University of Massachusetts Amherst
ScholarWorks@UMass Amherst

Masters Theses | Dissertations and Theses

November 2014

Deployment and Monitoring of an X-Band Dual-Polarization Phased Array Weather Radar

Lauren Masiunas
University of Massachusetts Amherst

Follow this and additional works at: https://scholarworks.umass.edu/masters_theses_2

Recommended Citation

Masiunas, Lauren, "Deployment and Monitoring of an X-Band Dual-Polarization Phased Array Weather Radar" (2014). *Masters Theses*. 101.
https://scholarworks.umass.edu/masters_theses_2/101

This Open Access Thesis is brought to you for free and open access by the Dissertations and Theses at ScholarWorks@UMass Amherst. It has been accepted for inclusion in Masters Theses by an authorized administrator of ScholarWorks@UMass Amherst. For more information, please contact scholarworks@library.umass.edu.

DEPLOYMENT AND MONITORING OF AN X-BAND DUAL-POLARIZATION PHASED ARRAY WEATHER RADAR

A Thesis Presented

by

LAUREN C. MASIUNAS

Submitted to the Graduate School of the
University of Massachusetts Amherst in partial fulfillment
of the requirements for the degree of

MASTER OF SCIENCE IN ELECTRICAL AND COMPUTER ENGINEERING

September 2014

Electrical and Computer Engineering

DEPLOYMENT AND MONITORING OF AN X-BAND DUAL-POLARIZATION PHASED ARRAY WEATHER RADAR

A Thesis Presented

by

LAUREN C. MASIUNAS

Approved as to style and content by:

Stephen Frasier, Chair

David McLaughlin, Member

Michael Zink, Member

C. V. Hollot, Department Chair
Electrical and Computer Engineering

to the people who supported me,
especially Krzysztof, Dave, Rob, Aunties, Dad, and Robin;
and to the people who told me I should be a waitress after college:
nothing pushes me to work harder than being told
I can't possibly succeed.

ABSTRACT

DEPLOYMENT AND MONITORING OF AN X-BAND DUAL-POLARIZATION PHASED ARRAY WEATHER RADAR

SEPTEMBER 2014

LAUREN C. MASIUNAS

B.A., SMITH COLLEGE

M.S.E.C.E., UNIVERSITY OF MASSACHUSETTS AMHERST

Directed by: Professor Stephen Frasier

This thesis describes the deployment of MIRSL's X-band dual-polarization Phase-Tilt Weather Radar (PTWR) at the University of Texas at Arlington during spring 2014. While this radar has been used to observe weather in Western Massachusetts, more observations of severe weather were required to determine the limits of its abilities in sensing more rapidly evolving weather systems. This site was chosen also for its proximity to the Dallas-Fort Worth Urban Testbed Network set up by the Center for Collaborative Adaptive Sensing of the Atmosphere (CASA), which provided the ability to compare and calibrate the PTWR data against another well-documented X-band weather radar. A data processing pipeline was developed for converting raw PTWR data to NetCDF format, which allows for easy sharing and mapping of weather data. Finally, this is the first in-depth documentation of the PTWR system and specifically the roof-mounted setup utilized for this deployment.

TABLE OF CONTENTS

Page

ABSTRACT . . . . . **iv**

LIST OF TABLES . . . . . **vii**

LIST OF FIGURES . . . . . **viii**

CHAPTER

INTRODUCTION **1**

1. HARDWARE DESCRIPTION **7**

1.1 Radar enclosure 7
1.2 RF subsystem 10

1.2.1 Upconversion 12
1.2.2 Antenna 14
1.2.3 Downconversion 14

1.3 Auxiliary hardware 16

1.3.1 Computer enclosure 17
1.3.2 Cooling 20
1.3.3 Temperature monitoring 22
1.3.4 Visual monitoring 24

1.4 System power 25

1.4.1 Radar enclosure power 25
1.4.2 netBooter power 27

2. OPERATION **29**

2.1 Remote access 29
2.2 GUI Description 29

3. DATA PROCESSING **35**

3.1 Data acquisition system 35
3.2 Data processing 37
3.3 Computation of polarimetric variables 41
3.4 Conversion to NetCDF 47
3.5 NetCDF plotter 50

4. OUTCOMES OF TEXAS DEPLOYMENT **52**

4.1 Observations 52
4.2 Qualitative comparison with DFW area radars 52
4.3 Quantitative comparison with CASA 54
4.4 Radar stability 56

5. FUTURE WORK **66**

5.1 Ettus transceiver 66
5.2 Cf/Radial NetCDF standard 67
5.3 Py-ART 67
5.4 Integration with CASA network 68
5.5 Temperature monitoring 68

APPENDICES

A. A BRIEF USER'S MANUAL **70**
B. DATASHEETS FOR UP-DOWN CONVERTER **82**

BIBLIOGRAPHY **146**

LIST OF TABLES

Table **Page**

1.1 PTWR parameters 8

1.2 Power within the radar enclosure. Side connectors indicate the power enters the radar enclosure through the military connectors on the side of the radar enclosure, as shown in Figure 1.4. 26

1.3 netBooter outlet descriptions. 28

2.1 Standard operating parameters for the PTWR deployment at UTA. 32

3.1 Header values 40

3.2 Global attributes saved to NetCDF files. 48

3.3 Variables saved to NetCDF files. All data types are 'f8' or 64-bit floating point. When polarization is unspecified, H is assumed. 49

4.1 List of observations taken by PTWR during deployment at UTA. All dates and times are listed in UTC and therefore may not match up with local time, i.e. "afternoon storm" may appear to be at night. During deployment, UTA was six hours behind UTC. 53

4.2 Characteristics of radar systems in the area during deployment at UTA. 54

A.1 Python programs written for PTWR processing. Inputs column indicates the default inputs; other options are described within the text. 73

A.2 Login and password information for setup and operation of the PTWR. 81

B.1 Companies and part numbers for the parts that make up the up/down converter. 83

LIST OF FIGURES

Figure **Page**

I.1 The Phase-Tilt Weather Radar during an observing run in Hadley, MA on 31 October 2013. 3

I.2 The CASA DFW Urban Demonstration Network during the spring 2014 deployment of the PTWR. Purple stars indicate working CASA radars, while purple circles indicate CASA radars that were not operating at the time of the deployment. Yellow diamonds indicate an NWS radar, KFWS, and an FAA radar, TDFW. Red pins indicate MIRSL radars in operation at the time, PTWR and XPOL. 6

1.1 A simplified system diagram. Solid lines indicate the path of the transmitted or received signal, while dashed lines indicate communication between different domains within the system. 8

1.2 Radar enclosure, as seen from the back with the metal plates removed. 9

1.3 Simplified schematic for the up-down converter. 10

1.4 Connections on the side of the radar enclosure. Top are military connectors for power, as explained in Section 1.4.1, while the bottom are BNC connectors for transmit, receive, trigger, and clock, connecting to the Pentek transceiver. 11

1.5 Picture of the Pentek PCI card in the back of the host computer. The top two connectors are for transmit (the bottom of the two is not used). The third connector down is receive, while the bottom is the input for a clock. Only one line on the ribbon cable is used, which is the trigger input from the FPGA. 13

1.6 A TR module without its metal casing, to show the PCB. (a) shows the path of a transmitted H-polarization signal, while (b) shows the path of a received V-polarization signal. The portion of the path both share is the common leg, which includes a digital attenuator and a phase shifter. 15

1.7 The PTWR mounted on the roof of Nedderman Hall at UTA. 18

1.8 The components inside the computer enclosure. 19

1.9 The PTWR roof mount cooling system. 21

1.10 Picture of the Arduino Uno-based temperature sensor, including the Uno, the ethernet shield, and the prototyping shield. 22

1.11 Schematic for the Arduino Uno-based temperature sensor inside the computer enclosure. 23

1.12 Screenshot of the last post on Twitter before the PTWR was taken down from the roof at UTA. 24

1.13 Lightning during the deployment on 3 April 2014, as seen from the security camera mounted beneath the radar. 25

2.1 GUI used for PTWR operation. 30

2.2 PPI live view in the PTWR GUI. 33

2.3 A-scope live view in the PTWR GUI. 34

3.1 The standard pulsing scheme for Texas deployment. Standard PRTs are shown, as well as PRTs used for multilag calculations. 36

3.2 The data acquisition process that runs the PTWR, including the new Level 1 and 2 processing. Pulse compression does not happen in real time, so here it is shown in an ideal real-time data processing scheme. 37

3.3 The structure of a binary file containing one PPI of data. These are saved as .dat files. 39

3.4 A plot of ϕ_{DP} before (green) and after (blue) smoothing and correcting for initial ϕ_{DP}, for one beam. 44

3.5 An example of a six-panel plot made en masse by the plotting program. 51

4.1 Comparison of the PTWR with three other DFW area radars. Range rings occur every 10 km and are centered on the PTWR's location. 55

4.2 PPIs of uncorrected reflectivity for a) XUTA at 23:31 UTC at an elevation angle of 5.28° averaged over 2° in azimuth, b) XUTA at 23:28 EST at an elevation angle of 7.4° averaged over 2° in azimuth, c) XUTA as an average of elevation angles 5.28 and 7.4°, and d) PTWR at 23:31 UTC at an elevation angle of 6°. All data was taken on 25 May 2014. 57

4.3 Histogram comparing CASA and PTWR data from similar scans, averaged for better comparison of illuminated volume. 58

4.4 Mean initial ϕ_{DP} plotted by beam for each deployment. Number of PPIs included in each day of observations (DEP) is listed in the legend. 59

4.5 RMS uncertainty in ϕ_{DP} plotted by beam, taken over eight days of observations. DEP5 is not included in this calculation, as it is considered an outlier. 60

4.6 Mean noise floor values plotted by beam for each deployment. Number of PPIs included in each day of observations (DEP) is listed in the legend. DEP 6 is an outlier here and was not included. 60

4.7 RMS uncertainty in noise floor plotted by beam, taken over seven deployments. DEP5 and DEP6 are not included in this calculation. 61

4.8 Mean noise floor values plotted by beam for each deployment. These lines are the same as Figure 4.6; however, each line has had its mean subtracted to be centered around 0. 62

4.9 Mean-subtracted noise floor from Figure 4.8, divided by the mean of the beam to show the variance by beam. 63

4.10 Uncertainty in variance from Figure 4.9. This is dominated by beam 65. 64

4.11 A histogram of uncertainty in noise floor variance. Beam 65 is not included. 65

A.1 Corner and level scheme of the radar enclosure frame. The first digit indicates corner, while the second indicates level. Corner 0 indicates the back right of the radar, from looking down from above; corner numbers increase clockwise around the frame. Level 0 indicates the ground level I-beam, while Level 3 indicates the topmost beam. 71

INTRODUCTION

Phased array radar technology

There are many problems with the current weather radar systems that have fueled the investigation of electronically scanned radars. One issue is that the mechanically scanned radars currently in use by most national weather services employ large spinning dish antennas that take a long time to scan the whole sky. These radars often provide revisit times on the order of five minutes. The long period between observations can result in severe weather warnings being issued too late. Another problem is that the current system employs a small number of high-power radars spread out over very large areas. Due to the curvature of the Earth, the radar beam is looking high in the sky at points far away from the radar. The weather at these altitudes often does not reflect the weather underneath the clouds; it often does not appropriately detect amount of rain, occurrence of hail, or such destructive forces as tornadoes. These issues and more have motivated interest in electronically scanned systems, which hold the promise to drop revisit times drastically.

The Center for Collaborative Adaptive Sensing of the Atmosphere (CASA) aims to eliminate the problem of the Earth's curvature within the large radar network [1]. CASA is testing this by building a system composed of a large number of short-range, low-power, low-cost dish radars set up on existing buildings and towers. Implementing phased arrays to focus only on areas of interest can drop revisit time and provide earlier warnings and more preparation time for those at risk.

The Multi-function Phased Array Radar (MPAR) is a proposed way to streamline the national radar system [2]. It aims to combine weather surveillance, wind profiling,

and air traffic control, reducing redundancies in current radar coverage. It accomplishes this using a single electronically scanned, dual-polarization radar in any one area. It uses the unique ability of pointing an electronically scanned radar beam from one point to another discontiguous point instantaneously without having to scan the whole sky. This uses the multi-functionality of the electronically scanned radar to direct the beam only where it is needed, rather than slowly scanning across the whole sky to look at a few targets of interest. This allows it to perform all of its tasks in a timely manner.

Over a decade ago, the Microwave Remote Sensing Lab (MIRSL) used its expertise in mobile weather radar to build an X-band dual-polarization mobile weather radar (XPOL) [3]. As technology advanced, it became possible to use this as a basis to build an electronically scanned weather radar, which is not hindered by mechanical scanning and can offer significant improvements in temporal resolution for rapidly evolving severe weather. Consequently, MIRSL has developed a mobile X-band dual polarization phased array weather radar at low cost, called the Phase-Tilt Weather Radar (PTWR, Figure I.1) [4]. This radar employs all the benefits of an electronically scanned radar, while also being mobile for serving areas that require better weather detection than is available from the national system.

While the PTWR had been used to observe weather in Western Massachusetts, more observations were required to determine the limits of its abilities in sensing more rapidly evolving weather systems. For this reason, MIRSL deployed the PTWR on a rooftop in Arlington, Texas, an area that typically yields the type of severe weather the PTWR was built to observe. This site was chosen also for its proximity to the Dallas-Fort Worth Demonstration Network set up by CASA [5]. This allows for a qualitative as well as quantitative comparison of weather observations from the CASA radar side-by-side with observations of the same weather system from the PTWR, for better calibration of the PTWR with respect to severe weather.

Figure I.1: The Phase-Tilt Weather Radar during an observing run in Hadley, MA on 31 October 2013.

CASA Dallas Fort Worth Demonstration Network

The PTWR was brought to the University of Texas at Arlington (UTA) for side-by-side comparison with CASA's Dallas-Fort Worth Demonstration Network. This network will deploy as many as eight X-band radars, including the four X-band radars previously deployed in CASA's Oklahoma Demonstration Network, which were refurbished and moved to the Dallas-Fort Worth metroplex. Two were operational during the PTWR deployment: one located at the University of Texas at Arlington (UTA), and one in Midlothian, TX. A map of the CASA radars during the PTWR deployment in spring 2014 can be found in Figure I.2.

The PTWR was deployed roughly 250m away from the CASA radar installed at UTA. This radar, like the other CASA radars, is a mechanically scanned dual-polarization parabolic antenna operating in X-band. The CASA radar and the PTWR were able to illuminate similar volumes at the same time. This provided a good opportunity to compare the benefits and hazards of electronic scanning. Having this side-by-side data for the first time allows for the investigation of phased array data against data from a radar whose products have been well-studied.

There are also two National Weather Service radars in the area. KFWS is a standard NEXRAD WSR-88D radar located in south Fort Worth, to the southwest of UTA. TDFW is an FAA TDWR radar, which are installed at airports where severe weather occurs. It has a narrower beam for high resolution, but typically observes only at lower elevation angles. This C-band radar is located northeast of UTA.

Also in the area during deployment was XPOL, the original MIRSL X-band radar. It was parked at the future location of the Fort Worth CASA radar near Lake Worth in hopes of testing the site. While data from this radar will not be included here, working with this radar while deployed in Fort Worth showed the benefits of the PTWR's roof mounting over the option of "truck turned permanent radar station"

method. This includes easier access to power and internet, as well as significantly fewer wild animals getting into the system and causing malfunctions.

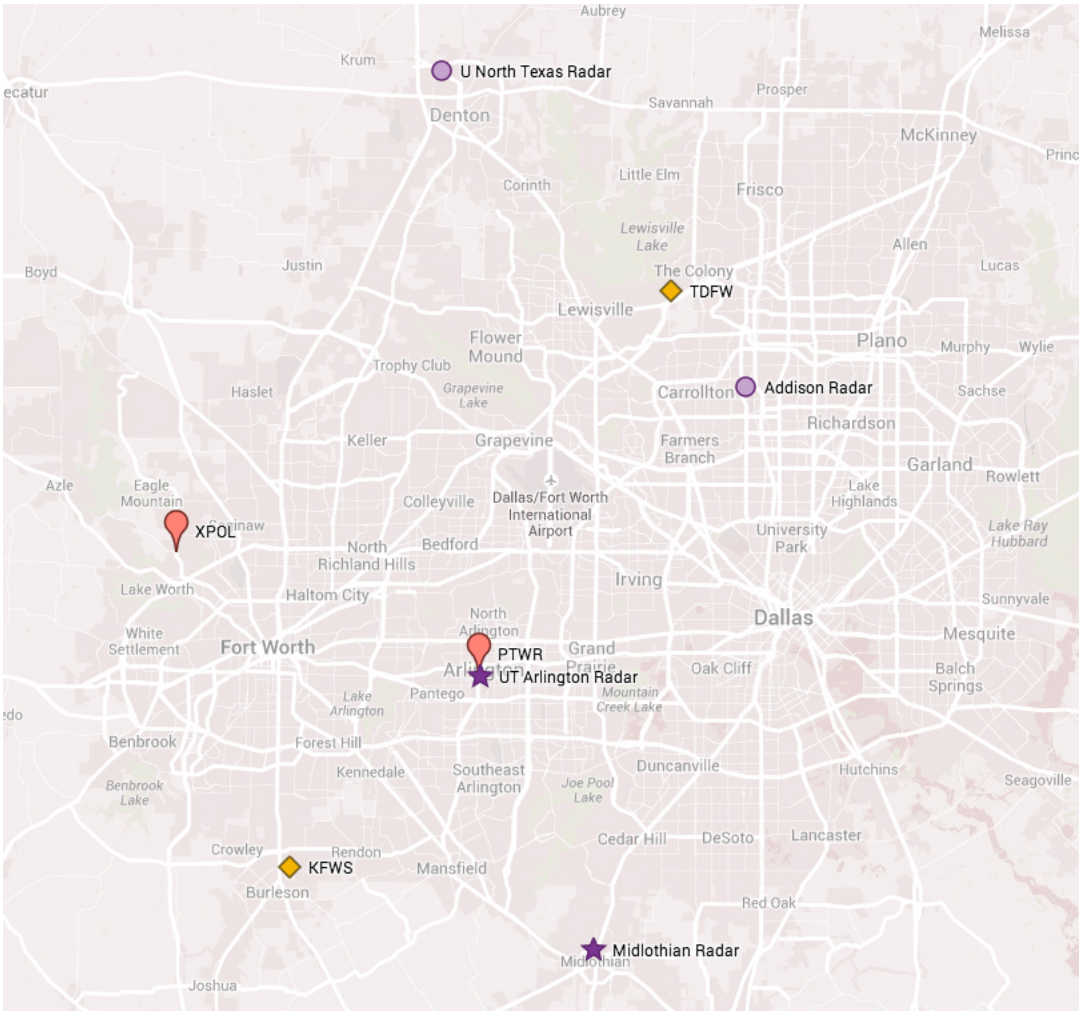

Figure I.2: The CASA DFW Urban Demonstration Network during the spring 2014 deployment of the PTWR. Purple stars indicate working CASA radars, while purple circles indicate CASA radars that were not operating at the time of the deployment. Yellow diamonds indicate an NWS radar, KFWS, and an FAA radar, TDFW. Red pins indicate MIRSL radars in operation at the time, PTWR and XPOL.

CHAPTER 1

HARDWARE DESCRIPTION

During the spring 2014 deployment, the PTWR consisted of a radar enclosure, computer enclosure, and pedestal. This radar setup is explained in this chapter. The radar is designed to scan electronically in azimuth and tilt in elevation using a pedestal, all while being controlled by a host computer. General parameters of the PTWR are listed in Table 1.1 [6]. A simplified system diagram is presented in Figure 1.1.

1.1 Radar enclosure

The radar enclosure contains the microwave components, including the up-down converter, transmit/receive (TR) modules, power supplies, array controller, and the antenna array. A figure of the radar enclosure, opened to show the components inside, can be found in Figure 1.2.

The radar enclosure is 1.47m wide, 0.82m tall, and 0.30m deep. It weighs about 82kg. It is made of an aluminum skeleton with a radome on one side, a metal plate on each side, two plates each on the top and bottom sides, and two metal plates on the back. It sits on a pedestal that enables it to move in elevation and azimuth.

The radome over the antenna array is a .5mm thick teflon sheet attached to a foam backing with an adhesive. The foam is cut into five pieces: one large sheet over the antenna, and four sheets along the border to add support. The teflon is bent around the edges of the radar enclosure and held in place by the plates on the sides of the radar. There are a few screws around the antenna to hold the foam in place.

Table 1.1: PTWR parameters

Parameter	**Specifications**
Radar system dimensions [m]	1.47 x 0.82 x 0.30
Weight [kg]	82
Frequency [GHz]	9.3 - 9.4
Transmit power (peak) [W]	60
Pulse compression gain [dB]	up to 20
Duty cycle	up to 30%
Beam width [°]	2 (azimuth) x 3.5 (elevation)
Integrated cross-pol isolation [dB]	< -15
Range resolution [m]	> 37.5
Polarization	alternate H & V

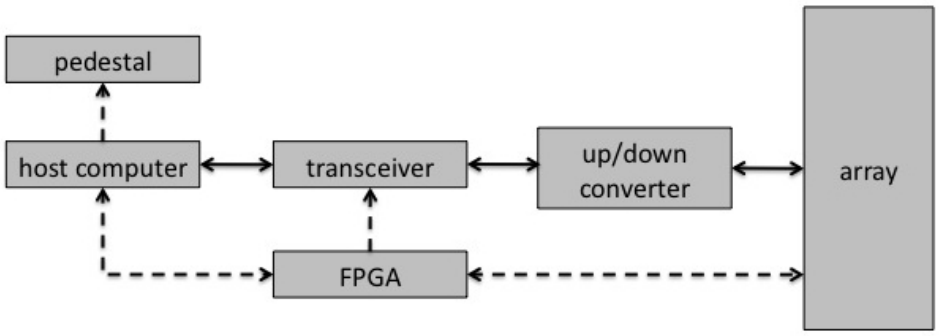

Figure 1.1: A simplified system diagram. Solid lines indicate the path of the transmitted or received signal, while dashed lines indicate communication between different domains within the system.

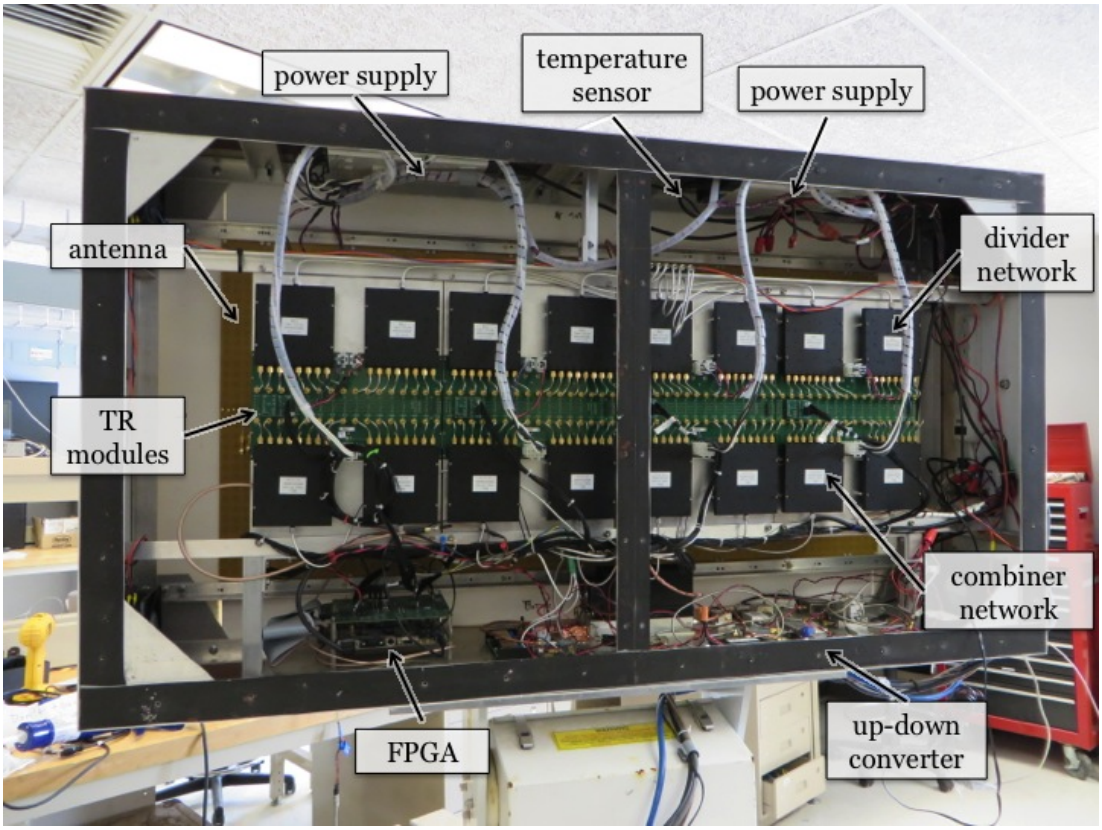

Figure 1.2: Radar enclosure, as seen from the back with the metal plates removed.

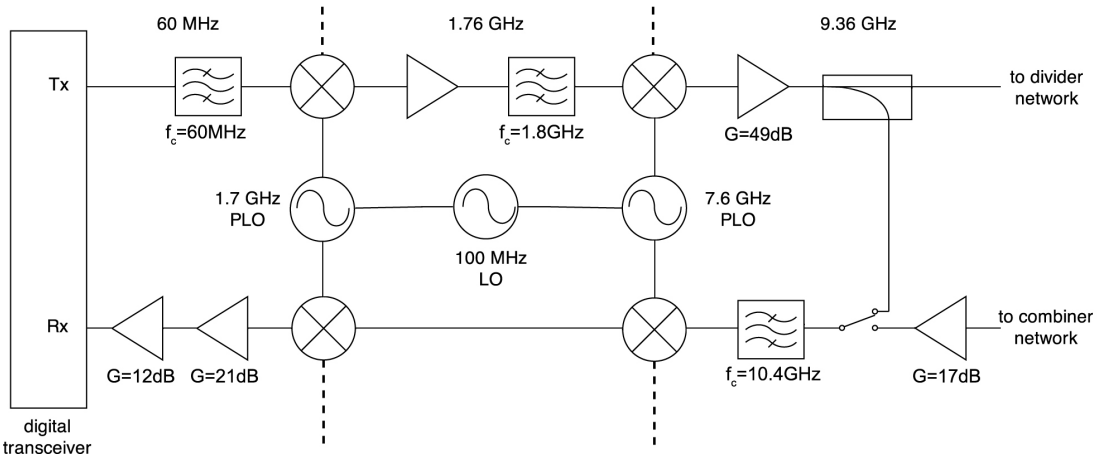

Figure 1.3: Simplified schematic for the up-down converter.

The transmission coefficient of this type of radome on a prototype of the PTWR has been found to be less than -0.4dB for an incident angle between 0 and 60° of azimuth angle [8], so the electromagnetic properties of this radome are good for the purposes of this radar.

There are some flaws in the radome, as it has been stored outside in extreme temperatures and in the sun and rain. The adhesive has detached in several places, causing the teflon to bubble up from the foam. Because of this, some of the screws holding the foam in place can no longer connect the foam to the frame. There is also a slit in the teflon where it meets the top of the radar enclosure, which has been sealed with duct tape. These degradations in the radar appear to have minimal effects on the data.

1.2 RF subsystem

The RF subsystem is contained within the radar enclosure, mounted on the bottom plate. Inputs and outputs go through the BNC connectors on the side of the radar enclosure, as shown in Figure 1.4. A schematic of the RF system is shown in Figure 1.3.

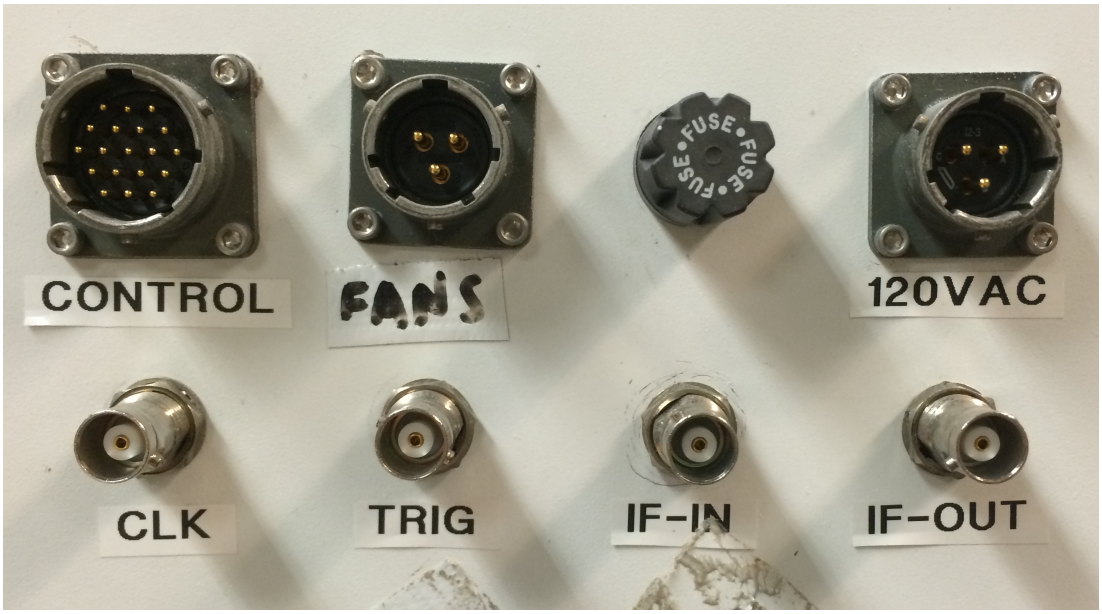

Figure 1.4: Connections on the side of the radar enclosure. Top are military connectors for power, as explained in Section 1.4.1, while the bottom are BNC connectors for transmit, receive, trigger, and clock, connecting to the Pentek transceiver.

The transceiver is a commercial digital transceiver, Pentek 7140. It is installed as a PCI card in the host computer, as shown in Figure 1.5. It has one transmit and one receive line, as well as a trigger and a clock input. The 100MHz clock is fed from the radar enclosure to the transceiver, as all parts of the system require the same clock. The transceiver also receives a trigger signal from the FPGA, to facilitate timing across the system. These cables are SMA, and come from the outputs at the side of the radar (from the BNC connectors in Figure 1.4), labelled "IF-IN" for transmit, "IF-OUT" for receive, "TRIG" for the trigger, and "CLK" for the clock. Since the PTWR operates in alternate transmit alternate receive (ATAR) mode, only one transmit and one receive line is required.

There is an attenuator on the transmit line, close to the Pentek. On the receive line, there is an anti-aliasing filter centered at 60MHz, then a limiter and a 3dB attenuator. The limiter assures that the Pentek never receives a signal above 10dBm, which would burn out the receiver.

Some of the cables in the RF system are wrapped in foil to increase isolation. At 9.36GHz, especially at the output of the high power amplifier, the signal can leak into the received data and will be visible in the data. The foil minimizes these effects.

The FPGA is connected to the computer via serial port TTYS0. This talks primarily to the `xdatalog` program described in Chapter 3. It receives a clock signal in order to appropriately time triggers. The FPGA daughter board converts the 100MHz sine wave from the system clock (the same that goes to the transceiver) to a square wave of the same frequency, as required by the FPGA. The triggering signals are generated at the FPGA and sent to the transceiver at every transmission to start recording data. The trigger also passes through a 100-pin connector to the FPGA daughter board, where they are split into four and sent to each of the four line replaceable units (to be explained in Subsection 1.2.2).

1.2.1 Upconversion

A 60MHz-centered chirp or pulse is sent from the transceiver through the IF-in cable (labelled "TX") into the radar enclosure. The signal travels through a bandpass filter with a 60MHz center frequency and 5MHz bandwidth to filter out spurious image signals from the transceiver. It is then mixed with a 1.7GHz phase-locked oscillator up to 1.76GHz. It is amplified and passed through another bandpass filter. It is mixed again with a 7.6GHz PLO to 9.36GHz. Finally, the signal goes through a high-power amplifier with over 40dB gain. This signal then enters the divider network and is split into eight, and those eight signals are split into eight again to produce the sixty-four signals for the TR modules.

With the signal split into sixty-four, plus the losses in the transmission line, there is 18dB of split loss and 3dB of transmission loss; the TR modules have a 30dB gain. Since the TR modules should be saturated with a 0dBm signal, the high power amplifier is necessary to make sure the signal is high enough before being

Figure 1.5: Picture of the Pentek PCI card in the back of the host computer. The top two connectors are for transmit (the bottom of the two is not used). The third connector down is receive, while the bottom is the input for a clock. Only one line on the ribbon cable is used, which is the trigger input from the FPGA.

split, providing roughly 5dBm to every TR module, with slight variations due to temperature variations.

A TR module without its casing is shown in Figure 1.6. Inside each of the 64 TR modules is a common leg shared between transmit and receive mode that includes the attenuators and phase shifters [7]. A switch at either end specifies transmit or receive mode. The signal is then fed through a polarization diversity switch before being transmitted through an antenna element. Each TR module has an FPGA inside with enough memory to save amplitude and phase values for the attenuator and phase shifter, fed from the host computer. Because each TR module can only transmit about 1W of power, the PTWR uses pulse compression techniques to increase sensitivity.

1.2.2 Antenna

The TR modules are connected to the antenna with two cables. Arrows on the TR modules indicate transmit and receive. The upper connector attached to the antenna is H-pol, while the lower connector is V-pol. These cables are SMA at the TR module and SMP at the antenna.

The antenna is made up of 64 dual-polarized antenna elements [8]. Each of these elements is a center-fed microstrip patch array antenna with 32 elements. The 64 antenna elements are broken up into four line replaceable units (LRUs) of 16 antenna elements each. There are also four terminated dummy elements on each side of the array, used to reduce negative effects from diffraction and non-uniform coupling at the array edges. Each of the 64 elements have a TR module capable of independent amplitude and phase control on transmit and receive.

1.2.3 Downconversion

Upon its return, the signal is fed back through the TR modules and into a combiner network, from sixty-four to eight to one. This signal is fed through an LNA to boost it above the noise floor of the receiver. It passes through a switch which is used

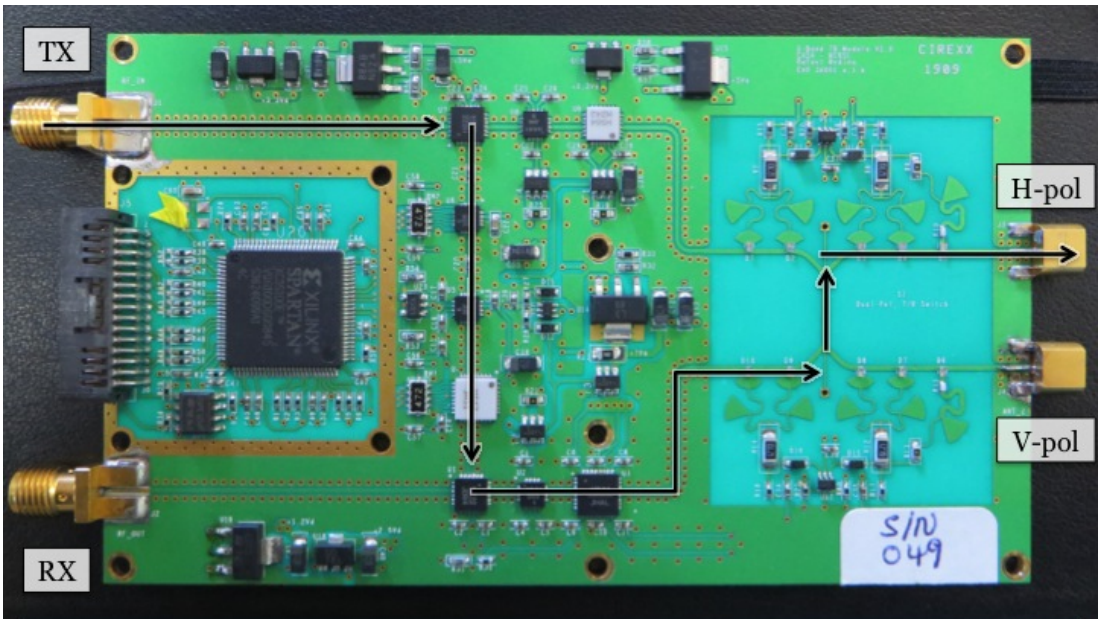

(a)

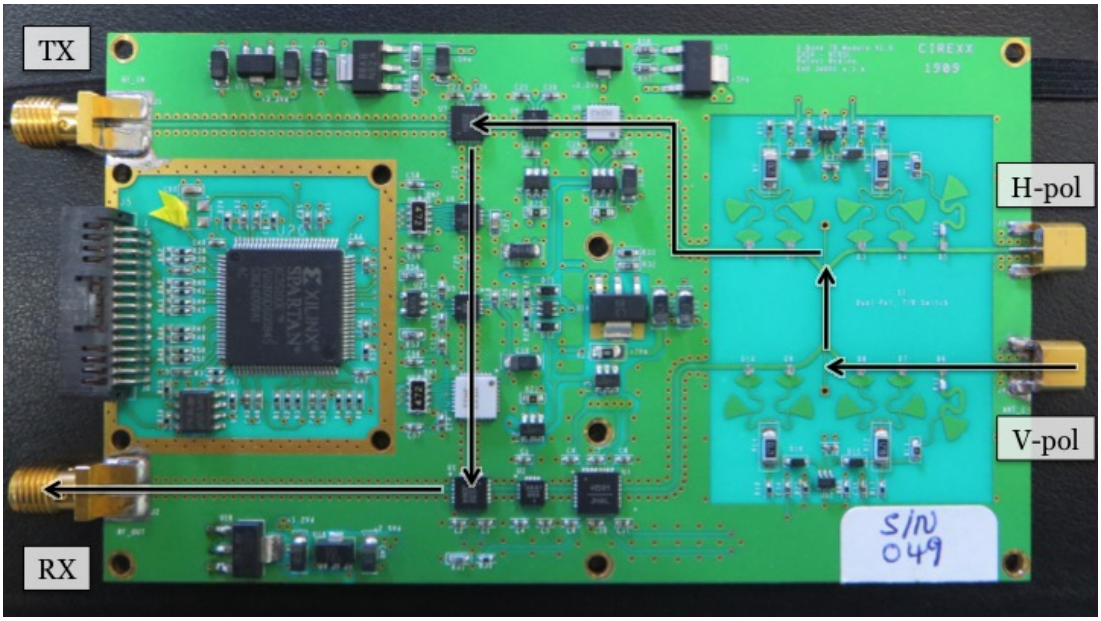

(b)

Figure 1.6: A TR module without its metal casing, to show the PCB. (a) shows the path of a transmitted H-polarization signal, while (b) shows the path of a received V-polarization signal. The portion of the path both share is the common leg, which includes a digital attenuator and a phase shifter.

primarily for diagnostics (described below) and a bandpass filter. It is then mixed with a 7.6GHz PLO (the same used in upconversion) down to 1.76GHz and again with the 1.7GHz PLO to 60MHz. It is amplified twice to make up for the loss from the mixers and attenuation from the filters. It passes out of the radar enclosure to the transceiver through the IF-out cable (labelled "RX").

The internal calibration switch is used to collect information about the transmitted waveform. When the radar is receiving, the signal comes from the TR modules to the digital transceiver, to record all received data as expected. When the radar is transmitting, the switch changes on every pulse. This allows the radar to receive normally but to record the transmitted waveform for calibration while transmitting the signal.

The switch records the transmitted signal from two places. One input comes through a 30dB coupler, which is fed into an attenuator before entering the switch. The coupler allows the transmitted signal to enter the divider network as expected while also collecting the signal through the switch and back into the receiver. The other input comes from the TR modules just after the LNA. This is important because during transmission, about -30dBm leaks through the transmit-receive switch in the joint leg of the TR modules. Since the signals are in phase, the signal from all 64 TR modules adds coherently. The switch works such that on pulses one and three, the recorded waveform comes through the path that bypasses the TR modules, while on pulses two and four, the signal comes through the path that includes the TR modules.

1.3 Auxiliary hardware

The PTWR was designed to be mounted on a truck; however, for this project, it was mounted on a roof, and so some changes were made to the setup, as shown in Figure 1.7. A climate-controlled enclosure for the host computer, positioner, and power strips was necessary. This computer enclosure is designed to be weatherproof,

though some holes have been cut to allow access for cables; every effort has been made to make these holes water-tight through use of silicone caulking and duct tape. The cords for controlling the radar exit the computer enclosure through a hole in the side of the computer enclosure.

A new mounting technique was contrived, including an extended structure for the radar enclosure and pedestal as well as a base for holding down the radar enclosure and computer enclosure. The system already included a pedestal for tilting and rotating the radar enclosure. Several I-beams were used to raise the radar enclosure and pedestal above the height of the wall surrounding the roof, roughly three feet. Two pieces of 3/4" thick plywood were used for the base. The I-beam structure and the computer enclosure were mounted to these with 3/8" stainless steel screws, fed from underneath and countersunk so as not to harm the lining of the roof. Cinder blocks were used as weight to ensure the roof mount would not blow away in severe weather.

The roof space allocated to the PTWR was less than ideal. The view to the east was blocked by a wall roughly 5m high. The south was blocked by a metal structure just over a meter high. To the west of the radar was a large dish antenna. Despite this, the PTWR had a generally unimpeded view to the southwest and northwest.

1.3.1 Computer enclosure

The computer enclosure houses the host computer, positioner controller, and two network-controlled power strips called netBooters. There is also a battery backup for power emergencies that the netBooters are connected to. (The battery backup aspect of the system fortunately never had to be used.) These components are all mounted within the computer enclosure, a large weatherproof Hardigg case with a rack mount. This case also includes the cooling for the system. The case and components are shown in Figure 1.8.

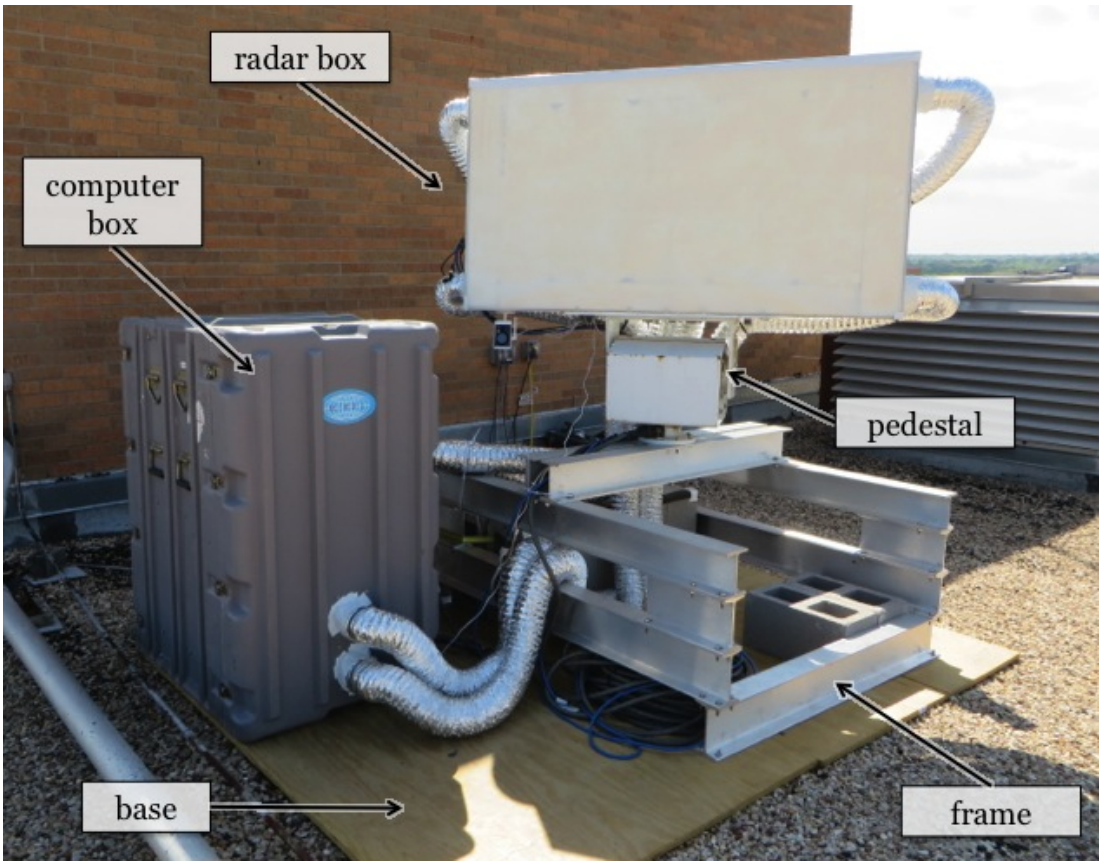

Figure 1.7: The PTWR mounted on the roof of Nedderman Hall at UTA.

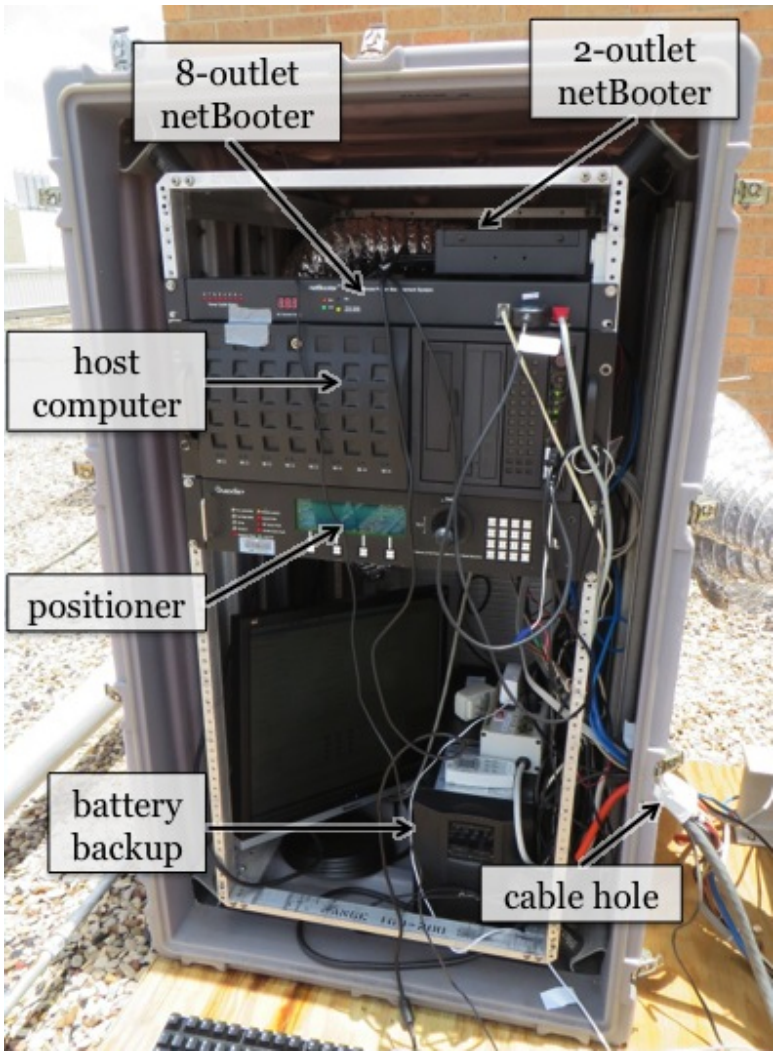

Figure 1.8: The components inside the computer enclosure.

The USB hub is for the keyboard and mouse as well as any external hard drives. The positioner and FPGA use the serial ports. This is because the two serial ports at the back of the computer are always named TTYS0 and TTYS1 by the host computer, and they are called specifically in the radar operation code in this way. The FPGA should always be TTYS0, and TTYS1 should always be the positioner, which uses a special female-female cable, and goes to the J2RS232 on the back of the positioner. The netBooters and the pitch and roll sensor use serial to USB adapters, since there are not enough serial ports in the host computer for all serial components. USB ports tend to change names randomly every time the computer is rebooted; this is addressed in Appendix A.

1.3.2 Cooling

For mounting on a roof, cooling and temperature monitoring had to be considered and added to the system, as these would no longer be provided by the truck. A window unit air conditioner was bought at low cost; a hole was cut into the back door of the computer enclosure to act as the "window" through which the air conditioner could be installed. The air conditioner uses an internal temperature sensor to maintain a predetermined temperature. It also has a remote control for easy temperature changing, as it is mounted at the back of the computer enclosure and can be hard to reach.

The TR modules have fans underneath them to keep them cool. The radar enclosure already had four fans mounted on the sides: two fans on the bottom for pulling cool air in from the environment, and two fans at the top that pull the cool air over the TR modules and push the warmed air back out. Repurposed dryer hoses were used as ducting between the computer enclosure and the radar enclosure, and were fed from holes cut in the computer enclosure to the fan openings. Dryer vents have the same diameter as the standard fan, so dryer louvers were installed in the fan

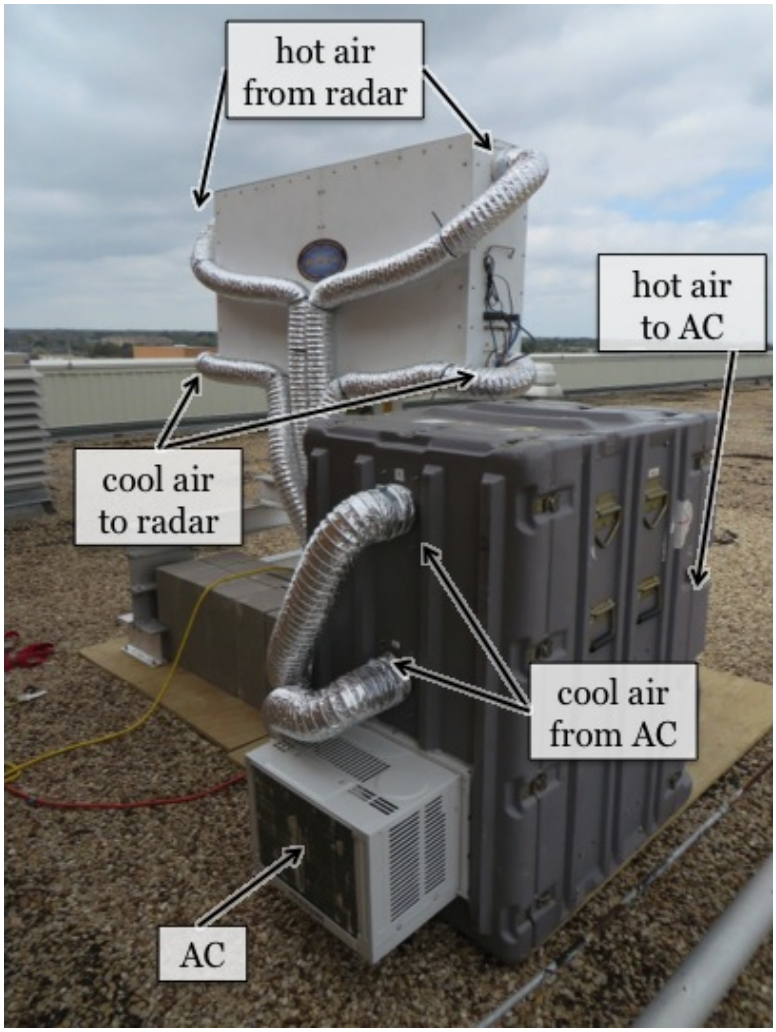

Figure 1.9: The PTWR roof mount cooling system.

openings to make the appropriate connections. The fans were reinstalled within the louvers to pull cool air through the ducting into the radar enclosure at the bottom and pump warm air back to the computer enclosure from the top. Inside the computer enclosure, the ducts for cool air leave from the side with the air conditioning, and the return ducts enter on the side opposite the air conditioner. It is sealed to form a closed loop to avoid problems with humidity and condensation on the radar components. The air inside the computer enclosure was air conditioned, so it stayed cool and dry.

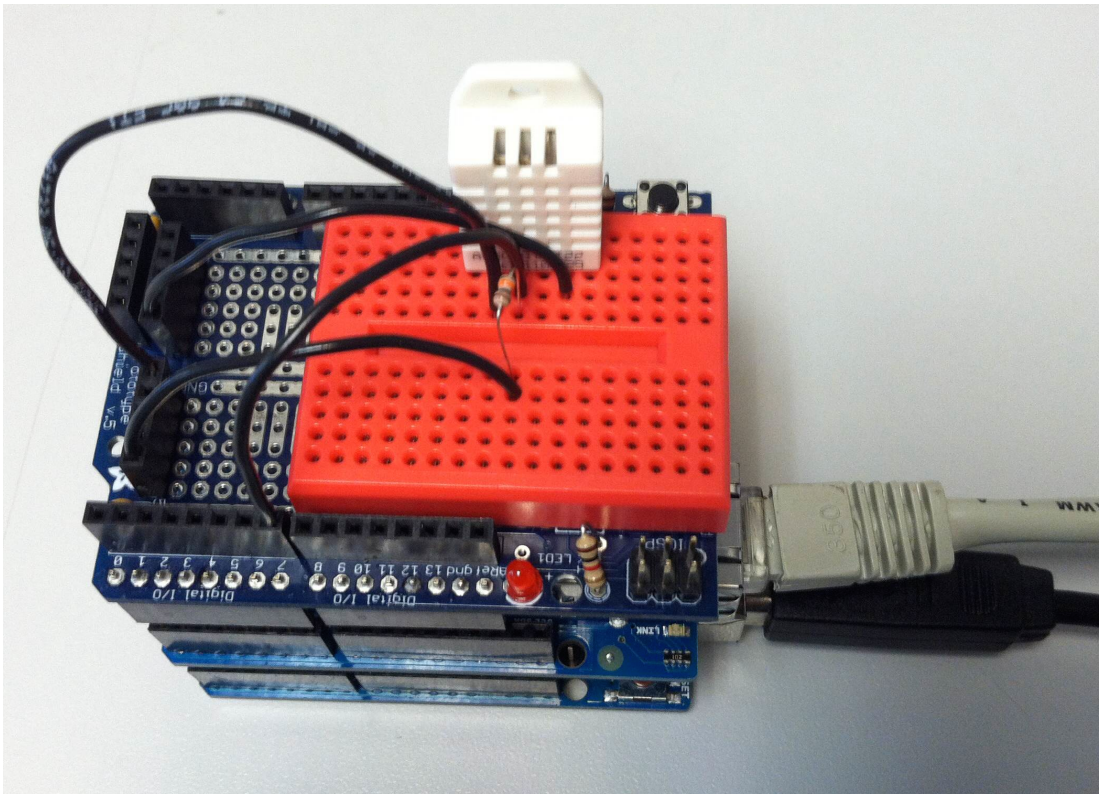

Figure 1.10: Picture of the Arduino Uno-based temperature sensor, including the Uno, the ethernet shield, and the prototyping shield.

1.3.3 Temperature monitoring

While the radar enclosure already had a temperature monitoring system inside, in the form of temperature sensors on the TR modules and a temperature sensor associated with the netBooters, the computer enclosure did not. The air conditioner was dependent upon the computer enclosure temperature, but there was no way of changing the air conditioner's temperature once set and the system closed. Therefore temperature monitoring was critical, since someone on-site would have to be called in to fix the air conditioner. A device was made for these monitoring purposes. Since there were also condensation concerns, a humidity sensor was included in this device to monitor the humidity and temperature and check it against the dew point in the area. This device is shown in Figure 1.10, with a circuit schematic in Figure 1.11.

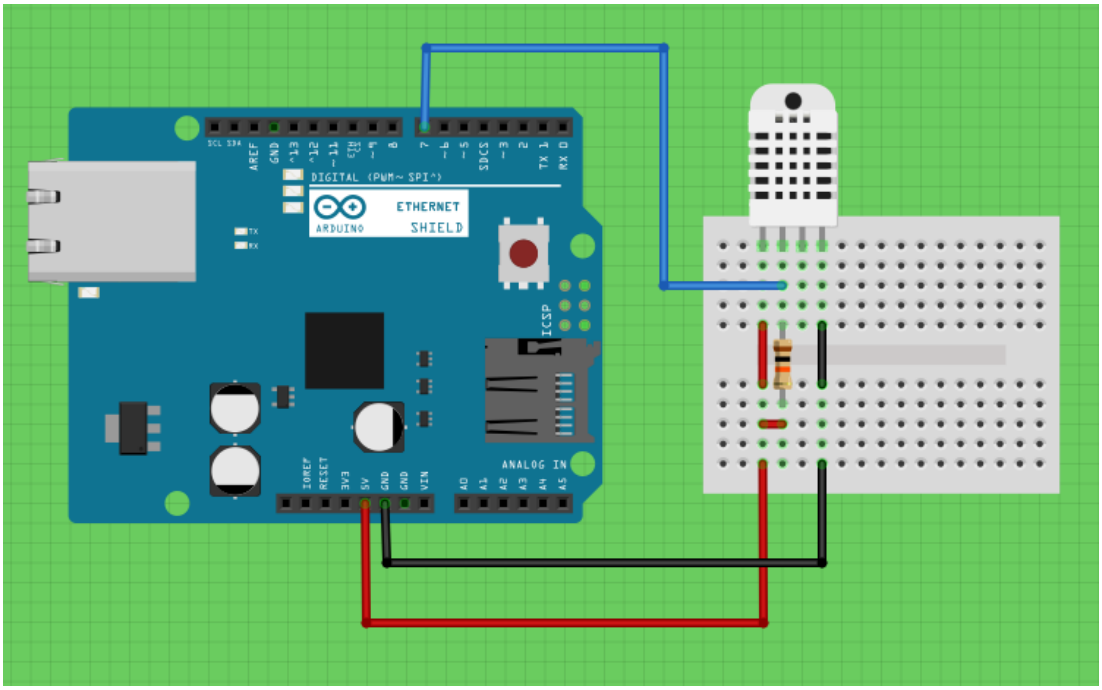

Figure 1.11: Schematic for the Arduino Uno-based temperature sensor inside the computer enclosure.

The device utilized an Arduino Uno microcontroller, an open-source electronics prototyping board. A DHT22 sensor was used for sensing temperature and humidity. This sensor can detect temperatures from -40 to 125° Celsius with ±0.5° accuracy, and humidity from 0-100% with 2-5% accuracy. (The humidity readings were often quite low, close to 1%. While this seems low, the air conditioner was designed for a much larger space than the computer enclosure and was run continuously for over two months. More testing is required to see how accurate this humidity sensor is.)

An ethernet shield was used to give the device connectivity. The device sent the temperature and humidity readings to a dedicated Twitter feed, @mirslradar, every five minutes; however, as per the Twitter protocol, duplicate tweets were discarded. An example tweet is shown in Figure 1.12. This Twitter feed served as the temperature and humidity monitoring point for the computer enclosure. The humidity

Figure 1.12: Screenshot of the last post on Twitter before the PTWR was taken down from the roof at UTA.

stayed below 25% for the duration of the deployment, and while the temperature did at times reach above 40° Celsius, the computer continued to work without a problem.

1.3.4 Visual monitoring

Also included in the system was a visual and audial monitoring system. This was achieved through the use of a D-Link DCS-2330L network-enabled outdoor security camera (seen on the bottom of the radar enclosure in Figure 1.7). This was mounted to the bottom of the radar enclosure during deployment. A web app as well as a smartphone app exist for viewing the camera when and wherever the operator desires.

This camera can be configured to take a picture or a video when it detects movement; this leads to some stunning photos of storm events as in Figure 1.13. This feature is triggered whenever the radar changes elevation during a scan; it also triggers from lightning, birds, and clouds. This can cause issues as these images are saved to a Micro SD card on the camera, which can fill fast and whose data must be removed manually.

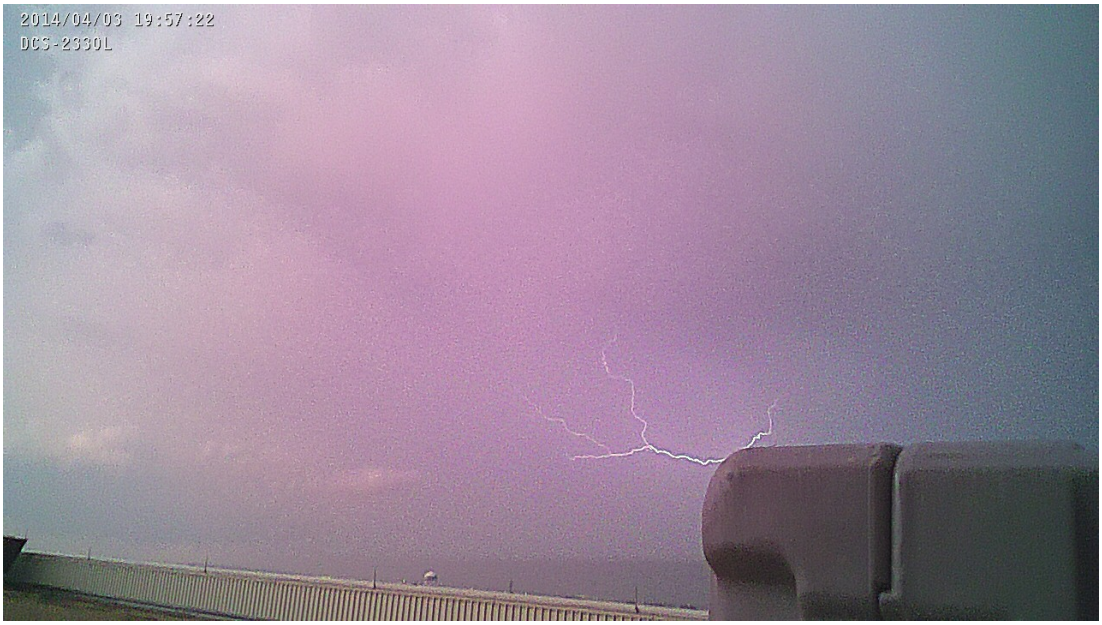

Figure 1.13: Lightning during the deployment on 3 April 2014, as seen from the security camera mounted beneath the radar.

1.4 System power

1.4.1 Radar enclosure power

Power enters the radar enclosure through military connectors on the side, as shown in Figure 1.4. The connections here are powered through the netBooters, so these connections can be controlled remotely, as described in Section 1.4.2. After entering the radar enclosure, power passes to two DC power supplies mounted on the top of the radar enclosure. These power supplies provide the various DC voltages needed by the radar components. They have cartridges inside that specify the output voltages of the supply and can be removed or replaced. They have fans that are positioned to blow hot air out the sides of the radar enclosure, toward the fans blowing air out of the radar enclosure. The DC supplies are attached to the top of the radar enclosure with screws, sealed from the top with silicone caulking and duct tape so no water leaks in through the top of the radar enclosure. They supply 12V to each of the four LRUs, the X-band high-power amplifier, and to the fans underneath the TR

Table 1.2: Power within the radar enclosure. Side connectors indicate the power enters the radar enclosure through the military connectors on the side of the radar enclosure, as shown in Figure 1.4.

Description	**Voltage**	**Origin**	**Wire color**
TR module fans	12V	DC power supply	black and red
TR modules	12V	DC power supply	black and white
TR modules	7.5V, -10V	DC power supply	black and red
DC power supply	120V AC	"120V AC" side connector	black and red
Up/down converter	12V	bottom rails	black and red
Side fans	120V AC	"Fans" side connector	orange and blue
FPGA	5V DC	"Control" side connector	black
High power amplifier	12V	DC power supply	red and black

modules. They also supply 12V, 7.5V, and -10V to the TR modules. An additional 12V line is passed to the voltage rails at the bottom of the radar enclosure to power the components in the up-down converter. One of these becomes the -12V required for the switch in the up-down converter.

The TR modules use three voltages. The power for the TR modules (12V, 7.5V, and -10V) enters through the backplane PCB between the splitter and combiner networks. The diodes on the PCB indicate whether there is power, regardless of color. However, not all the LEDs are currently functional, so checking the voltages is critical if a problem arises. The TR modules use 12V for internal power amplifiers. Quite a bit of amperage is required per LRU (one LRU in transmit mode requires 27A at 12V), so this voltage is fed to each LRU separately on the black and white twisted wires. The red and black twisted wires supply 7.5V to each LRU through the repeater board and is converted into 5V, 3.3V, 2.5V, and 1.2V as needed to the TR modules for the internal FPGAs and other logic. The voltage regulators inside the TR modules contribute to their heat generation. The -10V supplied to the repeater

boards are needed for transistors. The voltages enter the TR modules through the 20-pin connector in the backplane.

The FPGA requires 5V DC, so an adapter is used to turn 120V AC from the netBooters into the required DC voltage. The system is configured so that the FPGA is powered on after the rest of the system. If the FPGA is turned on first, it lacks a clock signal, which causes it to turn on in an undefined state. Similarly, the FPGA needs to be the last part of the system to turn off, since when powering down, the FPGA will send a final trigger and set the system into transmit mode.

There are small daughter boards in front of the TR modules. These are repeater boards, designed to keep the signal clean. They are connected to the FPGA by black cables.

1.4.2 netBooter power

The system utilizes netBooters for remote power management; that is, it acts as a power strip where individual outlets can be turned off and on remotely. There are two netBooters, one with eight outlets and one with two. The eight-outlet netBooter setup is described in Table 1.3.

The radar enclosure fans and TR module fans turn on when the radar is powered on, and off when the radar is powered off. The fans can also be controlled by a temperature sensor mounted in the top of the radar enclosure, so that if the temperature increases above a certain threshold temperature (set to 30° Celsius), the fans turn on, and when the temperature decreases again (below 28°), the fans turn off. The threshold temperatures for fan operation can be controlled over the netBooter software, to be described in Chapter 3. While this functionality was used in the past, it was not part of this deployment, since the cooling system was more complicated than during regular operation on the truck, and more cooling was needed.

Table 1.3: netBooter outlet descriptions.

netBooter	**Outlet**	**Description**	**Default state**
1	1	host computer	1
1	2	monitor	1
1	3	positioner	1
1	4	USB splitter	1
1	5	computer enclosure fan	0, 1 on radar on
1	6	radar main power	0, 1 on radar on
1	7	radar enclosure fans	0, 1 on radar on
1	8	FPGA	0, 1 on radar on
2	1	empty	0
2	2	AC	1

CHAPTER 2

OPERATION

2.1 Remote access

To access the computer remotely, the program TeamViewer is used. This program allows remote desktop access, since the radar has such a wide variety of functions that it is logical to run it through a GUI. TeamViewer can be installed on many operating systems and on mobile devices.

2.2 GUI Description

The system is run through a custom GUI created in Python using the Enthought Canopy GUI utility. Two GUIs currently exist on the host computer: one that implements 1024 gates, which was implemented for preliminary testing of the PTWR, and one that implements 2048 gates. All data sets taken during deployment at UTA have 2048 gates. It is shown in Figure 2.1.

The GUI is accessed through a Desktop icon. This opens the GUI window as well as a Terminal window with four tabs and two additional GtkTerm windows. The Terminal tabs are HTOP, NETBOOTER, AC CONTROL, and XDATALOG. HTOP displays the processes running on the computer, as well as which of sixteen CPUs are in use. All background processes should run on CPUs 1-8, while the radar operations use CPUs 9-16. TeamViewer is not restricted to a specific CPU, so CPUs 9-16 may show some usage even while the radar is not running. The NETBOOTER and AC CONTROL tabs typically are not used; instead, these can be controlled through the GtkTerm, for device access. XDATALOG displays the radar operations processes.

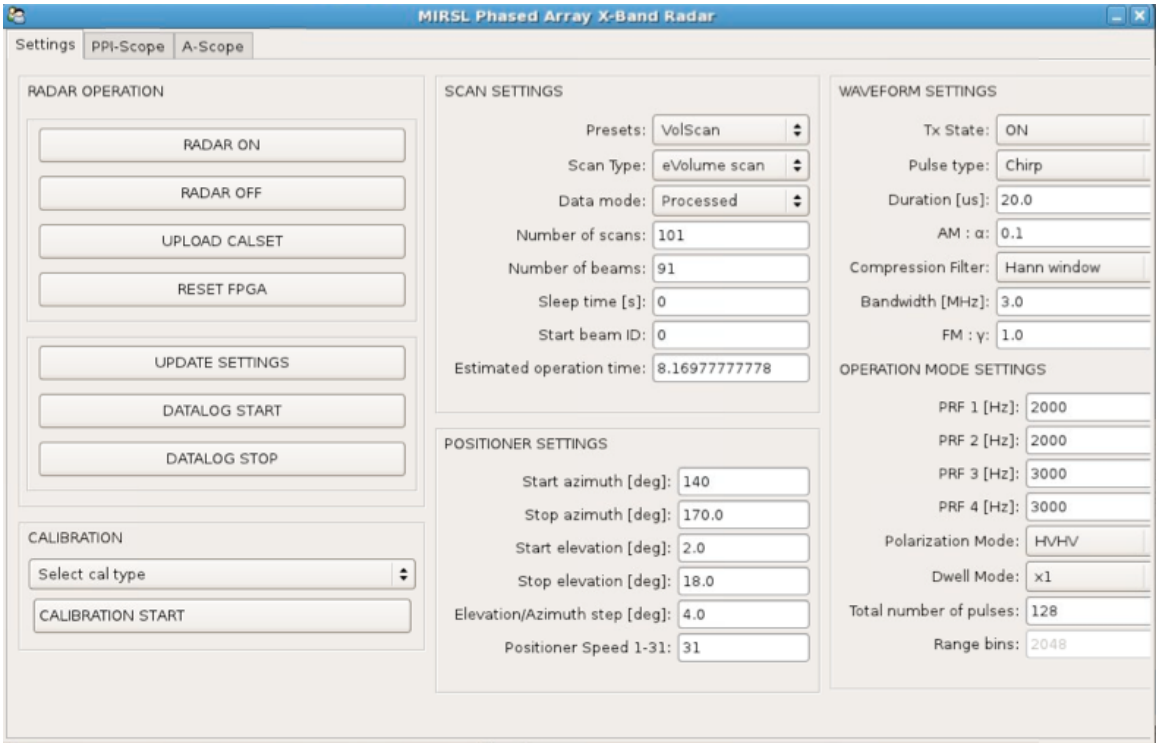

Figure 2.1: GUI used for PTWR operation.

This tab shows the outputs of the radar operation program, `xdatalog`, and indicates progress as the radar uploads calibrations, scans, and resets.

If an ethernet cable is plugged into the eight-outlet netBooter, a web application is available for power management. This is graphics-based and somewhat easier to use. It can be accessed from the netBooter's IP, which was static while within the UTA network (through the use of a VPN connection into UTA's network). This web application also allows control over outlets based on temperature, using the temperature sensor mounted in the top of the radar box. The web application also provides critical information about the current being drawn by the radar, an indicator of what state the radar is in.

The radar can be turned on using the "RADAR ON" button. Similarly, when operation is complete, "RADAR OFF" cuts power to the radar. As the radar starts up, the XDATALOG tab will display the appropriate outlets turning on. It will turn

on outlets 6, 8, 5, and 7, in that order; there is a longer delay of three seconds between 6 (radar on) and 8 (FPGA), since the clock needs to be up and running before the FPGA can be powered. The others are turned on one second after the previous outlet is turned on.

Once the radar is on, the calibrations must be uploaded to each TR module with the "UPLOAD CALSET" button. The TR modules have volatile memory, so the calibrations must be uploaded every time the radar is powered up. Lookup tables for phase shift, digital attenuation, and polarization for each beam are uploaded to the TR modules. While the computer communicates with each TR module, XDATALOG will display the temperature of the TR module to which it is uploading calibrations. If there is a problem with the TR module, it will appear here. Temperatures should be logical; if the listed temperatures are much higher or lower than ambient temperature, or temperature could not be read, likely something is wrong with the module. The radar operates at about 10° C above ambient temperature, but this is only after the radar has been running for some time, so when the radar is first powered on, it should be within a few degrees Celsius of ambient temperature.

The available scan settings are very flexible; the PTWR is highly configurable. Fortunately, the standard mode of operation, "VolScan", is a preset in the GUI (shown in Figure 2.1). Other options available are ePPI, which does a 90° PPI electronic scan; a chirp and a pulse calibration mode; an ESP mode for different calibration techniques; and a spaced antenna mode. Only the volume scan option was used for typical observations, and the other options will not be investigated in this thesis. The standard mode parameters are described in Table 2.1.

It must be noted that azimuths 220° and 320° in the table refer to degrees clockwise from north. During deployment, a 0° reading from the pedestal meant the radar was facing south, and so readings from the binary files will differ by 180°. This is corrected for in NetCDF conversion, to be described in Chapter 3.

Table 2.1: Standard operating parameters for the PTWR deployment at UTA.

Parameter	**Value**
Center azimuth	220 or 320°
Sector	±45°
Elevation	2 - 18°
Elevation step	4°
Dwell	128 pulses
PRF	2-3kHz
Range	50km
v_a	$\pm 45 m/s$
Pulse type	chirp
Pulse width	$20\mu s$
Bandwidth	3 MHz
Filter	Hann window
AM factor	.1
FM factor	1.0
Polarization mode	HVHV
Number of scans	101

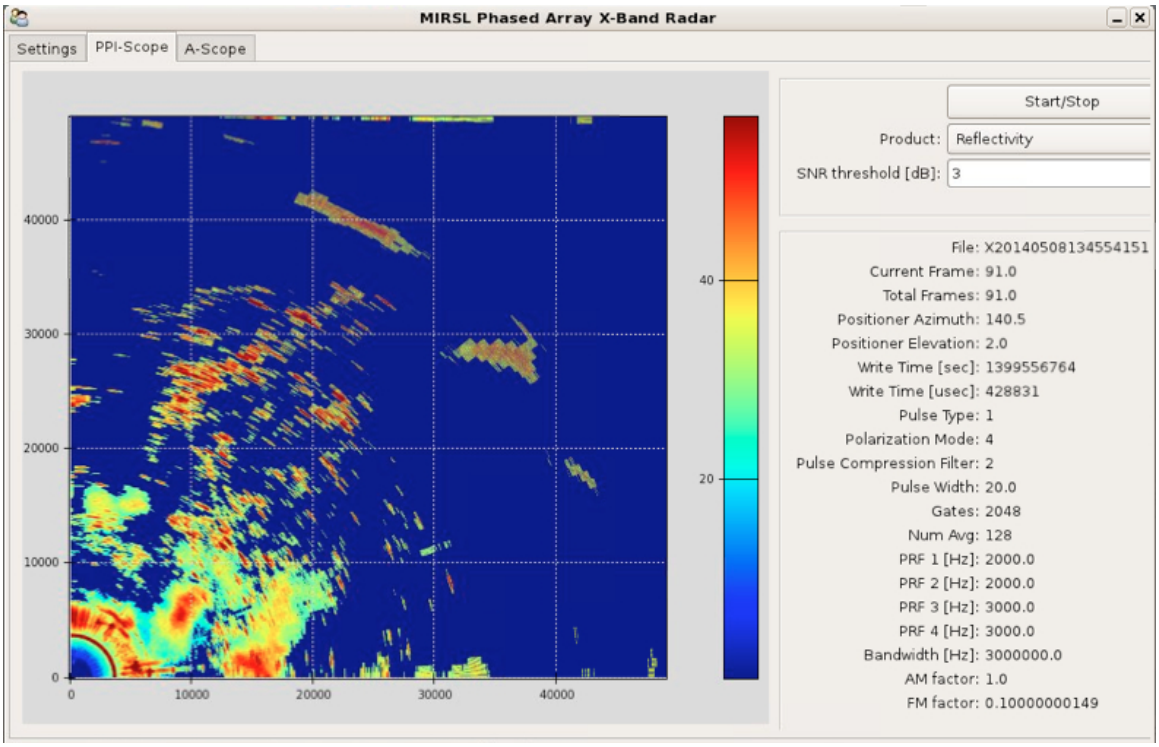

Figure 2.2: PPI live view in the PTWR GUI.

The GUI has three tabs: Settings, PPI, and A-scope. The PPI tab is a near-live view of reflectivity from the last scan received, as illustrated in Figure 2.2. There is also an option to change the SNR threshold for the field of view; the preset is 0dB.

The A-scope tab shows the power on the H and V channels, as seen in Figure 2.3. The tick rate option determines how quickly the next pulse is shown, in ms. The standard is 20ms. For more time between plot refreshes, this value should be set higher.

These plots are for real-time display only; they are not saved anywhere in a retrievable way. Data processing and plots are not performed in real-time with the current setup, but are made after raw data are collected.

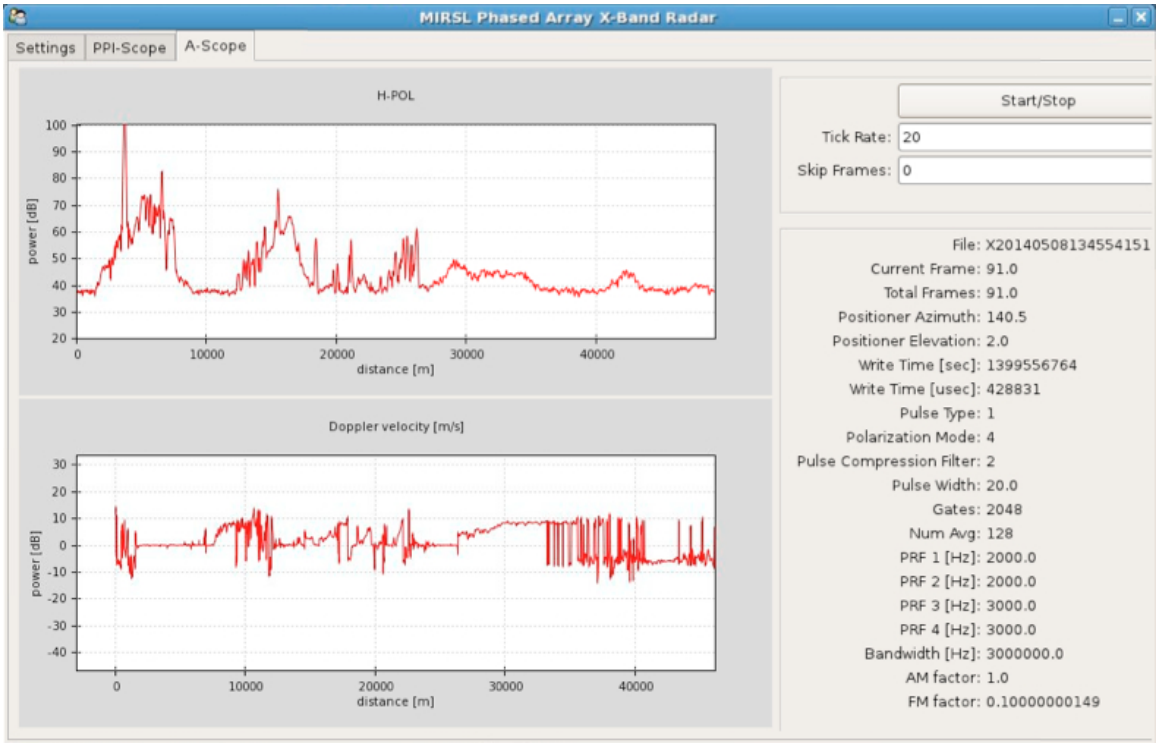

Figure 2.3: A-scope live view in the PTWR GUI.

CHAPTER 3

DATA PROCESSING

3.1 Data acquisition system

The custom GUI that controls the radar has a variety of waveform and pulsing options. The pulsing scheme typically used is such that pulses one (H) and two (V) have a PRF of 2000Hz, while pulses three (H) and four (V) have a PRF of 3000Hz. This allows for a maximum range of roughly 50km, depending on chirp duration. At the sampling frequency used there are 2048 gates per pulse, allowing for about 24m per range gate. Because of the use of 20μs waveforms, the first 157 gates or 3.75km are within the blind range, where the radar cannot see. The pulsing scheme is therefore H_{T_1}, V_{T_1}, H_{T_2}, V_{T_2}, where T_1 is $1/PRF_1$ or 500μs and T_2 is $1/PRF_2$ or 333μs. For each beam, 128 pulses are transmitted, meaning the $H_{T_1}V_{T_1}H_{T_2}V_{T_2}$ sequence is transmitted 32 times. This pulsing scheme is illustrated in Figure 3.1. The PTWR is a highly flexible system with a wide range of functionality, but for the purposes of this thesis, only this standard pulsing scheme will be considered.

Once a scanning procedure is defined by the user in the GUI (described in Chapter 2), an input parameter file is created and sent to the data acquisition process (DAQ). The DAQ sends a message to the pedestal to move to the appropriate elevation. Then the FPGA begins the process, generating a trigger for all subsystems, including the transceiver.

The DAQ begins collecting data, and pushes the received data from the four pulses from each azimuth angle into the buffer. The data processor then ingests the data. Raw IQ data are passed directly into a file; this is considered "Level 0" processing.

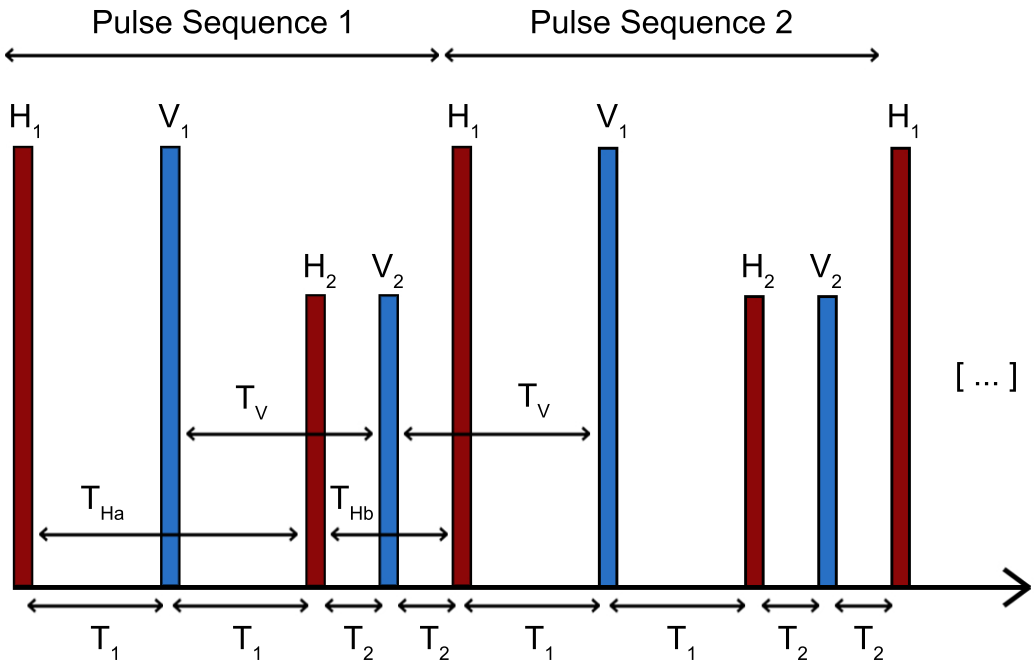

Figure 3.1: The standard pulsing scheme for Texas deployment. Standard PRTs are shown, as well as PRTs used for multilag calculations.

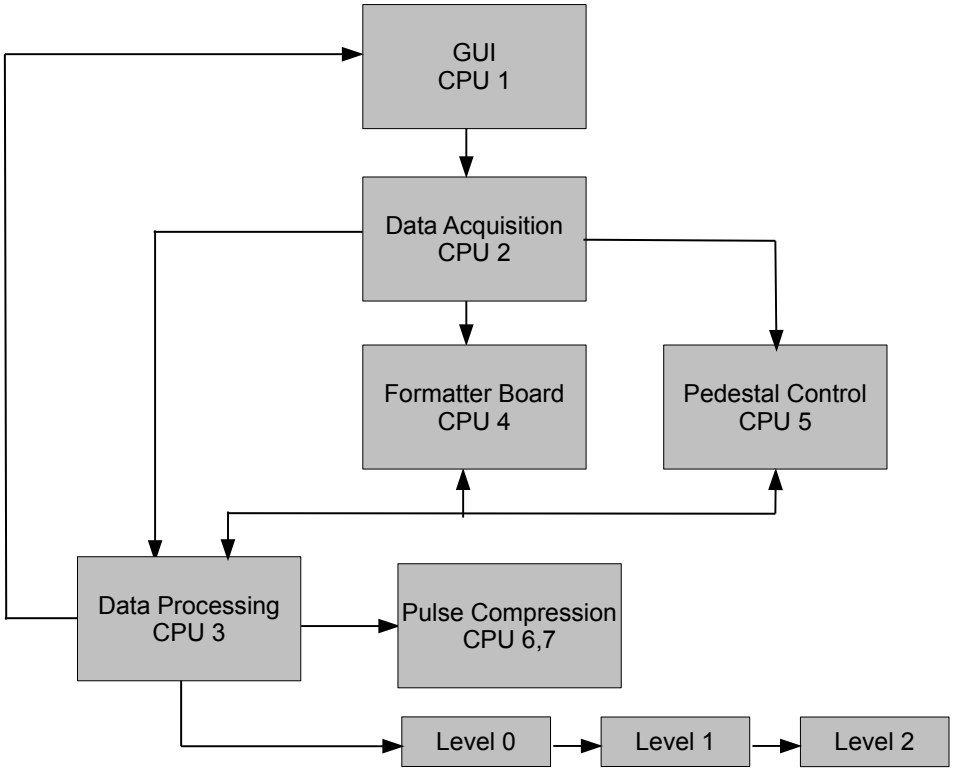

Figure 3.2: The data acquisition process that runs the PTWR, including the new Level 1 and 2 processing. Pulse compression does not happen in real time, so here it is shown in an ideal real-time data processing scheme.

The DAQ is multi-threaded, allowing these sub-processes to occur simultaneously on multiple dedicated CPUs. It relies on semaphores to ensure that the processes are synchronized and do not try to access the same memory location at the same time. The DAQ processes and their mapping to CPUs is shown in Figure 3.2.

3.2 Data processing

A number of new programs have been written in Python for processing PTWR data. These programs are designed to process the data as quickly as possible, taking a folder of raw IQ binary files and processing them into a useable format. New programs can be broken down into three files: one for determining what files are included in a folder, one for processing those files, and one for plotting them. They

are described in more detail in Appendix section A.3, including required Python libraries and operating system tests.

The raw IQ binary files are fed into a Python program called `ptwr` that processes them and outputs NetCDF files. One binary or NetCDF file contains one PPI. This is not yet implemented in real-time, but done separately after the data collection process so as not to interfere with the data acquisition. This is mainly because use of pulse compression requires two FFT calculations, and it is as yet unclear whether the computer would be able to handle so much computation reliably with the current multithreaded setup.

First, the raw IQ file is read in by the Python process. The structure of the binary files, including how many bytes are included in each section, is described in Figure 3.3. Each file contains a header followed by 91 beams of raw IQ data, in which each beam includes 128 pulses and a beam footer, for a total of 98403800 bytes. The header is two characters, three integers, and eight floating points, for a total of 40 bytes in length. The header includes pulse type, polarization sequence, number of range gates, pulses per beam, filter type, pulse width in microseconds, the PRFs for each pulse in Hz, the pulse bandwidth in Hz, and the FM and AM factors. These are listed in Table 3.1 along with the default values used for this deployment.

Due to a quirk of the system, the first data encountered in the binary file is from the previous scan. This occurs because the transceiver only pulls data from the buffer to the computer when it receives a trigger. Because of this, upon receiving the first trigger of a new scan, the data within the buffer contains the data of the last pulse from the previous scan and pushes that into the new scan file. This is stored as the first beam-length string within the raw binary file, in this case the first four sets of 4096 integers of the file. The scan header data comes after this. Because of this, each file contains an extra HVHV sequence (32768 bytes of data) that is not used, and is missing one HVHV sequence from the last beam.

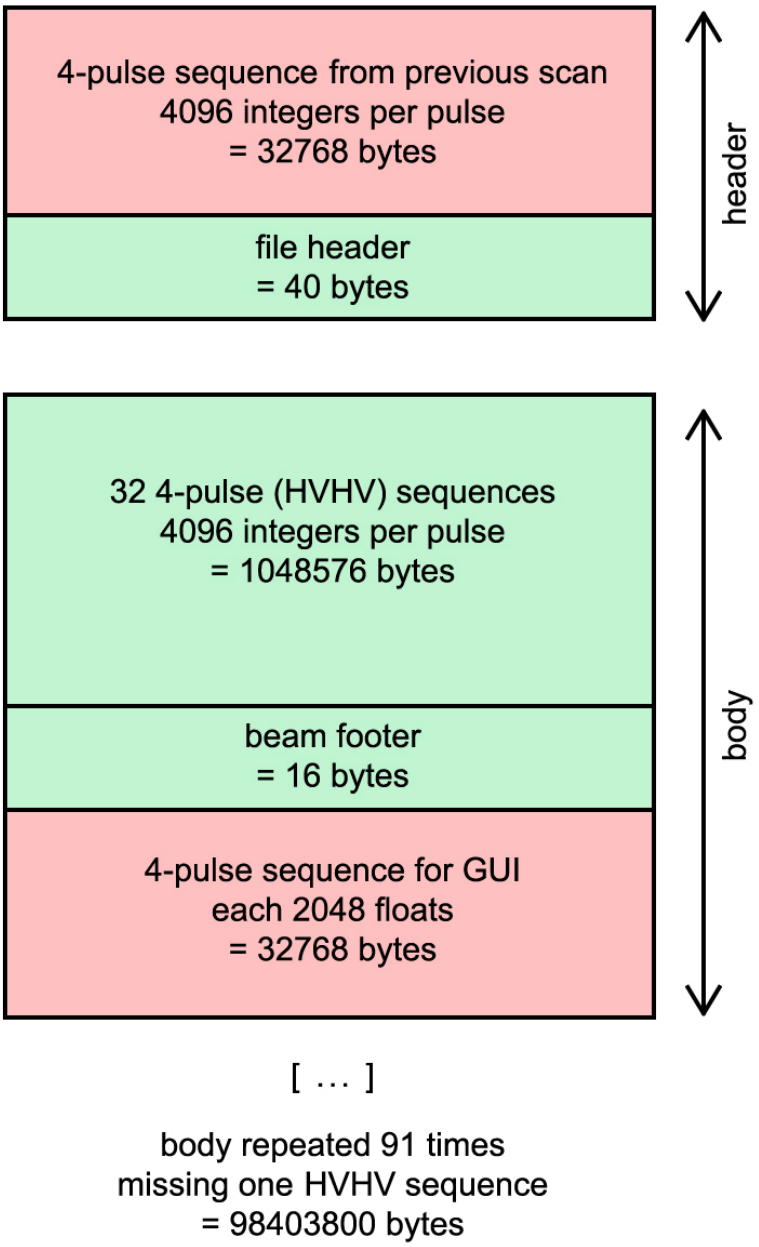

Figure 3.3: The structure of a binary file containing one PPI of data. These are saved as .dat files.

Table 3.1: Header values

Header	**Bytes**	**Description**	**Typical value**
char	1	pulse type	0 (pulse), 1 (chirp)
char	1	polarization sequence	4 (HVHV)
int	2	range gates	2048
int	2	pulses per beam	128
int	2	filter type	2 (Hann window)
float	4	pulsewidth [μs]	20
float	4	PRF for first pulse [Hz]	2000
float	4	PRF for second pulse [Hz]	2000
float	4	PRF for third pulse [Hz]	3000
float	4	PRF for fourth pulse [Hz]	3000
float	4	pulse bandwidth [Hz]	3000000
float	4	FM factor	1
float	4	AM factor	.1

After reading in 128 pulses with 4096 integers each, there is a beam footer. The beam footer records the elevation and azimuth readings from the pedestal as float values. It also stores time as an integer. After each beam footer, there is one last pulse of data. If the "processed" option is selected while using the GUI, the data processor also computes reflectivity, which it sends to the GUI in real-time for plotting either via a plan position indicator (PPI) for the full field of view or an A-scope for a pulse-by-pulse view. It is no longer of use in this case, and can be read out but ignored when processing the binary file.

Each pulse is read from the file as a profile of 4096 integers: even indices of the profile are the real part of the pulse while odd indices are the complex value. These are added together as I + jQ to make a total of 2048 complex values for one pulse.

This pulse is further processed to take into account the use of pulse compression. First, a copy of the transmitted pulse is multiplied by a Hanning window, and an FFT is taken. This is multiplied by a raw pulse on which an FFT has been taken. This product is then passed through an inverse FFT. This removes the effects of using a chirp rather than a pulse by taking advantage of the fact that performing a convolution in the time domain is equivalent to multiplication in frequency domain.

3.3 Computation of polarimetric variables

From these pulses, several different autocovariances at different lags can be computed [9]. This is considered "Level 1" processing from Fig 3.2, though it is not saved to file. In this case, the equations used are as follows:

$$R_{HH}(0) = \frac{1}{N}\sum_{i=1}^{N} H_1 \cdot H_1^* + \frac{1}{N}\sum_{i=1}^{N} H_2 \cdot H_2^* \tag{3.1a}$$

$$R_{VV}(0) = \frac{1}{N}\sum_{i=1}^{N} V_1 \cdot V_1^* + \frac{1}{N}\sum_{i=1}^{N} V_2 \cdot V_2^* \tag{3.1b}$$

$$R_{HH}(T_{Ha}) = \frac{2}{N}\sum_{i=1}^{N/2} H_2 \cdot H_1^* \tag{3.1c}$$

$$R_{HH}(T_{Hb}) = \frac{2}{N-2}\sum_{i=1}^{N/2-1} H_3 \cdot H_2^* \tag{3.1d}$$

$$R_{VV}(T_V) = \frac{2}{N}\sum_{i=1}^{N/2} V_2 \cdot V_1^* \tag{3.1e}$$

$$R_{VV}(T_V) = \frac{2}{N-2}\sum_{i=1}^{N/2-1} V_3 \cdot V_2^* \tag{3.1f}$$

$$R_{HV}(T_1) = \frac{2}{N}\sum_{i=1}^{N/2} H_2 \cdot V_1^* \tag{3.1g}$$

$$R_{VH}(T_1) = \frac{2}{N}\sum_{i=1}^{N/2} V_1 \cdot H_1^* \tag{3.1h}$$

$$R_{HV}(T_2) = \frac{2}{N-2}\sum_{i=1}^{N/2-1} H_3 \cdot V_2^* \tag{3.1i}$$

$$R_{VH}(T_2) = \frac{2}{N}\sum_{i=1}^{N/2} V_2 \cdot H_2^* \tag{3.1j}$$

where N is the number of pulses in a certain polarization, so N = 64 in the standard case. H_1 is the first H pulse in an HVHV sequence and H_2 is the second H pulse (and third pulse in total) in the sequence. H_3 refers to the first H pulse of the next sequence.

From these covariances, polarimetric products can be computed. Differential phase is computed as [9]:

$$\phi_{DP}(T_1) = \frac{1}{2}\arg(R_{VH}(T_1)) - \frac{1}{2}\arg(R_{HV}(T_1)) \tag{3.2a}$$

$$\phi_{DP}(T_2) = \frac{1}{2}\arg(R_{VH}(T_2)) - \frac{1}{2}\arg(R_{HV}(T_2)) \tag{3.2b}$$

The total differential phase can then be calculated as an average between the differential phase at the two times.

These differential phases can be folded, since R_{HV} and R_{VH} include a velocity component that can fold. Differential phase values are unfolded by multiplying by e^{j90° and subtracting π from values above 90°. It has been observed that in this radar, with its specific range, frequency, and transmit power, that the maximum range of ϕ_{DP} is 180°, with values above 120° being heavily attenuated. Therefore unfolding in this way maintains the appropriate ϕ_{DP} range.

These values are still typically quite noisy. This is due to a combination of low SNR and a small number of independent samples due to the relatively fast pulsing scheme. To smooth the values, a median filter is applied over a 2km window. A plot of ϕ_{DP} before and after smoothing and initial ϕ_{DP} correction is shown in Figure 3.4. The median filter used unfortunately pads the edges of the data with zeros, which is a problem since these values fall within a range of ±90° and the initial values are non-zero. A kilometer of data is repeated at the beginning and end of the data for the sake of better smoothed values.

The initial values of ϕ_{DP} must be close to zero for facilitating attenuation correction, so initial ϕ_{DP} must be calculated and subtracted. To do this, ϕ_{DP} is thresholded on SNR and reflectivity; values that do not meet the requirements are replaced with NAN. The first finite gate is considered the initial ϕ_{DP}, and this value is subtracted from the smoothed ϕ_{DP} values.

Doppler velocities are calculated in many ways and can be found in the `ptwr` code. However, those that are saved and plotted use the staggered PRT technique [10, eq. 7.6a]:

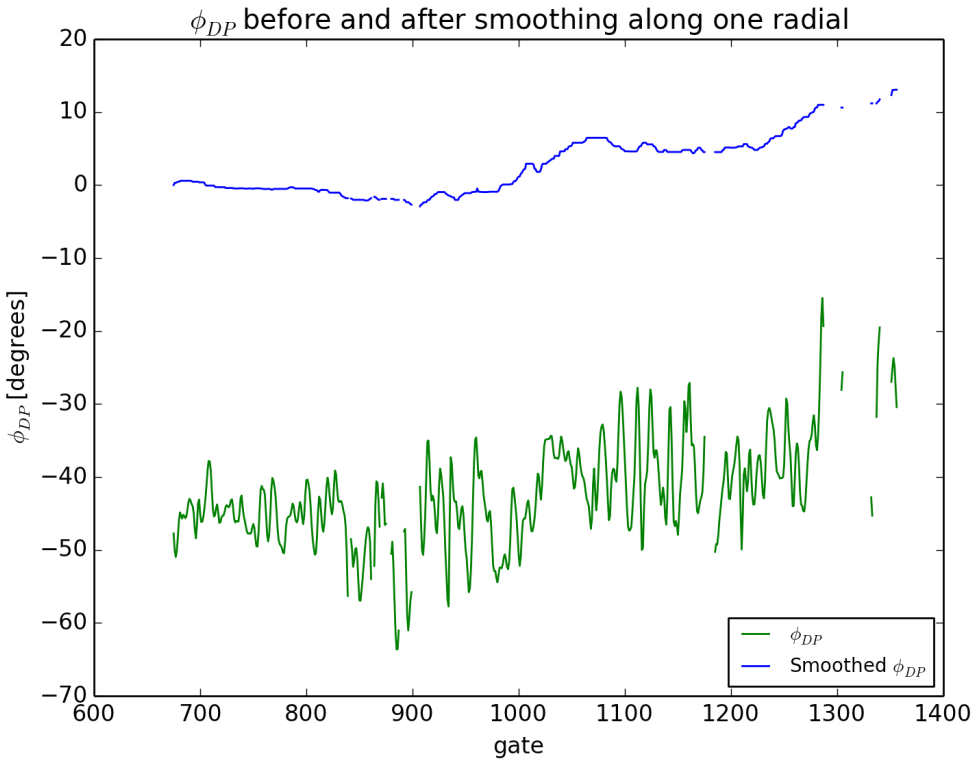

Figure 3.4: A plot of ϕ_{DP} before (green) and after (blue) smoothing and correcting for initial ϕ_{DP}, for one beam.

$$v_{crosspol} = \frac{\lambda}{4\pi \cdot (T_1 - T_2)} \cdot \angle \left(\frac{R_{VH}(T_1)e^{-j\phi_{DP}} + R_{HV}(T_1)e^{j\phi_{DP}}}{R_{VH}(T_2)e^{-j\phi_{DP}} + R_{HV}(T_2)e^{j\phi_{DP}}} \right) \tag{3.3a}$$

$$v_{copol} = \frac{\lambda}{4\pi \cdot (T_{Ha} - T_{Hb})} \cdot \angle \left(\frac{R_{HH}(T_{Hb})}{R_{HH}(T_{Ha})} \right) \tag{3.3b}$$

where T_{Ha} and T_{Hb} are showed in Figure 3.1 and defined as:

$$T_{Ha} = \frac{2}{f_1} \tag{3.4a}$$

$$T_{Hb} = \frac{2}{f_2} \tag{3.4b}$$

The correlation coefficient is found by first calculating [11, eq. 6.80c]:

$$\rho_{HV}(T_1) = \left| \frac{R_{HV}(T_1)}{\sqrt{|R_{HH}(0)|\,|R_{VV}(0)|}} \right| \tag{3.5a}$$

$$\rho_{HV}(T_2) = \left| \frac{R_{HV}(T_2)}{\sqrt{|R_{HH}(0)|\,|R_{VV}(0)|}} \right| \tag{3.5b}$$

Then, using a correction factor, $\rho_{HV}(0)$ can be calculated as [11, eq. 6.90]:

$$\rho_{HV}(0) = \rho_{HV}(T_1) \cdot \sqrt[4]{\frac{|R_{HH}(T_{H_a})|}{|R_{HH}(0)|}} \tag{3.6a}$$

$$\rho_{HV}(0) = \rho_{HV}(T_2) \cdot \sqrt[4]{\frac{|R_{HH}(T_{H_b})|}{|R_{HH}(0)|}} \tag{3.6b}$$

Next, the beam-by-beam noise power is calculated as the average of the power values in a beam corresponding to where ρ_{HV} is less than 0.3. From this:

$$SNR_H = \left| \frac{R_{HH}(0)}{PN_H} - 1 \right| \tag{3.7a}$$

$$SNR_V = \left| \frac{R_{VV}(0)}{PN_V} - 1 \right| \tag{3.7b}$$

where PN_H and PN_V are the beam-by-beam noise power arrays.

With SNR, reflectivity can now be calculated:

$$Z_H = C_H + 10\log_{10}(SNR_H \cdot PN) + 20\log_{10}(range) + 30 \tag{3.8a}$$

$$Z_V = C_V + 10\log_{10}(SNR_V \cdot PN) + 20\log_{10}(range) + 30 \tag{3.8b}$$

where C is the radar constant, for which there is one constant for each beam in both H and V polarizations, and PN is an estimate of the noise floor, as calculated by:

$$PN = kTf \cdot BW \tag{3.9}$$

where k is the Boltzmann constant in J/K, T is room temperature (300K), and f is the 5 dB noise figure of the system. Differential reflectivity is calculated by simply subtracting V-pol reflectivity from H-pol reflectivity, since this calculation puts reflectivity in dBZ.

An attenuation correction is applied to Z_H and Z_{DR}, using the appropriate correction for X-band [12]:

$$Z_{H,corrected} = Z_H + .28\phi_{DP} \tag{3.10a}$$

$$Z_{DR,corrected} = Z_{DR} + .04\phi_{DP} \tag{3.10b}$$

where ϕ_{DP} must be in degrees and Z_H and Z_{DR} are in dB.

Normalized coherent power is calculated as [11, eq. 6.87 and 6.88]:

$$NCP_H = \sqrt[4]{\left|\frac{R_{HH}(T_{H_b})}{R_{HH}(0)}\right|} \tag{3.11a}$$

$$NCP_V = \sqrt[4]{\left|\frac{R_{VV}(T_V)}{R_{VV}(0)}\right|} \tag{3.11b}$$

Finally, spectrum width is calculated as [10, eq. 7.7]:

$$\sigma = \frac{\lambda}{2\pi\sqrt{2\left(T_{Ha}^2 - T_{Hb}^2\right)}}\sqrt{\ln\left(\left|\frac{R_{HH}(T_{H_a})}{R_{HH}(T_{H_b})}\right|\right)} \tag{3.12}$$

3.4 Conversion to NetCDF

Once all of the polarimetric variables are calculated, they are saved into a Network Common Data Format (NetCDF) standard file. This is considered "Level 3" processing from Fig 3.2. This data type is the standard developed by UCAR and used by atmospheric scientists, including those at CASA. NetCDF files are self-describing, in that data as well as the names of the variables are saved. In this way, no extra explanation of the data is required, as is the case in binary files, which need to be read in bit by bit.

The same variable standard as CASA is used, making it easier to read NetCDF files from both (as explained in Appendix A.3. This is different from the Cf/Radial standard proposed by NCAR, to be explained in Chapter 5.

The single-value data are saved to the NetCDF as global attributes and are listed in Table 3.2. Those data that are in array form are saved as variables and are listed in Table 3.3. NetCDF variables are defined by specific dimensions; in this case, the dimensions are Radial (91 values) and Gate (2048 values).

Table 3.2: Global attributes saved to NetCDF files.

Name	**Description**
RadarName	PTWR Nedderman Hall UTA
Latitude	32.732373
Longitude	-97.113899
Freq	9.36 [GHz]
PulseType	Pulse or Chirp
PolSequence	HVHV
Pulses	hdrint[1]
Filter	Hanning
PulseWidth	hdrfloat[0]
PRF_H1	hdrfloat[1]
PRF_V1	hdrfloat[2]
PRF_H2	hdrfloat[3]
PRF_V2	hdrfloat[4]
Bandwidth	hdrfloat[5]
FMFactor	hdrfloat[6]
AMFactor	hdrfloat[7]
Elevation	Elevation reading from pedestal
BroadsideAzim	Azimuth reading from pedestal +180°
ZeroRange	Gate at which real data (not noise) starts; set to gate 30
UnixTime	Time in seconds since 1 January 1970 UTC
DataDate	Date in human-readable format, EDT
NetCDFCreated	Date of NetCDF creation
CreatedFrom	.dat file containing the original data

Table 3.3: Variables saved to NetCDF files. All data types are 'f8' or 64-bit floating point. When polarization is unspecified, H is assumed.

Name	**Dimensions**
Azimuth	Radial
DifferentialPhase	Radial, Gate
CrossPolCorrelation	Radial, Gate
NormalizedCoherentPower	Radial, Gate
NormalizedCoherentPowerV	Radial, Gate
SignalToNoiseRatio	Radial, Gate
SignalToNoiseRatioV	Radial, Gate
Reflectivity	Radial, Gate
ReflectivityV	Radial, Gate
VelocityCrosspol	Radial, Gate
VelocityCopol	Radial, Gate
SpectralWidth	Radial, Gate
DifferentialReflectivity	Radial, Gate
CorrectedReflectivity	Radial, Gate
CorrectedDifferentialReflectivity	Radial, Gate
InitialDifferentialPhase	Radial
NoiseFloor	Radial
NoiseFloorV	Radial

3.5 NetCDF plotter

Having processed data saved in NetCDF format allows for easy viewing, manipulation, and plotting. A series of plotting tools exist in Python. These include `matplotlib` [13], a plotting library created to imitate Matlab's plotting environment, and `wradlib` [14], which is primarily used to make arrays of radar data and easily plots PPIs without needing Cartesian to polar conversions. `wradlib` heavily relies on `matplotlib`'s `axisartist` namespace, and so it is highly customizable when making the plots, not requiring any edits to the source code.

The plotter developed can currently accept PTWR and CASA data. Since CASA utilizes adaptive scans, it sometimes scans a full 360° view and other times only scans a sector. It also scans clockwise and counter-clockwise. `wradlib` only accepts clockwise-scanned data, so the plotter first checks that the data scans clockwise, and if it finds counter-clockwise scanning, inverts the data and forces the azimuths to run clockwise. Since CASA infrequently scans the same sectors, the data is often better viewed as 360° PPIs, so plotting a full circle is an option when calling the function.

After this, the data is thresholded on reflectivity and SNR. This thresholding is used to create a mask that is applied to all polarimetric variables. Currently, wherever SNR is greater than 0dB and attenuation-corrected H-polarization reflectivity is less than 10dBZ is masked.

Once the data are manipulated into being clockwise and optionally padded for a full 360° view, they can be plotted. The program plots six polarimetric variables: attenuation corrected H-polarization reflectivity, attenuation corrected differential reflectivity, differential phase, correlation coefficient, Doppler velocity, and spectrum width. A range axis is applied, as well as custom color bars. These color bars are the same as those used by the Advanced Radar Research Center at the University of Oklahoma, and are similar to those used by the NWS. The color bars include units

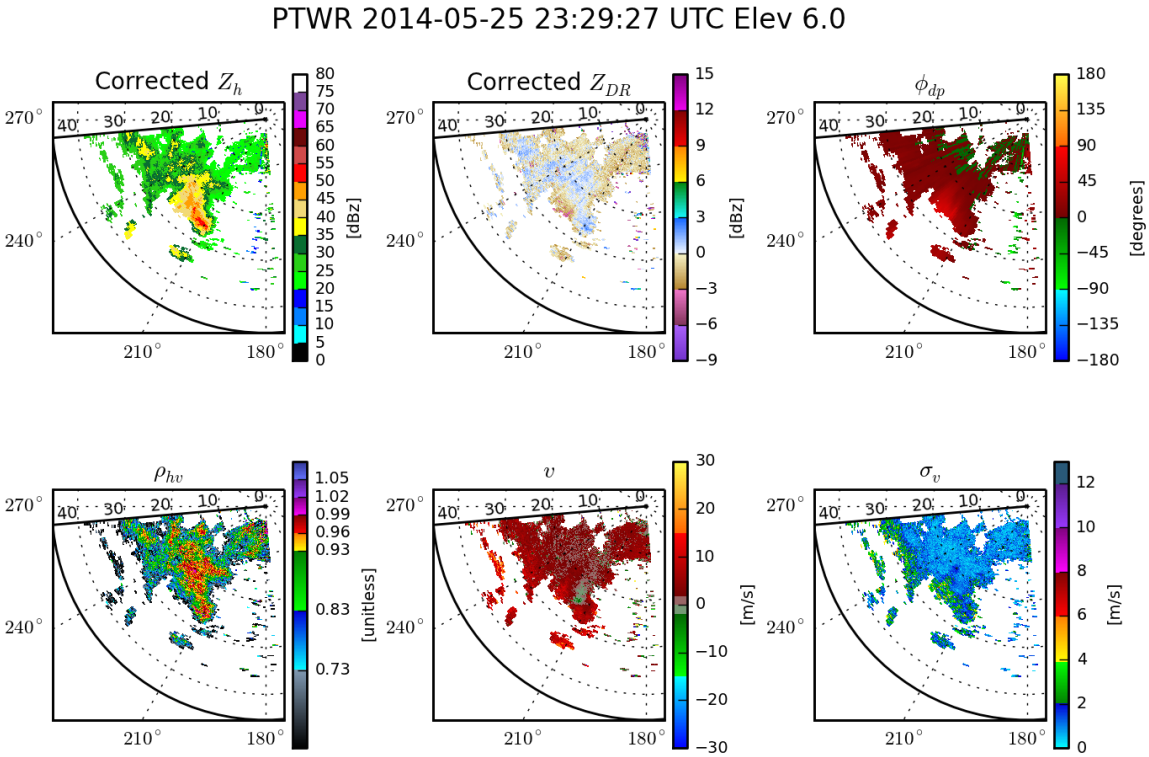

Figure 3.5: An example of a six-panel plot made en masse by the plotting program.

and ranges. A separate plot of corrected reflectivity is also saved, on a bigger scale for better viewing. An example of a PTWR plot is shown in Figure 3.5.

CHAPTER 4

OUTCOMES OF TEXAS DEPLOYMENT

4.1 Observations

All efforts were made to take data with the PTWR whenever there was a storm passing through the radius of the radar. The NWS radar, KFWS, was used to determine if there was rain in the area. Since XUTA was co-located with the PTWR and the two radars have a similar range, the CASA web application was used for determining whether rain was visible with the PTWR. A list of observations taken during deployment at UTA are listed in Table 4.1. For all observations, data from CASA XUTA and NEXRAD KFWS is also available.

Though not considered in this thesis, other modes of operation were used apart from the standard. These are shown for thoroughness in Table 4.1. Here, short pulse means a 1μs pulse, while medium pulse means a 10μs pulse width. Small BW refers to a bandwidth of 1, 1.5, or 2MHz. Straight PRF refers to a PRF of 2000Hz for all pulses in the pulse sequence, as well as 800 pulses per beam. ESP refers to a straight PRF of 3000Hz and a bandwidth of 3MHz. Calibration indicates a changed PRF, bandwidth, and pulse width, varying by the type of calibration.

4.2 Qualitative comparison with DFW area radars

For a qualitative comparison, corrected reflectivity from the area NEXRAD radar (KFWS) and the TDWR radar (TDFW) were collected. These were taken at 01:11:21 UTC and 01:10:59 UTC, respectively, on 4 April 2014. These can be compared against PTWR data taken at 01:11:32 and XUTA data from 01:12:53, during the

Table 4.1: List of observations taken by PTWR during deployment at UTA. All dates and times are listed in UTC and therefore may not match up with local time, i.e. "afternoon storm" may appear to be at night. During deployment, UTA was six hours behind UTC.

Date	**Observation**	**Begin**	**End**	**Files**	**Direction**	**Type**
3 April	afternoon storm	22:34	23:25	277	SW	standard, short pulse
4 April	evening storm	00:22	01:44	509	SW, NW	standard
7 April	evening rain	00:34	01:47	291	NW	standard
13 April	light rain	15:44	17:39	24	SW	standard, straight PRF
27 April	heavy rain	13:30	13:45	54	SW	straight, ESP
8 May	morning storm	13:16	14:23	435	NW, SW	standard
8 May	afternoon storm	19:33	21:43	428	NW, SW	standard, straight PRF, medium pulse
12 May	afternoon storm	19:11	22:44	380	NW, SW	standard, short pulse, small BW, calibration
14 May	stratiform rain	04:08	05:09	187	NW	standard, small BW
24 May	stratiform rain	21:29	03:12	190	SW	standard
25 May	evening storm	20:31	02:09	682	SW	standard, straight PRF
9 June	stratiform rain	12:05	13:43	177	NW, SW	standard
9 June	afternoon storm	19:06	20:05	282	NW	standard

Table 4.2: Characteristics of radar systems in the area during deployment at UTA.

Parameter	**PTWR**	**XUTA**	**KFWS**	**TDFW**
Peak power	60W	10.8kW	500kW	250kW
Frequency	9.36GHz	9.41GHz	3GHz	5.6GHz
Band	X-band	X-band	S-band	C-band
Beamwidth (az/el)	1.8°-2.6° / 3.6°	1.8°	1.25°	0.5°
Range resolution	60m	60m	1km	150m
Range coverage	45km	40km	460km	460km
PRF	2000-3000Hz	1600-2400Hz	320-1300Hz	800-1120Hz
Azimuthal resolution	1°	0.5°	1°	0.55°
Sector	90°	360°/adaptive	360°	360°
Pulse width	20μs	0.6μs	1.57-4μs	1.1μs
Pulse compression	yes	no	no	no

first observation of the deployment. A description of these radars can be found in Table 4.2.

These radars are not co-located and utilize different antennas at different wavelengths, as well as not looking at the same elevation angles (KFWS and TDFW regularly scan much lower than the PTWR and XUTA). However, given that this is the case, reflectivities match up quite well. All radars show high reflectivities in the same area, and the shapes swept out are roughly the same, as seen in Figure 4.1.

4.3 Quantitative comparison with CASA

While data from XUTA tends to look visually similar to PTWR data, it is not exact. One reason is that the area illuminated is not the same: XUTA scans to 5.3° and 7.4° in elevation, while PTWR scans to 6° in elevation. Also, while the

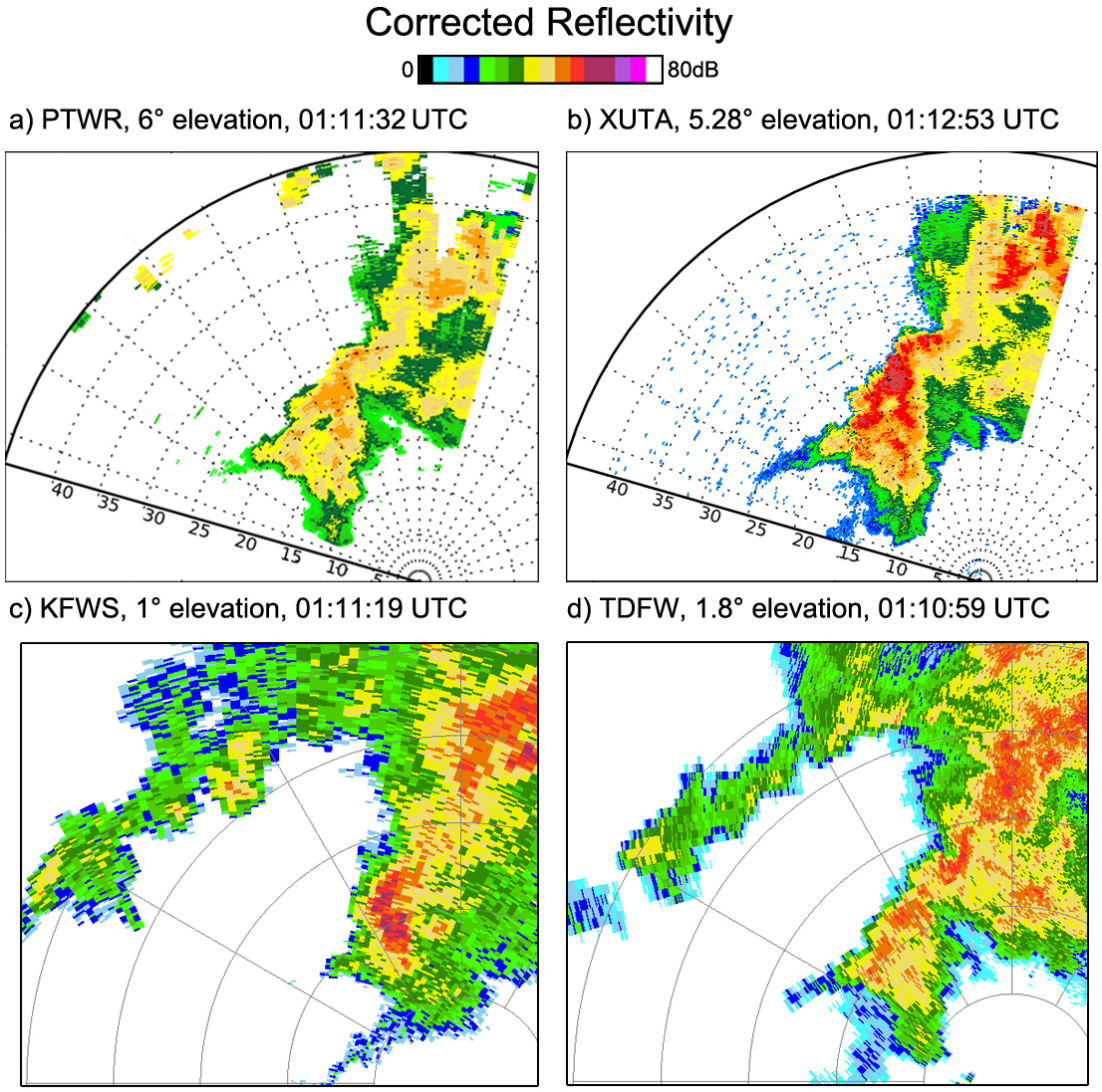

Figure 4.1: Comparison of the PTWR with three other DFW area radars. Range rings occur every 10 km and are centered on the PTWR's location.

beamwidths on the radars are similar in azimuth, XUTA beams occur at half-degree steps, while PTWR beams occur every degree.

To imitate a similar illuminated volume, XUTA data was first averaged in azimuth over 2°: beams were averaged with the next beam over, so a beam occurs every degree. Then these averages PPIs from 5.3° and 7.4° were averaged together, to get an approximate elevation angle just over 6°. From this averaged 6° XUTA scan, a better comparison with the PTWR can be made. This has done previously for an observation made on 3 April 2014 [15]; here observations made at the end of the deployment, on 25 May, will be compared to demonstrate the stability of the radar. Averaged PPIs of this observation are shown in Figure 4.2.

To make a histogram of the compared data, XUTA data was interpolated to have the same number of gates as the PTWR. Then, both PPIs were thresholded on PTWR SNR. A histogram of data can be made from these data points relating XUTA versus PTWR values (Figure 4.3).

The data chosen for this comparison visually looks similar once CASA is stretched to illuminate the same volume. However, it highlights some of the limitations of the PTWR; for example, no reflectivity values below roughly 20 dBZ can be seen past twenty kilometers. These differences make the best-fit slope on the histogram less than unity. This is due in part to the lower sensitivity of the PTWR compared to CASA.

4.4 Radar stability

To characterize the stability of the radar over the course of a two-month deployment, statistics for noise floor and initial ϕ_{DP} were computed. These were calculated on a beam-by-beam basis for each day of observations during the deployment.

The initial ϕ_{DP} (Figure 4.4) stayed relatively stable throughout the deployment, differing by about 15° over the course of two months One day of observations, DEP5,

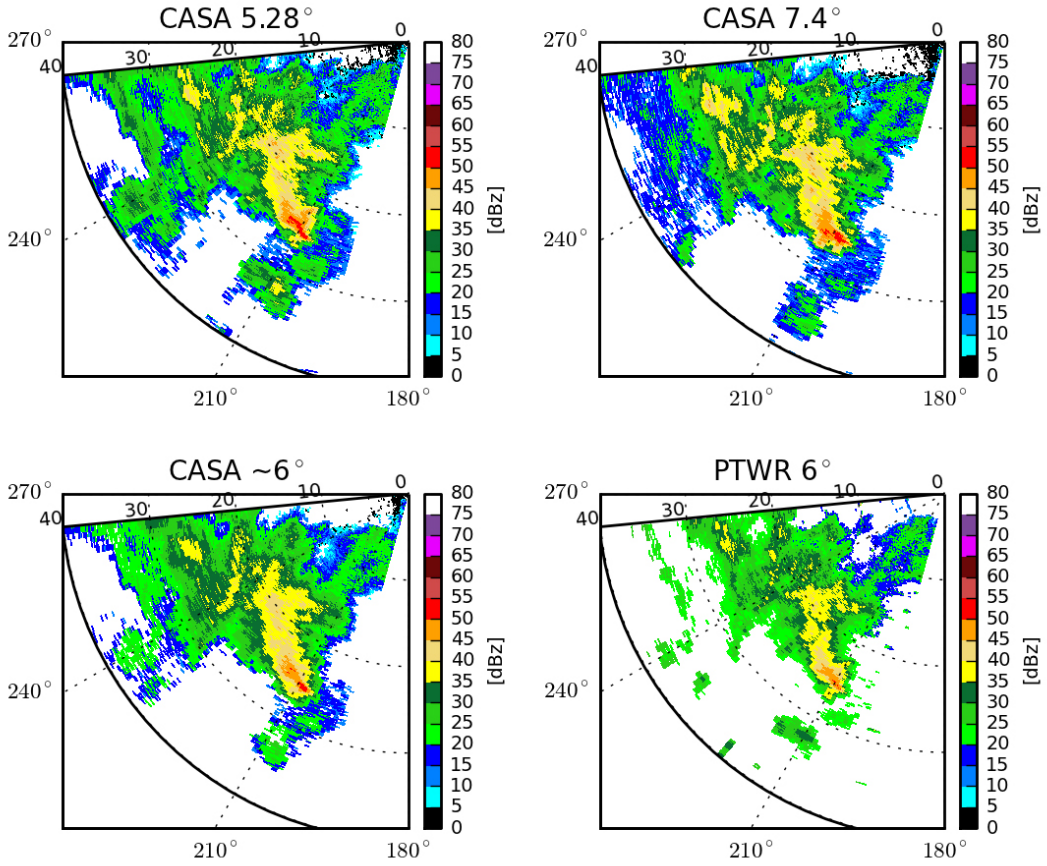

Figure 4.2: PPIs of uncorrected reflectivity for a) XUTA at 23:31 UTC at an elevation angle of 5.28° averaged over 2° in azimuth, b) XUTA at 23:28 EST at an elevation angle of 7.4° averaged over 2° in azimuth, c) XUTA as an average of elevation angles 5.28 and 7.4°, and d) PTWR at 23:31 UTC at an elevation angle of 6°. All data was taken on 25 May 2014.

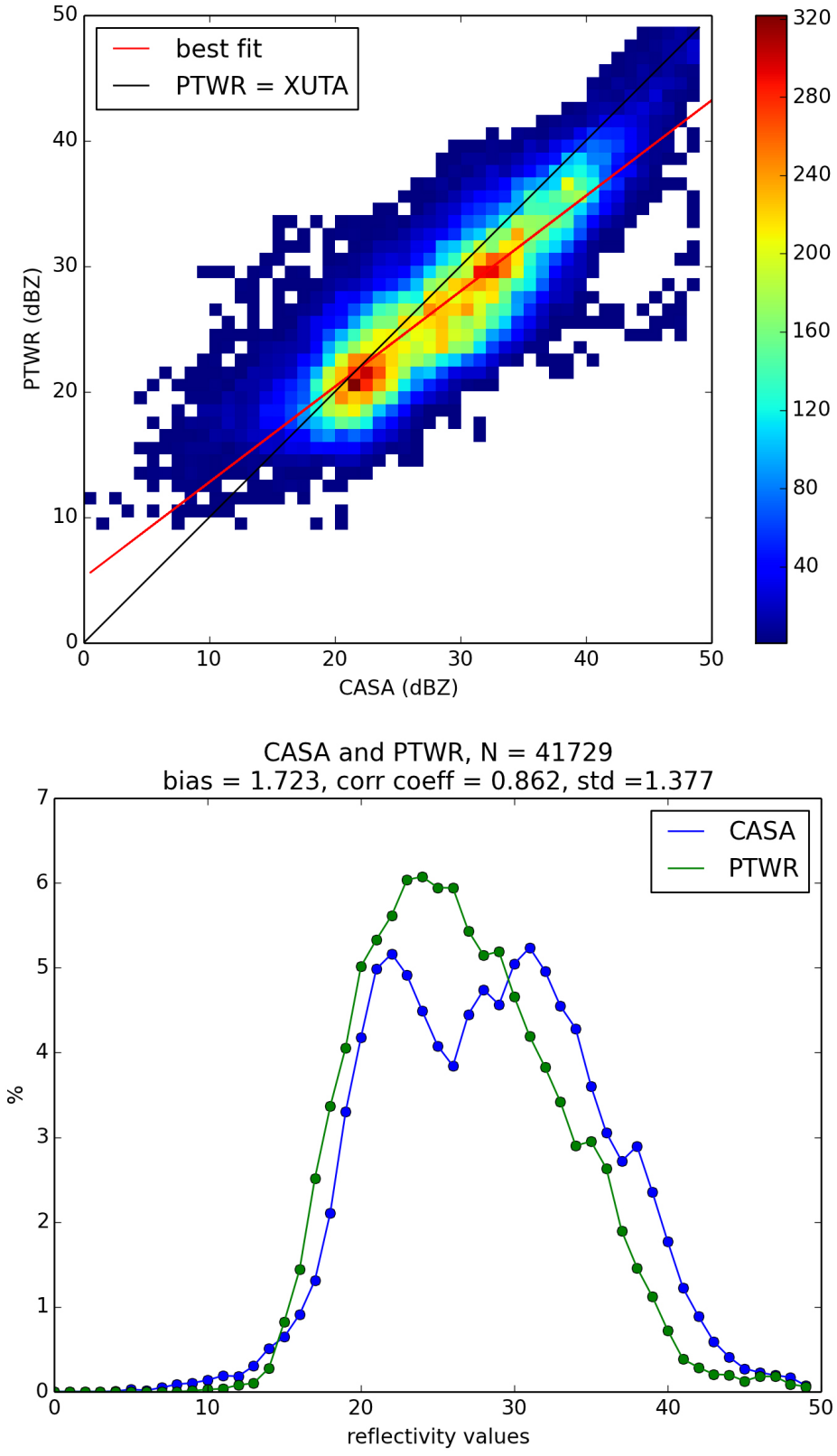

Figure 4.3: Histogram comparing CASA and PTWR data from similar scans, averaged for better comparison of illuminated volume.

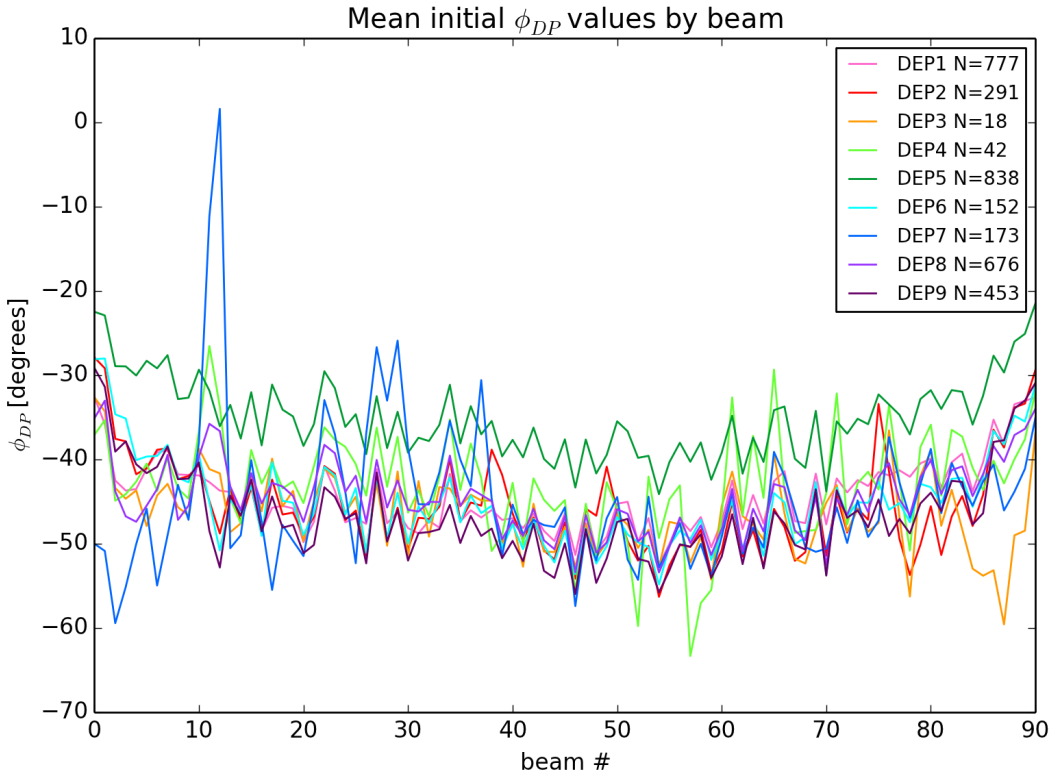

Figure 4.4: Mean initial ϕ_{DP} plotted by beam for each deployment. Number of PPIs included in each day of observations (DEP) is listed in the legend.

is an obvious outlier by about 10°. However, for this day, there was rain within the radar blind range (determined by looking at CASA and NEXRAD data from that day) and so this may indicate a method of judging how much rain is falling between the radar and the end of the blind range.

The noise floor is shown in Figure 4.6. Noise floor is also effected by rain on the radome; DEP5 can again be seen with higher values than the average. Rain changes the antenna temperature, which raises the noise floor by more than a dB in this case. Other differences in noise floor can be attributed to ambient temperature (.15 dB / °C, as found in the laboratory during initial PTWR calibrations).

Using these statistics, uncertainty to be expected in these measurements can be calculated. They are plotted in Figures 4.5 and 4.7. The median RMS uncertainty

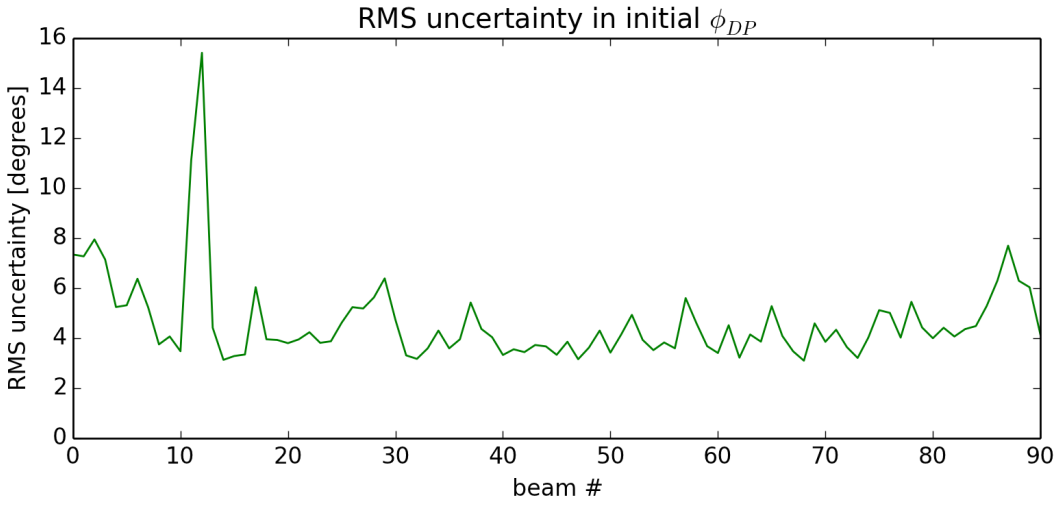

Figure 4.5: RMS uncertainty in ϕ_{DP} plotted by beam, taken over eight days of observations. DEP5 is not included in this calculation, as it is considered an outlier.

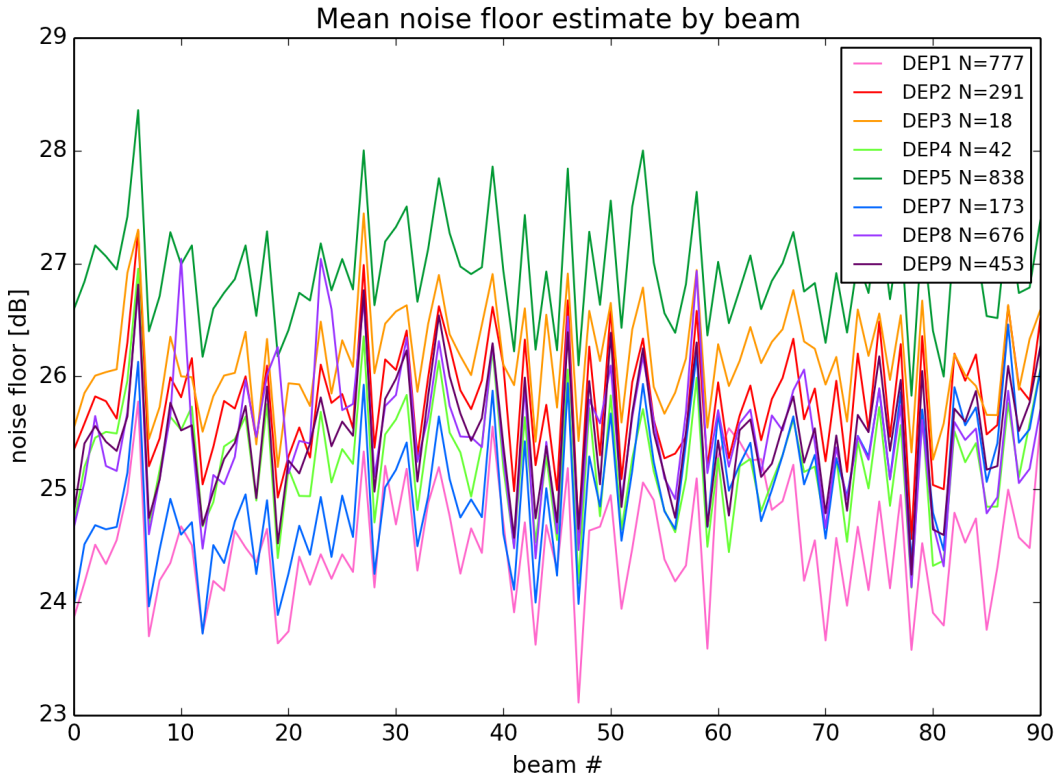

Figure 4.6: Mean noise floor values plotted by beam for each deployment. Number of PPIs included in each day of observations (DEP) is listed in the legend. DEP 6 is an outlier here and was not included.

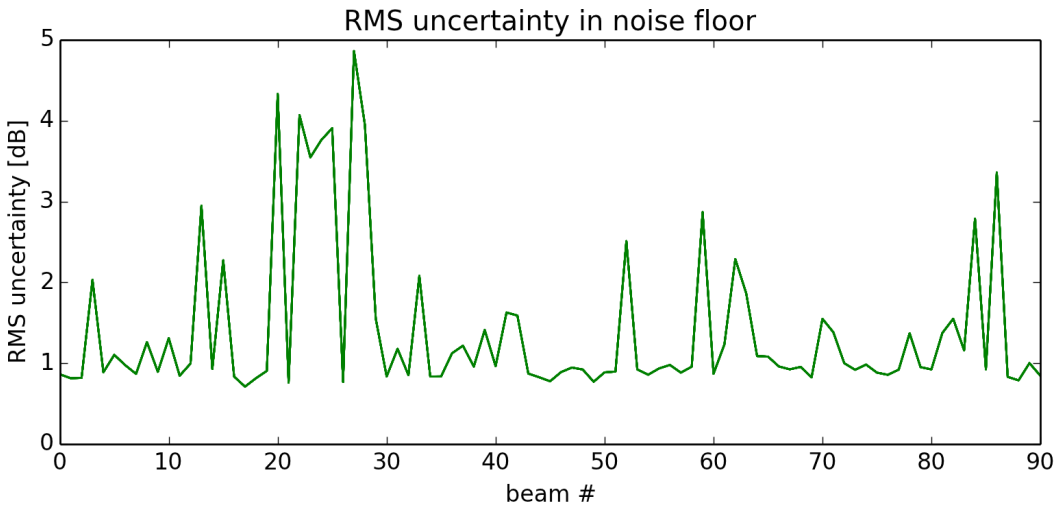

Figure 4.7: RMS uncertainty in noise floor plotted by beam, taken over seven deployments. DEP5 and DEP6 are not included in this calculation.

in initial ϕ_{DP} is 4.08°, while the median RMS uncertainty in noise floor is .957 dB. Looking at these plots, it is suggested that this uncertainty is caused by clutter. In the southwest observations, a large clutter field is visible in ϕ_{DP}. This is caused by tall signs and a water tower on Cooper Street, which stretches south and southwest from UTA. This can cause high initial ϕ_{DP} measurements in beams 10 through 25.

It is interesting to note that the noise floor appears to have a periodic trend shared by each day of observations. It is thought that this periodicity is due to losses in the TR modules, caused by different attenuator and phase shifter settings for each beam as well as a large loss in the power combiner. There is not enough gain in the TR modules before this loss, and because of the design of the power combiner, the signal combines coherently while the noise does not.

To investigate this, the mean of each day of observations was subtracted, bringing each line down to the same mean, as plotted in Figure 4.8. The variance, calculated by dividing each data point in a beam by the mean of the beam, is shown in Figure 4.9.

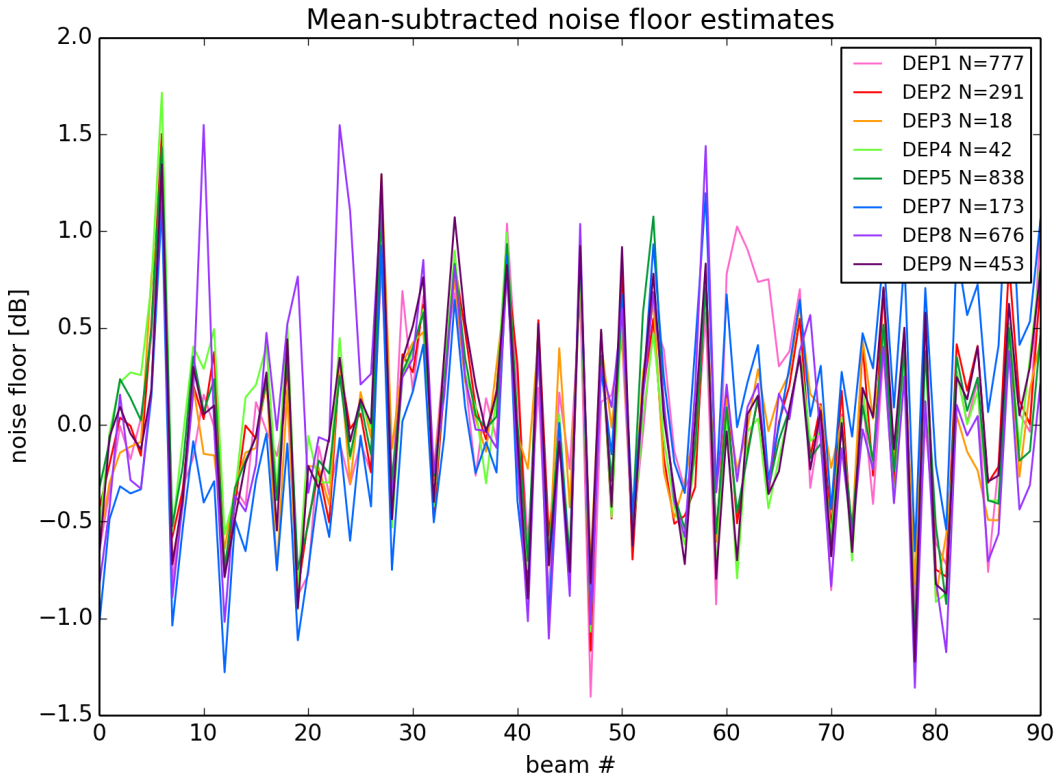

Figure 4.8: Mean noise floor values plotted by beam for each deployment. These lines are the same as Figure 4.6; however, each line has had its mean subtracted to be centered around 0.

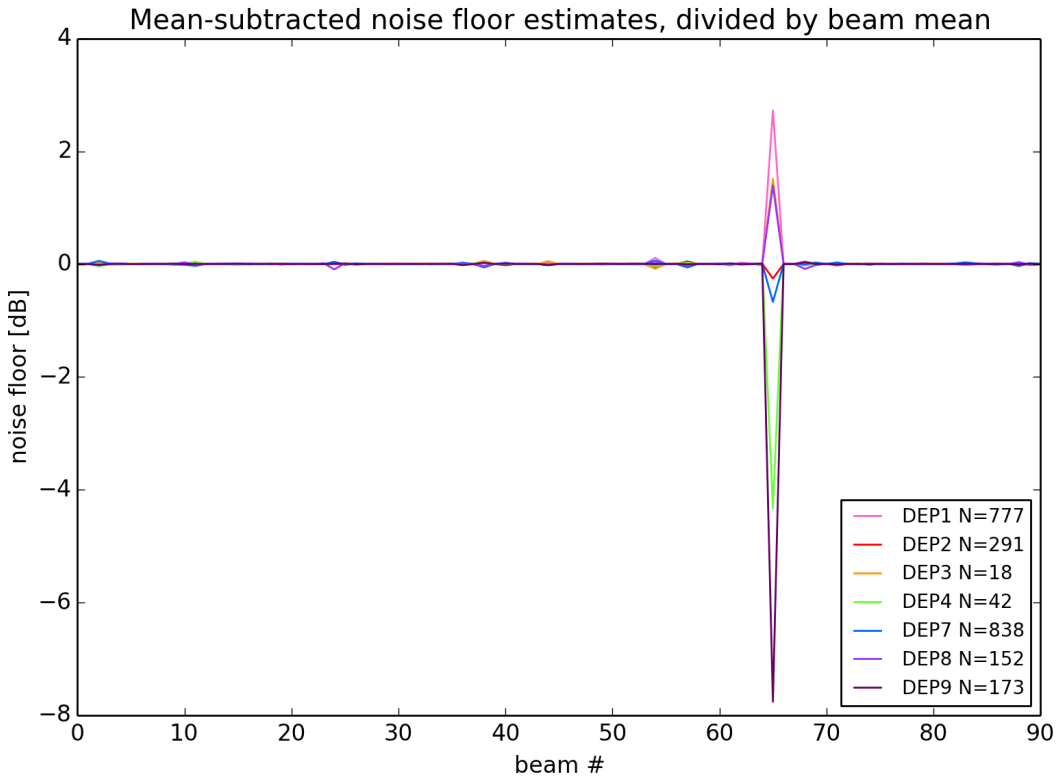

Figure 4.9: Mean-subtracted noise floor from Figure 4.8, divided by the mean of the beam to show the variance by beam.

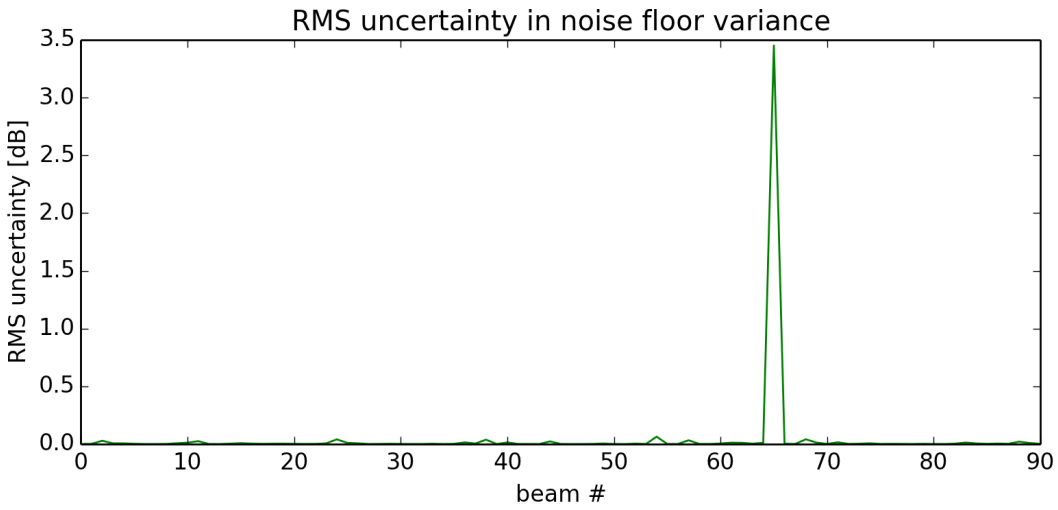

Figure 4.10: Uncertainty in variance from Figure 4.9. This is dominated by beam 65.

The RMS uncertainty in this variance can be calculated as well, as shown in Figure 4.10. The uncertainty on beam 65 is quite high, so a histogram serves better to show the RMS uncertainties (Figure 4.11). This histogram shows that when this periodicity is removed, more than 70 beams have an RMS uncertainty of 0.01 dB. This RMS uncertainty is much closer to the statistically expected variance, which is calculated to be closer 0.003 dB for the number of samples included on the day with the most observations (DEP5).

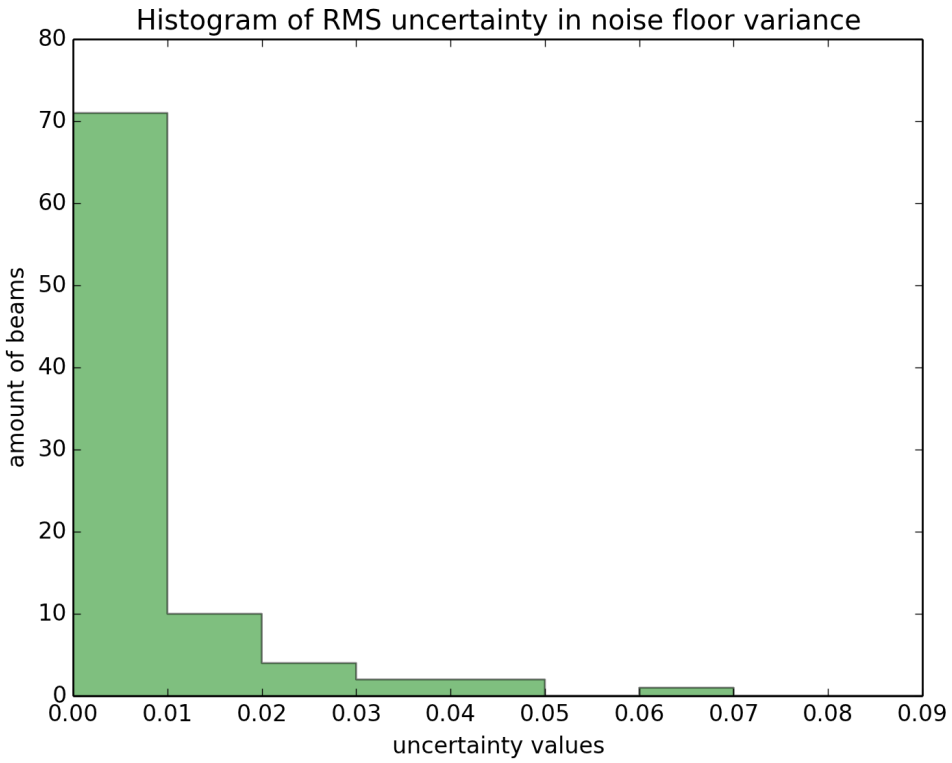

Figure 4.11: A histogram of uncertainty in noise floor variance. Beam 65 is not included.

CHAPTER 5

FUTURE WORK

This thesis proved that the PTWR, which was designed to be deployed on a truck, can also be converted into a fixed radar system at low cost. This fixed PTWR fits into a van, and can be transported to Texas in as few as three days. It can be set up in less than a day, and can be installed without the use of cranes or helicopters; in fact, only two pieces (radar enclosure and computer enclosure) required heavy lifting by three or so strong people up a single flight of stairs.

Along with this, where the data from the PTWR once required processing by hand done in Matlab, products can now be mass-processed with little effort on any computer that can run Python and the packages required by the program, all of which are free and open-source.

5.1 Ettus transceiver

One of the main problems with the system is that it employs a Pentek 7140 transceiver. This transceiver limits the host computer's abilities drastically due to operating system requirements for the transceiver drivers as well as low reliability. They are very sensitive to being physically bumped, and on a system that now travels in a van from Massachusetts to Texas and back, it is challenging to make sure the Pentek is clear and bump-free.

It has been suggested to upgrade this transceiver to a modifed Ettus transceiver. While this is outside the scope of this thesis, it remains that this upgrade would be a significant improvement over the challenge of the Pentek transceiver. An Ettus has

been installed in XPOL; however, the pulsing scheme of that radar is much simpler, for example it does not utilize pulse compression. Much work would be involved to get the Ettus transceiver to operate over the full range of parameters the PTWR is designed to be capable of.

5.2 Cf/Radial NetCDF standard

The National Center for Atmospheric Research (NCAR) has developed a NetCDF standard, Cf/Radial. The Cf/Radial format is attempts to standardize the NetCDF variable and global attribute names.

Unfortunately, the NWS does not use the NetCDF standard. A java program distributed by NCAR will convert the files from the archive service to NetCDF, but these converted files do not conform to the Cf/Radial standard. These files also cannot be read easily, as folding in ϕ_{DP} is still present, causing higher reflectivity values to wrap. Images in this thesis from NEXRAD-run radars were made using NCAR's Integrated Data Viewer (IDV), which reads in NetCDFs and plots them, but is also far from user friendly.

Because of this, it was decided to follow the CASA standard of NetCDF variable naming. If, one day, the Cf/Radial standard is to be upheld by PTWR data as well as CASA, a script could easily be written to pull data out of the existing NetCDFs and reformat the variable and global attribute names to the Cf/Radial standard.

5.3 Py-ART

Py-ART is a toolkit for plotting radar products in Python, similar to `wradlib`. Py-ART is more widely used than `wradlib`, and likely will have better support over time as required packages like Matplotlib are upgraded. It claims to be capable of taking NEXRAD data as downloaded from the archive as an input without any

special NetCDF conversion. Since it uses `matplotlib` for plotting, many of the more challenging calls to edit the axes and gridlines will likely remain largely unchanged.

The choice to use `wradlib` was simply due to this library being suggested first. Likely the use of Py-ART would be more prudent for plotting; however, that was determined not to be within the scope of this thesis, since much of the plotting program was already developed before Py-ART was discovered.

5.4 Integration with CASA network

One upgrade that would be very useful would be integration into the CASA network. CASA uses adaptive scanning, finding areas of a storm system that require closer monitoring, and spend more observation time on those areas while minimally scanning the rest of the sky for new cells. Since there are limitations to the scanning area of the PTWR on the roof of Nedderman Hall, this may be impossible. However, better integration and communication with CASA regarding when to observe and where could mean the difference between a good observation and a bad one. If the PTWR is to be used in a system similar to this in the future, it would be good to know what integration into the CASA system would require.

5.5 Temperature monitoring

Temperature readings are useful for checking that a change in noise floor is from ambient temperature and not some other factor, as well as generally monitoring the radar to make sure it isn't harmed by extreme temperatures. Having a way to monitor the temperature in the computer enclosure was crucial; however, Twitter was not a particularly useful medium through which to receive this information. The largest problem is that despite Twitter's claims that an archive of tweets can be obtained, actually retrieving this archive proves to be extremely difficult, and this problem still has not been resolved.

A different platform should be used for temperature monitoring in the future. One suggestion is to use the website Xively, which was designed with long-term monitoring and statistics in mind. Another is to utilize a RaspberryPi, which is capable of uploading temperature readings to remote data storage, including Google Drive. Since the RaspberryPi essentially runs an operating system, it can run Python scripts. This would allow easy programming of, for example, a script that emails the radar operator if the temperature exceeds some threshold limit.

APPENDIX A

A BRIEF USER'S MANUAL

A.1 Roof mount assembly

The new mounting technique for the PTWR involves assembly of many parts; it was built to be modular, so it can be taken apart and fit into a van for easy transportation. It was custom built, having been cut and drilled in the MIRSL machine shop. Because of this, it can be a challenge to put together; this section endeavors to explain how to rebuild the mount.

Two plywood pieces serve as the base of the mount. Bolts go into counter-sunk holes from the bottom of the wood, as not to tear the lining of the Nedderman Hall roof. The plywood has been marked roughly as to the location of the radar and the computer enclosure, however the location of the bolt holes are also a good indicator of where the computer and radar enclosure are to be mounted.

The computer enclosure is mounted to the base with four bolts. Holes have been drilled through the bottom of the computer enclosure for this purpose.

The radar enclosure frame is made of aluminum I-beams and is mounted to the base with eight bolts. It is then built up following a corner and level scheme, as shown in Figure A.1. The first number refers to the corner, while the second number refers to the level above the ground. Bolts connect the I-beams through beveled sections to ensure a flat interface. A portion of the old frame from the truck mount is included as the top portion of the roof mount.

The radar enclosure is attached to the pedestal via bolts that enter tapped holes in the bottom of the radar enclosure. (It is important to note that only some of the

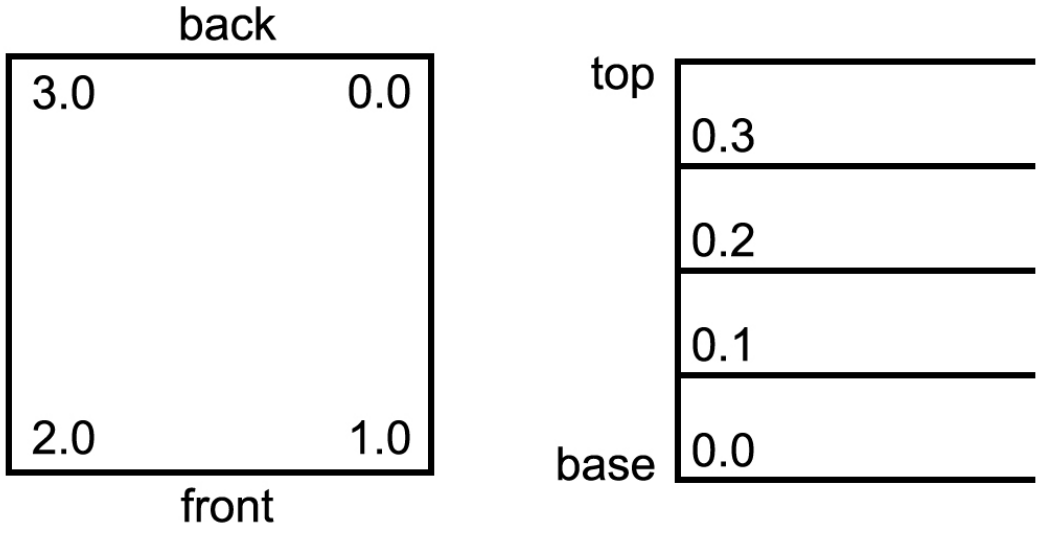

Figure A.1: Corner and level scheme of the radar enclosure frame. The first digit indicates corner, while the second indicates level. Corner 0 indicates the back right of the radar, from looking down from above; corner numbers increase clockwise around the frame. Level 0 indicates the ground level I-beam, while Level 3 indicates the topmost beam.

holes in the pedestal align with holes in the radar enclosure; about eight holes in total are aligned properly.)

A.2 RF subsystem assembly and disassembly

If the power dividers or splitters must be removed, it is important to remember which of the sixteen identical components are for up conversion and which are for downconversion. The power dividers in the upconverter are to the top of the radar enclosure, while the power combiners are to the bottom. This can be remembered through the use of a pneumonic: up (top) is the up(conversion), while down (bottom) is the down(conversion).

These components have also been known to leak through the screwholes when exposed to water. This causes damage to the system, dropping the power transmitted or received significantly. The TR modules have also been known to leak; however,

they can catch fire when wet. For these reasons, it is imperative that the seal between the two metal plates making up the top side of the radar enclosure is checked regularly. (To quote Krzysztof, who had the misfortune of replacing a burned TR module: "It's not good to get water into your radar.")

To that end, removing the TR modules from the radar enclosure is not recommended, but sometimes required. To do this, the fans below the TR modules must first be disconnected from power. There are seven places a TR module is connected to the enclosure: four cables and three screws. Two screws are close to the LRU backplane (one on the top and one on the bottom), while the last is close to the antenna (on the bottom of the TR module). The TR modules are held in place by two L-beams running along the length of the antenna array. Replacing a TR module back into the system can be tricky, as the fit is designed to be tight. If it seems an L-beam has slipped or a TR module simply will not fit, the aluminum casing surrounding the module can be filed slightly. When replacing a TR module, the 20-pin connector must be properly aligned; while the SMA cables slide into the backplane nicely, the 20-pin connector can be challenging.

A.3 Data processing programs

Three main programs have been written for data processing, as shown in Table A.1. One is for preliminary information about the data by opening the binary data files and printing the headers to a text file for inspection. One is for full processing of the data, outputting NetCDF files. The last is a program for plotting the data and saving it to an image file.

The preliminary data program, called `print_headers`, allows easy access to what data is in a folder without processing it first, saving time by not processing unwanted data. It accepts a folder as an input and outputs a text file with the data from all

Table A.1: Python programs written for PTWR processing. Inputs column indicates the default inputs; other options are described within the text.

Name	Module	Inputs	Outputs
`ptwr`	`go`	`'folder', plot=False`	NetCDF files
`mplotall`	`go`	`'folder', type='other', plround=True`	folders by elevation with six-panel plots and attenuation corrected reflectivity plots
`print_headers`	`go`	`'folder'`	text file with header information from each file plus a count of how many files are included

the files in the folder. The first line of the text file lists how many files were found in the folder. It can be called by:

```
>>> import print_headers
>>> print_headers.go('data/day/')
```

where `data/day/` is a folder containing binary files for one day's worth of observations. Often it is easier to run this program on a day-by-day basis, so that it can be easy to find differences in scan type. This also makes it easier to see what date and times are included in the observation run. However, it easily finds files within folders, so it can be run on an entire deployment.

The main processing program, `ptwr`, processes the raw binary files into radar products in NetCDF format, as described in Chapter 3. It can be run by calling:

```
>>> import ptwr
>>> ptwr.go('data/day/',True)
```

Here, `True` indicates that the user wants the program to make plots after the data has been processed, by calling `mplotall`. The program defaults to `False` for this input, so if only NetCDfs without plots are desired, this can be left blank.

The plotting program, `mplotall`, can be used to plot any NetCDF files named according to CASA's standards. It can be called by:

```
>>> import mplotall
>>> mplotall.go('data/day/','ptwr',False)
```

The first optional input describes the type. Small differences between the PTWR and CASA data requires this. For example, `wradlib` requires data to sweep clockwise. Sometimes, CASA data sweeps counterclockwise; therefore, if the type is CASA, a check must be done on the direction the data sweeps out. Also, the plotter must make a mask of values set to NAN. NetCDFs created by `ptwr` output arrays with NANs. However, CASA data uses -99900.0 instead of NAN; any data points with this value must be set to NAN before they can be plotted. This NAN mask is required for plotting with `wradlib`. Since both CASA and PTWR files can be fed into `mplotall`, specifying which type of file is being plotted is required. The second optional input describes whether the user wants a plot with a full 360° view; here, `False` indicates sectors of the full PPI are desired.

The title and file name of the six-panel plot will be set to a string including the radar type (PTWR or CASA), the data and time of the observation, and the elevation in degrees. These are then saved in .png format into folders by elevation for easier sorting.

If an empty file list is found for any of these programs, Python will most likely output the following error:

```
Traceback (most recent call last):
  File "<stdin>", line 1, in <module>
  File "ptwr.py", line 105, in go
    fid = open(flist[0],'rb')
IndexError: list index out of range
```

If this occurs, often it means the the input folder must be changed. Each program is capable of searching sub-folders for files, but the number of levels between the input folder and the files in question can cause problems in some cases. The programs check whether the folder ends with a slash and appends one as necessary, so when troubleshooting, this is not a problem to be considered.

The radar operation program `xdatalog` writes the binary files as the super user on the radar computer. Because of this, either the file owner must be changed using the `chmod` command, or the super user must be logged in. Once this is done, Python can be run and the data can be accessed.

A.3.1 System requirements

The Python programs were written in Aquamacs, an Emacs editor built for OSX, using a MacBook Pro running OSX 10.9 (Mavericks). It was also tested to run on a MIRSL computer running CentOS 6.4, as well as the radar computer, which runs CenOS 5.8. It successfully ran on all of these operating systems.

Part of this OS flexibility comes from the Python distribution used. In all cases, Enthought was the method of installing Python. Enthought ships with Python 2.7.6, as well as useful libraries for mathematics and plotting. Enthought is currently released as Enthought Canopy, which includes many graphical interfaces. In the case of the radar computer, the Enthought Python Distribution (EPD) was necessary to maintain stability of the older OS. However, the radar operation GUI requires libraries specific to EPD, so the Enghought requirement is for both radar operation and data processing.

Rather than write over the existing version of Python, Enthought installs in a separate location and both the pre-existing Python as well as the Enthought distribution can be run. The version can be checked by entering `python` into the terminal and seeing what version is printed. For example, in OSX:

```
$ python
Enthought Canopy Python 2.7.6 | 64-bit | (default, Apr 11 2014, 11:55)
[GCC 4.2.1 (Apple Inc. build 5666) (dot 3)] on darwin
Type "help", "copyright", "credits" or "license" for more information.
>>>
```

When Enthought is installed, Enthought Python becomes the default that runs from the terminal. It does this by adding the following line to the bash profile:

```
VIRTUAL_ENV_DISABLE_PROMPT=1 source /pathtoEnthought/User/bin/activate
```

in which the path to Enthought may vary by operating system. If Enthought is no longer the desired default from the terminal, this line can be commented out of the bash profile with a `#` at the beginning of the line.

In both Canopy and EPD, a Python package manager is included. This can be accessed graphically in Canopy and in the terminal in EPD using the call `enpkg`. This is particularly useful, as installing some of the required libraries for `wradlib` can be a challenge without a Python package manager. Fortunately, most of the required libraries come installed: `szlib`, `numpy`, and `matplotlib` are already included. Other required libraries can be downloaded easily with the package manager: `h5py`, `numpydoc`, `netCDF4`, and `gdal` can be found through this tool. They can be installed without Enthought, but this has proved challenging compared to the ease of using Enthought's package manager. The only library that must be downloaded and installed manually is `wradlib`, which can be found easily online. It can be installed by running

```
$ cd /pathtowradlib/
$ python setup.py install
```

from the terminal.

`wradlib`'s `cg_plot_ppi`, in the `vis` module, is used for plotting PPIs without having to first convert to polar coordinates. It has been found that this method, which is employed in the PPI tab on the radar operation GUI due to it being faster, creates undesirable artifacts. This library heavily relies on `matplotlib`'s `axisartist` namespace, and all plots can be manipulated using calls to this namespace. This makes the plotting function highly customizable; the plots output by `mplotall` do not look like the standard output due to a great deal of calls to manipulate the gridlines, axes, and colorbars. However, this means it contains the same quirks of `matplotlib`, including inconsistent naming schemes in ticks and labels: some must be "got" before manipulating, while others can simply be edited. This often requires a trial and error technique, and much of the code in `mplotall` is dedicated to making these plots consistent and not too busy.

`cg_plot_ppi` is highly adaptable, as it can be used to plot 360° PPIs as well as sectors by merely calling different columns from a data array. It can be fed azimuth values; if none are given, it will assume 360° of data were given and create a fake azimuth array based on the number of columns of data given. It can also be passed an array of radii; otherwise, it will assume 1 unit per range bin of data.

A.4 Radar operation notes

A.4.1 GUI operation

Before the radar is powered on, the idle state of the system is roughly 2A. When the radar is on but not transmitting, it draws roughly 6.5A. While transmitting, it draws about 8A, depending on the duty cycle. If the radar does not complete its transmit process correctly (if, for example, the "DATALOG STOP" button is pressed), the TR modules may get stuck in transmit mode. This is not good for the system and may break the TR modules. In this case, the FPGA should be reset using the "RESET FPGA" button, which clears out commands and resets the state

machine in the FPGA. If that does not work, the radar should be shut down using the "RADAR OFF" button, cutting power to the TR modules and the FPGA before they are damaged.

When using the PPI and A-scope tabs in the radar operation GUI, "Processed" mode must be used; otherwise, the PPI and A-scope will not display. The scale bar on the PPI viewer can be changed by right-clicking with the mouse and dragging from one desired extreme to another. Zooming out or in is done with the scrolling wheel on a mouse.

The tick rate option in the A-scope tab determines how quickly the next pulse is shown in ms. The standard is 20ms. For more time between A-scope refreshes, this value should be changed to a larger number. However, this will also slow down the speed at which the PPI refreshes.

To close the GUI, click the red circle in the top right-hand corner of the GUI itself. This will close all the other windows as well. When powering down the radar, it is important to check the current from the netBooter before closing the GUI.

All programs required for operating the radar, including the GUI and `xdatalog`, are stored within one directory. To access these files, simply:

```
$ cd home/radarop/Dropbox/PhasedArray/Software
```

A.4.2 TR module check

Diagnosis of the FPGA can be done through the GtkTerm by connecting to `/dev/TTYS0` at the highest speed. Entering "v" for verbose into the command line ensures all relevant data will be printed to the GtkTerm. The command `j` will reset the FPGA and clear any old commands or data. Checking a specific TR module can be accomplished by entering `t` (for temperature) and then the hex address (for example, `3F` for 64) of the TR module. (When the radar is first powered on and calibrations are uploaded to the TR modules, the modules are again listed by their hex

address.) This ensures communication with the TR module functions correctly, and if the temperature is within a few degrees Celsius of ambient, is a valuable check on the TR module's proper functioning. Before quitting GtkTerm, "V" for quiet mode must be entered, as the radar operation code requires the FPGA to be in quiet mode.

An easier way to check the connectivity with and temperature on the TR modules is to run `TRMtemp` from the CalSet directory. This will print the temperature of each TR module, which checks connectivity and proper TR module functionality.

A.4.3 netBooters

The netBooters are connected to the computer through two serial to USB connectors, as the radar computer does not have enough serial ports. GtkTerm windows can be used to communicate directly with the netBooters. A full list of netBooter commands can be accessed by typing `help`. One useful command is `pshow`, which lists all the outlets and their current state (on or off). To set the state of a particular outlet, `pset n v`, is used. For this command, n is the number of the outlet and v is the value, so turning outlet 7 on would be entered as `pset 7 1`. Network settings can also be accessed through GtkTerm.

Unfortunately, the two USB connections with the netBooters, TTYUSB0 and TTYUSB1, are named randomly when the computer first powered on. This is a problem, as the netBooters address is hard-coded into the software. Therefore, when the computer boots, steps must be taken to ensure the radar operation code can access the netBooters properly. GtkTerm can be used to determine which netBooter corresponds to which address: `pshow` will list either two outlets or eight.

Once the appropriate address for each is determined, this must be checked against the `nboot.c` program. Line 17, which reads `define COMM/dev/ttyusbX`, must contain the address of the eight-outlet netBooter. If this is changed, `nboot.c` must be recompiled by entering `make -B nboot` in the command line.

The netBooters can be controlled manually through use of the yellow button on the front, without need for GtkTerm or the web application. This button should be pressed until the LED for the outlet to be changed begins to flash. Press and hold the button until the LED changes to the desired state: LED on indicated the outlet is powered, and LED off indicated the outlet is disconnected from power.

A.4.4 Security camera

The security camera has a short ethernet cable that cannot be removed. Because of this, a a male-male connector is required for use. The camera is wifi capable, but the firewalls at both UMass and UTA have requirements that the security camera cannot operate.

The camera has an internal SD card to hold photos and videos. It can be accessed through the screws in the back of the camera. However, the SD card cannot be accessed over the network. The option of saving a photo or video when the camera senses motion can be turned on and off from the web app. This is useful in case storage on the SD card becomes scarce.

A.4.5 Positioner

When the positioner is first powered on, the joystick must be calibrated before it can be used to move the pedestal. Commands will appear on the screen to move the joystick on the positioned to its extremes. Unfortunately, this is required every time the positioner is powered on, including if the system loses power. This is the only part of the roof mount that must be done manually.

A.4.6 TeamViewer

TeamViewer runs automatically when the radar computer is booted up. If the TeamViewer application is closed on the host computer, the computer must be re-booted using the netBooter web application (outlet 1 on the eight outlet netBooter).

Table A.2: Login and password information for setup and operation of the PTWR.

Service	**Username**	**Password**
Computer	radarop	tornado
TeamViewer	227 390 181	tornado
Camera over IP	admin	tornado
netBooter over IP	admin	admin
MyDLink	korzel@engin.umass.edu	tornado
Twitter	mirslradar	tornado
CASA webapp	contact Eric Lyons for a login and password	

When the computer restarts, TeamViewer will automatically begin running and the computer can be accessed again.

A.5 Login information for radar operations

Many passwords are involved when running the PTWR. These can be hard to keep track of; therefore, a list of useful login and password combinations for operation of the radar are described in Table A.2.

CASA has a web application for viewing the DFW area CASA data in real-time. The website is `http://droc1.srh.noaa.gov/dfw/` and requires a login and password, which can be obtained from Eric Lyons (`elyons@cs.umass.edu`). This is useful for determining when there is rain in the range of the PTWR, as the radars are co-located and have a similar range.

APPENDIX B

DATASHEETS FOR UP-DOWN CONVERTER

The up-down converter uses commercial parts. These are described in Table B.1. Datasheets for these parts are appended to this Appendix, in the order in which they are found in the up-down converter, as shown in Figure 1.3. It must be noted that the first amplifier in the upconversion and the second amplifier in the downconversion have the same part number.

Table B.1: Companies and part numbers for the parts that make up the up/down converter.

Location	**Part**	**Company**	**Part number**
up	1st filter	Lark	MC60-5-3AA
up	1st mixer	Mini-Circuits	ZEM-M2TMH
up	1st amp	Mini-Circuits	ZJL-4G+
up	2nd filter	Lorch	8EZ4-1800/A100-S
up	2nd mixer	Mini-Circuits	ZX05-153MH+
up	power amp	Microwave Amplifiers Ltd	AM49-06-053RB
up/down	switch	Narda	S133DH
up/down	power splitter/ combiner	Richardson RFPD	RPDC020180A8S
down	LNA	Planar	PE2-17-9R5G-2R0-8-12-SFF
down	1st filter	K&L	4FV20-10400/T3000-O/O
down	1st mixer	Mini-Circuits	ZX05-153LH+
down	2nd mixer	Mini-Circuits	ZFM-15
down	1st amp	Mini-Circuits	ZFL-500
down	2nd amp	Mini-Circuits	ZJL-4G+

MC SERIES

NO. OF SECTIONS	2	3	4	5	6 OR MORE
1.5/1 VSWR BW MIN. 3 dB BW	0.4	0.7	0.8	0.85	0.9

SPECIFICATIONS	STANDARD	*SPECIAL
ELECTRICAL		
Center Frequency (Fc)	1 to 5000 MHz	0.1 to 5000 MHz
3dB Relative Bandwidth (% of Fc)	2 to 50	3 to 100
Number of Sections Available	3 to 6	2 to 10
Nominal Impedance	50Ω	50 to 300Ω
Maximum Insertion Loss	See Curve	See Curve
Maximum VSWR	1.5/1	1.3/1
Attenuation in the Stopband	See Page 14	See Page 14
Maximum Input Power (Average) (Watts to 10,000 ft.)	2	4
Maximum Input Power (Peak) (Watts to 10,000 ft.)	20	40
ENVIRONMENTAL		
Shock	20 G's	75 G's
Vibration	10 G's	30 G's
Humidity	95% relative	100% relative
Altitude	Unlimited	Unlimited
Temperature Range (Operating)	- 40°C to + 85°C	- 55°C to + 125°C
Temperature (Non-Operating)	- 65°C to + 125°C	- 65°C to + 150°C
MECHANICAL		
Approximate Weight in Grams	L + 10	L + 10
Mounting Provisions	See Next Page	See Next Page
Special Configurations	Consult Lark	Consult Lark

*Contact Lark Engineering

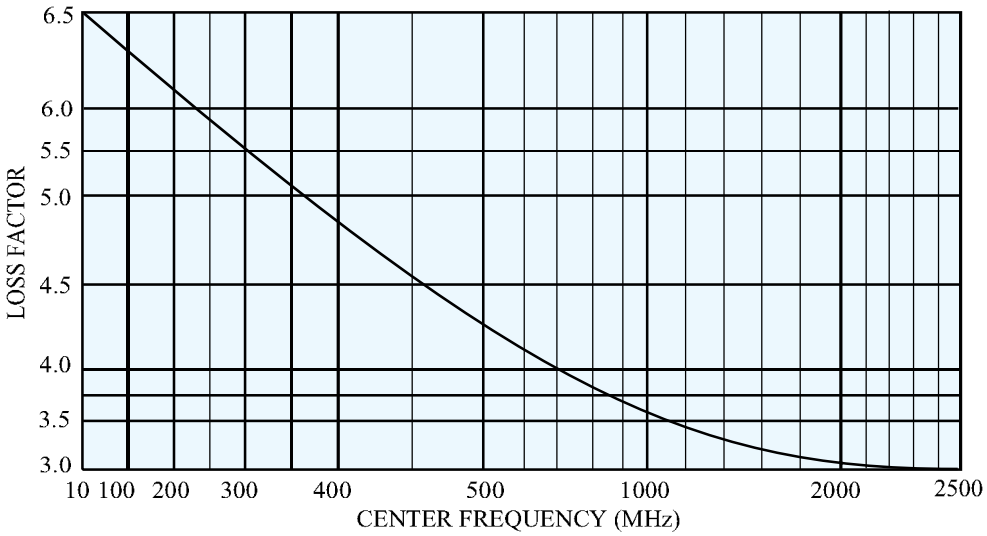

INSERTION LOSS:

The maximum Insertion Loss at center frequency is equal to:

$$\frac{LF \times (N+0.5)}{\%\ 3\ dB\ BW} + 0.2$$

Where:

LF = Loss Factor

N = Number of Sections

% 3dB BW:

$$\frac{3dB\ BW\ (MHz) \times 100}{CENTER\ FREQUENCY\ (MHz)}$$

Example:

A 3 section MC with a center frequency of 700 MHz and a 3dB BW of 70 MHz would be:

$$\frac{4.0 \times 3.5}{10} = \frac{14}{10} = 1.4$$

1.4 + 0.2 = 1.6 dB

MECHANICAL SPECIFICATIONS

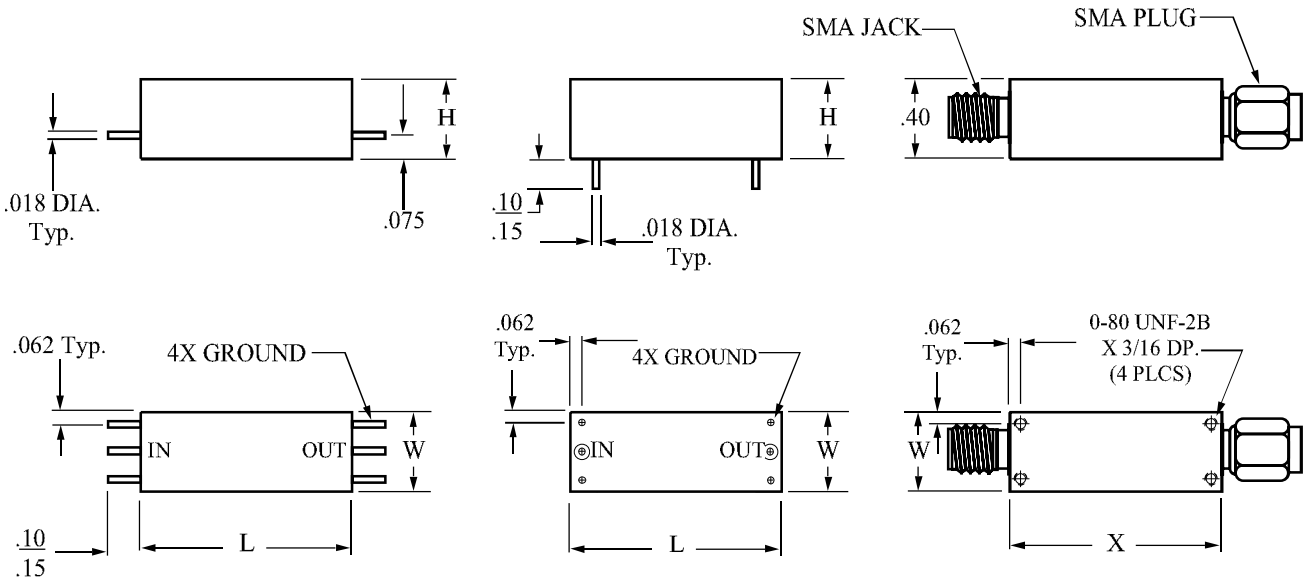

CONNECTORS AVAILABLE ON MC SERIES:

LARK CODE	TYPE	LARK CODE	TYPE
A	SMA Jack	M	Solder Pin Radial
B	SMA Plug	S	Special
L	Solder Pin Axial		

FREQUENCY RANGE	NUMBER OF SECTIONS	W	H	L	X
1 - 9.9 MHz	2 to 3	0.75	0.50	1.50	1.75
	4 to 5	0.75	0.50	2.50	2.75
	6 to 7	0.75	0.50	3.50	3.75
10 - 100 MHz	2 to 3	0.55	0.40	1.00	1.25
	4 to 5	0.55	0.40	1.50	1.75
	6 to 7	0.55	0.40	1.75	2.00
101 - 300 MHz	2 to 3	0.44	0.40	0.75	1.00
	4 to 5	0.44	0.40	1.00	1.25
	6 to 7	0.44	0.40	1.50	1.75
301 - 3000 MHz	2 to 3	0.44	0.31	0.75	1.00
	4 to 5	0.44	0.31	0.75	1.00
	6 to 7	0.44	0.31	1.25	1.50

OVER 7 SECTIONS - CONSULT LARK ENGINEERING

NOTE: ALL STANDARD UNITS WITH SMA CONNECTORS ARE SUPPLIED WITH H=.40”

The size shown is a standard used by Lark to facilitate low cost, easily reproduced units. Should you require another size, please submit all of your requirements, both electrical and mechanical, to Lark Engineering. This will enable Lark to quote the optimum design for your application.

STOPBAND ATTENUATION

The graphs on the following pages define the normal specification limits on attenuation for Lark's MC and MS bandpass filter series. The minimum level of attenuation in dB is shown as a "number of 3dB bandwidths from center frequency". Since the frequency characteristics vary for differing bandwidths, it is necessary to establish specifications for each bandwidth. The different graphs represent various 3dB percentage bandwidths. Intermediate values should be interpolated. The 3dB percentage bandwidth is defined as follows:

$$\frac{\text{3dB Bandwidth (MHz) x 100}}{\text{Center Frequency (MHz)}}$$

The exact relationship is as follows:

$$\text{3dB Bandwidths From Center Frequency} = \frac{\text{Rejection Frequency (MHz) - Center Frequency (MHz)}}{\text{3dB Bandwidth (MHz)}}$$

Example:
Given: Center Frequency = 500 MHz
Minimum 3dB Bandwidth = 50 MHz
Number of Sections = 5

Find: Minimum attenuation levels at 425 MHz and 585 MHz.

$$\text{3dB BW's from Fc} = \frac{425 - 500}{50} = -1.5$$

$$\text{and } \frac{585 - 500}{50} = +1.7$$

The answer can be read directly from the 10% graph. Using the 5 section curve at the point -1.5 (425 MHz) we find the minimum level of attenuation is 40dB. At +1.7 (585 MHz) the minimum level of attenuation is 39dB.

NOTE: The attenuation curves shown for the "MC" and "MS" series are for our standard designs. Other topologies may be utilized yielding different attenuation characteristics.

For special requirements, please contact our Engineering Department.

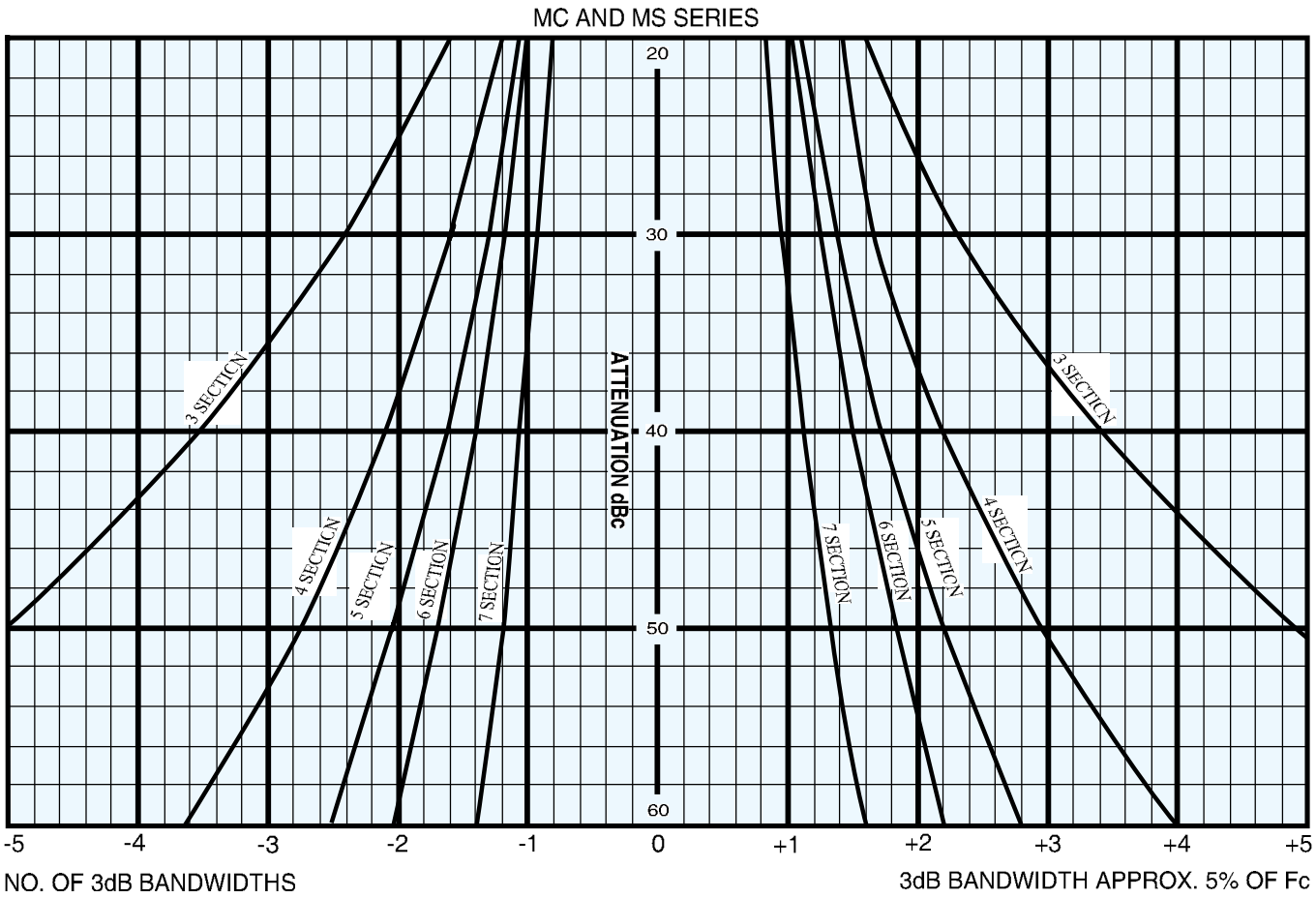

Coaxial

Frequency Mixer

ZEM-M2TMH+
ZEM-M2TMH

Level 13 (LO Power +13 dBm) 10 to 2400 MHz

CASE STYLE: V37

Connectors	Model	Price	Qty.
SMA	ZEM-M2TMH(+)	$114.95	(1-9)

+ RoHS compliant in accordance with EU Directive (2002/95/EC)

The +Suffix identifies RoHS Compliance. See our web site for RoHS Compliance methodologies and qualifications.

Maximum Ratings

Operating Temperature	-55°C to 100°C
Storage Temperature	-55°C to 100°C
RF Power	200mW
IF Current	40mA

Permanent damage may occur if any of these limits are exceeded.

Coaxial Connections

LO	3
RF	2
IF	1

Features

- low conversion loss, 6.9 dB typ.
- excellent isolation, 43 dB typ. L-R, 44 dB typ. L-I
- wideband, 10 to 2400 MHz

Applications

- VHF/UHF
- cellular
- GPS

Outline Drawing

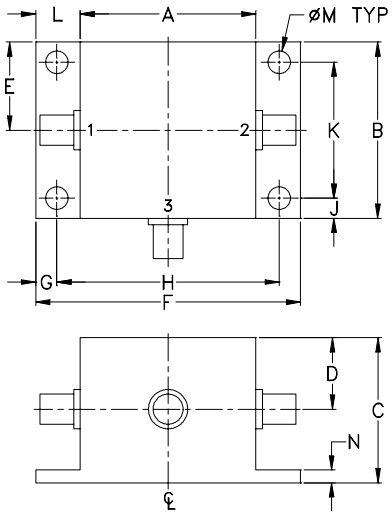

Outline Dimensions (inch / mm)

A	B	C	D	E	F	G
.83	.83	.75	.37	.42	1.25	.10
21.08	21.08	19.05	9.40	10.67	31.75	2.54

H	J	K	L	M	N	wt
1.050	.10	.640	.21	.106	.06	grams
26.67	2.54	16.26	5.33	2.69	1.52	22.0

Electrical Specifications

FREQUENCY (MHz)		CONVERSION LOSS (dB)				LO-RF ISOLATION (dB)						LO-IF ISOLATION (dB)					
LO/RF	IF	Mid-Band m			Total Range	L		M		U		L		M		U	
f_L-f_U		$\overline{X}$	σ	Max.	Max.	Typ.	Min.	Typ.	Min.	Typ.	Min.	Typ.	Min.	Typ.	Min.	Typ.	Min.
10-2400	10-1000	6.9	0.10	9.0	9.5	49	40	43	35	42	35	49	40	44	30	40	30

1 dB COMP.: +9 dBm typ.

L = low range [f_L to 10 f_L] M = mid range [10 f_L to f_U/_] U = upper range [f_U/2 to f_U]
m= mid band [2f_L to f_U/2]

Typical Performance Data

Frequency (MHz)		Conversion Loss (dB)	Isolation L-R (dB)	Isolation L-I (dB)	VSWR RF Port (:1)	VSWR LO Port (:1)
RF	LO	LO +13dBm	LO +13dBm	LO +13dBm	LO +13dBm	LO +13dBm
10.00	40.00	6.87	48.7	47.5	1.06	1.43
25.00	55.00	6.77	48.7	47.4	1.02	1.43
40.00	70.00	6.83	48.9	47.3	1.02	1.43
70.00	100.00	6.69	48.9	47.0	1.04	1.39
100.00	130.00	6.64	49.1	46.9	1.06	1.41
200.00	230.00	6.44	47.6	45.9	1.13	1.44
400.00	430.00	6.25	44.0	43.4	1.31	1.56
600.00	630.00	6.31	40.9	41.7	1.40	1.59
700.00	730.00	6.37	40.6	41.2	1.51	1.58
800.00	830.00	6.39	40.6	40.3	1.53	1.59
1000.00	1030.00	6.45	43.2	37.9	1.46	1.62
1200.00	1230.00	6.40	41.9	37.3	1.42	1.74
1300.00	1330.00	6.46	40.3	37.5	1.42	1.81
1500.00	1530.00	6.73	38.5	36.9	1.43	1.80
1700.00	1730.00	6.98	38.8	37.4	1.45	1.83
1800.00	1830.00	7.26	39.3	37.0	1.57	1.85
2000.00	2030.00	7.60	40.2	36.3	1.84	1.73
2200.00	2230.00	7.88	42.3	36.4	1.92	1.56
2300.00	2330.00	7.91	44.9	35.8	1.83	1.50
2400.00	2430.00	7.74	49.9	34.2	1.65	1.44

Electrical Schematic

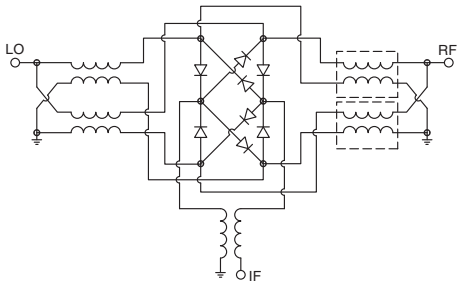

Notes: 1. Performance and quality attributes and conditions not expressly stated in this specification sheet are intended to be excluded and do not form a part of this specification sheet. **2.** Electrical specifications and performance data contained herein are based on Mini-Circuit's applicable established test performance criteria and measurement instructions. **3.** The parts covered by this specification sheet are subject to Mini-Circuits standard limited warranty and terms and conditions (collectively, "Standard Terms"); Purchasers of this part are entitled to the rights and benefits contained therein. For a full statement of the Standard Terms and the exclusive rights and remedies thereunder, please visit Mini-Circuits' website at www.minicircuits.com/MCLStore/terms.jsp.

REV. A
M98898
ZEM-M2TMH
DJ/TD/CP/AM
091006

Performance Charts

ZEM-M2TMH
CONVERSION LOSS
at IF Freq of 30 MHz

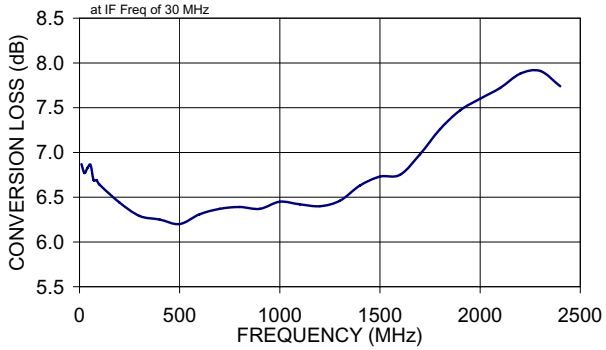

ZEM-M2TMH
L-R ISOLATION

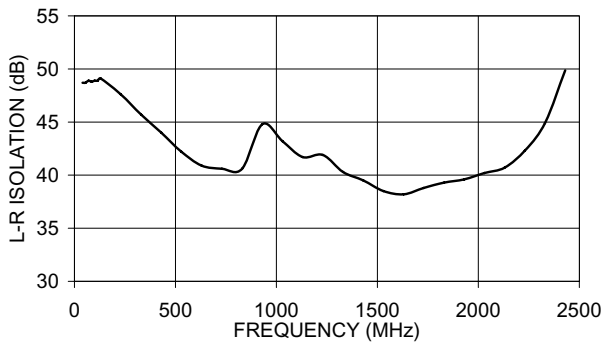

ZEM-M2TMH
L-I ISOLATION

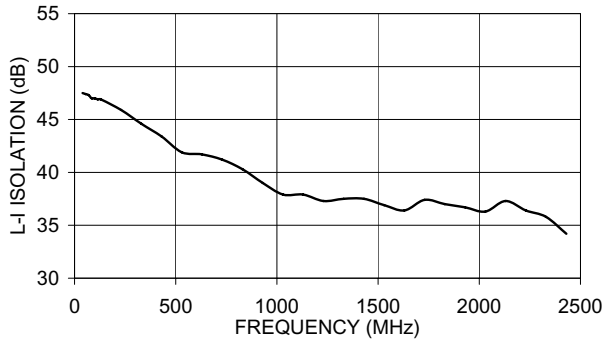

ZEM-M2TMH
RF VSWR

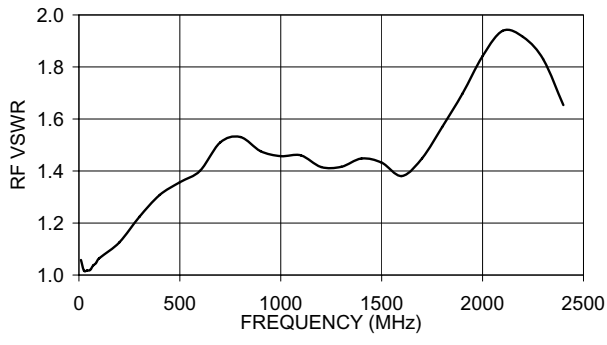

ZEM-M2TMH
LO VSWR

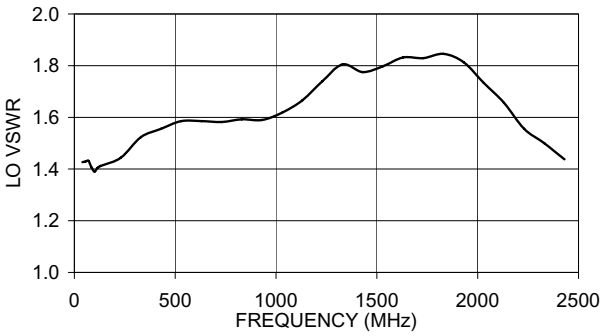

ZEM-M2TMH
IF VSWR

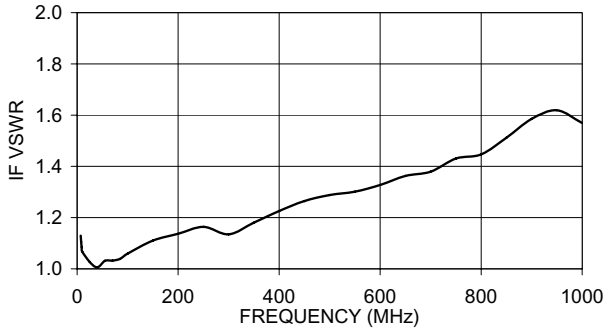

Notes: 1. Performance and quality attributes and conditions not expressly stated in this specification sheet are intended to be excluded and do not form a part of this specification sheet. **2.** Electrical specifications and performance data contained herein are based on Mini-Circuit's applicable established test performance criteria and measurement instructions. **3.** The parts covered by this specification sheet are subject to Mini-Circuits standard limited warranty and terms and conditions (collectively, "Standard Terms"); Purchasers of this part are entitled to the rights and benefits contained therein. For a full statement of the Standard Terms and the exclusive rights and remedies thereunder, please visit Mini-Circuits' website at www.minicircuits.com/MCLStore/terms.jsp.

Coaxial

Amplifier

ZJL-4G+
ZJL-4G

50Ω Medium Power 20 to 4000 MHz

CASE STYLE: BW459

Connectors	Model	Price	Qty.
SMA	ZJL-4G(+)	$129.95 ea.	(1-9)

+ RoHS compliant in accordance with EU Directive (2002/95/EC)

The +Suffix identifies RoHS Compliance. See our web site for RoHS Compliance methodologies and qualifications.

Features

- wideband, 20 to 4000 MHz
- high IP3, +30.5 dBm typ.
- rugged, compact case, 1.07"x0.61" (including mounting bracket)
- protected by US Patent, 6,943,629

Applications

- radar
- instrumentation
- lab use

Amplifier Electrical Specifications

MODEL NO.	FREQUENCY (MHz)		GAIN (dB)			MAXIMUM POWER (dBm)			DYNAMIC RANGE		VSWR (:1) Typ.		DC POWER	
						Output (1 dB Compr.)								
	f_L	f_U	Typ.	Min.	Flatness[1] Typ.	L	U	Input (no damage)	NF (dB) Typ.	IP3 (dBm) Typ.	In	Out	Volt (V) Nom.	Current (mA) Max.
ZJL-4G(+)	20	4000	12.4	10.0	±0.25	+13.5	+11	+20	5.5	+30.5	1.4	1.6	12	75

1. Flatness specified to 0.75 fU, dynamic range at 2 GHz.

L= low range (f_L to $f_U/2$) U= upper range ($f_U/2$ to f_U)

Open load is not recommended, potentially can cause damage.
With no load derate max input power by 20 dB

Maximum Ratings

Operating Temperature	-40°C to 75°C
Storage Temperature	-55°C to 100°C
DC Voltage	+13V Max.

Outline Drawing

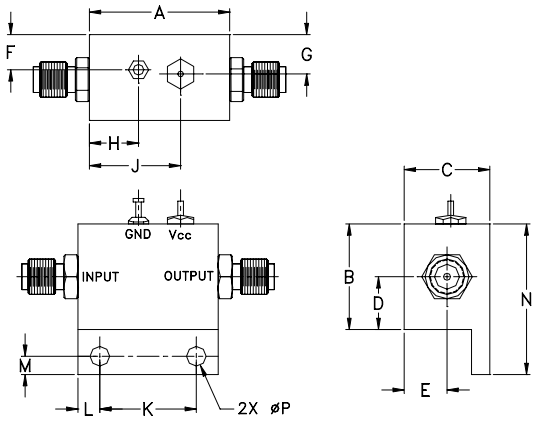

Outline Dimensions (inch / mm)

A	B	C	D	E	F	G	H	J	K	L	M	N	P	wt
1.00	.75	.61	.38	.29	.25	.26	.35	.65	.688	.156	.13	1.07	.140	grams
25.40	19.05	15.49	9.65	7.37	6.35	6.60	8.89	16.51	17.48	3.96	3.30	27.18	3.56	25

Typical Performance Data/Curves

FREQUENCY (MHz)	GAIN (dB)			DIRECTIVITY (dB)			VSWR (:1)		NOISE FIGURE (dB)	POUT at 1 dB COMPR. (dBm)
	9V	12V	13V	9V	12V	13V	IN	OUT	12V	12V
20.00	12.22	12.49	12.48	6.96	7.21	7.38	1.38	1.79	5.03	16.85
320.00	12.43	12.83	12.87	6.59	6.59	6.61	1.37	1.65	4.94	17.37
620.00	12.43	12.84	12.88	6.53	6.50	6.51	1.37	1.57	5.04	17.61
820.00	12.48	12.88	12.92	6.45	6.41	6.41	1.35	1.51	5.05	17.73
1120.00	12.56	12.98	13.02	6.26	6.16	6.16	1.29	1.39	5.04	17.85
1420.00	12.64	13.07	13.12	6.06	5.90	5.90	1.21	1.28	5.02	17.72
1720.00	12.58	13.02	13.10	6.21	5.89	5.89	1.12	1.16	5.03	17.51
2020.00	12.47	12.94	13.00	6.38	6.02	6.02	1.07	1.10	5.03	17.23
2320.00	12.29	12.76	12.83	6.78	6.38	6.38	1.14	1.16	5.08	17.02
2620.00	12.11	12.54	12.60	7.05	6.76	6.76	1.24	1.24	5.13	16.57
2920.00	12.04	12.41	12.46	7.45	7.25	7.25	1.31	1.31	5.23	16.06
3120.00	11.91	12.25	12.29	7.38	7.59	7.57	1.34	1.34	5.29	15.69
3420.00	11.65	11.95	11.98	8.44	8.36	8.36	1.35	1.36	5.33	14.92
3720.00	11.40	11.68	11.70	8.86	8.84	8.84	1.33	1.34	5.29	14.20
4000.00	11.21	11.45	11.47	9.37	9.38	9.38	1.29	1.30	5.34	13.39

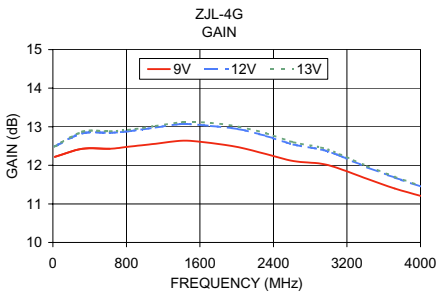

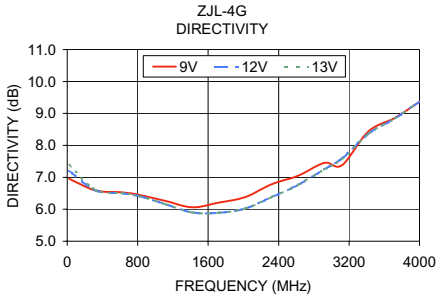

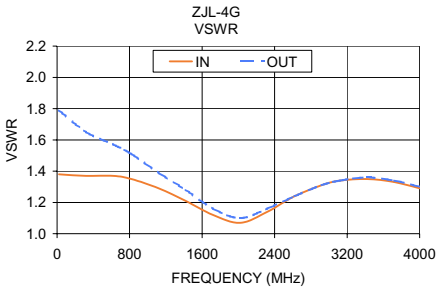

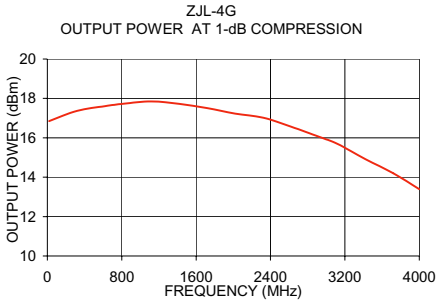

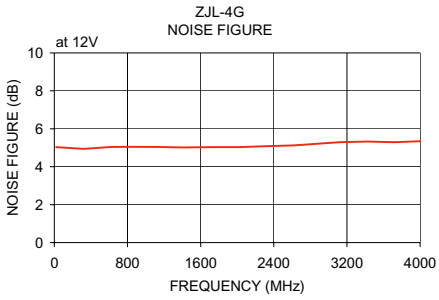

Cavity Filters

- 30 MHz to 40 GHz
- 3 dB Bandwidths from <0.5 to >66%
- High "Q", Low Loss
- High Power
- Computer-Aided Designs
- Helical, Combline, Interdigital
- Waveguide
- 12 Stock Series

Lorch Microwave's cavity filter designs are available in the frequency range of 30 MHz to 40 GHz and with bandwidth options from less than 0.5% to over 66%. Cavity filters offer the user very low insertion loss, steep skirt selectivity, and narrower bandwidths than discrete component filters. Cavity filter performance is based on parts selection and physical layout of the helical coils, resonators, as well as the shape and size of the cavity housing. Lorch Microwave offers the user 12 unique stock designs to satisfy the majority of applications. At lower frequencies a helical coil is used to excite the electromagnetic field, while a 1/8 to 1/4 wave capacitively loaded design is used at higher frequencies. A cylindrical waveguide design is used to achieve narrow bandwidths and high power operation.

Each filter is custom designed to your exact specification so that you will receive the optimum performance at the lowest cost. Filter performance is easily predicted using our proprietary software, while CAD files are generated for our CNC machine and fabrication center. At Lorch Microwave, even complex designs and working drawings can be generated in a matter of a few hours…not weeks.

Standard cavity filters generally are designed using aluminum as the base metal. As most raw metals are inherently lossy, filter housings are silver plated for improved electrical characteristics and current flow. Brass, copper, aluminum or bi-metal resonators are used to minimize frequency drift over temperature.

LORCH MICROWAVE
1725 N. Salisbury Blvd. · PO Box 2828 · Salisbury, MD 21802
Phone 800.780.2169, 410.860.5100 · Fax 410.860.1949
www.lorch.com · lorchsales@lorch.com

The tables, graphs and curves on the following pages have been prepared to enable you to determine an approximation of the electrical performance and physical size you can expect. If by chance your requirements cannot be met from the units described herein, please contact our technical marketing staff for assistance. With over 30 years of filter designs in our data bank, chances are good that we have successfully solved a similar problem in the past.

Narrowband - 0.5% to 4%

P/N	Frequency (MHz)	% 3 dB Bandwidth	VSWR (Typical)	Number of Sections	Avg. Power (Watts)	Operating Temp. (°C)	Relative Humidity
CP	30 - 2000	0.5 - 4	1.5:1	2 - 6	10	-55 to +85	95%
CF2	500 - 2000	0.5 - 4	1.5:1	2 - 8	10	-55 to +85	95%
CF3	500 - 2500	0.5 - 4	1.5:1	2 - 8	10	-55 to +85	95%
CF4	2000 - 3000	0.5 - 4	1.5:1	2 - 8	10	-55 to +85	95%
CF6	2000 - 8000	0.5 - 4	1.5:1	2 - 8	10	-55 to +85	95%
CF7	4000 - 26000	0.5 - 4	1.5:1	2 - 8	10	-55 to +85	95%

Narrowband (Combline) - 1% to 25%

P/N	Frequency (MHz)	% 3 dB Bandwidth	VSWR (Typical)	Number of Sections	Avg. Power (Watts)	Operating Temp. (°C)	Relative Humidity
EZ3	500 - 6000	1 - 25	1.5:1	2 - 17	10	-55 to +85	95%
EZ4	1000 - 8000	1 - 25	1.5:1	2 - 17	10	-55 to +85	95%
EZ5	2000 - 12000	1 - 25	1.5:1	2 - 17	10	-55 to +85	95%
EZ6	4000 - 18000	1 - 25	1.5:1	2 - 17	10	-55 to +85	95%
EZ7	6000 - 26000	1 - 25	1.5:1	2 - 17	10	-55 to +85	95%

Wideband (Interdigital) -25% to 66%

P/N	Frequency (MHz)	% 3 dB Bandwidth	VSWR (Typical)	Number of Sections	Avg. Power (Watts)	Operating Temp. (°C)	Relative Humidity
IZ3	500 - 6000	25 - 66	2.0:1	2 - 17	10	-55 to +85	95%
IZ4	1000 - 8000	25 - 66	2.0:1	2 - 17	10	-55 to +85	95%
IZ5	2000 - 12000	25 - 66	2.0:1	2 - 17	10	-55 to +85	95%
IZ6	4000 - 18000	25 - 66	2.0:1	2 - 17	10	-55 to +85	95%
IZ7	6000 - 26000	25 - 66	2.0:1	2 - 17	10	-55 to +85	95%

Shock 10G
Vibration 20G

See pages 12-14 for mechanical outlines and dimensions.
Contact factory for specific requirements not listed above.

Specifying Cavity Filters

Cavity Filter Part Number Description

4 CF2 - 1200 / A15 - S / SM
1 2 3 4 5 6

1. Number of Sections
2. Series and Package Size
3. Center Frequency, MHz
4. Bandwidth and Code (3 dB BW Standard)
5. Input Connector
6. Output Connector (if different from input)

Bandwidth	Designator
3 dB	/(blank)
1 dB	/A
equi-ripple	/R
special	/X

CONNECTORS

Connector Type	Designator
BNC Female (1)	B
BNC Male (1)	BM
Blind Mate	BP
N Female (1)	N
N Male (1)	NM
RF Pin (2)	P
SMA Female	S
SMA Male	SM
SMA Removable	SR
Special	X
TNC Female (1)	T
TNC Male (1)	TM

(1) Requires Minimum Cross Section of 0.88"

(2) Requires SMA Removable Connectors at High Frequencies

Calculating Number of Sections

The following curves show the stopband frequencies normalized to the 3 dB bandwidth for filters with 2 to 13 sections. A ratio of stopband frequency to 3 dB bandwidth is used.

The curve on the next page shows a slightly asymmetric frequency response resulting from the circuit used. Other schematics may be utilized to yield different attenuation characteristics (i.e. steeper on the high frequency side of the passband and shallower on the low side).

Example:
A CF-Series filter has a center frequency of 1000 MHz and a 3 dB bandwidth of 10 MHz. A stopband attenuation of 60 dB is required at 980 MHz and 1030 MHz.

The percentage bandwidth is 1%, calculated as follows:

$$\frac{\text{3 dB BW (MHz)}}{F_O\text{ (MHz)}} \times 100 = \frac{10}{1000} \times 100 = 1\%$$

For the first stopband requirement: Number of 3 dB bandwidths from center frequency = $\frac{(1000 - 980)}{10} = 2.0$

From the CP/CF series attenuation curve, we find that a minimum of 7 sections are required.

The second stopband requirement is: Number of 3 dB bandwidths from center frequency = $\frac{(1030 - 1000)}{10} = 3.0$

From the CP/CF series attenuation curve, we find that 5 sections minimum are required.

The greater number of sections must always be used to insure full specification compliance; therefore, a 7 section should be used.

LORCH MICROWAVE
1725 N. Salisbury Blvd. · PO Box 2828 · Salisbury, MD 21802
Phone 800.780.2169, 410.860.5100 · Fax 410.860.1949
www.lorch.com · lorchsales@lorch.com

Insertion Loss Calculation

Knowing the number of sections, center frequency and bandwidth of the filter, insertion loss may be calculated using the following formula:

$$\text{Loss} = \frac{N - 1.5}{Q \times \%3\text{dB BW}} + 0.2$$

Example: 5CF2-915/25-N

1. Percentage BW = 25 / 915 x 100 = 2.7%
2. Q from CF series curves = 2.9
3. Number of Sections = 5
4. $\text{Loss} = \frac{5 - 1.5}{2.9 \times 2.7} + 0.2$

Example: 9EZ6-8725/1375-S

1. Percentage BW = 1375/8725 x 100 = 15.8%
2. Q from EZ series curves = 1.1
3. Number of Sections = 9
4. $\text{Loss} = \frac{9 - 1.5}{1.1 \times 15.8} + 0.2 = 0.63$ dB

"Q"-CF, CP Series, Narrowband Cavities

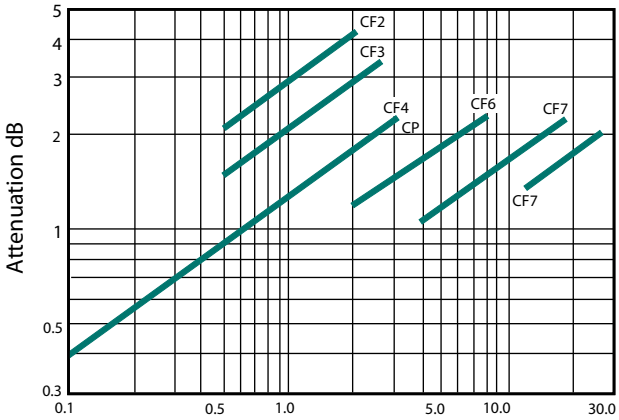

"Q"-EZ, IZ Series, Wideband Cavities

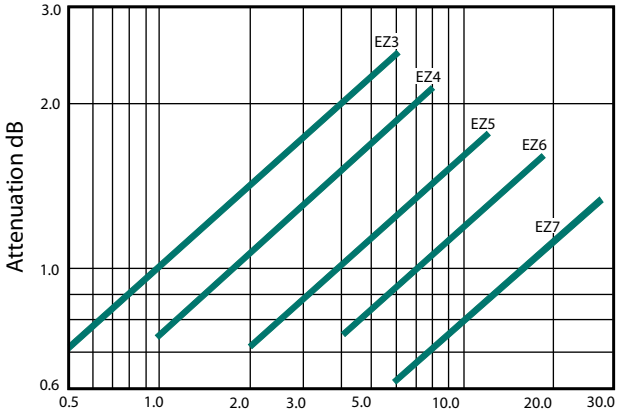

CP and CF Series Attenuation Characteristics

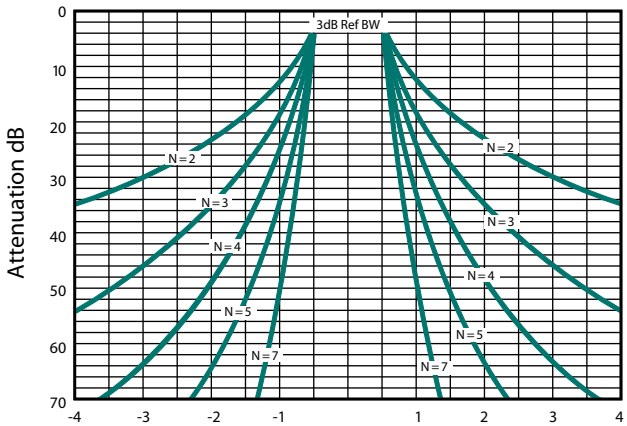

EZ and IZ Series Attenuation Characteristics

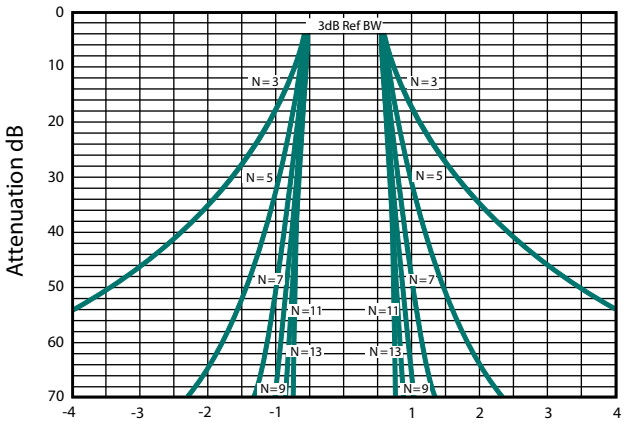

1725 N. Salisbury Blvd. · PO Box 2828 · Salisbury, MD 21802
Phone 800.780.2169, 410.860.5100 · Fax 410.860.1949
www.lorch.com · lorchsales@lorch.com

LORCH MICROWAVE

Cavity Filter Outline Drawings

CP, BRP Series

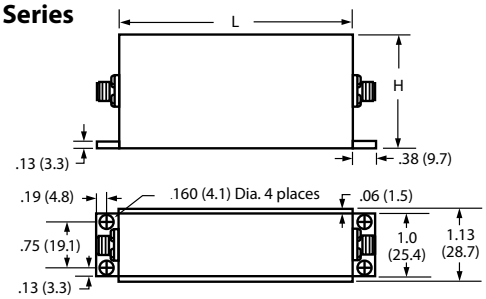

CF2 Series

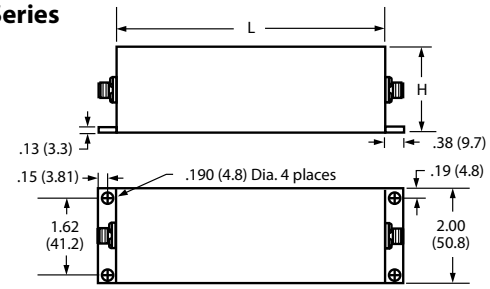

CP Series

Frequency (MHz)	Width Inches (mm)	Height Inches (mm)	Length vs. Number of Sections — Inches (mm) 2	3	4	5	6
30 - 50	1.13 (28.7)	3.88 (98.6)	2.50 (63.5)	3.63 (92.2)	4.75 (120.7)	5.88 (149.4)	7.00 (177.8)
51 - 65	1.13 (28.7)	2.88 (73.2)	2.50 (63.5)	3.63 (92.2)	4.75 (120.7)	5.88 (149.4)	7.00 (177.8)
66 - 100	1.13 (28.7)	2.38 (60.5)	2.50 (63.5)	3.63 (92.2)	4.75 (120.7)	5.88 (149.4)	7.00 (177.8)
101 - 500	1.13 (28.7)	1.88 (47.8)	2.50 (63.5)	3.63 (92.2)	4.75 (120.7)	5.88 (149.4)	7.00 (177.8)
501 - 600	1.13 (28.7)	4.88 (124.0)	2.50 (63.5)	3.63 (92.2)	4.75 (120.7)	5.88 (149.4)	7.00 (177.8)
601 - 900	1.13 (28.7)	3.88 (98.6)	2.50 (63.5)	3.63 (92.2)	4.75 (120.7)	5.88 (149.4)	7.00 (177.8)
901 - 1300	1.13 (28.7)	2.88 (73.2)	2.50 (63.5)	3.63 (92.2)	4.75 (120.7)	5.88 (149.4)	7.00 (177.8)
1301 - 1800	1.13 (28.7)	2.38 (60.5)	2.50 (63.5)	3.63 (92.2)	4.75 (120.7)	5.88 (149.4)	7.00 (177.8)
1801 - 2000	1.13 (28.7)	1.88 (47.8)	2.50 (63.5)	3.63 (92.2)	4.75 (120.7)	5.88 (149.4)	7.00 (177.8)

BRH Series

Frequency (MHz)	Width Inches (mm)	Height Inches (mm)	Length vs. Number of Sections — Inches (mm) 2	3	4	5	6
30 - 50	1.13 (28.7)	4.88 (124.0)	2.50 (63.5)	3.63 (92.2)	4.75 (120.7)	5.88 (149.4)	7.00 (177.8)
51 - 65	1.13 (28.7)	3.88 (98.6)	2.50 (63.5)	3.63 (92.2)	4.75 (120.7)	5.88 (149.4)	7.00 (177.8)
66 - 100	1.13 (28.7)	3.38 (85.9)	2.50 (63.5)	3.63 (92.2)	4.75 (120.7)	5.88 (149.4)	7.00 (177.8)
101 - 500	1.13 (28.7)	2.88 (73.2)	2.50 (63.5)	3.63 (92.2)	4.75 (120.7)	5.88 (149.4)	7.00 (177.8)
501 - 600	1.13 (28.7)	5.88 (149.4)	2.50 (63.5)	3.63 (92.2)	4.75 (120.7)	5.88 (149.4)	7.00 (177.8)
601 - 900	1.13 (28.7)	4.88 (124.0)	2.50 (63.5)	3.63 (92.2)	4.75 (120.7)	5.88 (149.4)	7.00 (177.8)

CF2 Series

Frequency (MHz)	Width Inches (mm)	Height Inches (mm)	Length vs. Number of Sections — Inches (mm) 2	3	4	5	6
500 - 750	2.0 (50.8)	6.6 (167.6)	3.9 (99.1)	5.7 (145)	7.6 (193.1)	9.4 (238.8)	11.2 (285)
751 - 1000	2.0 (50.8)	4.6 (116.8)	3.9 (99.1)	5.7 (145)	7.6 (193.1)	9.4 (238.8)	11.2 (285)
1001 - 1500	2.0 (50.8)	3.7 (94.0)	3.9 (99.1)	5.7 (145)	7.6 (193.1)	9.4 (238.8)	11.2 (285)
1501 - 2000	2.0 (50.8)	2.7 (68.6)	3.9 (99.1)	5.7 (145)	7.6 (193.1)	9.4 (238.8)	11.2 (285)

All dimensions are approximate. Contact factory for actual sizes. All length dimensions are excluding connectors.

LORCH MICROWAVE
1725 N. Salisbury Blvd. · PO Box 2828 · Salisbury, MD 21802
Phone 800.780.2169, 410.860.5100 · Fax 410.860.1949
www.lorch.com · lorchsales@lorch.com

CF3 Series

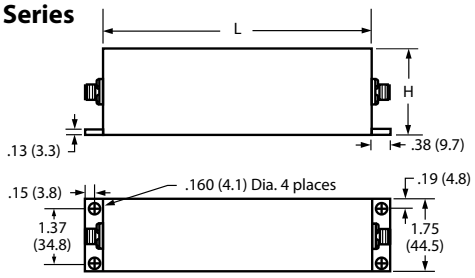

CF4 Series

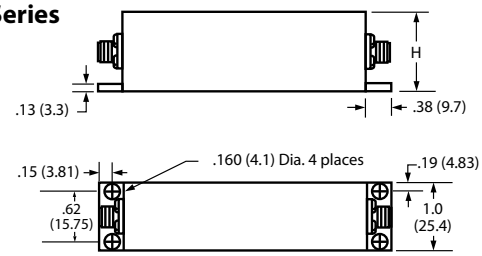

CF3 Series

Frequency (MHz)	Width Inches (mm)	Height Inches (mm)	Length vs. Number of Sections — Inches (mm) 2	3	4	5	6
500 - 750	1.75 (44.45)	6.6 (167.6)	3.00 (76.2)	4.3 (109.5)	5.6 (142.25)	6.9 (175.26)	8.3 (210.82)
751 - 1000	1.75 (44.45)	4.6 (116.8)	3.00 (76.2)	4.3 (109.5)	5.6 (142.25)	6.9 (175.26)	8.3 (210.82)
1001 - 1500	1.75 (44.45)	3.7 (94.0)	3.00 (76.2)	4.3 (109.5)	5.6 (142.25)	6.9 (175.26)	8.3 (210.82)
1501 - 2000	1.75 (44.45)	2.7 (68.6)	3.00 (76.2)	4.3 (109.5)	5.6 (142.25)	6.9 (175.26)	8.3 (210.82)

CF4 Series

Frequency (MHz)	Width Inches (mm)	Height Inches (mm)	Length vs. Number of Sections — Inches (mm) 2	3	4	5	6
2001-3000	1.0 (25.4)	2.1 (53.4)	2.00 (50.8)	2.80 (71.1)	3.60 (91.4)	4.40 (111.8)	5.20 (132.1)

CF6 Series

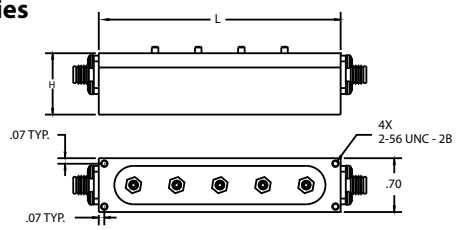

CF7 Series

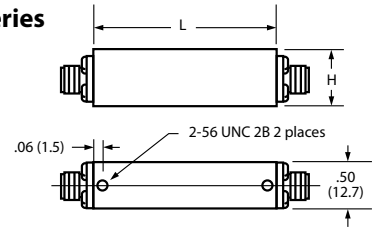

CF6 Series

Frequency (MHz)	Width Inches (mm)	Height Inches (mm)	Length vs. Number of Sections — Inches (mm) 2	3	4	5	6
2000 - 4000	0.7 (17.8)	1.9 (48.3)	1.50 (38.1)	2.0 (50.8)	2.6 (66.1)	3.2 (81.3)	3.7 (94.0)
4001 - 6000	0.7 (17.8)	1.2 (30.5)	1.50 (38.1)	2.0 (50.8)	2.6 (66.1)	3.2 (81.3)	3.7 (94.0)
6001 - 8000	0.7 (17.8)	0.9 (22.9)	1.50 (38.1)	2.0 (50.8)	2.6 (66.1)	3.2 (81.3)	3.7 (94.0)

CF7 Series

Frequency (MHz)	Width Inches (mm)	Height Inches (mm)	Length vs. Number of Sections — Inches (mm) 2	3	4	5	6
4000 - 7000	0.5 (12.7)	1.15 (29.2)	0.9 (22.8)	1.3 (33.1)	1.6 (40.7)	1.9 (48.3)	1.95 (49.6)
7001 - 13000	0.5 (12.7)	0.85 (21.6)	0.9 (22.8)	1.3 (33.1)	1.6 (40.7)	1.9 (48.3)	1.95 (49.6)
13000 - 26000	0.5 (12.7)	0.65 (16.6)	0.9 (22.8)	1.3 (33.1)	1.6 (40.7)	1.9 (48.3)	1.95 (49.6)

All dimensions are approximate. Contact factory for actual sizes. All length dimensions are excluding connectors.

1725 N. Salisbury Blvd. · PO Box 2828 · Salisbury, MD 21802
Phone 800.780.2169, 410.860.5100 · Fax 410.860.1949
www.lorch.com · lorchsales@lorch.com

Cavity Filter Outline Drawings

EZ3, EZ4, EZ5 Series and IZ3, IZ4, IZ5 Series

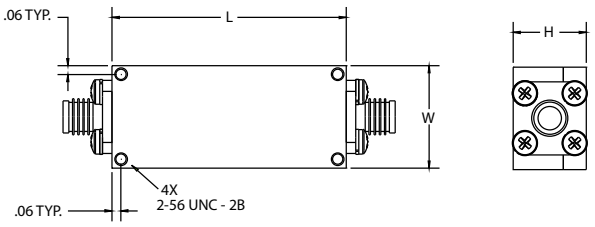

EZ6, EZ7 Series and IZ6, IZ7 Series

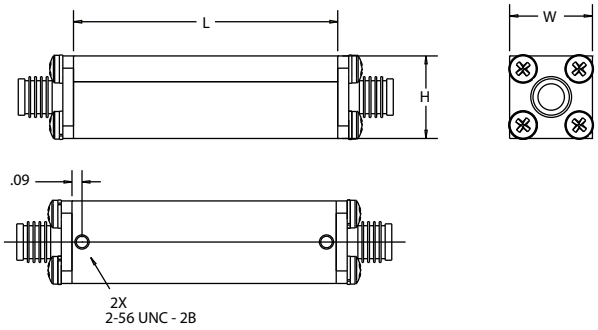

EZ Series Length VS. Number of Sections, 1 - 25% BW

Series	Frequency (MHz)	Width In. (mm)	Height In. (mm)	Length vs. Number of Sections — Inches (mm) 3	4	5	6	7	8	9	10	11	12	13
EZ3	0.5-6.0	4.00 (101.6)	0.75 (19.1)	2.6 (66.0)	3.2 (81.3)	3.7 (94.0)	4.3 (109.2)	4.8 (121.9)	5.5 (139.7)	6.2 (157.5)	6.9 (175.3)	7.6 (193.0)	8.3 (210.8)	9.0 (228.6)
EZ4	1.0-8.0	2.1 (53.4)	0.59 (15.0)	1.9 (48.8)	2.4 (61.0)	2.8 (71.1)	3.2 (81.3)	3.6 (91.5)	4.1 (104.1)	4.6 (116.8)	5.1 (129.5)	5.6 (142.2)	6.1 (154.9)	6.6 (167.6)
EZ5	2.0-12.0	1.5 (38.1)	0.63 (16.0)	1.4 (35.6)	1.8 (45.7)	1.9 (48.8)	2.3 (58.4)	2.6 (66.0)	2.9 (73.7)	3.3 (83.8)	3.6 (91.5)	4.0 (101.6)	4.3 (109.2)	4.7 (119.4)
EZ6	4.0-18.0	0.9 (22.9)	0.50 (12.7)	1.1 (28.0)	1.2 (30.5)	1.5 (38.1)	1.8 (45.7)	2.1 (53.3)	2.4 (61.0)	2.7 (68.6)	3.0 (76.2)	3.3 (83.8)	3.6 (91.4)	3.9 (99.1)
EZ7	6.0-20.0	0.7 (17.8)	0.50 (12.7)	1.0 (25.4)	1.1 (28.0)	1.2 (30.5)	1.3 (33)	1.4 (35.6)	1.6 (40.6)	1.7 (43.2)	1.9 (48.3)	2.0 (50.8)	2.2 (55.9)	2.4 (61.0)

All dimensions are approximate, based on % BW. Contact factory for actual sizes. All length dimensions are excluding connectors. Dimensions for width are a maximum. The final width will vary with frequency.

IZ Series Length VS. Number of Sections, 25 - 66% BW

Series	Frequency (MHz)	Width In. (mm)	Height In. (mm)	Length vs. Number of Sections — Inches (mm) 3	4	5	6	7	8	9	10	11	12	13
IZ3	0.5-6.0	6.5 (165.1)	0.75 (19.1)	1.1 (28.0)	1.5 (38.1)	1.9 (48.3)	2.3 (58.4)	2.7 (68.6)	3.1 (78.7)	3.5 (88.9)	3.9 (99.1)	4.3 (109.2)	4.7 (119.4)	5.1 (129.5)
IZ4	1.0-8.0	3.5 (88.9)	0.59 (15.0)	1.0 (25.4)	1.2 (30.5)	1.5 (38.1)	1.8 (45.7)	2.1 (53.3)	2.5 (63.5)	2.8 (71.1)	3.2 (81.3)	3.5 (88.9)	3.9 (99.1)	4.2 (106.7)
IZ5	2.0-12.0	2.0 (50.8)	0.63 (16.0)	1.0 (25.4)	1.1 (28.0)	1.2 (30.5)	1.3 (33.0)	1.5 (38.1)	1.8 (45.7)	2.0 (50.8)	2.3 (58.4)	2.5 (63.5)	2.8 (71.1)	3.1 (78.7)
IZ6	4.0-18.0	1.25 (31.8)	0.50 (12.7)	0.9 (22.9)	1.0 (25.4)	1.1 (28.0)	1.2 (30.5)	1.3 (33.0)	1.5 (38.1)	1.6 (40.6)	1.8 (45.7)	2.0 (50.8)	2.2 (55.9)	2.3 (58.4)
IZ7	6.0-20.0	1.00 (25.4)	0.50 (12.7)	0.8 (20.3)	0.9 (22.9)	1.0 (25.4)	1.1 (28.0)	1.2 (30.5)	1.3 (33.0)	1.4 (35.6)	1.5 (38.1)	1.6 (40.6)	1.7 (43.2)	1.8 (45.7)

All dimensions are approximate, based on % BW. Contact factory for actual sizes. All length dimensions are excluding connectors. Dimensions for width are a maximum. The final width will vary with frequency.

LORCH MICROWAVE
1725 N. Salisbury Blvd. · PO Box 2828 · Salisbury, MD 21802
Phone 800.780.2169, 410.860.5100 · Fax 410.860.1949
www.lorch.com · lorchsales@lorch.com

Coaxial

Frequency Mixer WIDE BAND

ZX05-153MH+

Level 13 (LO Power +13 dBm) 3200 to 15000 MHz

CASE STYLE: FL905

Connectors	Model	Price	Qty.
SMA	ZX05-153MH-S+	$48.95	(1-24)

+ RoHS compliant in accordance with EU Directive (2002/95/EC)

The +Suffix has been added in order to identify RoHS Compliance. See our web site for RoHS Compliance methodologies and qualifications.

Maximum Ratings

Operating Temperature	-40°C to 85°C
Storage Temperature	-55°C to 100°C
RF Power	50mW

Permanent damage may occur if any of these limits are exceeded.

Coaxial Connections

LO	2
RF	3
IF	1

Features

- wide bandwidth, 3200 to 15000 MHz
- low conversion loss, 6.5 dB typ.
- high L-R isolation, 36 dB typ.
- excellent IF BW, DC to 4000 MHz
- rugged construction
- small size
- useable as up and down converter
- protected by US patents, 6,790,049 and 7,027,795

Applications

- satellite up and down converters
- defense radar and communications
- line of sight links
- federal fixed service
- WIFI
- blue tooth
- VSAT
- ISM

Outline Drawing

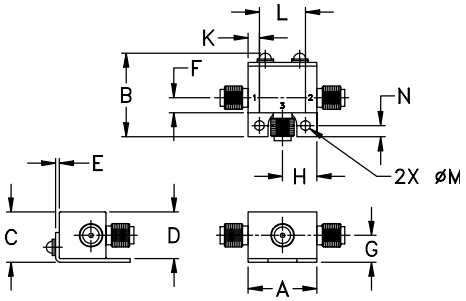

Outline Dimensions (inch / mm)

A	B	C	D	E	F	G
.74	.90	.54	.50	.04	.16	.29
18.80	22.86	13.72	12.70	1.02	4.06	7.37

H	J	K	L	M	N	wt
.37	--	.122	.496	.106	.122	grams
9.40	--	3.10	12.60	2.69	3.10	20.0

Electrical Specifications

FREQUENCY (MHz)		CONVERSION LOSS* (dB)			LO-RF ISOLATION (dB)		LO-IF ISOLATION (dB)		IP3 at center band (dBm)
LO/RF f_L-f_U	IF	Typ.	σ	Max.	Typ.	Min.	Typ.	Min.	Typ.
3200-15000	**DC-4000**								
3200-4500		6.4	0.2	9.3	40	34	19	13	15
4500-5100		6.2	0.2	8.0	35	32	14	10	18
5100-14000		7.5	0.4	13.6	34	22	17	9	17
14000-15000		7.0	0.3	10.5	26	14	24	11	13

1 dB COMPR.: +5 dBm typ.

* Conversion loss at 30 MHz IF. σ is a measure of repeatability from unit to unit.

Typical Performance Data

Frequency (MHz)		Conversion Loss (dB)	Isolation L-R (dB)	Isolation L-I (dB)	VSWR RF Port (:1)	VSWR LO Port (:1)
RF	LO	LO +13dBm	LO +13dBm	LO +13dBm	LO +13dBm	LO +13dBm
3193.10	3223.10	7.79	47.11	20.82	2.39	17.57
3791.60	3821.60	6.32	51.86	19.59	2.88	7.44
4484.60	4514.60	5.92	41.93	16.09	2.33	3.48
5083.10	5113.10	5.94	40.95	12.87	2.75	1.90
5618.60	5648.60	6.29	38.97	14.17	3.46	2.65
6217.10	6247.10	5.90	40.72	16.68	2.79	3.90
6815.60	6845.60	5.61	39.73	18.51	2.14	4.30
7414.10	7444.10	5.33	37.25	16.36	1.52	3.19
8012.60	8042.60	5.50	30.38	12.32	1.56	2.13
8611.10	8641.10	5.72	37.50	19.00	2.22	1.83
9209.60	9239.60	6.31	33.03	22.52	3.30	1.99
10028.60	10058.60	8.48	31.28	17.81	4.62	1.90
10627.10	10657.10	8.76	36.89	23.65	4.95	2.47
11225.60	11255.60	8.77	37.44	29.08	5.33	3.65
11824.10	11854.10	8.51	32.31	34.91	4.78	4.83
12422.60	12452.60	8.67	30.24	37.24	4.13	4.80
13021.10	13051.10	7.66	26.56	37.10	3.67	3.60
13997.60	14027.60	7.84	29.74	30.66	3.20	4.00
14627.60	14657.60	8.55	26.54	22.01	2.75	3.80
15005.60	15035.60	8.82	19.09	16.55	2.05	3.01

Electrical Schematic

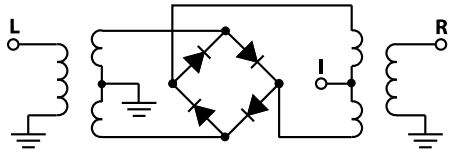

Notes: 1. Performance and quality attributes and conditions not expressly stated in this specification sheet are intended to be excluded and do not form a part of this specification sheet. **2.** Electrical specifications and performance data contained herein are based on Mini-Circuit's applicable established test performance criteria and measurement instructions. **3.** The parts covered by this specification sheet are subject to Mini-Circuits standard limited warranty and terms and conditions (collectively, "Standard Terms"); Purchasers of this part are entitled to the rights and benefits contained therein. For a full statement of the Standard Terms and the exclusive rights and remedies thereunder, please visit Mini-Circuits' website at www.minicircuits.com/MCLStore/terms.jsp.

REV. OR
M111660
ZX05-153MH+
ED-12902/10
DJ/AM
091007

ZX05-153MH+
CONVERSION LOSS
at IF= 30 MHz

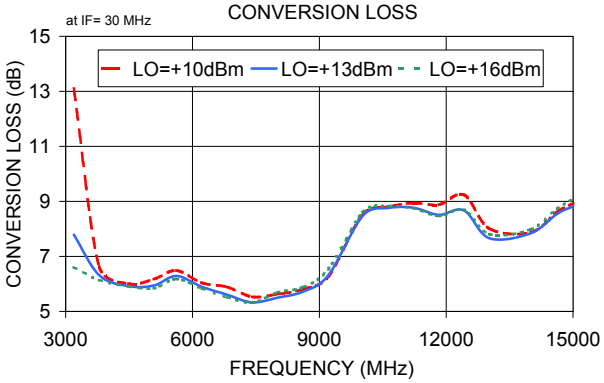

ZX05-153MH+
CONVERSION LOSS VARIABLE IF
RF= 3190 MHz

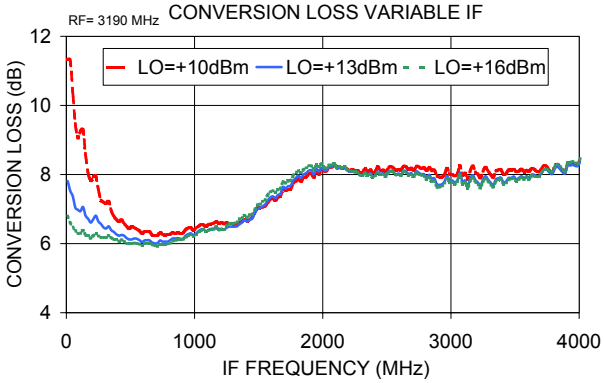

ZX05-153MH+
L-R ISOLATION

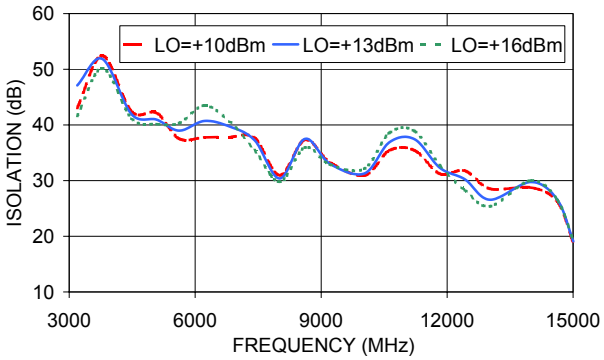

ZX05-153MH+
L-I ISOLATION

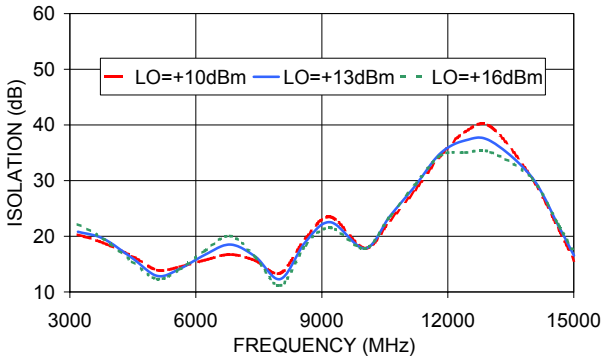

ZX05-153MH+
RF VSWR

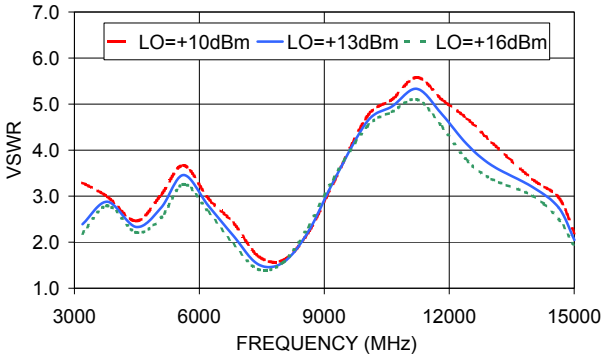

ZX05-153MH+
LO VSWR

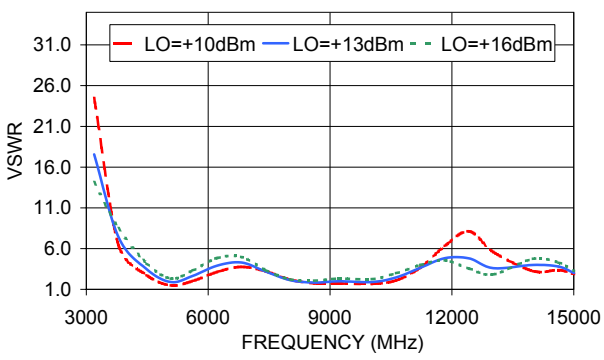

ZX05-153MH+
IF VSWR

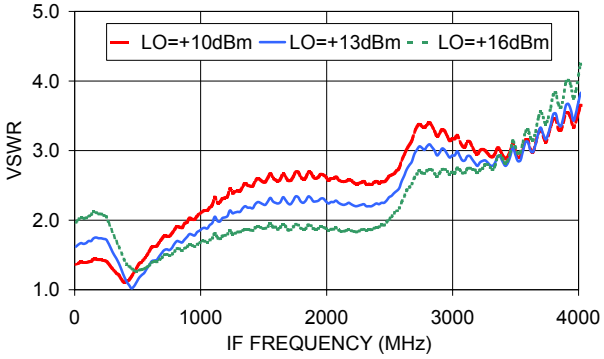

ZX05-153MH+
IP3
at IF= 30 MHz

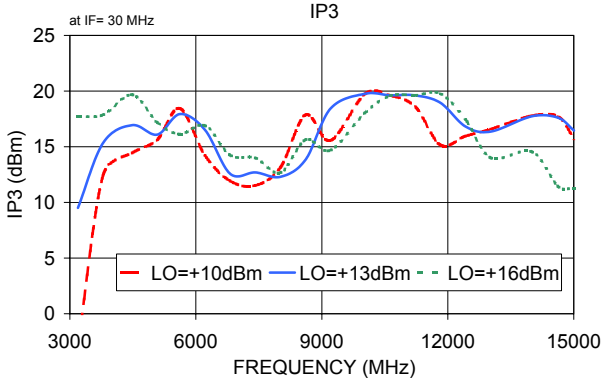

Notes: 1. Performance and quality attributes and conditions not expressly stated in this specification sheet are intended to be excluded and do not form a part of this specification sheet. **2.** Electrical specifications and performance data contained herein are based on Mini-Circuit's applicable established test performance criteria and measurement instructions. **3.** The parts covered by this specification sheet are subject to Mini-Circuits standard limited warranty and terms and conditions (collectively, "Standard Terms"); Purchasers of this part are entitled to the rights and benefits contained therein. For a full statement of the Standard Terms and the exclusive rights and remedies thereunder, please visit Mini-Circuits' website at www.minicircuits.com/MCLStore/terms.jsp.

Microwave Amplifiers Ltd

PRODUCT SPECIFICATION

AM49-06-053RB

Model no : AM49-9.4S-47-49P

ELECTRICAL PARAMETERS:

Frequency Range		9.3-9.5GHz
Small Signal Gain		47dB min, 49dB typ
Gain Flatness		1dB p-p max
Maximum Input Power		+15dBm max
Output Power @ 1dB GCP		+48dBm min, +48.5dBm typ
Output Power Saturated		+48.5dBm min, +49dBm typ
Non-Harmonic Spurious		-80dBc min
Noise Figure @ 25C		8dB max
Input Return Loss		14dB min, 17dB typ
Output Return Loss		14dB min, 17dB typ
TTL Pulse Control Rise Time		5uS max, 3uS typ (see note 1) TTL High = ON
TTL Pulse Control Fall Time		5uS max, 4uS typ (see note 1) TTL Low = OFF, OC = OFF
DC Detector		+5V min @ Pout +48dBm (see note 2)
Power Supply +Ve		+12V DC, +/-0.1V (see note 3)
Supply Current +Ve		38A max
Standby Supply Current		100mA nom
Power Supply –Ve		-8 to -12V DC, 100mA nom
Connectors	RF Input	SMA Female
	RF Output	N Female
	DC	Power D-Type
Dimensions (LWH)		245x180x110mm
Operating Temp Range (Baseplate)		-30 to +70C
Storage Temp Range		-40 to +80C

Microwave Amplifiers Ltd

PRODUCT SPECIFICATION

AM49-06-053RA

Model no : AM49-9.4S-47-49P

Notes:

1. TTL pulse control switching times are measured with CW RF input signal applied.
2. DC detector is RF coupled shottky barrier diode giving DC output approximately proportional to RF.
3. The maximum permissible +V supply is +12.5V.

General Description:

The AM49 power amplifier is a class A linear GaAs fet amplifier designed for optimum RF performance with minimum power consumption. With fast TTL controlled switching, these amplifiers are ideally suited to applications requiring high efficiency with low weight and heat generation and are constructed using the latest GaAs FET devices and high stability composite materials to ensure reliable performance.

Design Features:

Class A Linear design
Fast switching speed
Unconditional stability
Reverse polarity protection
Open & short circuit protection
Over temperature protection
Internally sequenced bias protection
Machined from Solid Aluminium alloy enclosure
Alocrom or Alodine passivated finish

Environmental Performance:

These products are not supplied qualified to any environmental standards. Design practices are employed which will enable the products to operate in harsh industrial environments, and components of appropriate grade are selected for the operating temperature ranges specified.
This product is not suitable for operation in environments subject to water exposure, or in condensing high humidity.

MTBF:

MTBF is estimated to be 100,000Hrs under normal operating conditions.

CE Certification:

All Microwave Amplifiers Ltd products are supplied CE marked where appropriate.

Warranty:

All Microwave Amplifiers Ltd products are supplied with 2 year warranty.

Solid State PIN Control Products

0.5-18 GHz and 2-18 GHz

Super-Slim High Performance Drop-In PIN Switches

- Reflective and Absorptive
- SPST thru SP6T and Transfer (Standard)
- High Speed
- High Isolation – up to 80 dB
- Low Insertion Loss
- Drop-In Applications
- Integral TTL Drivers
- Hermetically Sealed
- Full MIL Specifications

Description

The super-slim series of broadband, hermetically sealed switches offers fast switching speed and low insertion loss in very compact packages. Both 0.5 to 18 GHz and 2 to 18 GHz models are available. The switches are gold plated and have removable SMA connectors for use in drop-in applications. Superior RF performance is achieved over the entire bandwidth due to the use of selected PIN diodes and optimum RF circuit designs.

All models include integral drivers with reverse voltage protection. The drivers are TTL compatible and are tailored to each RF circuit to give optimum switching performance.

The small size, high speed, broad bandwidth and low insertion loss make these switches ideal for EW systems, automatic test equipment and simulators.

Solid State PIN Control Products

Specifications

Reflective Switches, SMA (F), 0.5 to 18 GHz

MODEL	TYPE	SWITCHING TIME MODULATION (ns)	BAND SEGMENTS (GHz)	INSERTION LOSS (dB max.)	VSWR (max.)	ISOLATION (dB min.)	POWER HANDLING (mW)	POWER SUPPLY REQUIREMENTS	
								mA @+5 V	mA @-12 V
SS212DHS	SPST	15	0.5-2 2-4 4-8 8-12 12-18	1.1 1.3 1.6 2.1 2.6	1.6 1.7 1.8 1.9 2.0	70 70 70 70 70	200	50	50
SS122DHS	SP2T	20	0.5-2 2-4 4-8 8-12 12-18	1.5 1.5 2.0 2.4 2.9	1.8 1.9 1.9 2.0 2.0	70 75 70 65 60	200	90	60
SS132DHS	SP3T	20	0.5-2 2-4 4-8 8-12 12-18	1.5 1.5 2.0 2.5 3.0	1.8 1.9 1.9 2.0 2.0	70 75 70 65 60	200	90	60
SS142DHS	SP4T	20	0.5-2 2-4 4-8 8-12 12-18	1.6 1.6 2.1 2.6 3.2	1.8 1.9 1.9 2.0 2.0	70 75 70 65 60	200	110	70
SS152DHS	SP5T	20	0.5-2 2-4 4-8 8-12 12-18	2.0 2.0 2.5 3.0 3.6	1.8 1.9 2.0 2.0 2.0	70 70 70 65 60	200	220	90
SS162DHS	SP6T	20	0.5-2 2-4 4-8 8-12 12-18	2.0 2.0 2.5 3.0 3.6	1.8 1.9 2.0 2.0 2.0	70 70 70 65 60	200	260	100

narda microwave-east an L3 company

www.nardamicrowave.com **E-MAIL:** nardaeast@L-3com.com **TEL:** +1 631 231-1700

Absorptive Switches, SMA (F), 0.5 to 18 GHz

MODEL	TYPE	SWITCHING TIME MODULATION (ns)	BAND SEGMENTS (GHz)	INSERTION LOSS (dB max.)	VSWR (max.)	ISOLATION (dB min.)	POWER HANDLING (mW)	POWER SUPPLY REQUIREMENTS	
								mA @+5 V	mA @-12 V
SS212DHTS	SPST	30	0.5-12 12-18	2.4 2.8	1.9 2.0	55 50	200	50	60
SS212DHTS-80	SPST	30	0.5-12 12-18	2.4 2.8	1.9 2.0	70 80	200	60	60
SS122DHTS	SP2T	30	0.5-12 12-18	2.7 3.1	1.9 2.0	60 55	200	60	60
SS122DHTS-80	SP2T	30	0.5-12 12-18	2.2 2.9	2.0 2.0	80 80	200	90	60
SS132DHTS	SP3T	30	0.5-12 12-18	2.9 3.4	1.9 2.0	60 45	200	105	75
SS142DHTS	SP4T	30	0.5-12 12-18	2.9 3.4	1.9 2.0	60 45	200	110	80
SS152DHTS	SP5T	30	0.5-12 12-18	3.3 4.0	2.0 2.0	60 50	200	220	90
SS162DHTS	SP6T	30	0.5-12 12-18	3.3 4.0	2.0 2.0	60 50	200	250	100

Solid State PIN Control Products

Specifications

Reflective Switches, SMA (F), 2 to 18 GHz

MODEL	TYPE	SWITCHING TIME MODULATION (ns)	BAND SEGMENTS (GHz)	INSERTION LOSS (dB max.)	VSWR (max.)	ISOLATION (dB min.)	POWER HANDLING (mW)	POWER SUPPLY REQUIREMENTS	
								mA @+5 V	mA @-12 V
SS213DHS	SPST	15	2-4 4-8 8-12 12-18	1.2 1.4 1.9 2.4	1.8 1.9 1.9 2.0	50 65 60 60	500	50	50
SS213DHS-80	SPST	15	2-4 4-8 8-12 12-18	1.3 1.5 1.9 2.5	1.8 1.9 2.0 2.0	80 80 80 80	500	60	40
SS123DHS	SP2T	15	2-4 4-8 8-12 12-18	1.5 2.0 2.4 2.9	1.9 1.9 2.0 2.0	75 70 65 60	200	90	60
SS123DHS-80	SP2T	15	2-4 4-8 8-12 12-18	1.5 1.9 2.2 2.9	1.8 1.9 2.0 2.0	80 80 80 80	200	90	60
SS133DHS	SP3T	15	2-4 4-8 8-12 12-18	1.5 2.0 2.5 3.0	1.9 1.9 2.0 2.0	75 70 65 60	200	90	60
SS143DHS	SP4T	15	2-4 4-8 8-12 12-18	1.6 2.1 2.6 3.0	1.9 1.9 2.0 2.0	75 70 65 60	200	110	70
SS153DHS	SP5T	20	2-4 4-8 8-12 12-18	2.0 2.5 3.0 3.6	1.9 2.0 2.0 2.0	70 70 65 60	200	220	90
SS163DHS	SP6T	20	2-4 4-8 8-12 12-18	2.0 2.5 3.0 3.6	1.9 2.0 2.0 2.0	70 70 65 60	200	250	100

Transfer Switch, SMA (F), 2 to 18 GHz

MODEL	TYPE	SWITCHING TIME (ns)	BAND SEGMENTS (GHz)	INSERTION LOSS (dB max.)	VSWR (max.)	ISOLATION (dB min.)	POWER HANDLING (mW)	POWER SUPPLY REQUIREMENTS	
								mA @+5 V	mA @-12 V
XSS323CDHS	XFER	50	2-4 4-8 8-12 12-18	1.8 2.2 2.1 2.6	1.8 1.9 2.0 2.0	70 70 60 55	200	80	80

narda microwave-east an L3 company

www.nardamicrowave.com **E-MAIL:** nardaeast@L-3com.com **TEL:** +1 631 231-1700

Solid State PIN Control Products

Absorptive Switches, SMA (F), 2 to 18 GHz

MODEL	TYPE	SWITCHING TIME MODULATION (ns)	BAND SEGMENTS (GHz)	INSERTION LOSS (dB max.)	VSWR (max.)	ISOLATION (dB min.)	POWER HANDLING (mW)	POWER SUPPLY REQUIREMENTS	
								mA @+5 V	mA @-12 V
SS213BDHTS	SPST	20 20 20 25 25	2-4 4-8 8-12 12-16 16-18	1.5 1.7 2.1 2.5 2.5	1.9 1.9 1.9 2.0 2.0	65 60 55 50 50	200	40	60
SS123BDHTS	SP2T	20 20 20 25 25	2-4 4-8 8-12 12-16 16-18	1.6 1.8 2.5 2.9 2.9	1.9 1.9 1.9 2.0 2.0	65 65 60 55 55	200	60	60
SS133BDHTS	SP3T	20 20 20 25 25	2-4 4-8 8-12 12-16 16-18	1.8 2.0 2.7 3.2 3.2	1.9 1.9 1.9 2.0 2.0	65 65 60 50 45	200	105	75
SS143BDHTS	SP4T	20 20 20 25 25	2-4 4-8 8-12 12-16 16-18	1.8 2.0 2.7 3.2 3.2	1.9 1.9 1.9 2.0 2.0	65 65 60 50 45	200	105	75
SS153BDHTS	SP5T	25 25 25 25 25	2-4 4-8 8-12 12-16 16-18	2.2 2.7 3.2 3.8 3.8	1.9 2.0 2.0 2.0 2.0	65 65 60 50 50	200	220	90
SS163BDHTS	SP6T	25 25 25 25 25	2-4 4-8 8-12 12-16 16-18	2.2 2.7 3.2 3.8 3.8	1.9 2.0 2.0 2.0 2.0	65 65 60 50 50	200	250	100

Solid State PIN Control Products

Electrical Specifications

TTL CONTROL LOGIC
Logic 0 (0-0.8 V, 1.6 mA max. sink @ 0.4 V) = Insertion Loss
Logic 1 (2.0-5.5 V, 40 µA max. source @ 2.4 V) = Isolation

FOR TRANSFER SWITCH (XSS323CDHS)
Logic 0: J1-J4 and J2-J3 at Insertion Loss
Logic 1: J1-J2 and J4-J3 at Insertion Loss

SWITCHING TIME
T on = 50% TTL to 90% of RF voltage
T off = 50% TTL to 10% of RF voltage

SWITCHING RATE
5 MHz max. PRF @50% duty cycle

DRIVER
Reverse voltage protected

SURVIVAL POWER at 25°C (Cold Switching)
1.0 W CW, 20W Peak (1µs max. pulse width, 5% duty cycle)
Derate linearly to 50% at +95°C

Environmental Specifications

TEMPERATURE
Operating -54°C to +95°C
Storage -65°C to +125°C

HUMIDITY
Per MIL-STD-202F, method 103B, condition B
(96 hours at 95% R.H.)

SHOCK
Per MIL-STD-202F, method 213B, condition B
(75 G, 6 ms)

ALTITUDE
Per MIL-STD-202F, method 105C, condition B
(50,000 feet)

VIBRATION
Per MIL-STD-202F, method 204D, condition B
(.06" double amplitude or 15 G, whichever is less)

THERMAL SHOCK
Per MIL-STD-202F, method 107D, condition A (5 cycles)

Options

- Very Low Loss Video Leakage
- Inverted TTL Logic Control
- BCD Decoder Driver
- Package Configuration
- Over Voltage Protection

narda microwave-east an L3 company
www.nardamicrowave.com E-MAIL: nardaeast@L-3com.com TEL: +1 631 231-1700

Outline Drawings

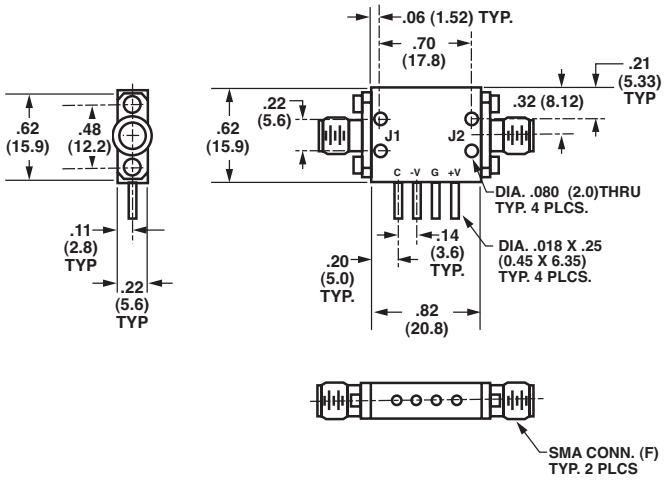

SS213DHS, SS213BDHTS

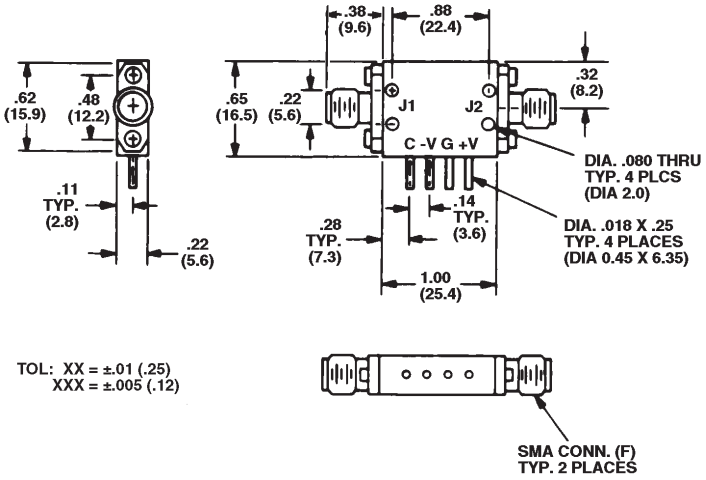

SS213DHS-80, SS212DHS, SS212DHTS

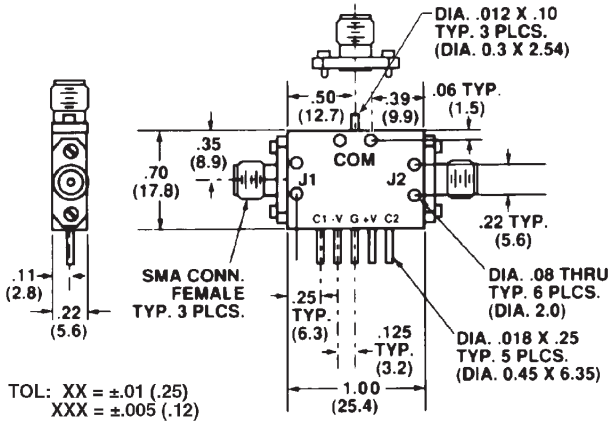

SS123DHS, SS123BDHTS, SS122DHS, SS123DHS-80, SS122DHTS

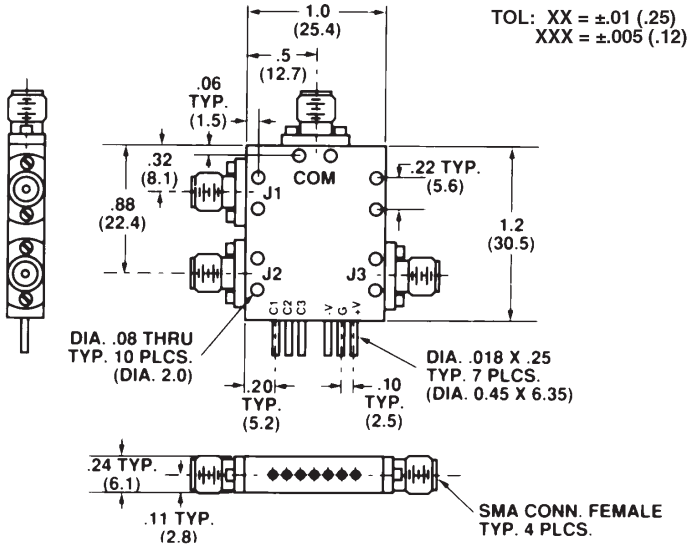

SS133DHS, SS133BDHTS, SS132DHS, SS132DHTS

Dimensions in inches (mm in parentheses), unless otherwise specified.

Solid State PIN Control Products

Outline Drawings

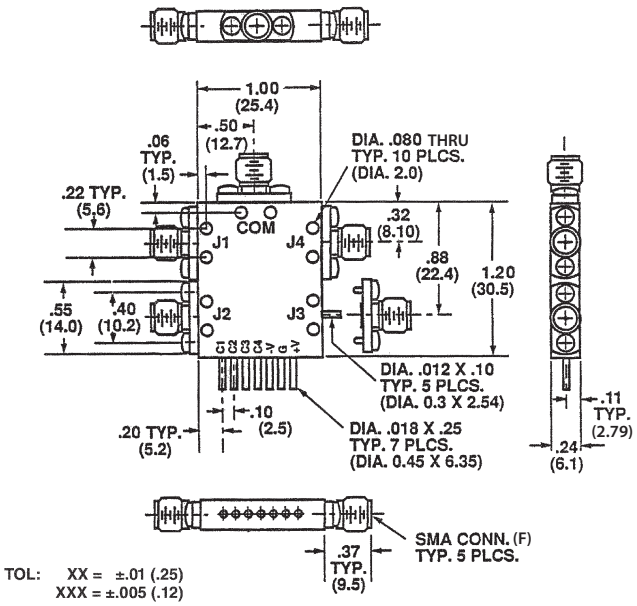

SS143DHS, SS143BDHTS, SS142DHS, SS142DHTS

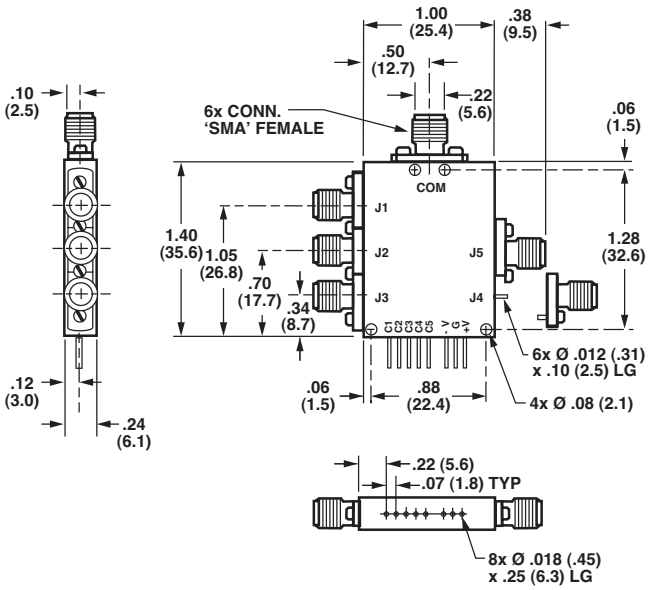

SS153DHS, SS153BDHTS, SS152DHTS, SS152DHS

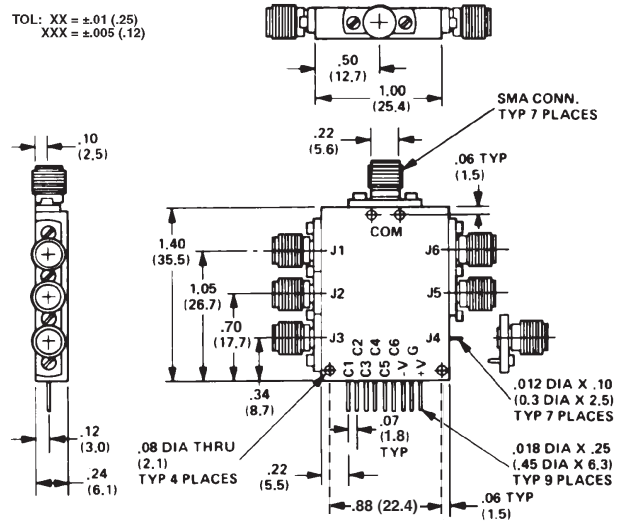

SS163DHS, SS163BDHTS, SS162DHS, SS162DHTS

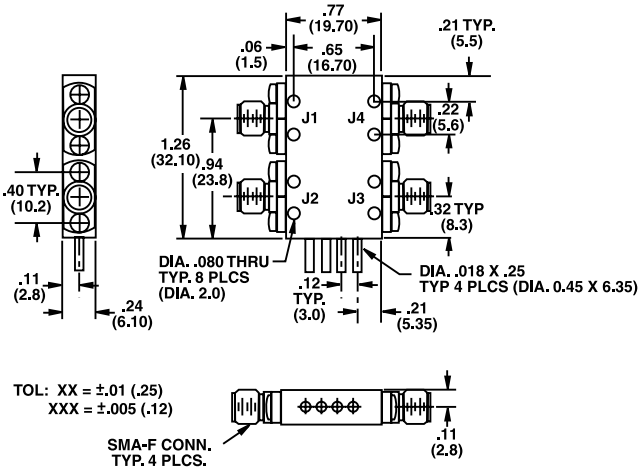

XSS323CDHS

Dimensions in inches (mm in parentheses), unless otherwise specified.

narda microwave-east an L3 company
www.nardamicrowave.com E-MAIL: nardaeast@L-3com.com TEL: +1 631 231-1700

2- 18 GHz 8-Way Power Divider/Combiner – RPDC020180A8S (Richardson RFPD)

Key Attributes	Value
Package Type	Rectangular, SMA Connectors
Divide By	8
Frequency	18 GHz
Impedance	50 Ω
Isolation	16 dB
IL	3 dB
VSWR (~:1)	1.8:1
Amplitude Balance	±0.4 dB
Phase Balance	±5 °

S-parameters measurement at 9.36 GHz

Unit #	worst case S11 [dB]	worst case S22 [dB]	phase unbalance [°]	amp unbalance [dB]	max loss [dB]	min isolation [dB]
1	-13.70	-13.56	2.02	0.49	1.51	
2	-14.61	-16.24	2.44	0.33	1.33	-31.78
3	-13.46	-15.23	2.76	0.47	1.59	
4	-14.86	-15.12	1.52	0.3	1.27	
5	-17.12	-14.39	2.19	0.49	1.53	
6	-16.64	-14.94	1.86	0.53	1.32	
7	-13.98	-14.45	3.10	0.43	1.30	
8	-12.29	-13.18	1.83	0.52	1.52	
9	-14.81	-13.92	1.30	0.29	1.40	
10	-14.08	-13.62	2.26	0.31	1.42	
11	-20.13	-16.76	1.20	0.32	1.27	-40.30
12	-12.62	-13.78	1.33	0.54	1.70	-33.45
13	-14.95	-15.03	2.62	0.35	1.29	
14	-13.50	-14.24	2.98	0.32	1.32	
15	-15.93	-13.23	3.54	0.76	1.70	-26.13
16	-13.96	-13.82	2.86	0.4	1.50	
17	-15.53	-14.05	3.26	0.27	1.42	
18	-15.03	-15.57	2.49	0.2	1.35	
19	-15.25	-14.91	2.66	0.16	1.27	
20	-16.66	-16.10	2.26	0.49	1.41	
21	-12.01	-14.33	2.93	0.22	1.52	
22	-16.47	-15.13	3.9	0.3	1.38	
23	-13.44	-14.97	1.39	0.32	1.44	
24	-13.30	-15.24	1.49	0.52	1.52	
25	-15.13	-14.58	0.76	0.27	1.22	
26	-19.83	-17.25	1.68	0.38	1.17	
27	-14.63	-14.59	1.72	0.47	1.42	
28	-12.62	-12.31	2.74	0.31	1.53	
29	-11.71	-12.70	1.96	0.80	2.02	-28.00
30	-14.46	-15.15	3.38	0.54	1.51	
31	-12.99	-14.25	1.17	0.20	1.36	
32	-16.19	-16.11	1.09	0.23	1.10	
33	-14.01	-14.07	3.38	0.59	1.41	
34	-12.73	-12.66	2.43	0.43	1.50	-32.11
35	-15.95	-16.54	1.21	0.22	1.32	
36	-15.60	-14.92	3.65	0.73	1.43	
Avr	-14.73	-14.64	2.26	0.40	1.42	
Min	-20.13	-17.25	0.76	0.16	1.10	
Max	-11.71	-12.31	3.90	0.80	2.02	
σ	1.88	1.14	0.83	0.16	0.17	

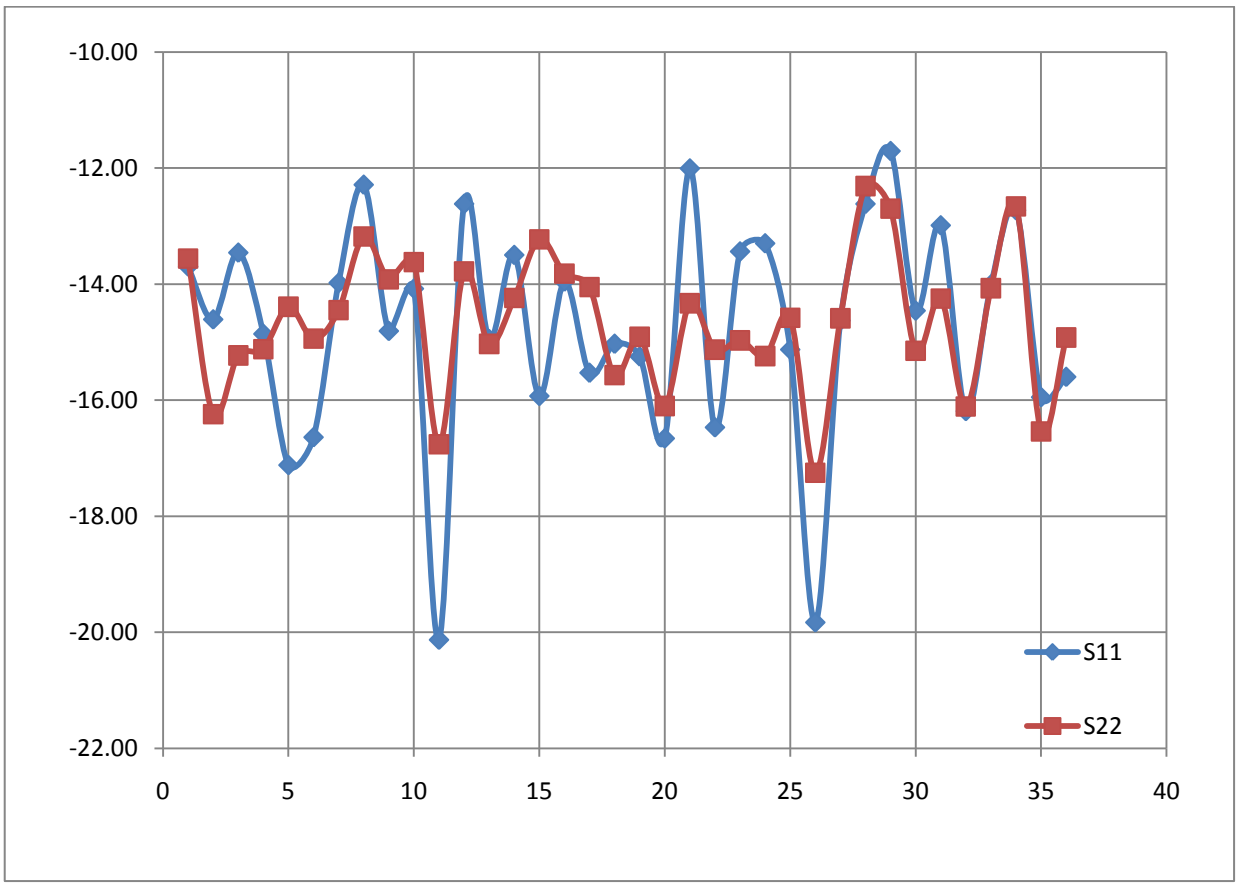
-10.00
-12.00
-14.00
-16.00
-18.00
-20.00
-22.00
0
5
10
15
20
25
30
35
40
S11
S22

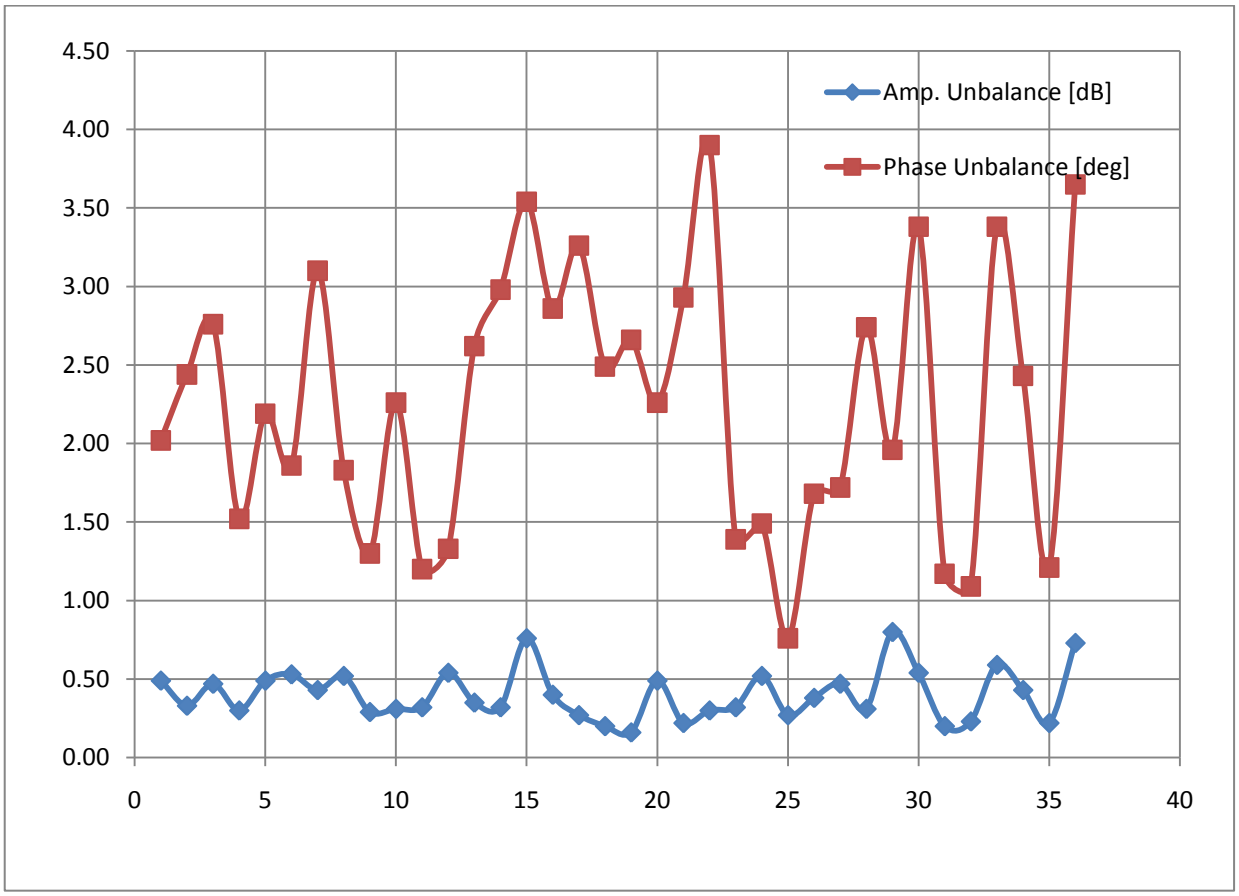
4.50
4.00
3.50
3.00
2.50
2.00
1.50
1.00
0.50
0.00
0
5
10
15
20
25
30
35
40
Amp. Unbalance [dB]
Phase Unbalance [deg]

POWER DIVIDER #001

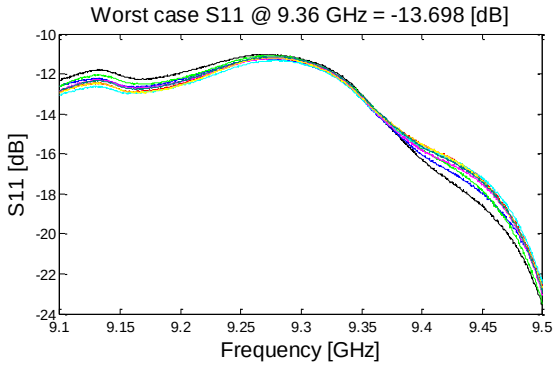

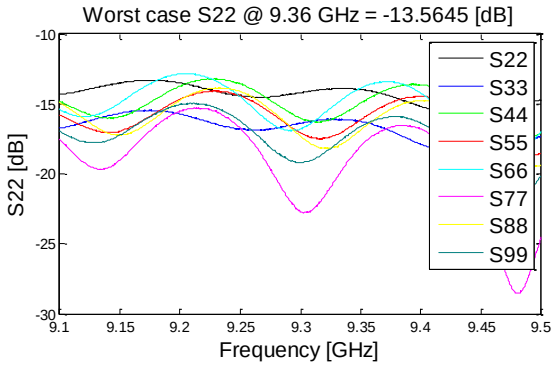

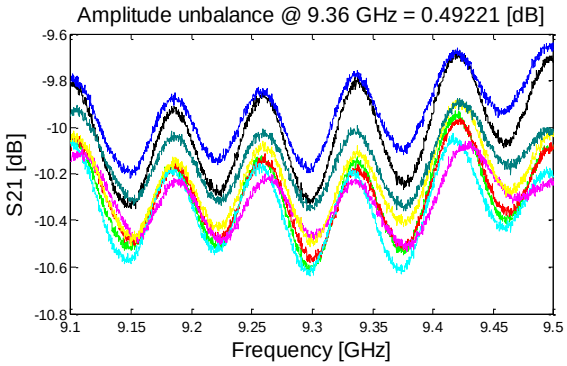

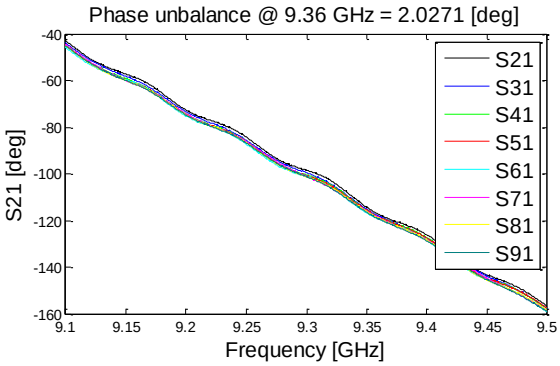

POWER DIVIDER #002

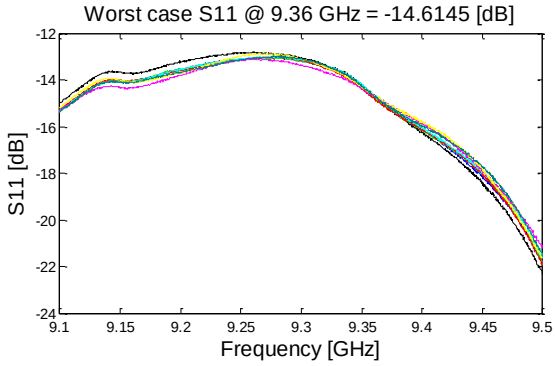

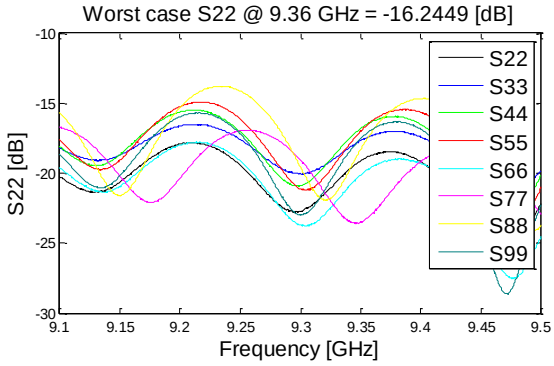

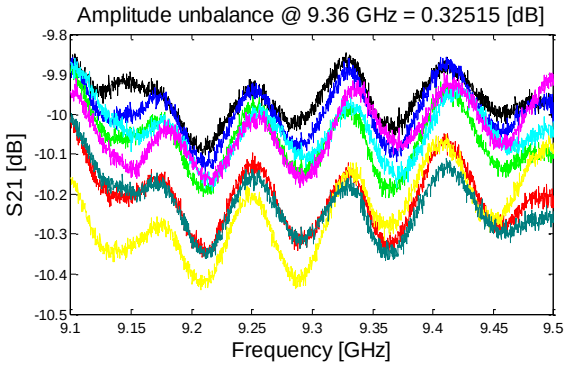

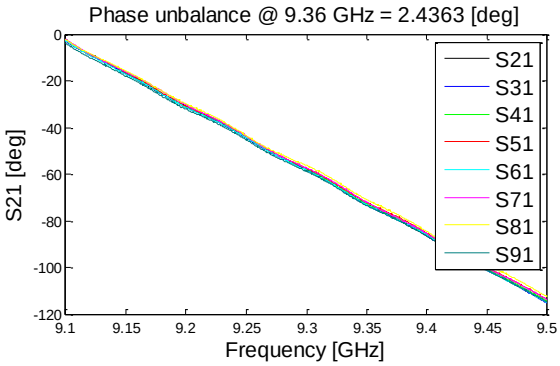

POWER DIVIDER #003

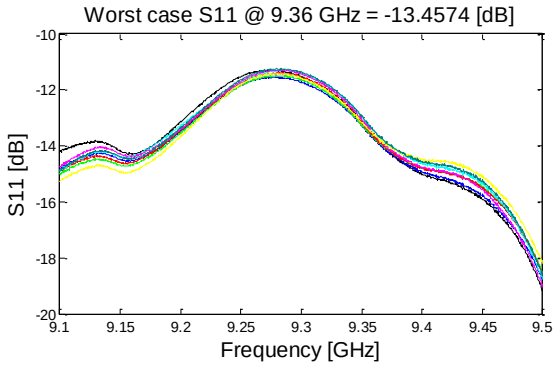

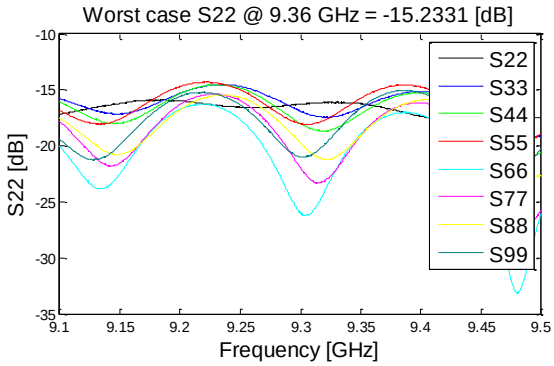

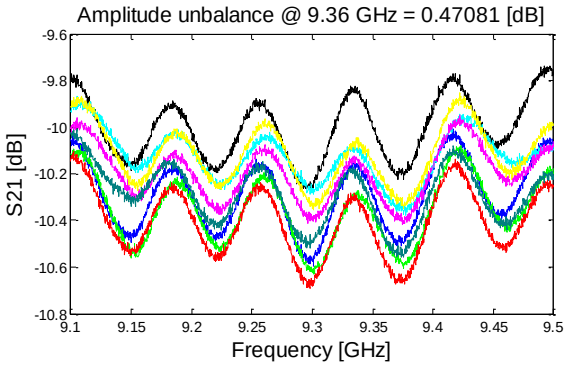

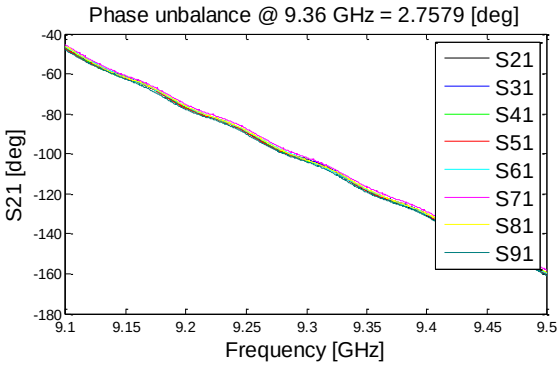

POWER DIVIDER #004

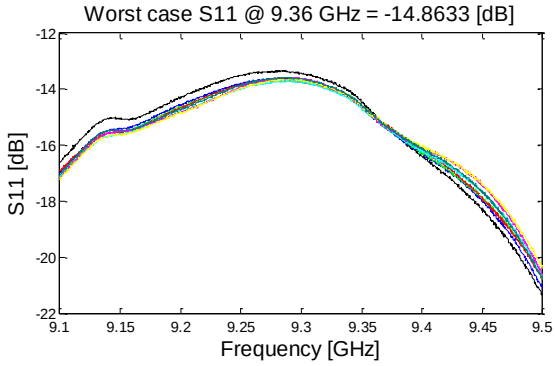

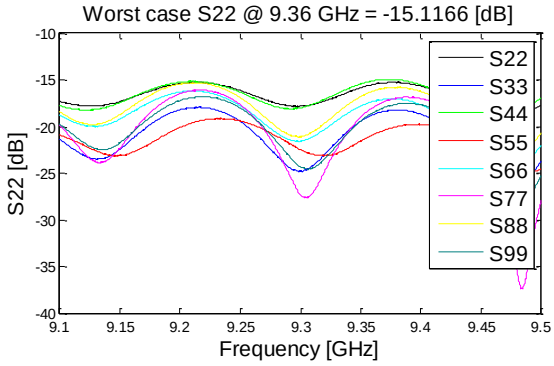

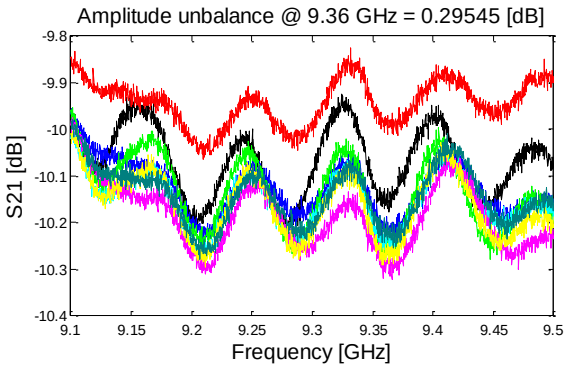

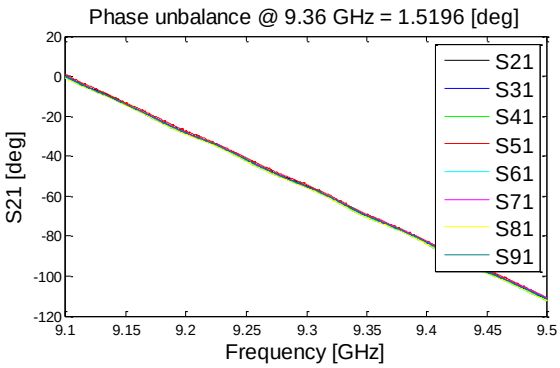

POWER DIVIDER #005

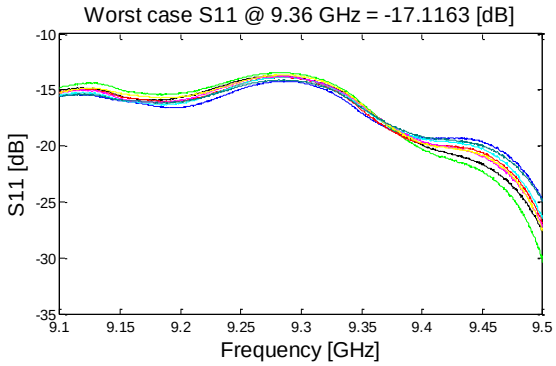

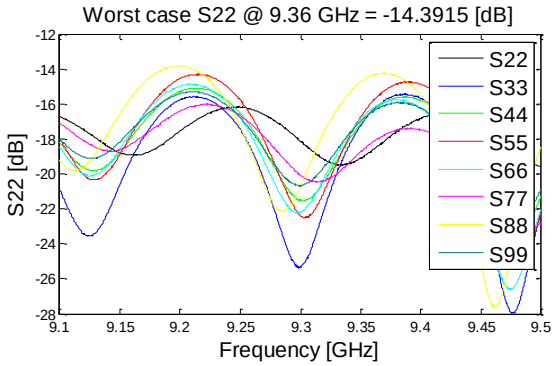

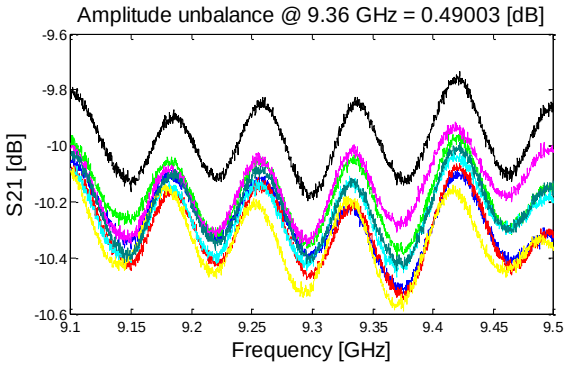

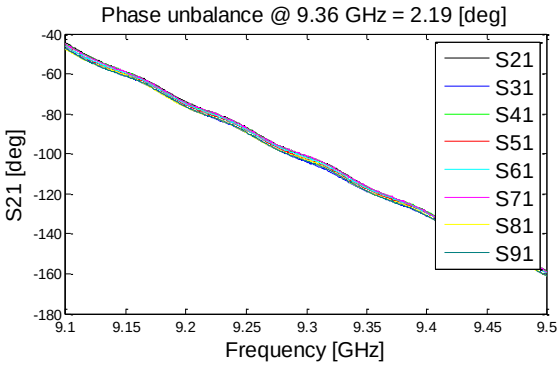

POWER DIVIDER #006

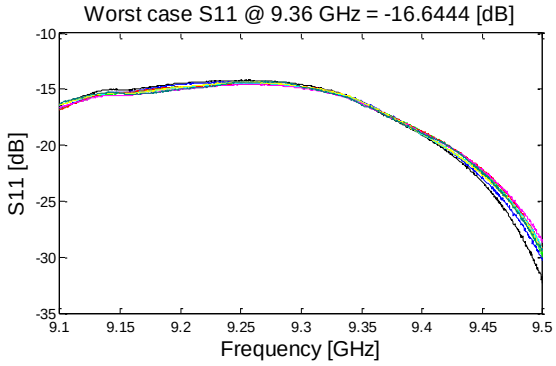

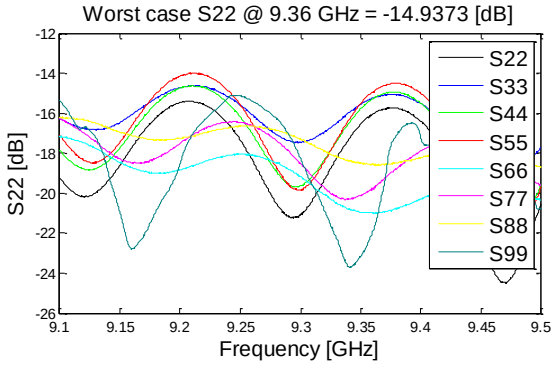

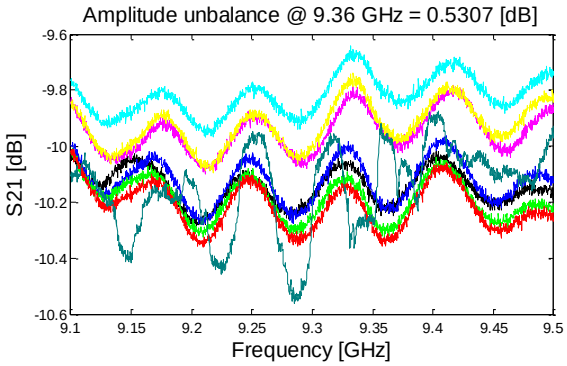

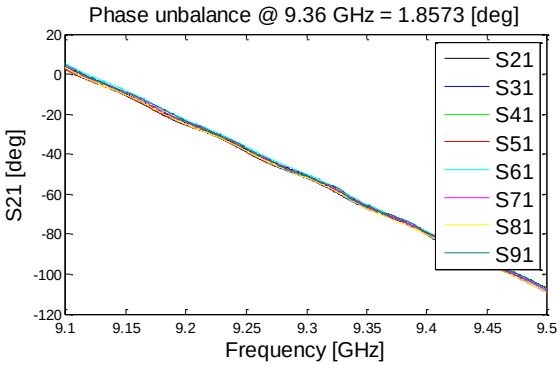

POWER DIVIDER #007

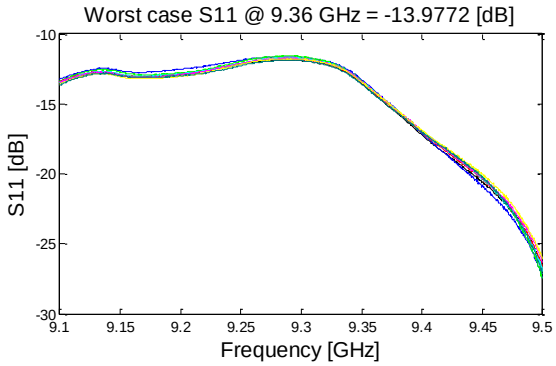

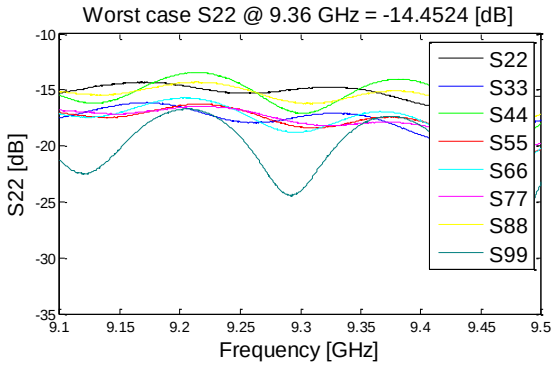

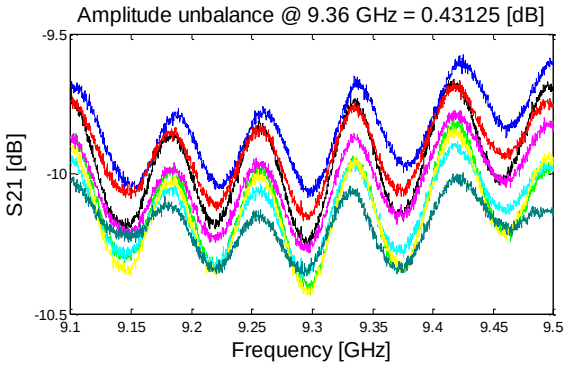

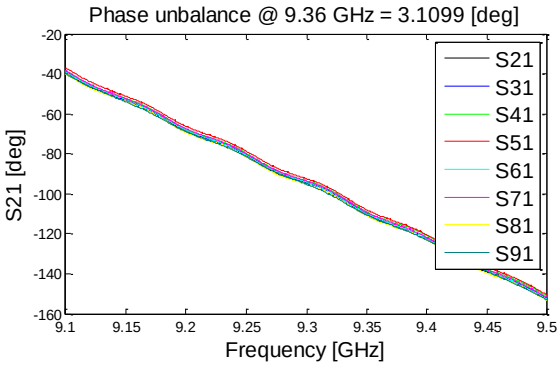

POWER DIVIDER #008

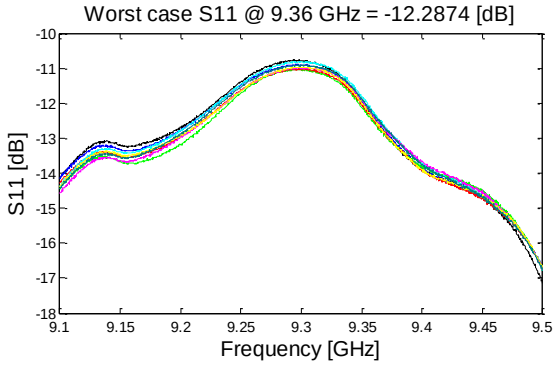

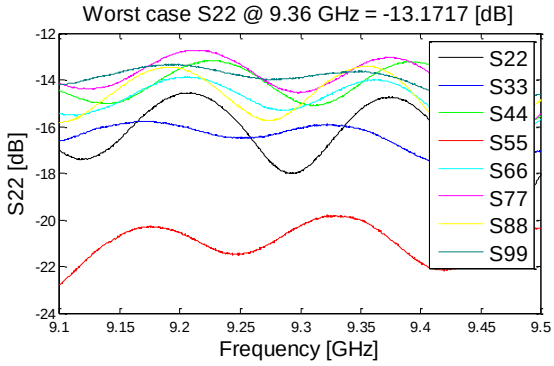

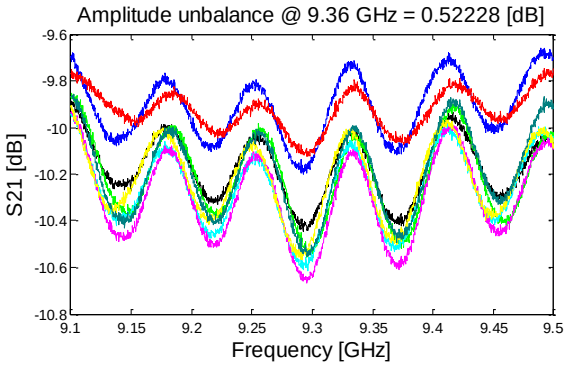

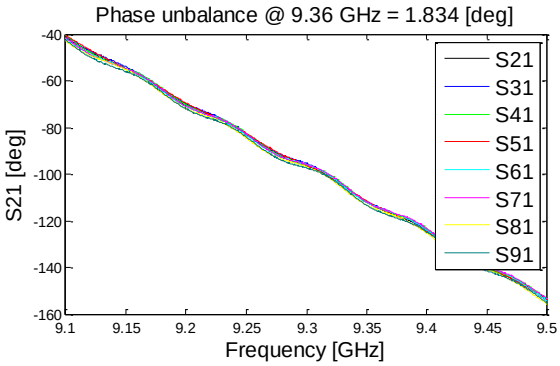

POWER DIVIDER #009

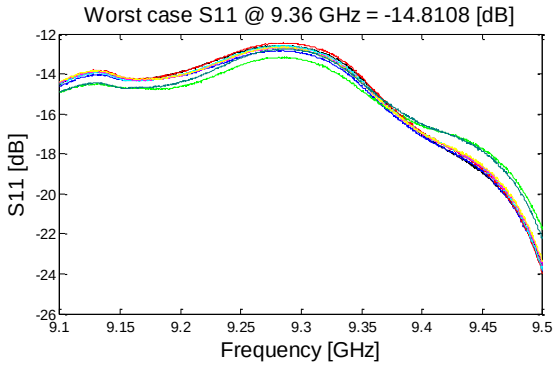

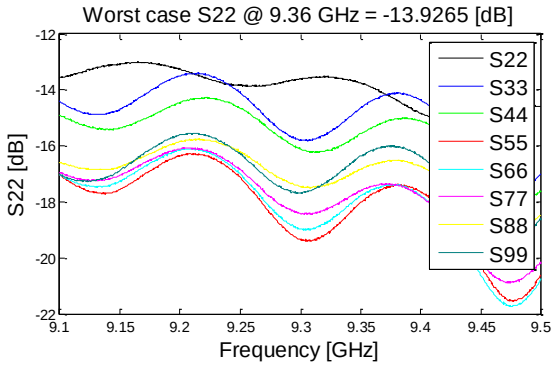

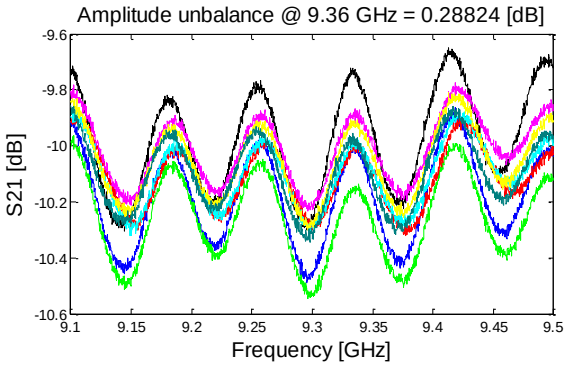

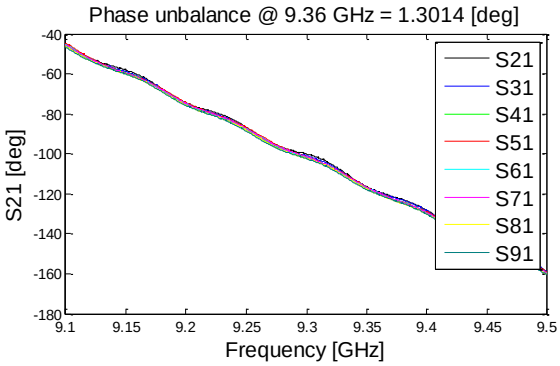

POWER DIVIDER #010

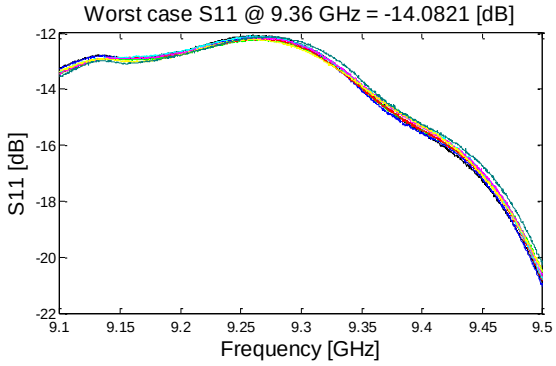

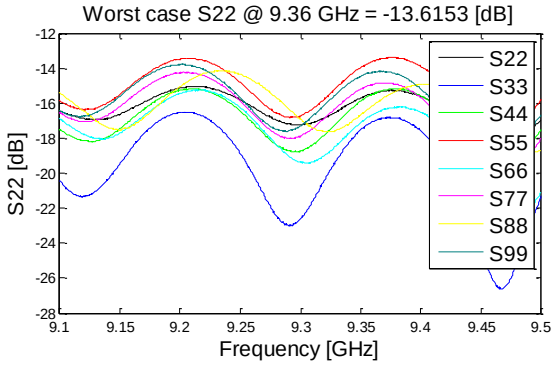

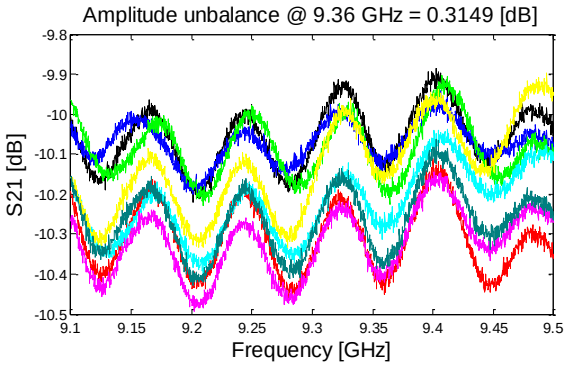

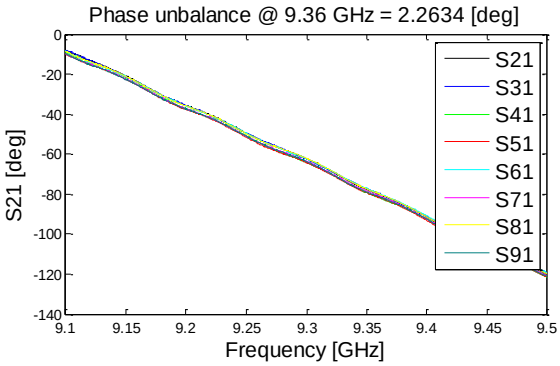

POWER DIVIDER #011

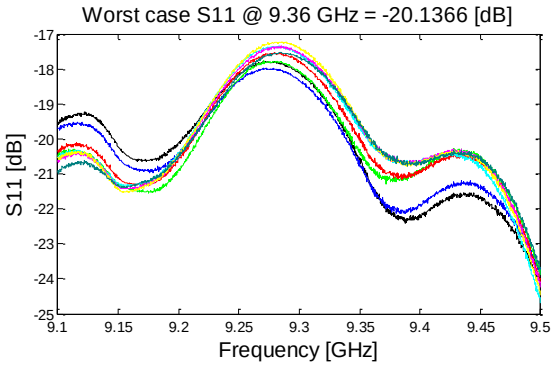

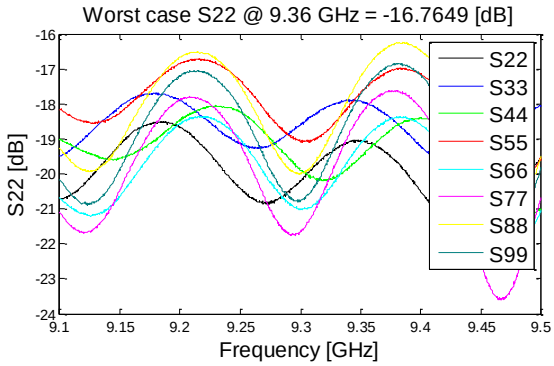

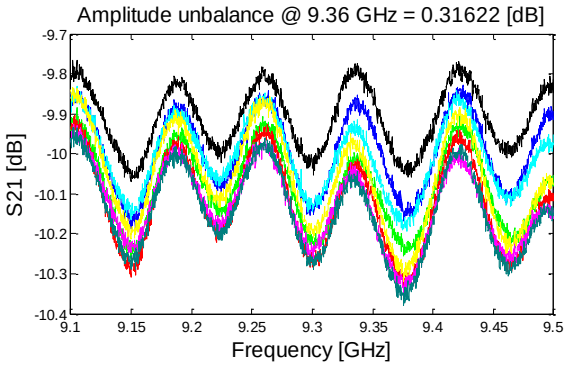

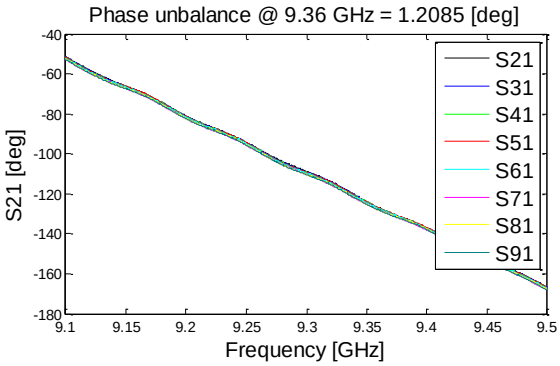

POWER DIVIDER #012

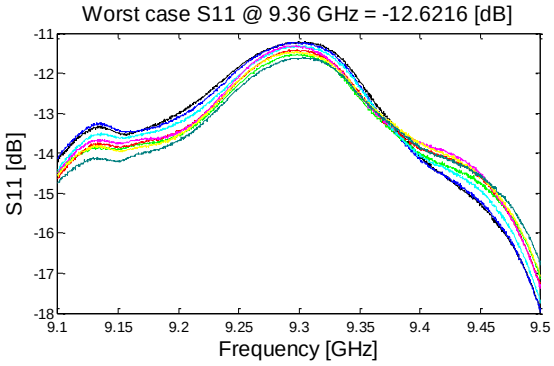

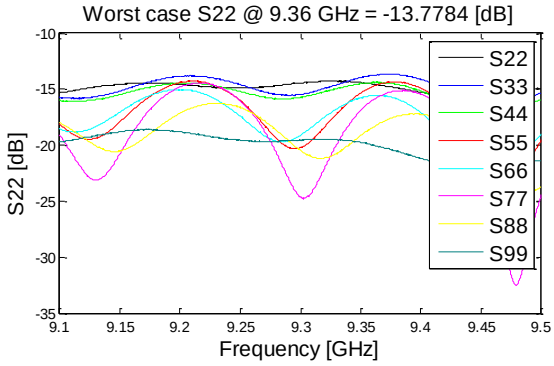

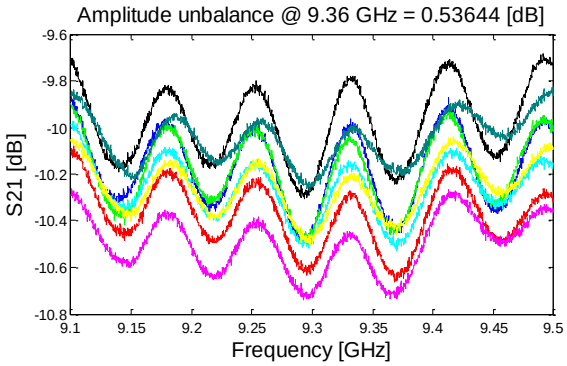

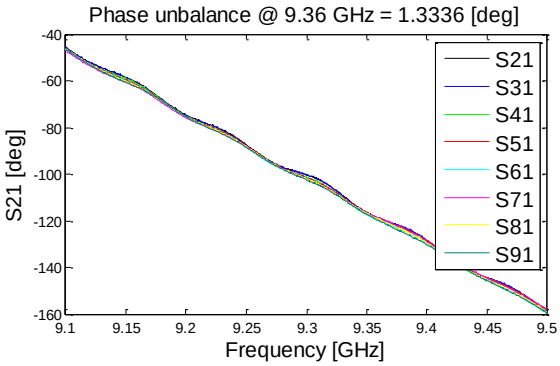

POWER DIVIDER #013

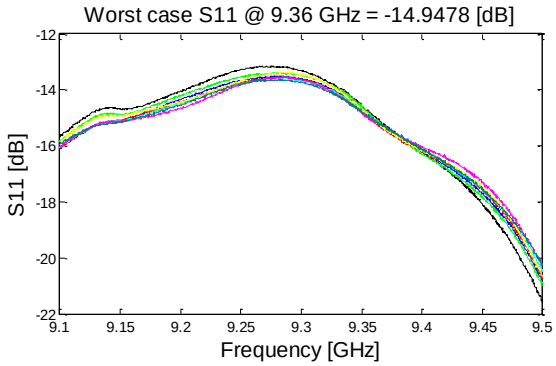

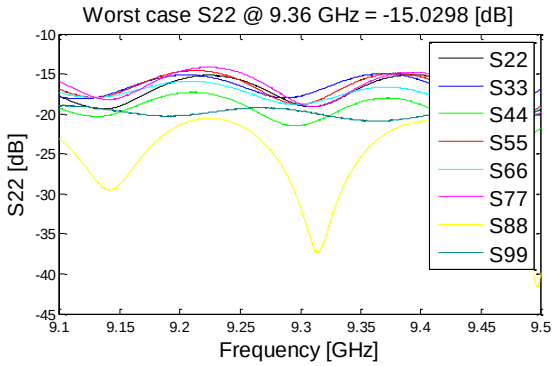

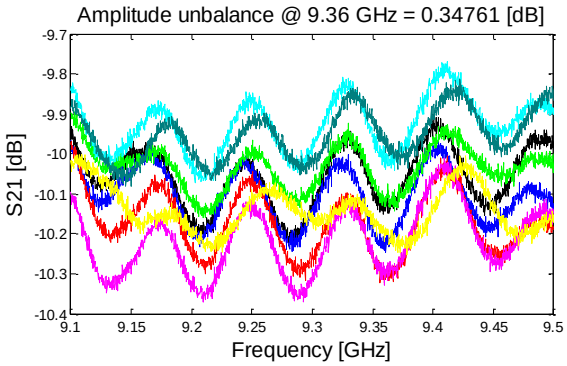

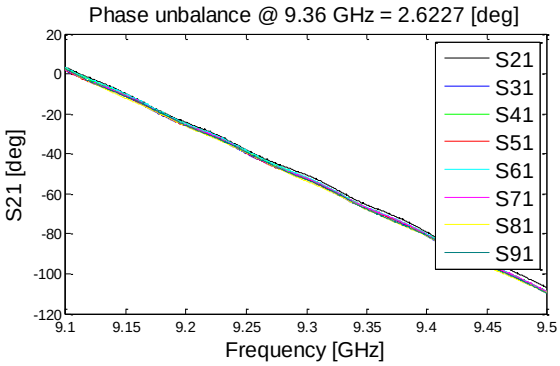

POWER DIVIDER #014

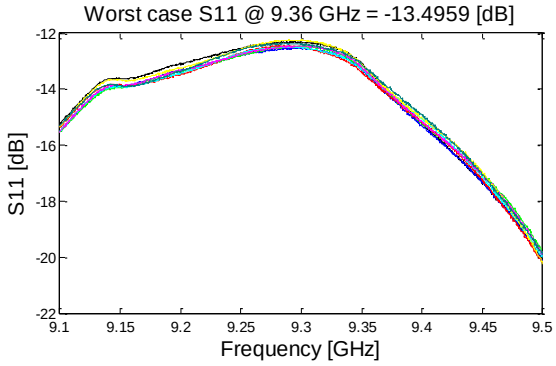

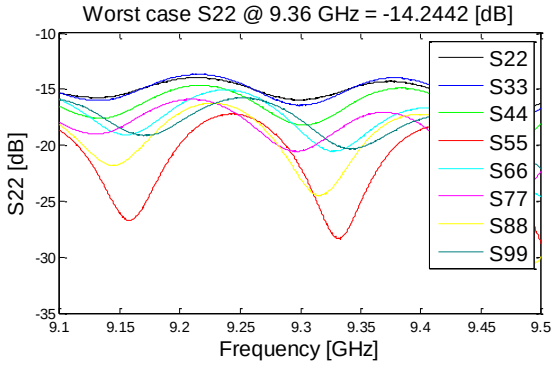

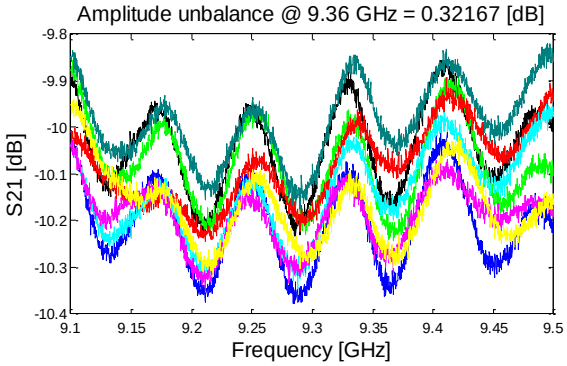

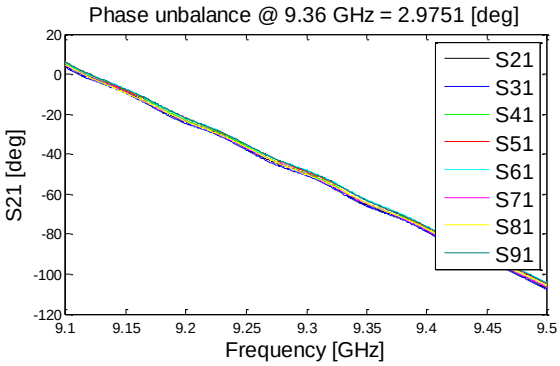

POWER DIVIDER #015

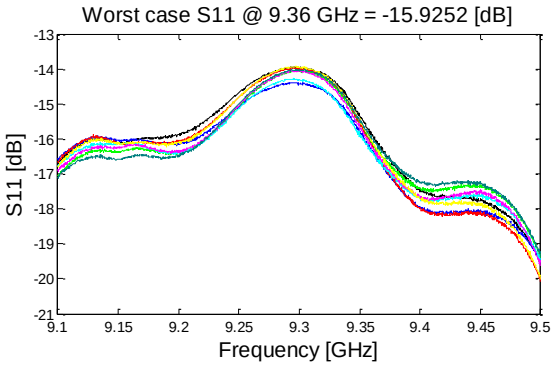

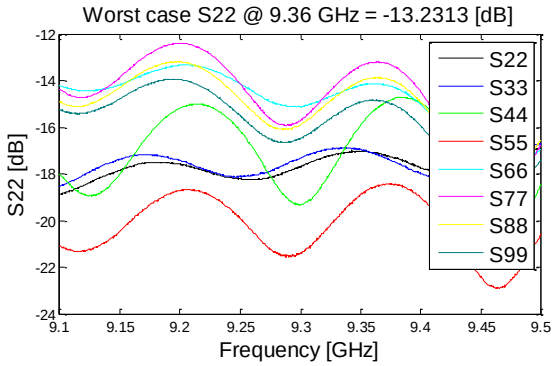

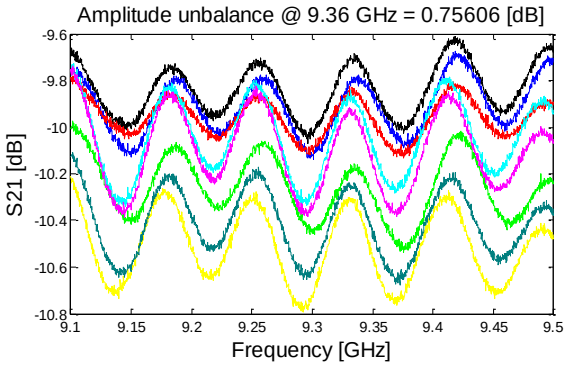

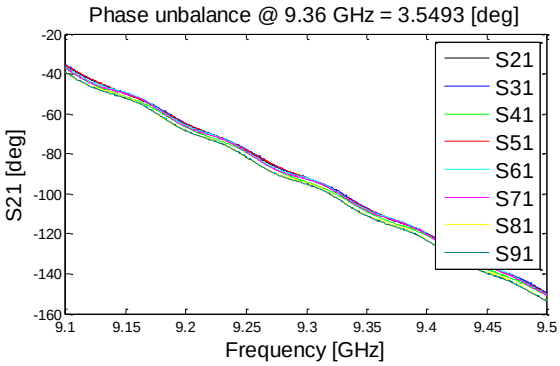

POWER DIVIDER #016

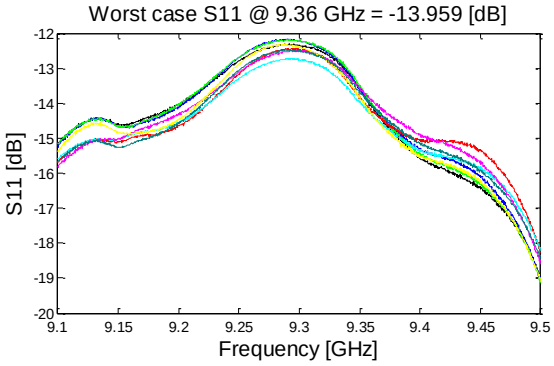

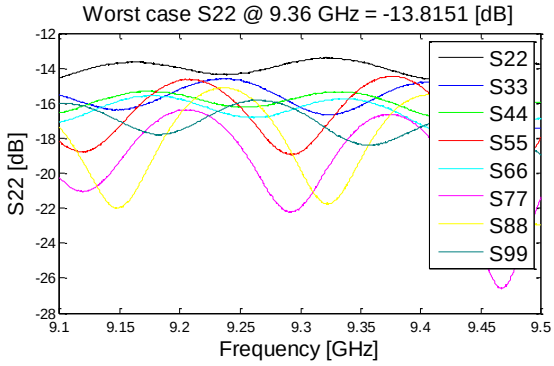

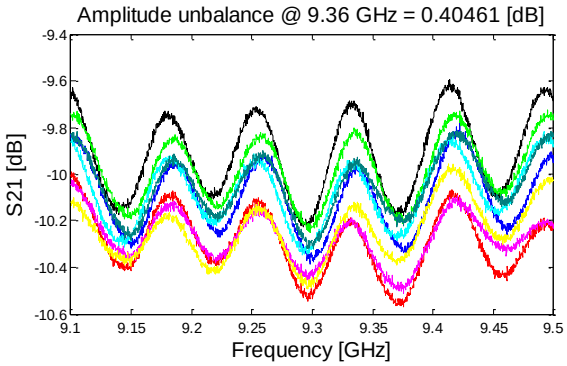

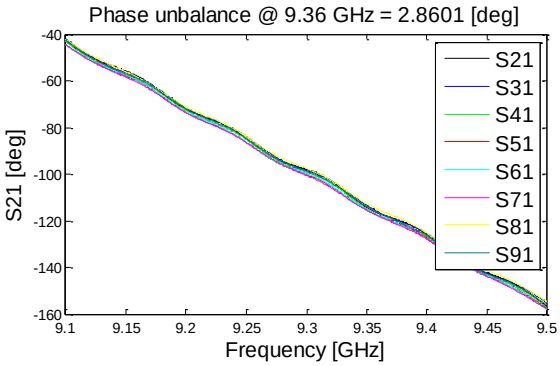

POWER DIVIDER #017

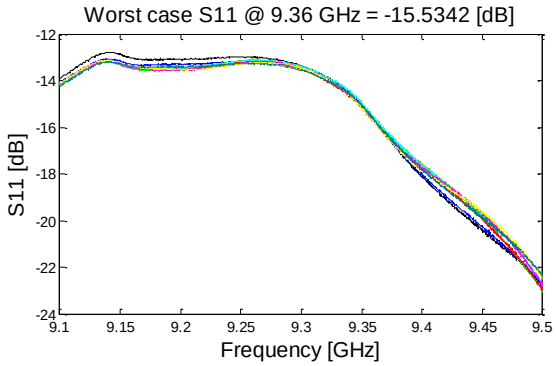

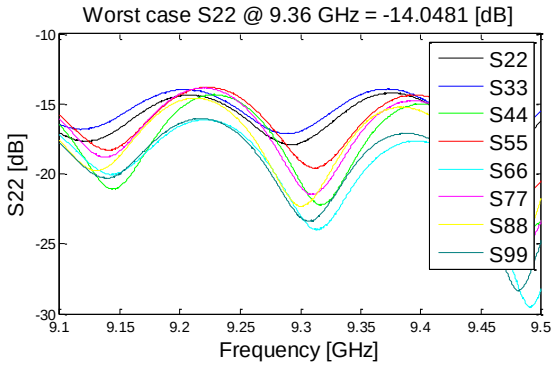

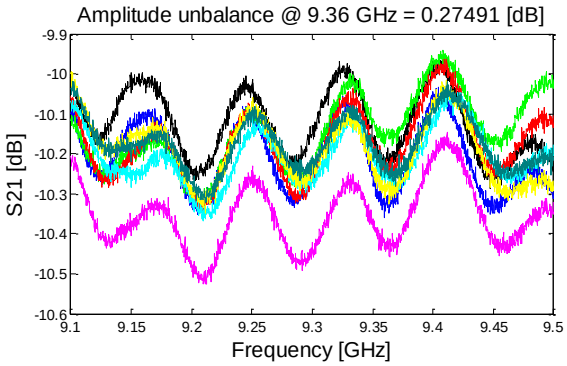

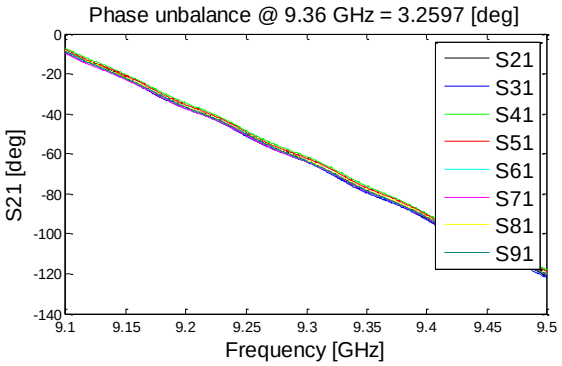

POWER DIVIDER #018

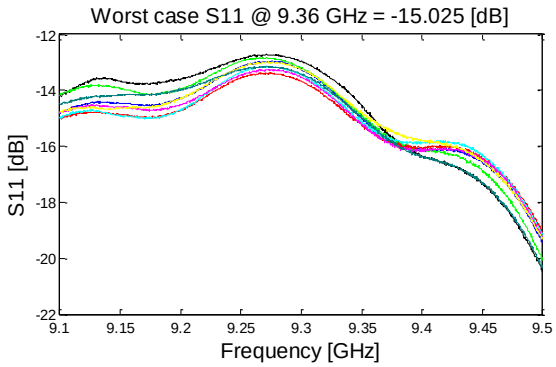

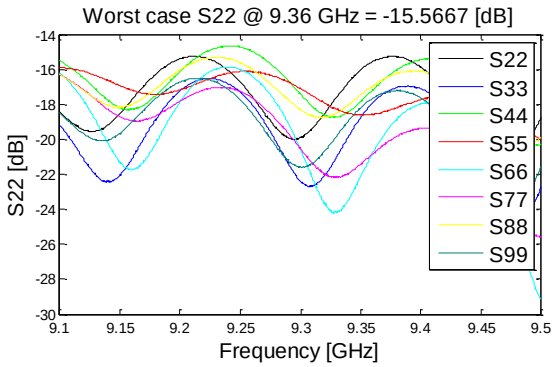

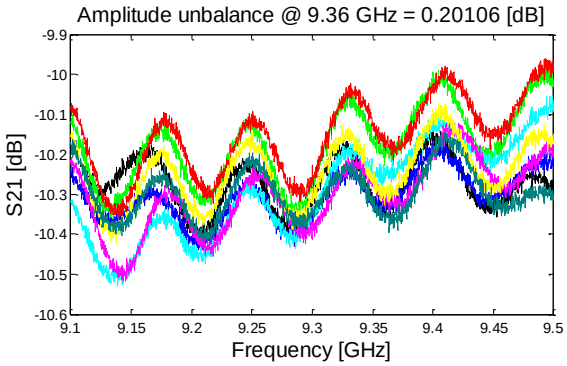

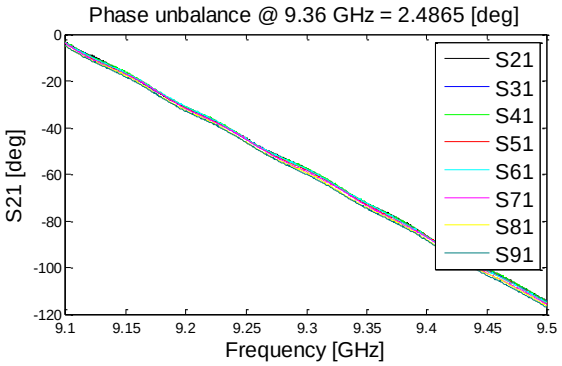

POWER DIVIDER #019

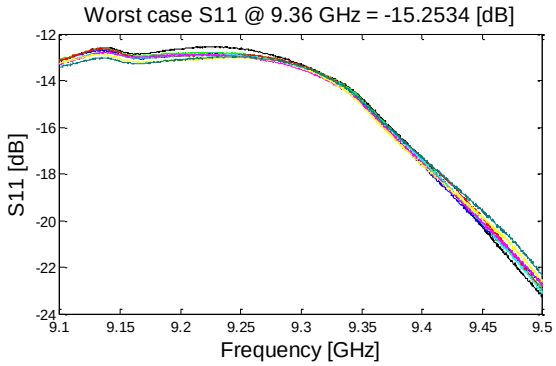

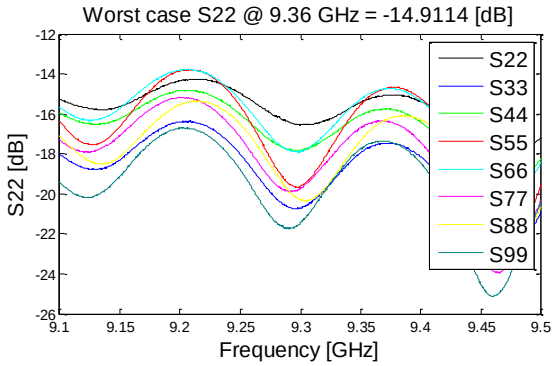

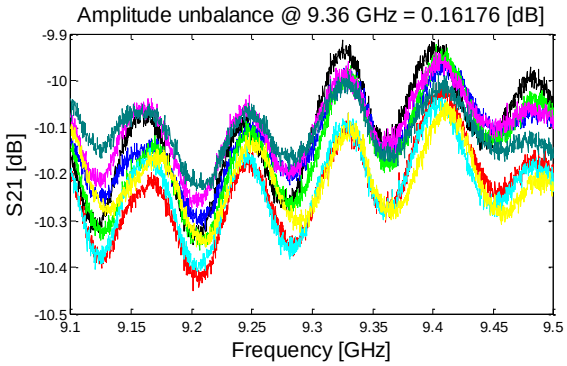

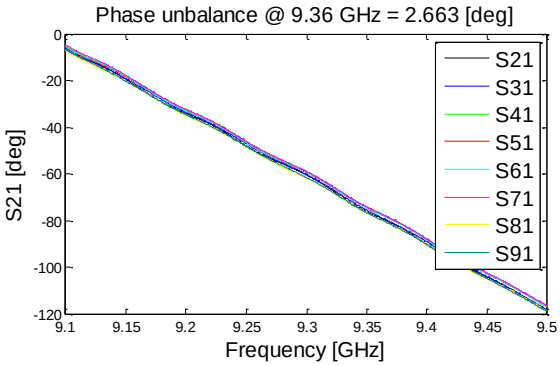

POWER DIVIDER #020

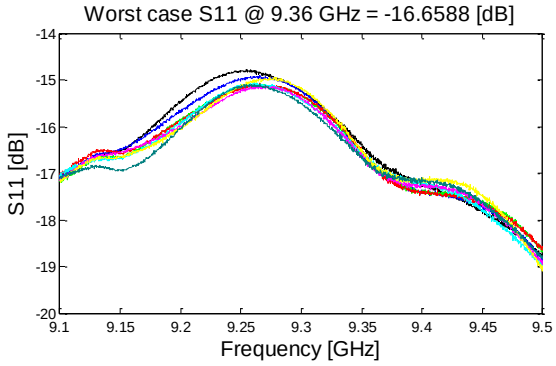

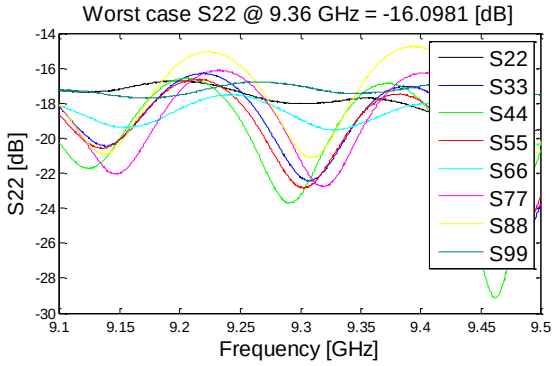

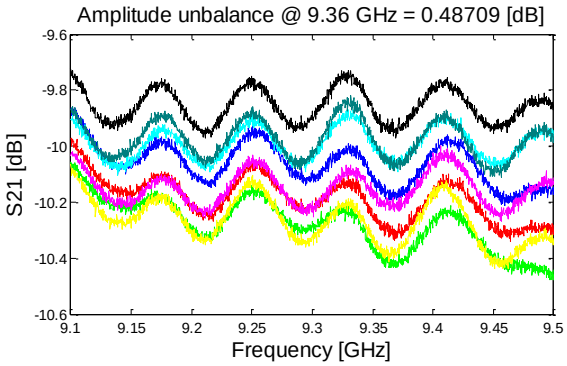

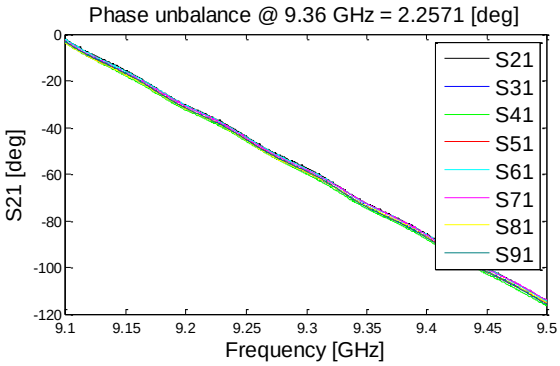

POWER DIVIDER #021

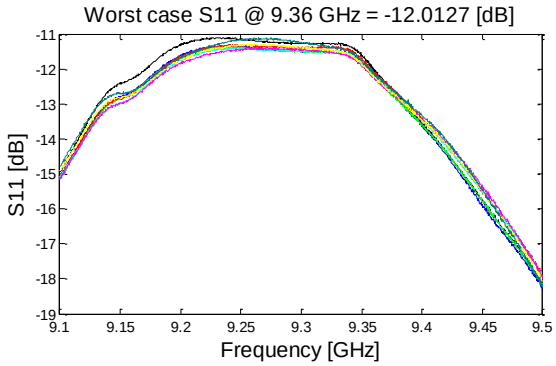

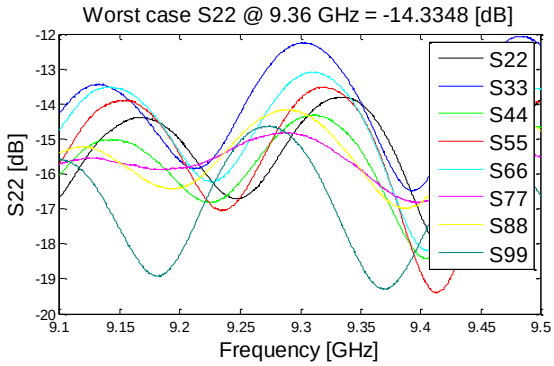

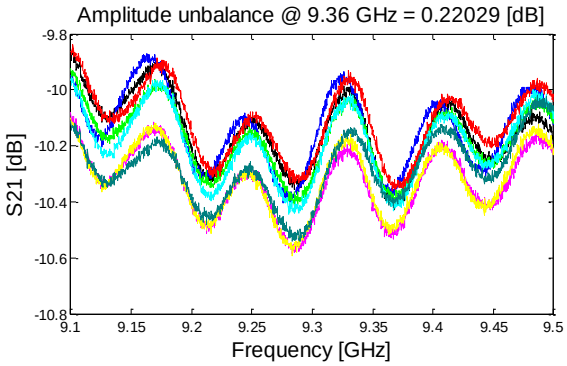

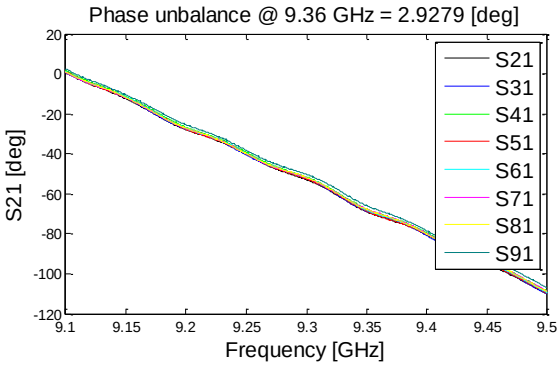

POWER DIVIDER #022

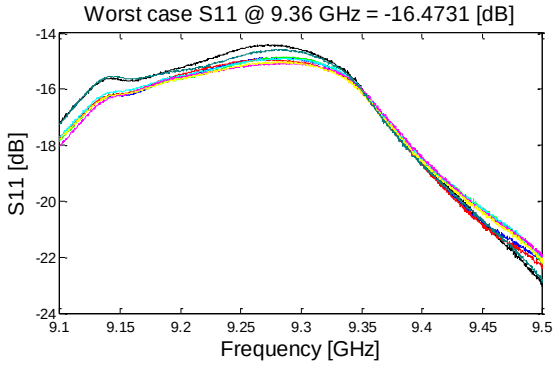

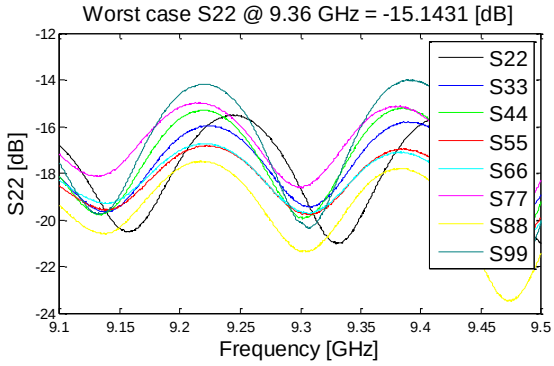

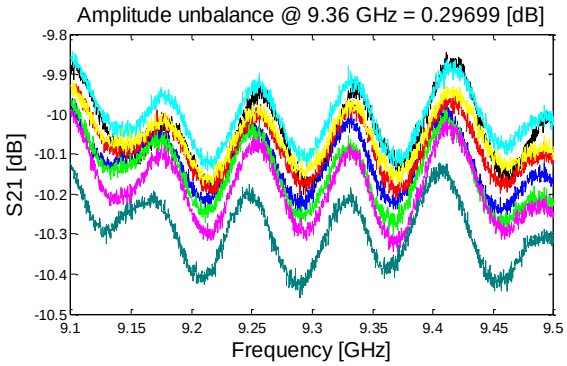

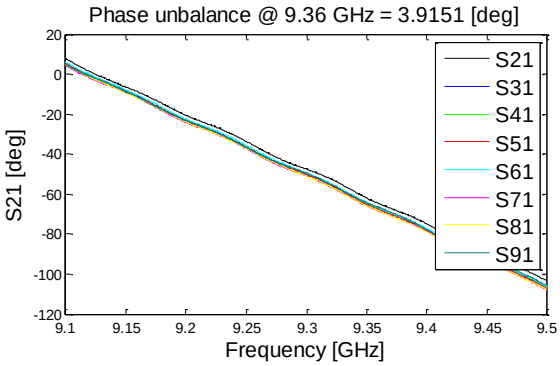

POWER DIVIDER #023

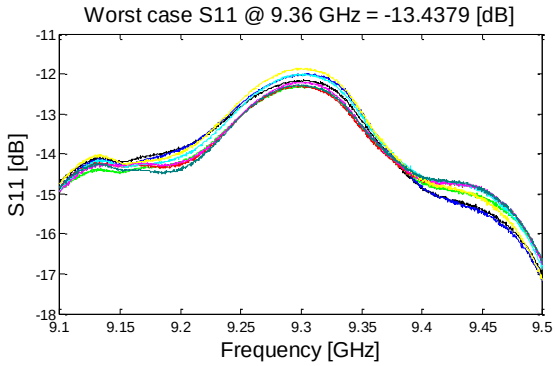

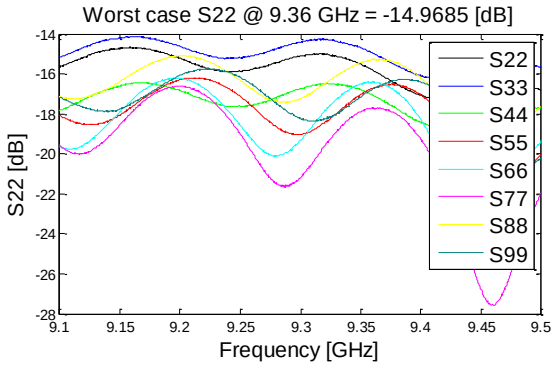

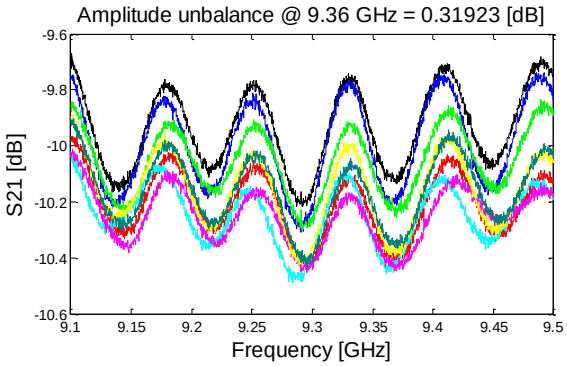

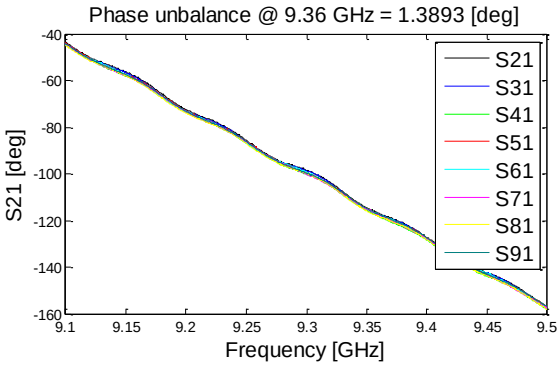

POWER DIVIDER #024

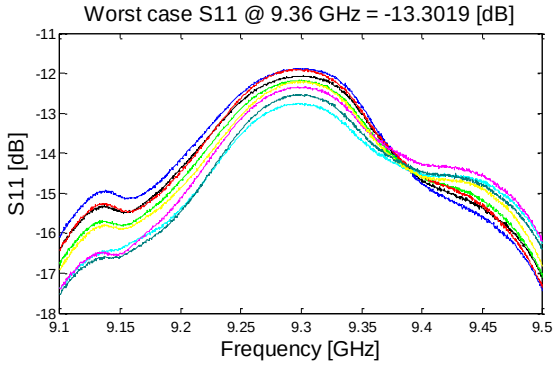

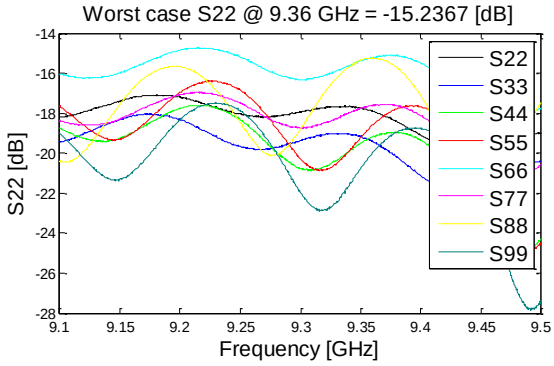

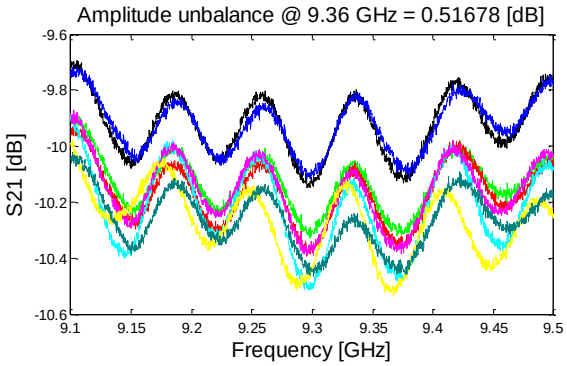

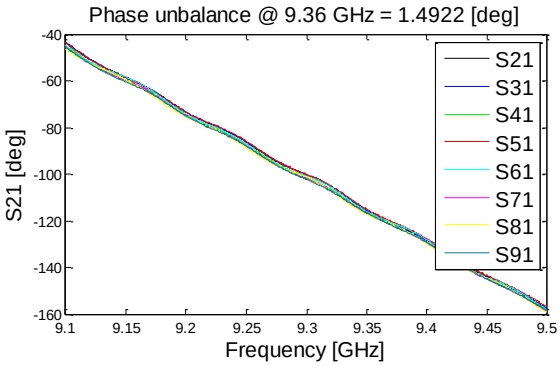

POWER DIVIDER #025

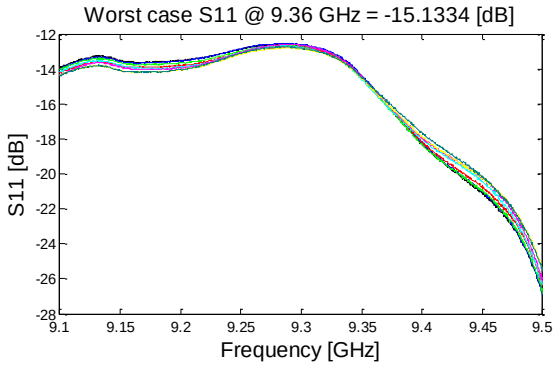

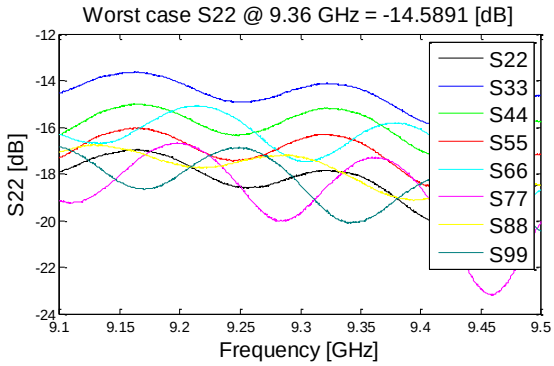

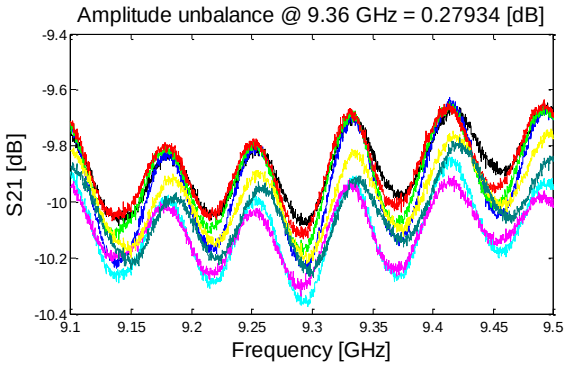

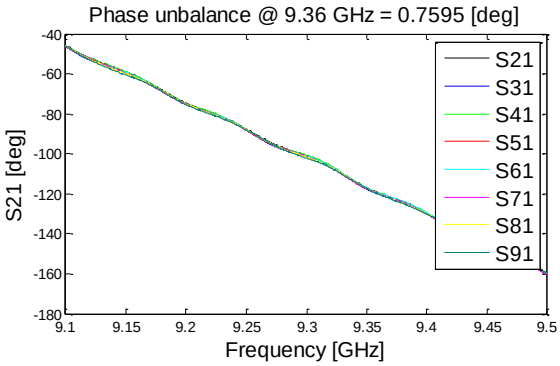

POWER DIVIDER #026

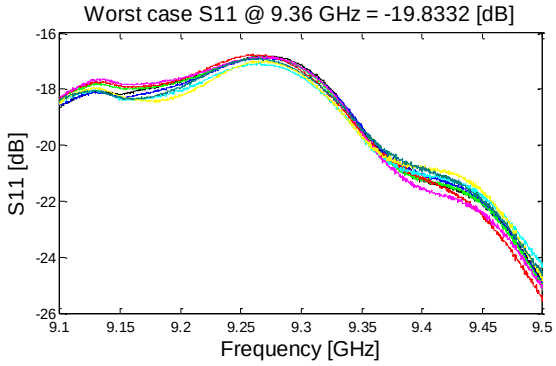

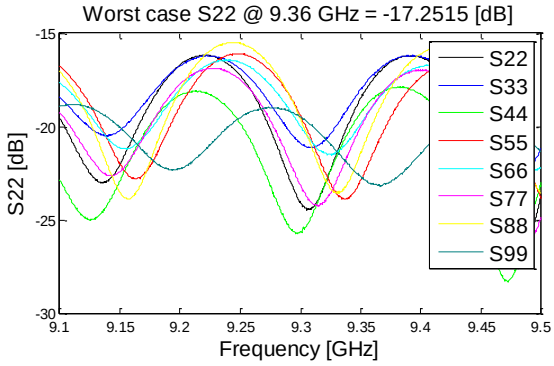

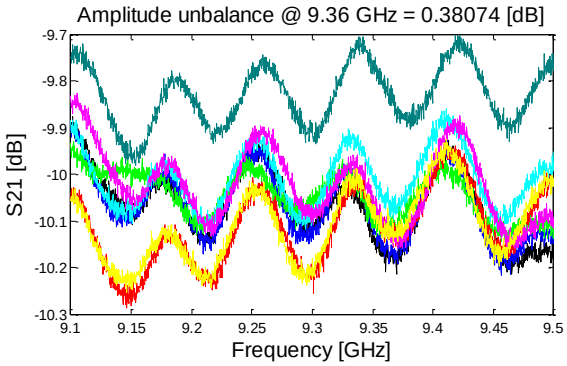

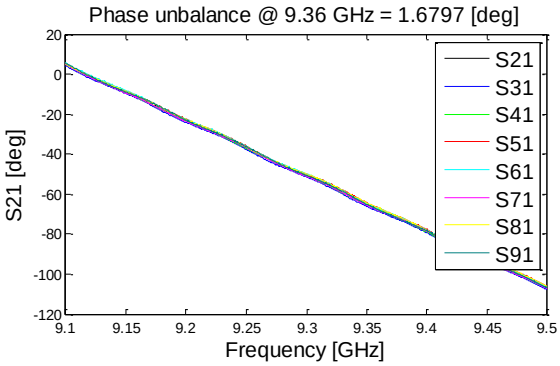

POWER DIVIDER #027

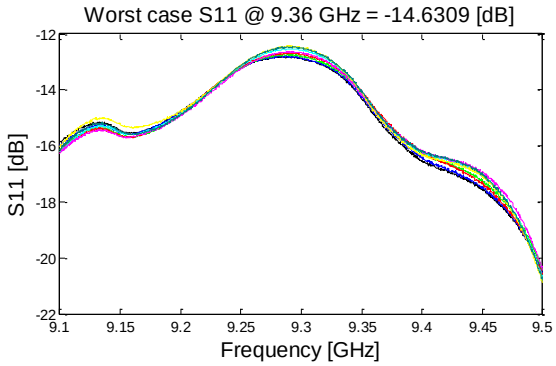

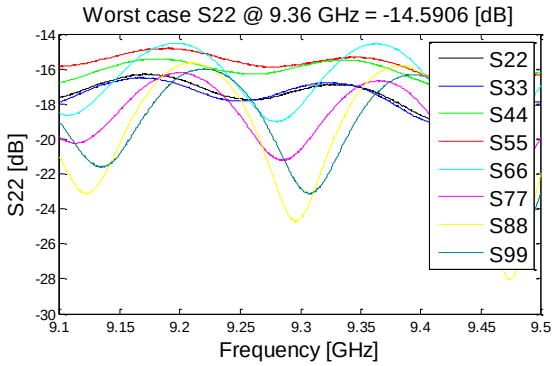

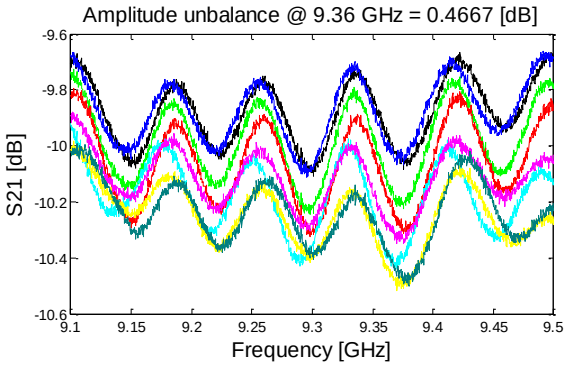

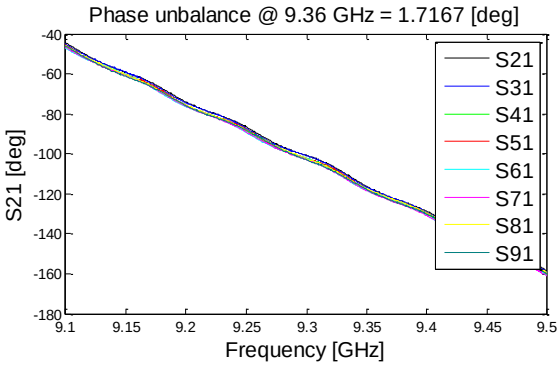

POWER DIVIDER #028

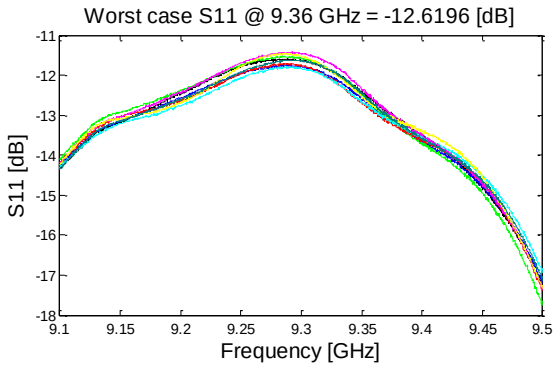

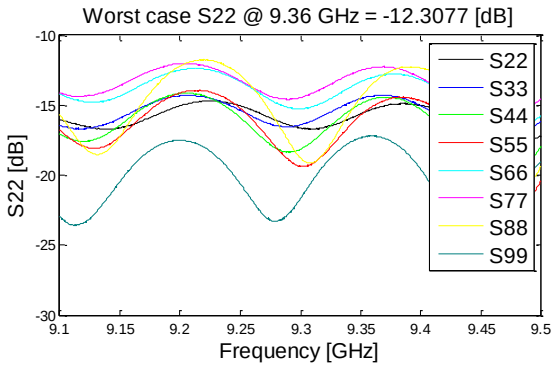

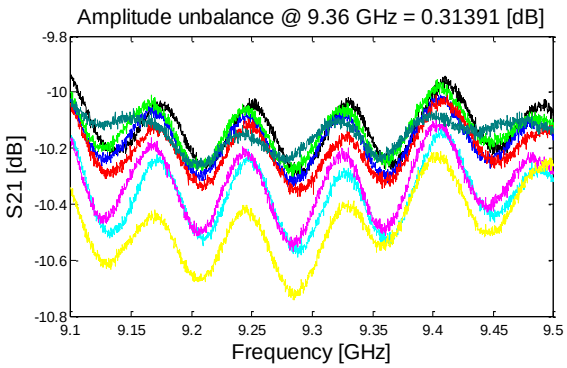

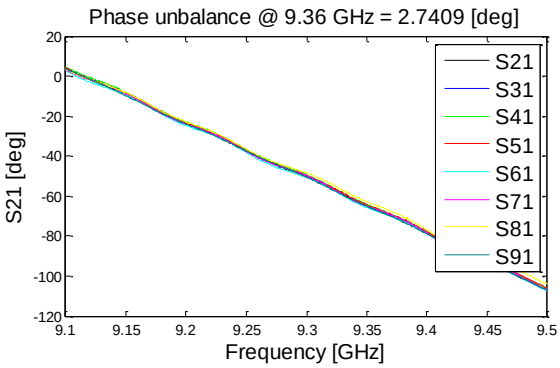

POWER DIVIDER #029

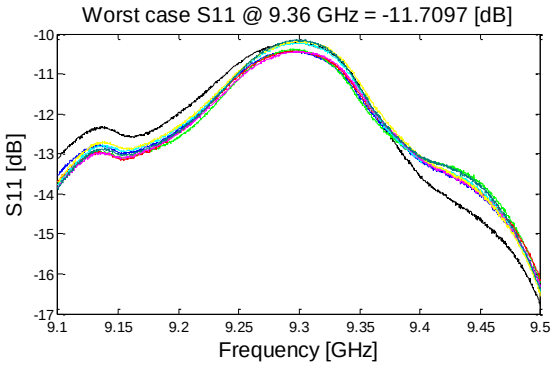

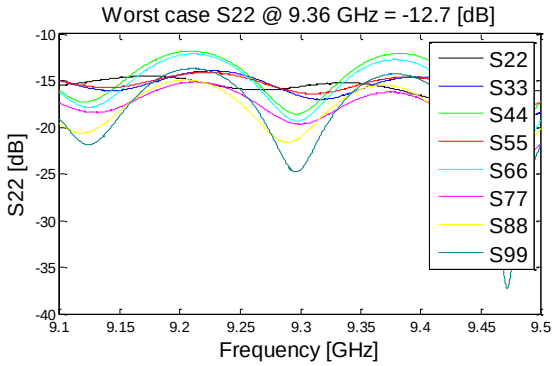

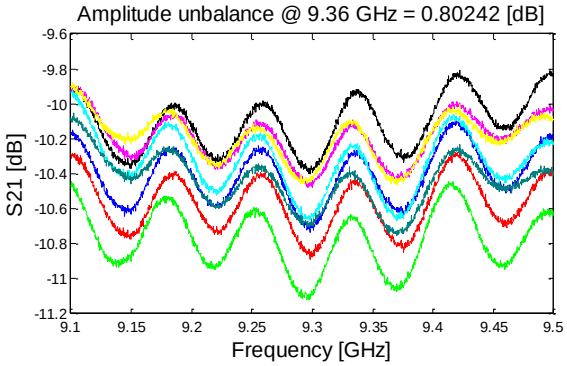

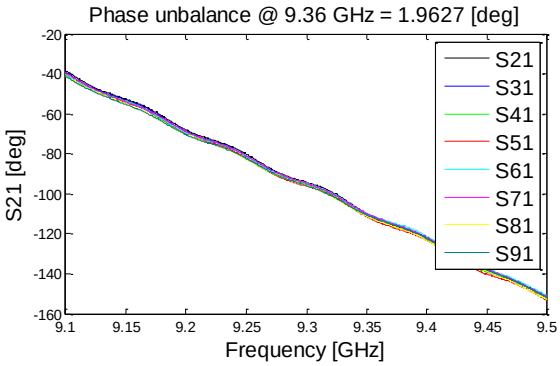

POWER DIVIDER #030

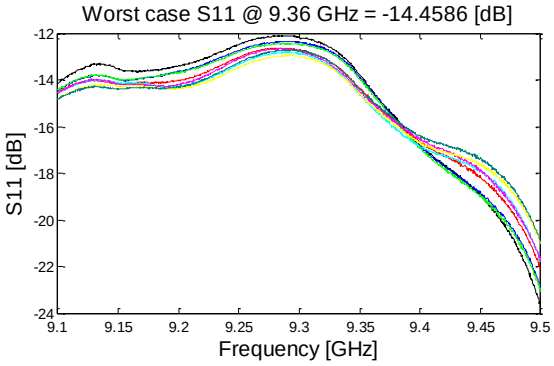

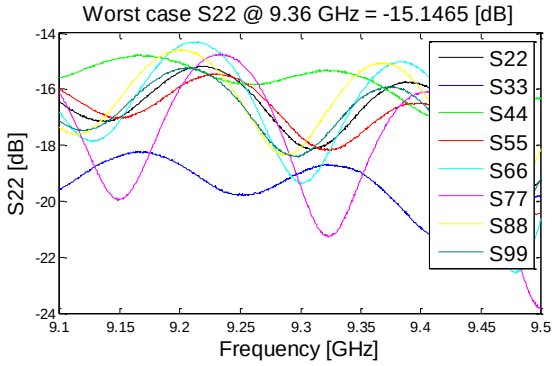

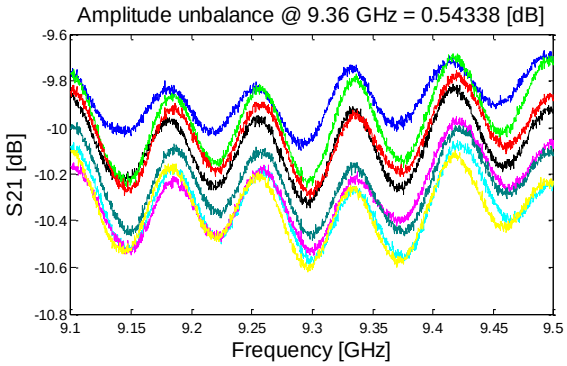

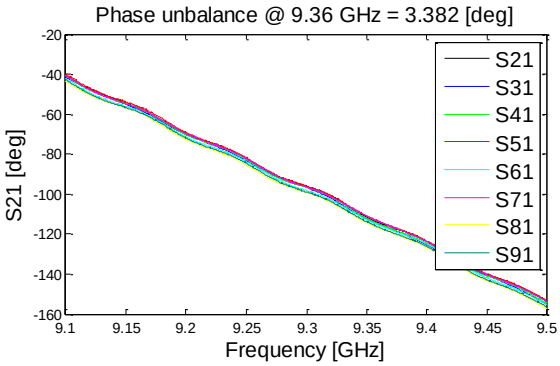

POWER DIVIDER #031

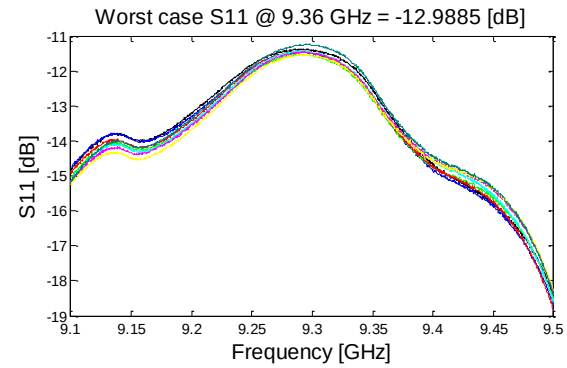

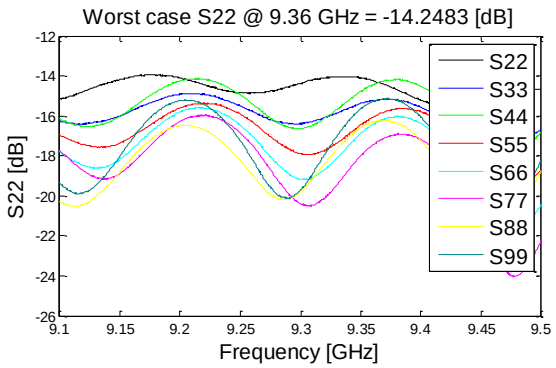

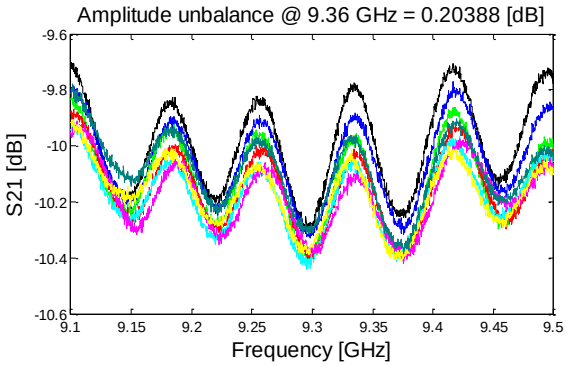

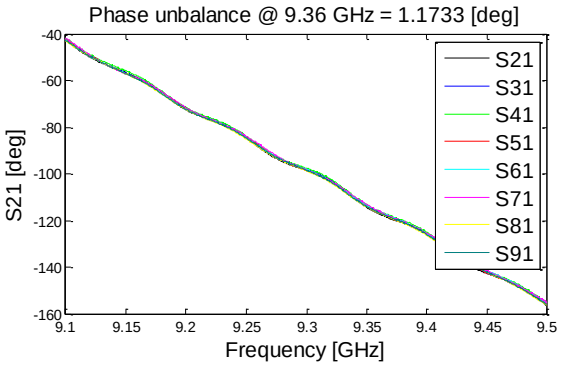

POWER DIVIDER #032

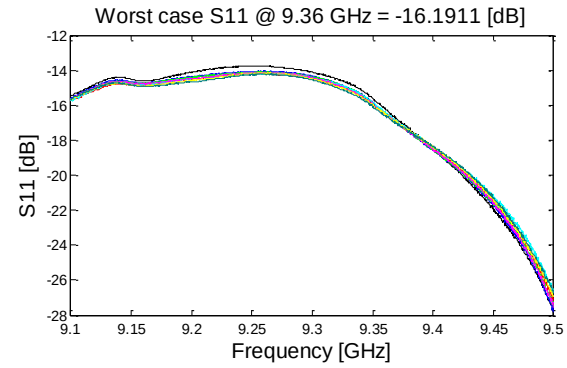

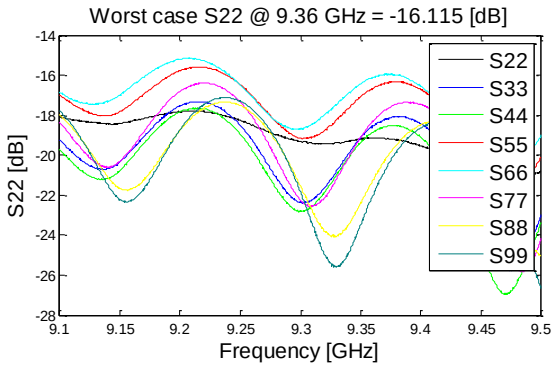

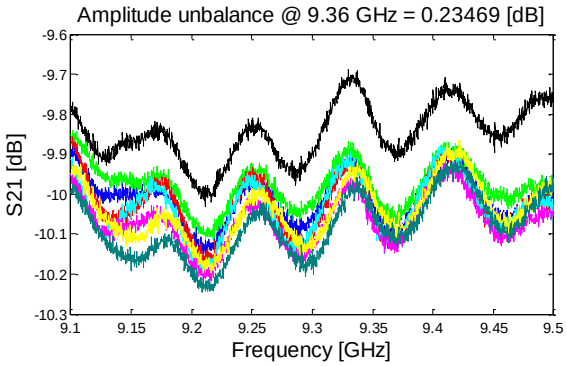

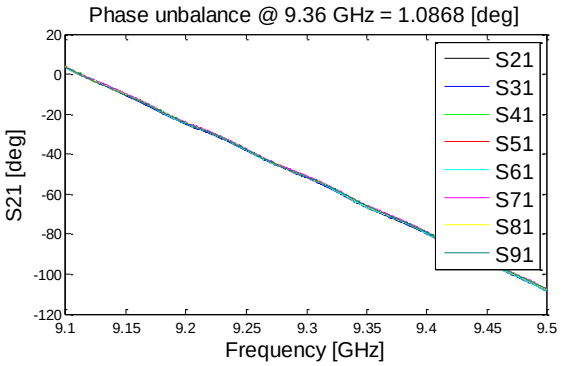

POWER DIVIDER #033

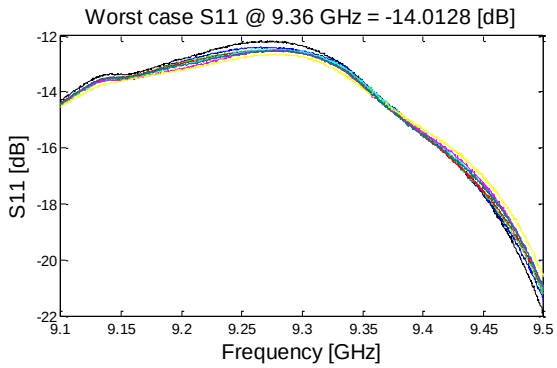

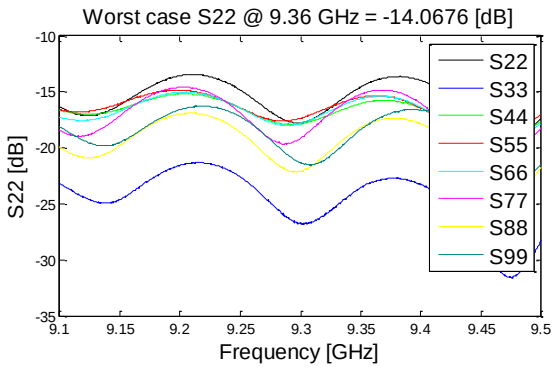

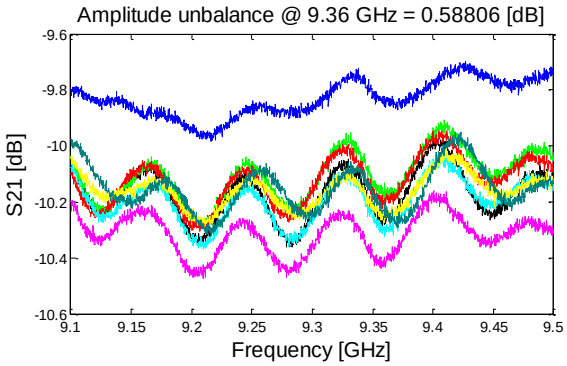

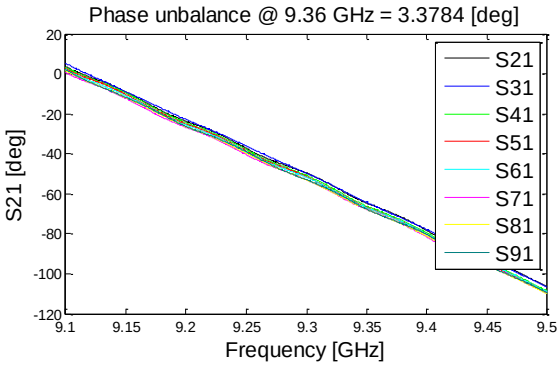

POWER DIVIDER #034

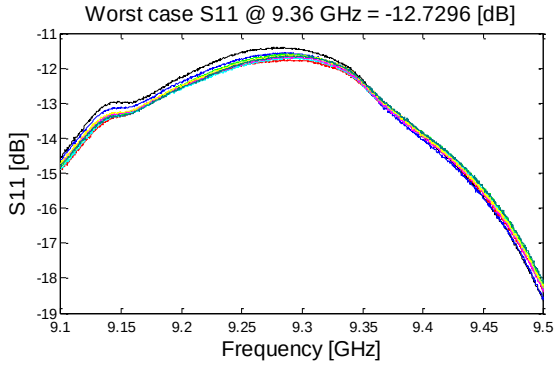

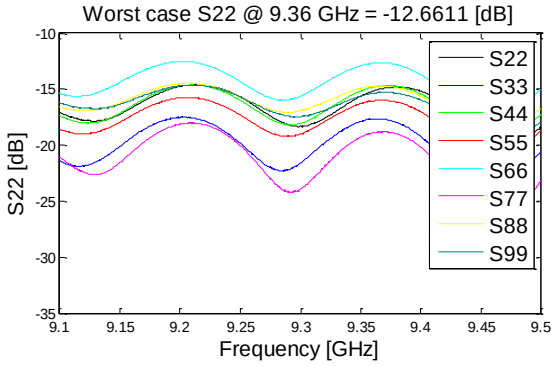

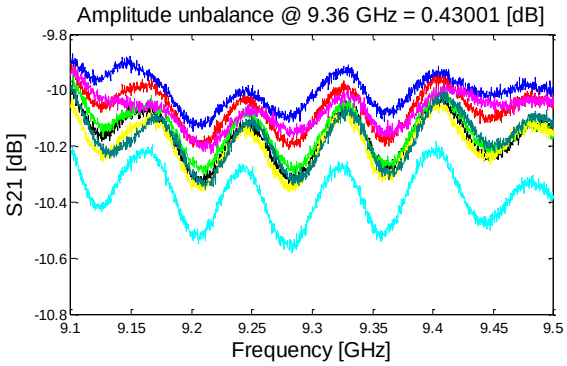

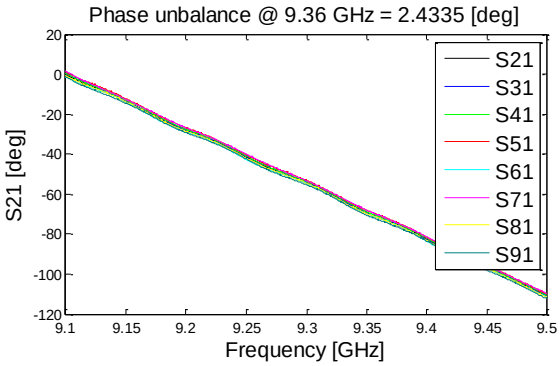

POWER DIVIDER #035

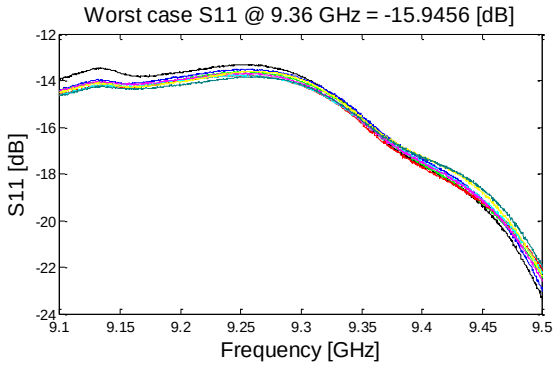

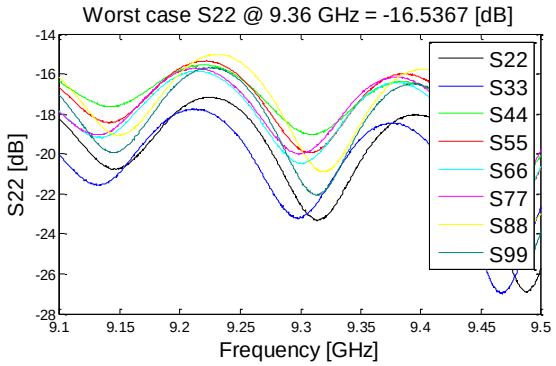

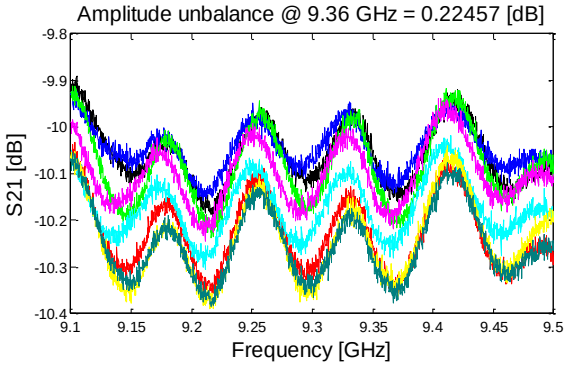

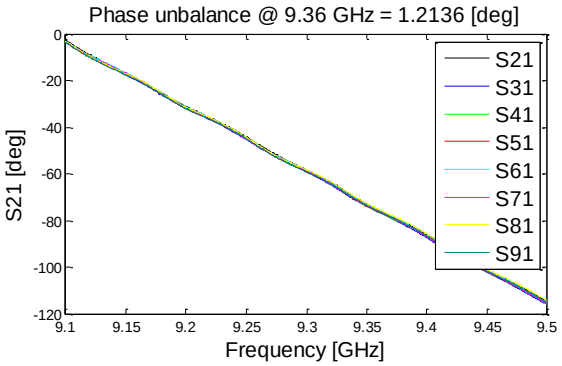

POWER DIVIDER #036

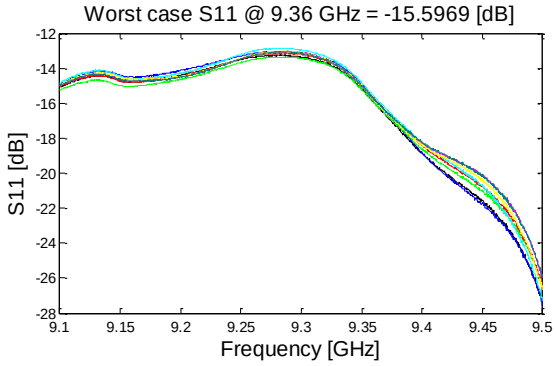

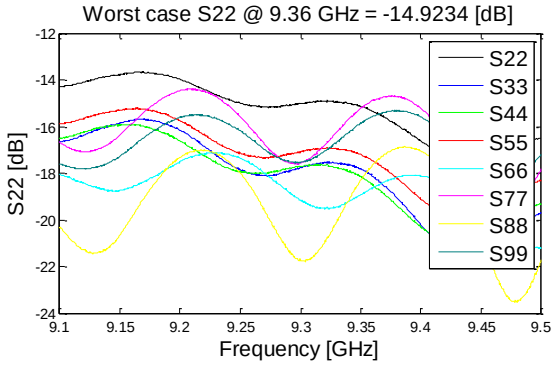

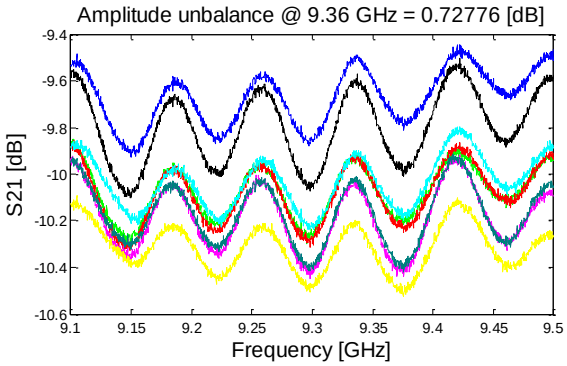

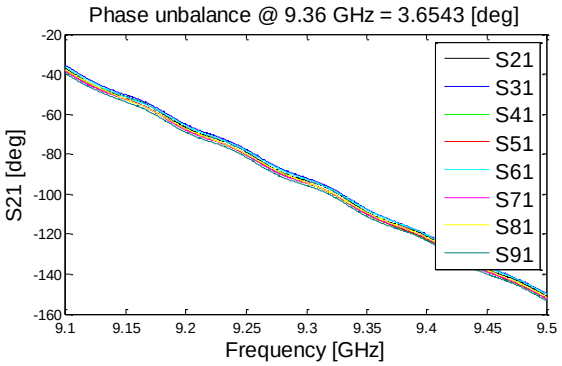

ISOLATION

POWER DIVIDER #002

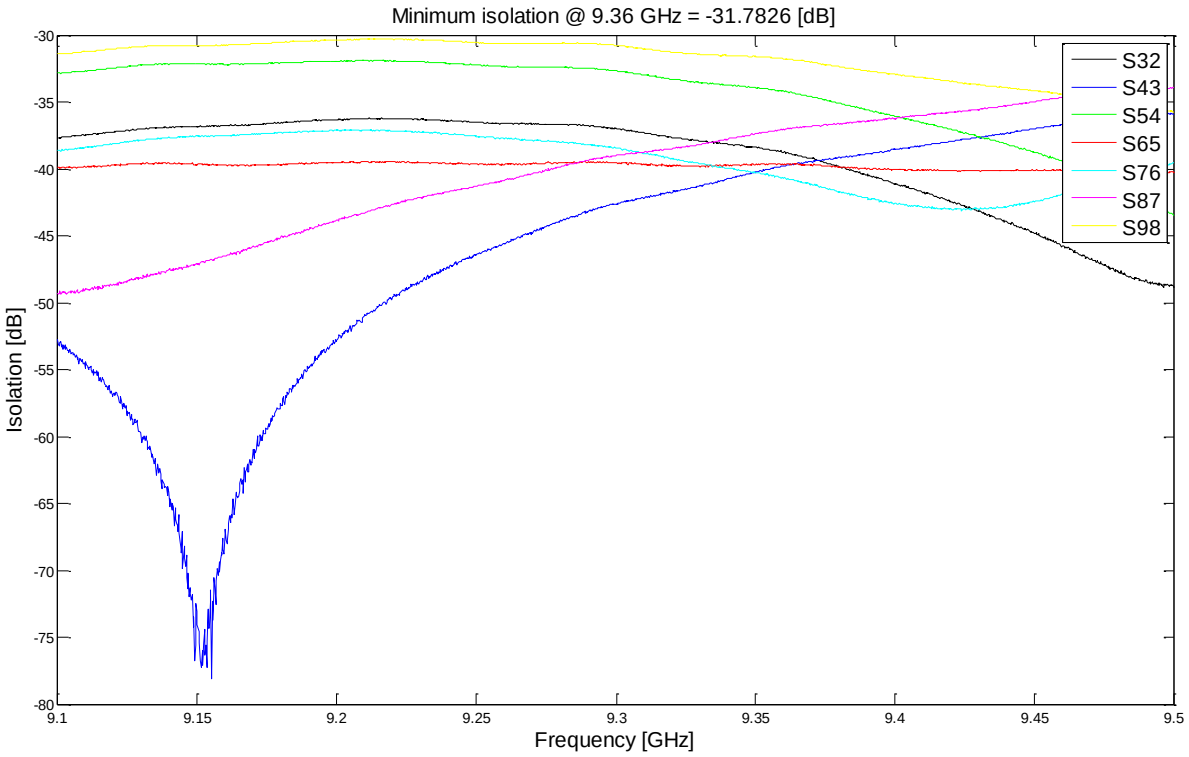

POWER DIVIDER #011

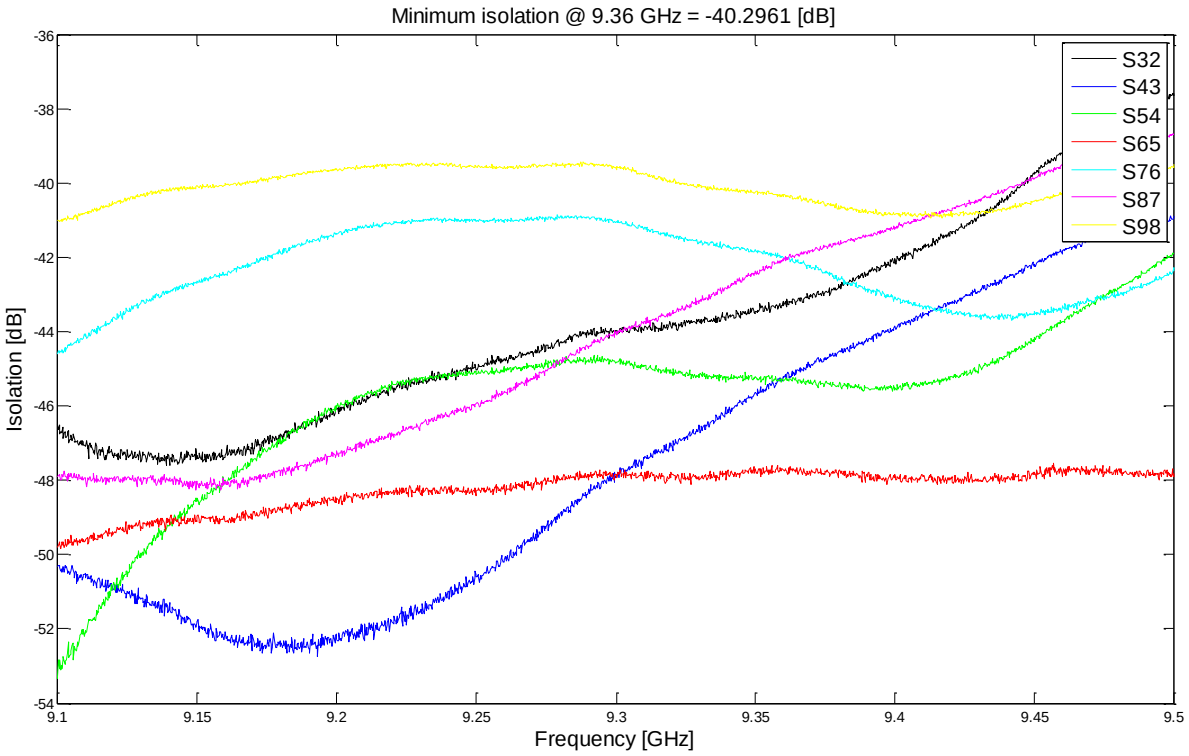

POWER DIVIDER #012

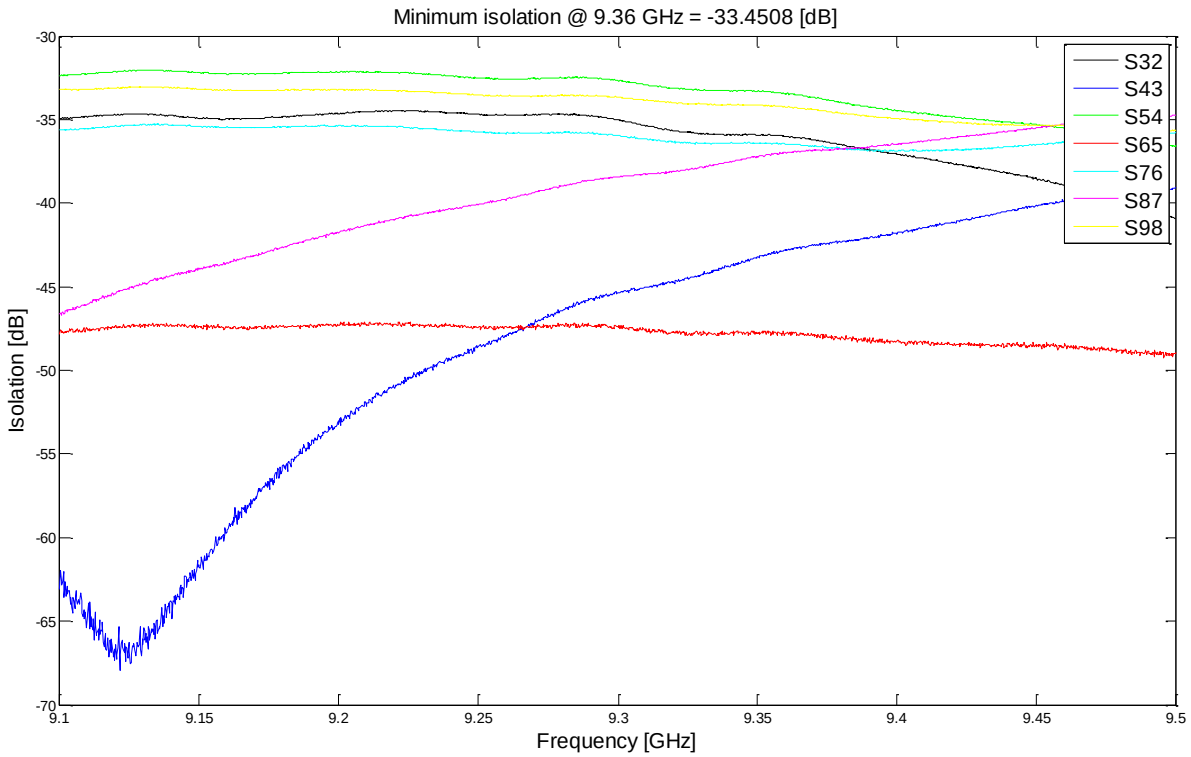

POWER DIVIDER #015

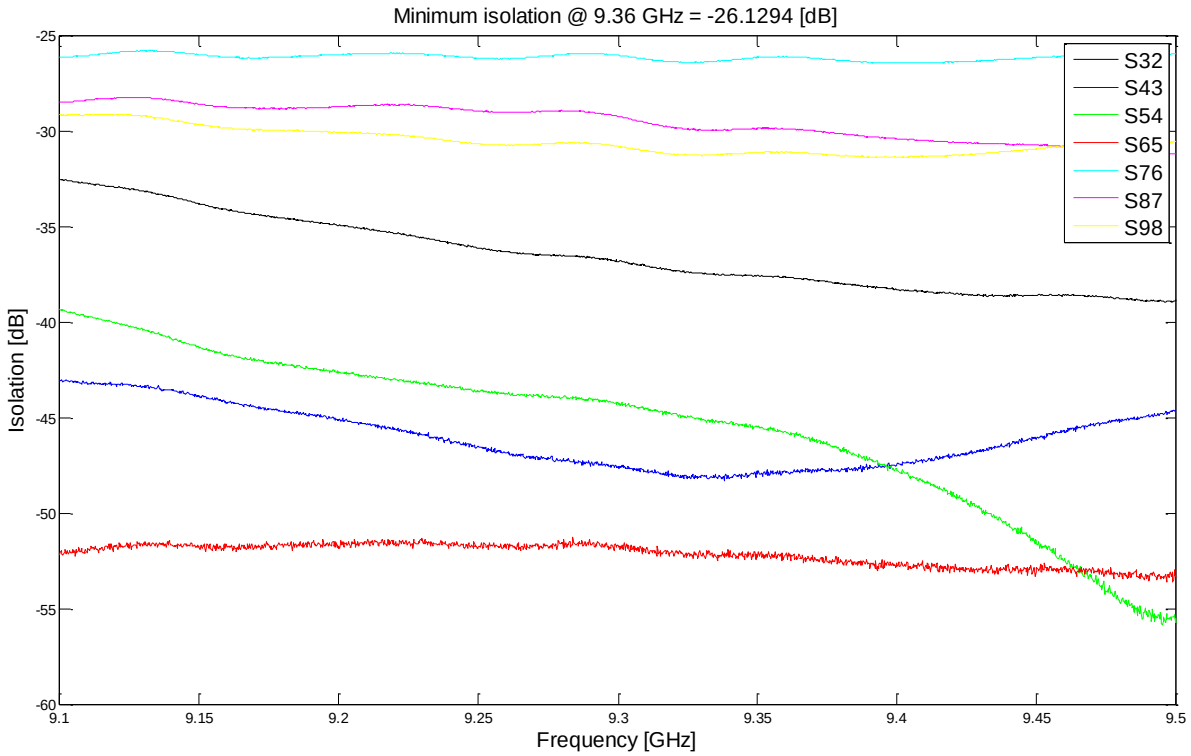

POWER DIVIDER #029

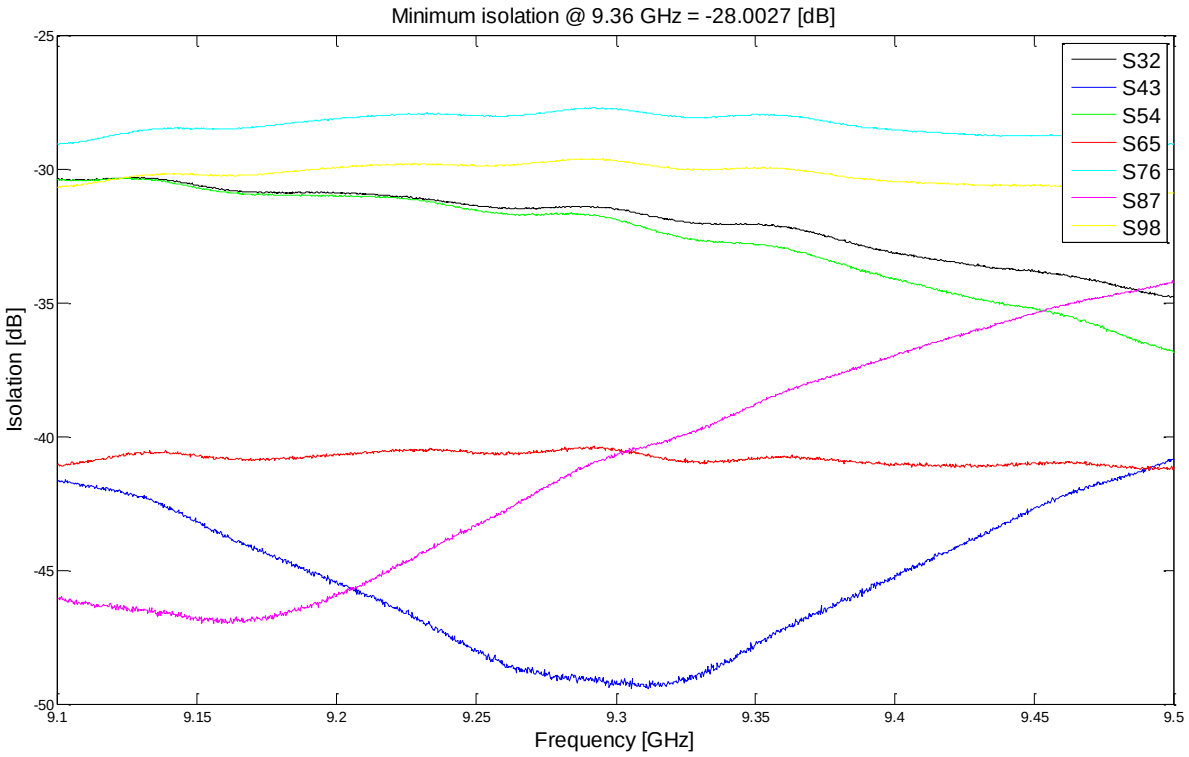

POWER DIVIDER #034

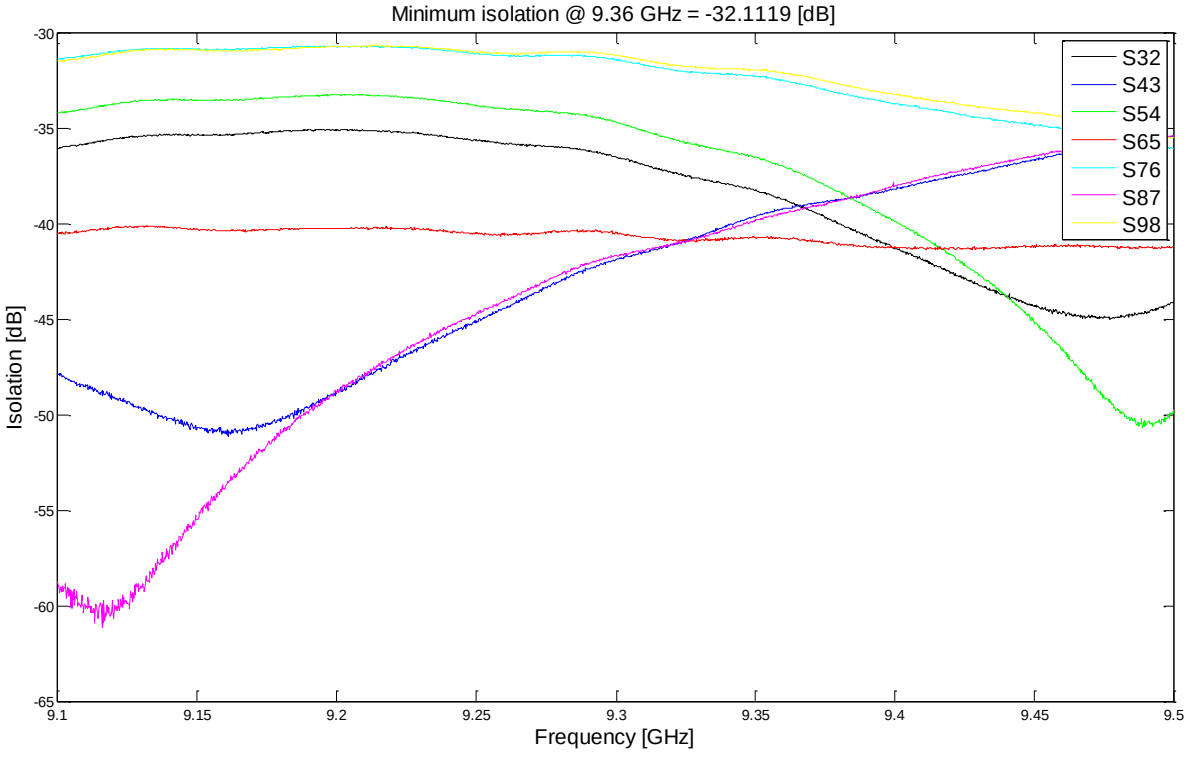

SUMMARY TEST DATA
ON
AMPLIFIER

Customer	**: University of Massachusetts**	**Tested By**	**: K. Mason**
Job No	**: PE504273**	**Temperature**	**: +25°C**
Model No	**: PE2-17-9R5G-2R0-8-12-SFF**	**Date**	**: 05/05/05**
Serial No	**: PL1697/0520**		

TEST ITEM NO.	PARAMETERS	SPECIFIED VALUE	MEASURED VALUE	REMARKS QA/QC
1	Frequency Range:	9.4-9.55GHz	Pass	
2	Gain:	+17dB Typ.	Pass (See Plot)	
3	Flatness:	± 0.5dB Max.	± 0.08dB	
4	Noise Figure:	2.0dB Max.	Pass (See NF Plot)	
5	Pout @ 1dB Compression:	+8dBm Min.	> +8dBm	
6	VSWR:	Input : 2.0:1 Output: 2.0:1 (Max.)	Pass (See Plots)	
7	DC Supply:	80mA @ +12 to +15VDC Max.	84mA @ +12 to +15VDC	+4mA
8	RF Input Power:	+12dBm CW Max.	Pass	

Production Manager Approval: _____ **Date: 05/05/05**

QA/QC Approval: _____ **Date: 05/05/05**

5715 Industry Lane, Unit 11, Frederick, MD 21704 USA Phone: (301)662-5019 Fax: (301)662-1731
email: sales@planarelec.com

VNA Plot

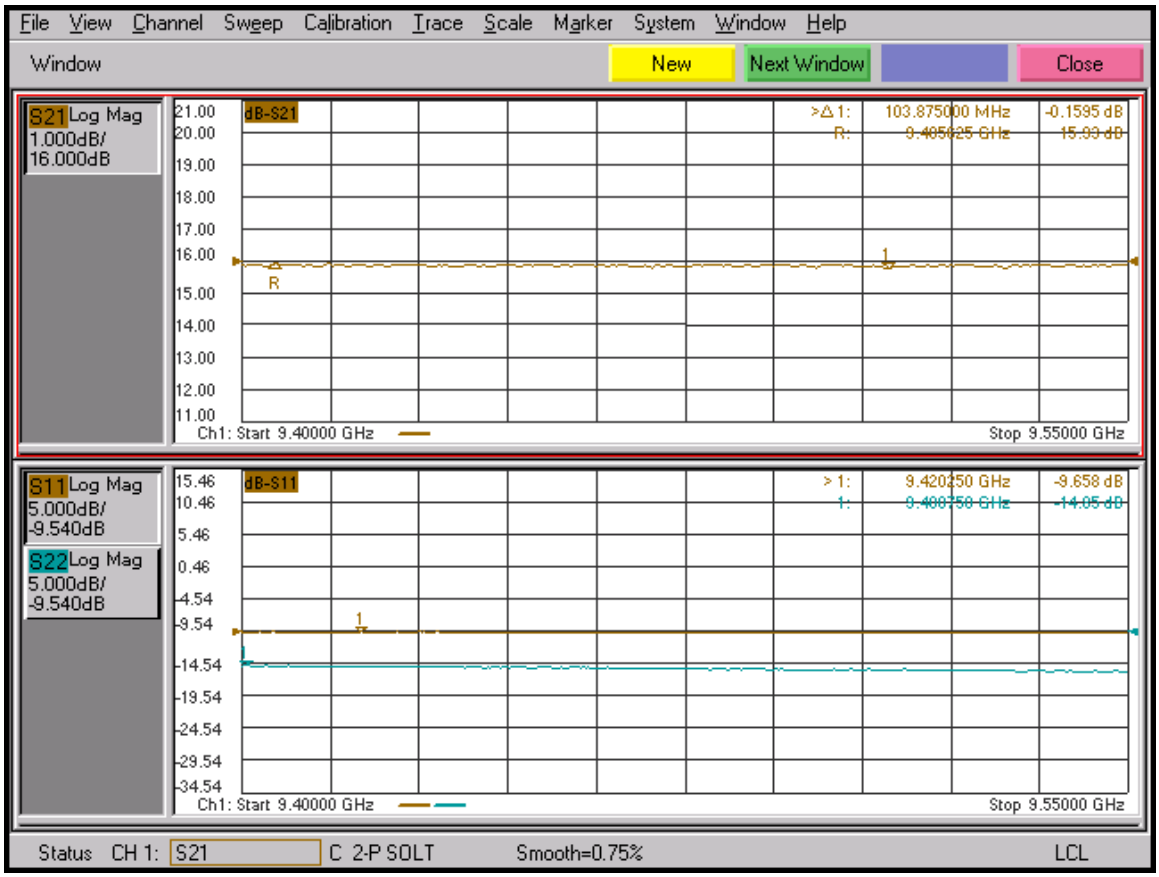

5715 Industry Lane, Unit 11, Frederick, MD 21704 USA Phone: (301)662-5019 Fax: (301)662-1731
email: sales@planarelec.com

Noise Figure Plot

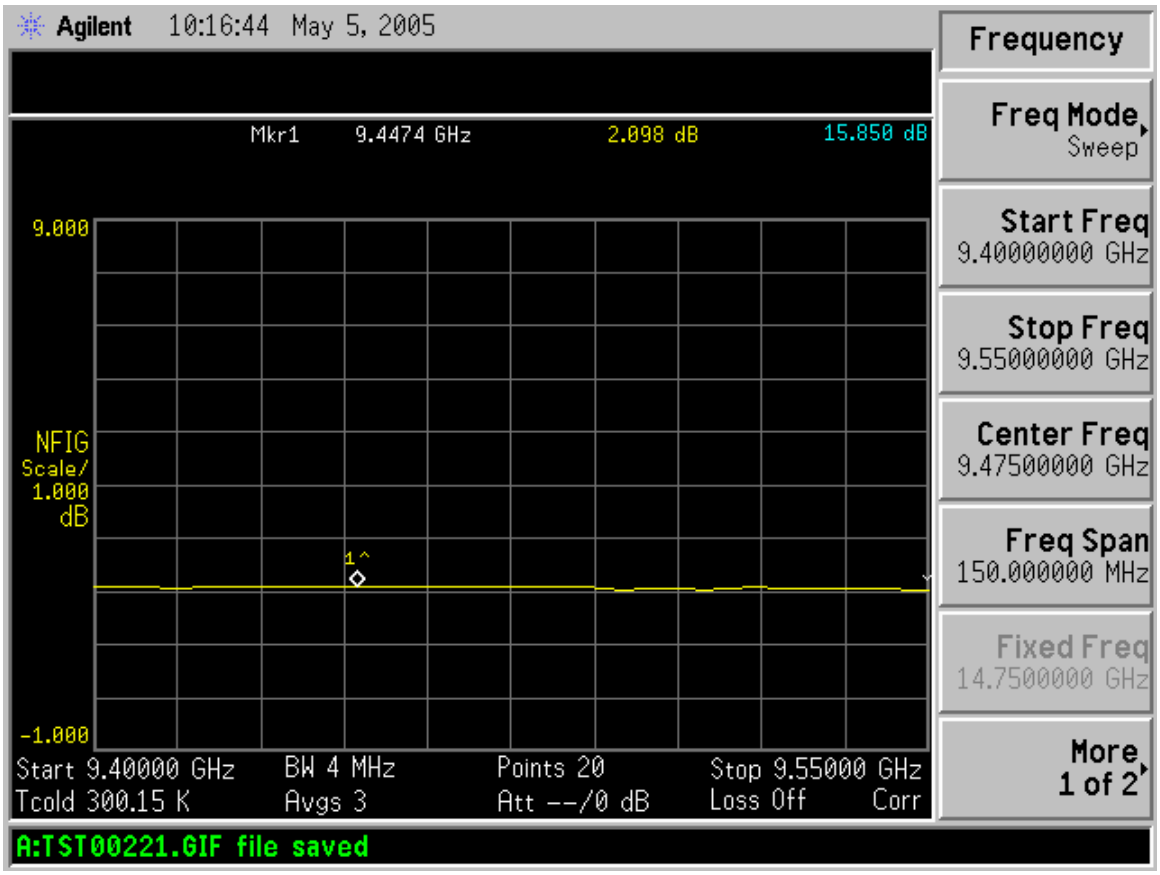

5715 Industry Lane, Unit 11, Frederick, MD 21704 USA Phone: (301)662-5019 Fax: (301)662-1731
email: sales@planarelec.com

High Frequency, Medium Bandwidth — FV Series

Features:

- Small Package Design, High "Q" Response
- Ruggedized Package Design
- Covers the 500 MHz to 40 GHz Frequency Range
- Combline Design Results in Low Insertion Loss Performance
- 3 dB BW Available from 3-18%
- Designs Available in 2-17 Sections
- Custom Package Designs Available

Specifications:

Model	Frequency (GHz)	3 dB % BW	VSWR	Insertion Loss	Passband Return	Impedance (Ohms)	No. of Sections	Shock	Vibration	Temperature	Relative Humidity
FV-50	.5-2	3-18	1.5:1	0.1 dB per section @ BW ≥ 5%	≥ 3.5 X f_0	50	2-17	20 G's, 1/2 Sine, 11 Ms	10 G's, 10 Hz-2000 Hz	-55 to +85 °C	0-95%
FV-40	2-5										
FV-30	3-8										
FV-20	4-10										
FV-10	7-18										

To Order:

5 FV 20 — 6575 / T 750 - O / O
1 2 3 4 5 6 7 8

Code	Description
1	Number of Sections
2	Series (FV-Combline)
3	Package Designator 20 Series
4	Center Frequency (MHz)
5	Supplemental Codes (See Page 13)
6	Bandwidth (MHz)
7	Input Connector
8	Output Connector

Connectors:

Connector	Code
SMA Female	O
SMA Male	OP
N Female	N*
N Male	NP*
TNC Female	T*
TNC Male	TP*
RF Pins	P
Removable SMA	RO
Blind Mate	OB

*Requires .75 W and .75 H

High Frequency, Medium Bandwidth — FV Series

◆ Attenuation:

The adjacent curve is used to determine the out-of-band or stopband attenuation for K&L's combline filters. This curve shows the attenuation as multiples of the 3 dB bandwidth for filters up to 13 sections. The formula for approximate stopband attenuation:

$$\text{3 dB BW from } f_0 = \frac{\text{Reject Frequency-Center Frequency}}{\text{3 dB BW}}$$

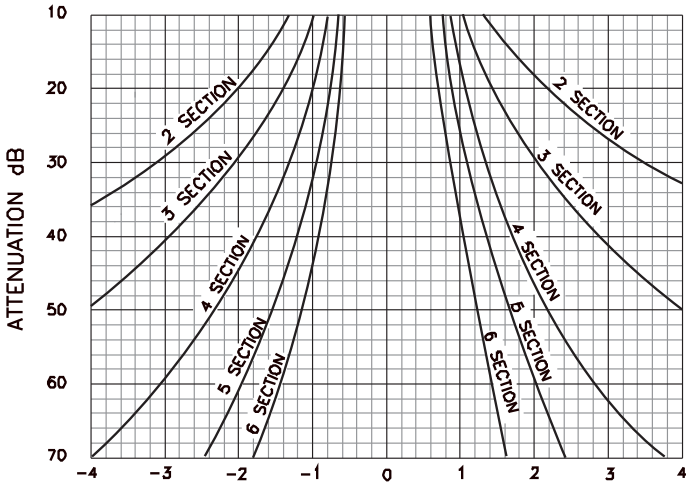

Note: For more stringent rejection requirements, contact the factory.

Example:

Center Frequency = 6575 MHz
3 dB Bandwidth = 750 MHz
Number of Sections = 6

Find the attenuation at 5600 MHz and 7550 MHz by substituting in the formula:

$$\text{3 dB BW from } f_0 = \frac{5600-6575}{750} = -1.3 \text{ BW}$$

$$\text{3 dB BW from } f_0 = \frac{7550-6575}{750} = +1.3 \text{ BW}$$

From the 6 section curves -1.3 BW and +1.3 BW yield approximately 54 dB.

◆ Mechanical:

The mechanical dimensions and mounting hole locations are dependent upon the design parameters specified by the customer. Contact K&L Microwave for details.

Phone: 410-749-2424 • FAX: 443-260-2268
Email: sales@klmicrowave.com
2250 Northwood Drive
Salisbury, MD 21801
www.klmicrowave.com • www.klfilterwizard.com

Explanation of Supplemental Codes

(Can be one or two characters)

/A Amplitude Matched
/B Bessel Response
/C Contiguous Multiplexer
/D Delay Matched
/E Equiripple Bandwidth
/H Half dB Bandwidth
/N Non-contiguous Multiplexer
/P Phased Matched
/Q High Power Requirements
/T Three dB Bandwidth
/U One dB Bandwidth
/W Butterworth Response
/X Special

Multiplexer

Four character medium and topology code
_ Z _ _ Diplexer
_ M _ _ Multiplexer

Special Packaging

"1" is used as 3rd character in medium topology code.
__ __ 1 __

Explanation of Topology of Codes

LP/HP/BP
0 - Special
1 - Chebyshev
2 - S.E.L.F.
Symmetrical Equiripple
Lumped Filter

BP
0 - Special
1- Resonant Ladder
2 - Capacitively Coupled "tank"
3 - "tank" with Tubular End Sections
4 - Lowpass/Highpass Cascade
5 - Lumped Tubular or "mesh"
6 - Narrowband S.E.L.F.
7 - Broadband S.E.L.F.
8 - General Parameter
9 - Unspecified

Specific Examples for Each Product Line are:

9B111-500/H50-O/O 9 section Chebyshev filter in a **one and a quarter inch tubular,** center frequency 500 MHz with a half dB bandwidth of 50 MHz and SMA female connectors on both ends.

6C42-1000/UW30-O/OP 6 section Butterworth **cavity filter** in a 42 series package, center frequency 1000 MHz, one dB bandwidth 30 MHz, SMA female on input and SMA male on the output.

9ED30-4000/U2000-N/NP 9 section **interdigital filter** in a 30 series package, center frequency of 4000 MHz, its 1 dB bandwidth is 2000 MHz and it has N-type connectors, input female and output male.

6IB33-2500/TA212-O/O 6 section **IB filter**, tank circuit with tubular end sections in an IB package, center frequency 2500 MHz with a 3 dB bandwidth of 212 MHz, SMA female connectors on both ends, amplitude matching is specified.

3MC10-500/TD45-O/OP 3 section **miniature cavity filter,** center frequency of 500 MHz with a 3 dB bandwidth of 45 MHz. Delay matching is specified and the connectors are SMA female on input and SMA male on the output.

Multiplexers

In a multiplexer the second character in the medium and topology code is replaced by a Z in the case of a diplexer and by M in case of any other multiplexer. The lowest and highest passband frequencies are specified in the part number.

Multiplexers

7FZ30-3000/TC4500-O This **diplexer** consists of 2 seven-section combline filters in a 30 series package. The lower channel bandedge is at 3000 MHz and the channels are contiguous passing up to 4500 MHz. All three connectors are SMA female.

Coaxial

Frequency Mixer WIDE BAND

ZX05-153LH+

Level 10 (LO Power +10 dBm) 3200 to 15000 MHz

CASE STYLE: FL905

Connectors	Model	Price	Qty.
SMA	ZX05-153LH-S+	$48.95	(1-24)

+ RoHS compliant in accordance with EU Directive (2002/95/EC)

The +Suffix has been added in order to identify RoHS Compliance. See our web site for RoHS Compliance methodologies and qualifications.

Maximum Ratings

Operating Temperature	-40°C to 85°C
Storage Temperature	-55°C to 100°C
RF Power	50mW

Permanent damage may occur if any of these limits are exceeded.

Coaxial Connections

LO	2
RF	3
IF	1

Features

- wide bandwidth, 3200 to 15000 MHz
- low conversion loss, 6.6 dB typ.
- high L-R isolation, 36 dB typ.
- excellent IF BW, DC to 4000 MHz
- rugged construction
- small size
- useable as up and down converter
- protected by US patents, 6,790,049 and 7,027,795

Applications

- satellite up and down converters
- defense radar and communications
- line of sight links
- federal fixed service
- WIFI
- blue tooth
- VSAT
- ISM

Outline Drawing

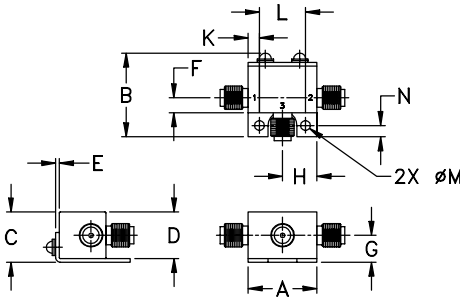

Outline Dimensions (inch / mm)

A	B	C	D	E	F	G
.74	.90	.54	.50	.04	.16	.29
18.80	22.86	13.72	12.70	1.02	4.06	7.37

H	J	K	L	M	N	wt
.37	--	.122	.496	.106	.122	grams
9.40	--	3.10	12.60	2.69	3.10	20.0

Electrical Specifications

FREQUENCY (MHz)		CONVERSION LOSS* (dB)			LO-RF ISOLATION (dB)		LO-IF ISOLATION (dB)		IP3 at center band (dBm)
LO/RF f_L-f_U	IF	Typ.	σ	Max.	Typ.	Min.	Typ.	Min.	Typ.
3200-15000	**DC-4000**								
3200-4500		6.6	0.1	8.5	40	36	18	12	12
4500-5100		6.2	0.1	7.5	38	34	12	9	16
5100-14000		7.0	0.3	14.2	34	22	18	9	15
14000-15000		7.8	0.4	11.2	25	15	23	12	10

1 dB COMPR.: +2 dBm typ.

* Conversion loss at 30 MHz IF. σ is a measure of repeatability from unit to unit.

Typical Performance Data

Frequency (MHz)		Conversion Loss (dB)	Isolation L-R (dB)	Isolation L-I (dB)	VSWR RF Port (:1)	VSWR LO Port (:1)
RF	LO	LO +10dBm	LO +10dBm	LO +10dBm	LO +10dBm	LO +10dBm
3200.10	3230.10	7.32	46.50	21.25	2.52	15.26
3800.10	3830.10	6.59	46.23	19.58	2.93	7.41
4400.10	4430.10	6.34	40.60	15.17	2.41	3.94
5000.10	5030.10	6.14	37.06	12.14	2.71	1.91
5600.10	5630.10	6.06	35.48	13.32	3.23	2.53
6200.10	6230.10	6.18	38.40	15.97	2.68	4.09
7000.10	7030.10	5.46	36.65	17.39	2.13	4.47
7600.10	7630.10	5.70	39.03	14.07	1.64	3.30
8200.10	8230.10	5.35	30.91	14.22	1.95	1.90
9000.10	9030.10	5.93	34.96	24.70	3.33	2.03
9600.10	9630.10	6.39	28.80	20.15	4.07	2.07
10200.10	10230.10	6.77	31.31	20.86	5.58	2.07
10800.10	10830.10	7.55	38.50	26.81	3.29	2.75
11400.10	11430.10	8.97	39.43	33.14	6.89	5.25
12000.10	12030.10	10.33	36.37	37.96	2.84	7.08
12600.10	12630.10	11.08	32.60	39.88	5.49	6.63
13200.10	13230.10	12.27	26.20	36.26	3.02	4.45
13800.10	13830.10	10.81	24.44	32.04	4.59	3.97
14400.10	14430.10	8.30	26.38	27.04	2.28	3.58
15000.10	15030.10	7.79	24.05	20.42	1.80	2.49

Electrical Schematic

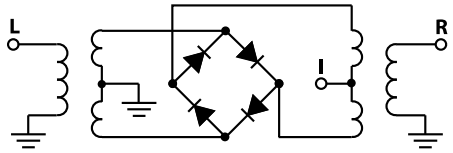

Notes: 1. Performance and quality attributes and conditions not expressly stated in this specification sheet are intended to be excluded and do not form a part of this specification sheet. **2.** Electrical specifications and performance data contained herein are based on Mini-Circuit's applicable established test performance criteria and measurement instructions. **3.** The parts covered by this specification sheet are subject to Mini-Circuits standard limited warranty and terms and conditions (collectively, "Standard Terms"); Purchasers of this part are entitled to the rights and benefits contained therein. For a full statement of the Standard Terms and the exclusive rights and remedies thereunder, please visit Mini-Circuits' website at www.minicircuits.com/MCLStore/terms.jsp.

REV. OR
M111660
ZX05-153LH+
ED-12902/9
DJ/AM
091007

ZX05-153LH+
CONVERSION LOSS

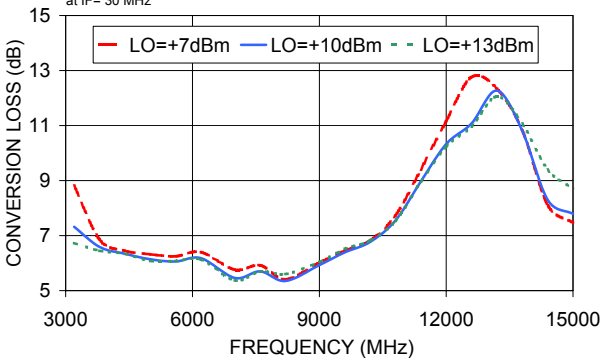

ZX05-153LH+
CONVERSION LOSS VARIABLE IF

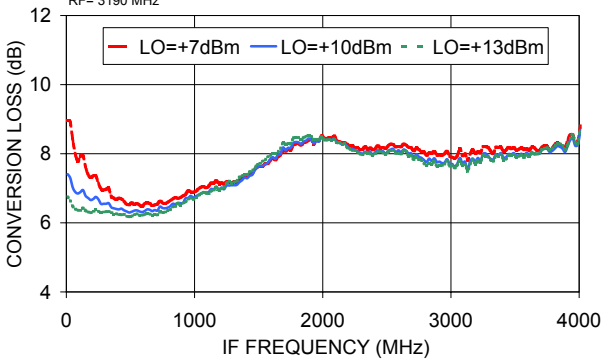

ZX05-153LH+
L-R ISOLATION

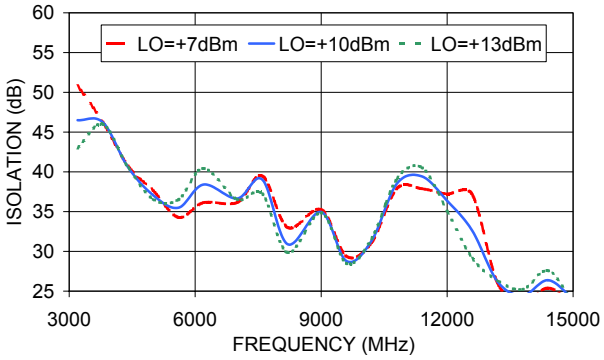

ZX05-153LH+
L-I ISOLATION

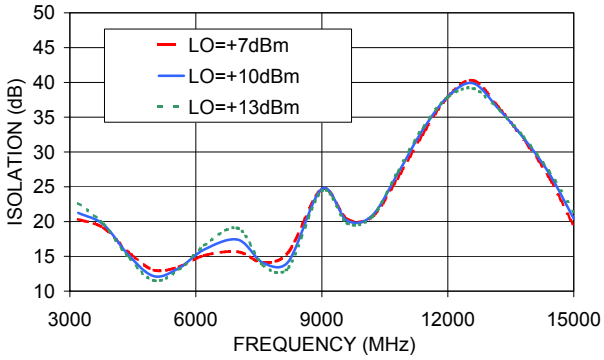

ZX05-153LH+
RF VSWR

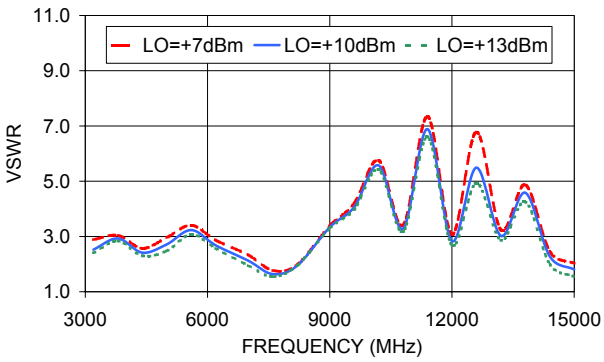

ZX05-153LH+
LO VSWR

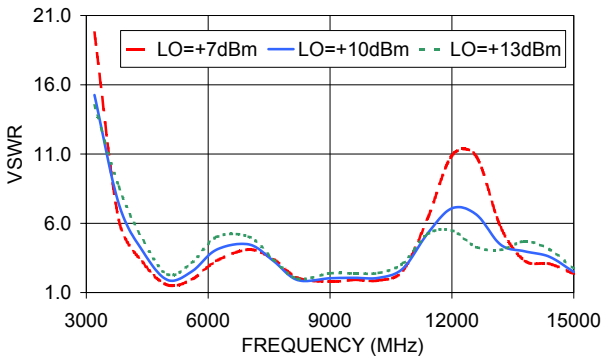

ZX05-153LH+
IF VSWR

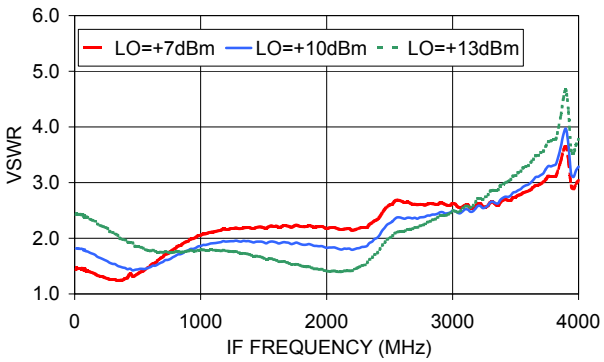

ZX05-153LH+
IP3

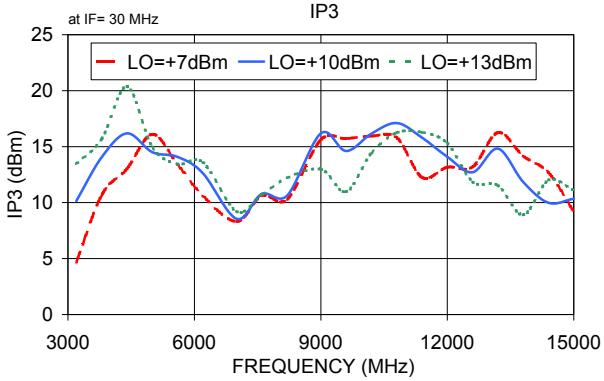

Notes: 1. Performance and quality attributes and conditions not expressly stated in this specification sheet are intended to be excluded and do not form a part of this specification sheet. **2.** Electrical specifications and performance data contained herein are based on Mini-Circuit's applicable established test performance criteria and measurement instructions. **3.** The parts covered by this specification sheet are subject to Mini-Circuits standard limited warranty and terms and conditions (collectively, "Standard Terms"); Purchasers of this part are entitled to the rights and benefits contained therein. For a full statement of the Standard Terms and the exclusive rights and remedies thereunder, please visit Mini-Circuits' website at www.minicircuits.com/MCLStore/terms.jsp.

Coaxial

Frequency Mixer

Level 10 (LO Power +10 dBm) 10 to 3000 MHz

ZFM-15+
ZFM-15

SMA version shown
CASE STYLE: K18

Connectors	Model	Price	Qty.
BNC	ZFM-15(+)	$89.95 ea.	(1-9)
SMA	ZFM-15-S+	$94.95 ea.	(1-9)
BRACKET (OPTION "B")		$5.00	(1+)

+ RoHS compliant in accordance with EU Directive (2002/95/EC)

The +Suffix identifies RoHS Compliance. See our web site for RoHS Compliance methodologies and qualifications.

Maximum Ratings

Operating Temperature	-55°C to 100°C
Storage Temperature	-55°C to 100°C
RF Power	50mW
IF Current	40mA

Permanent damage may occur if any of these limits are exceeded.

Coaxial Connections

LO	1
RF	2
IF	3

Features

- low conversion loss, 6.13 dB typ.
- good L-R isolation, 35 dB typ, L-I, 30 dB typ.
- wideband, 10 to 3000 MHz
- rugged shielded case

Applications

- cellular
- GPS
- MMDS
- ISM
- instrumentation

Outline Drawing

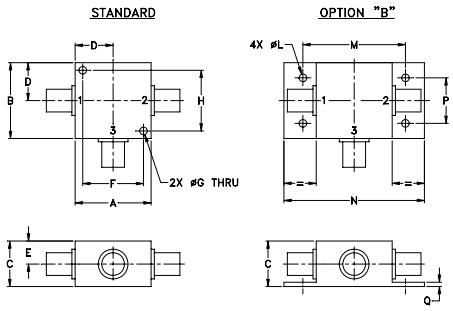

Outline Dimensions (inch / mm)

A	B	C	D	E	F	G	H
1.25	1.25	.75	.63	.38	1.00	.125	1.000
31.75	31.75	19.05	16.00	9.65	25.40	3.18	25.40

J	K	L	M	N	P	Q	wt
--	--	.125	1.688	2.18	.75	.07	grams
--	--	3.18	42.88	55.37	19.05	1.78	70.0

Electrical Specifications

FREQUENCY (MHz)		CONVERSION LOSS (dB)				LO-RF ISOLATION (dB)						LO-IF ISOLATION (dB)					
		Mid-Band m			Total Range	L		M		U		L		M		U	
LO/RF f_L-f_U	IF	$\overline{X}$	σ	Max.	Max.	Typ.	Min.	Typ.	Min.	Typ.	Min.	Typ.	Min.	Typ.	Min.	Typ.	Min
10-3000	10-800	6.13	0.14	8.0	8.5	35	25	35	25	35	25	30	20	30	20	30	30

1 dB COMP.: +5 dBm typ.

L = low range [f_L to 10 f_L] M = mid range [10 f_L to f_U/2] U = upper range [f_U/2 to f_U]
m= mid band [2f_L to f_U/2]

Typical Performance Data

Frequency (MHz)		Conversion Loss (dB)	Isolation L-R (dB)	Isolation L-I (dB)	VSWR RF Port (:1)	VSWR LO Port (:1)
RF	LO	LO +10dBm	LO +10dBm	LO +10dBm	LO +10dBm	LO +10dBm
10.00	40.00	6.53	26.10	25.08	1.84	1.71
20.00	50.00	6.60	30.38	29.74	1.54	1.51
100.00	70.00	6.55	35.82	35.93	1.50	1.37
200.00	170.00	6.60	37.35	38.21	1.55	1.44
400.00	370.00	6.74	36.49	39.50	1.72	1.40
500.00	470.00	6.52	35.42	38.00	1.99	1.34
790.00	760.00	6.70	32.94	33.60	2.45	1.33
920.00	890.00	6.76	32.80	33.97	2.70	1.36
1180.00	1150.00	7.30	31.62	32.89	2.85	1.36
1310.00	1280.00	7.30	31.27	34.31	2.75	1.38
1500.00	1470.00	6.54	29.76	32.85	2.28	1.30
1700.00	1670.00	6.91	28.49	30.87	1.94	1.27
1830.00	1800.00	6.97	29.46	28.22	1.44	1.29
2000.00	1970.00	7.07	28.32	27.77	1.25	1.34
2200.00	2170.00	6.97	27.89	27.68	1.42	1.34
2480.00	2450.00	6.93	28.37	24.64	1.97	1.44
2610.00	2580.00	7.08	27.10	23.13	2.18	1.52
2740.00	2710.00	7.45	26.79	21.95	2.37	1.93
2870.00	2840.00	7.56	26.23	21.25	2.09	2.25
3000.00	2970.00	8.31	29.30	20.32	2.18	2.63

Electrical Schematic

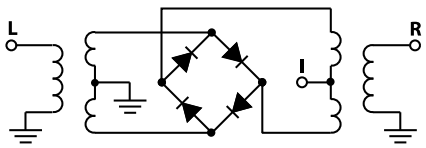

Notes: 1. Performance and quality attributes and conditions not expressly stated in this specification sheet are intended to be excluded and do not form a part of this specification sheet. **2.** Electrical specifications and performance data contained herein are based on Mini-Circuit's applicable established test performance criteria and measurement instructions. **3.** The parts covered by this specification sheet are subject to Mini-Circuits standard limited warranty and terms and conditions (collectively, "Standard Terms"); Purchasers of this part are entitled to the rights and benefits contained therein. For a full statement of the Standard Terms and the exclusive rights and remedies thereunder, please visit Mini-Circuits' website at www.minicircuits.com/MCLStore/terms.jsp.

REV. B
M113397
ZFM-15
DJ/TD/CP
120306

Performance Charts

ZFM-15
CONVERSION LOSS
at IF Freq of 30 MHz

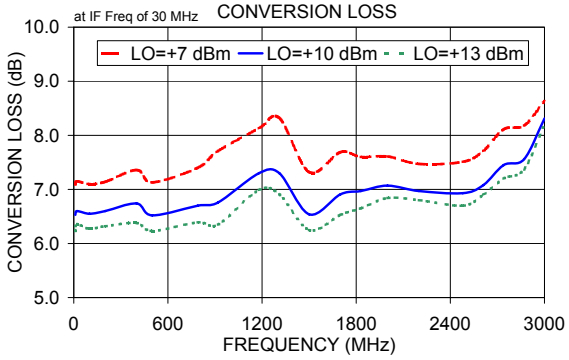

ZFM-15
L-R ISOLATION

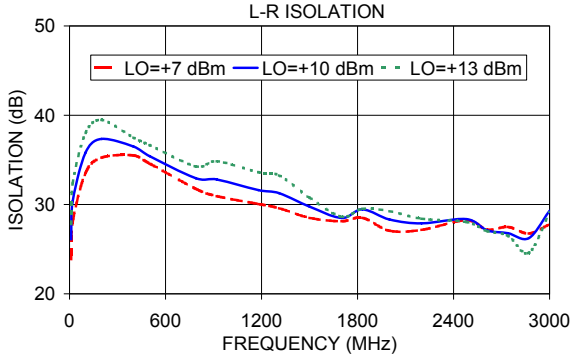

ZFM-15
L-I ISOLATION

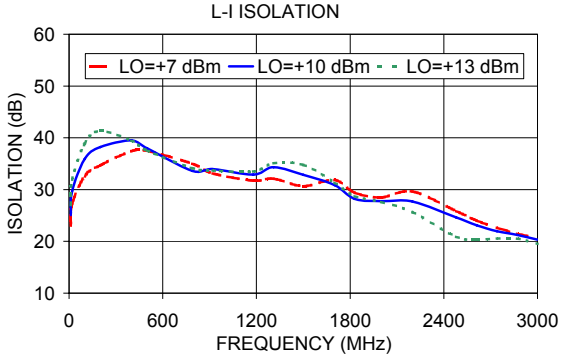

ZFM-15
RF VSWR

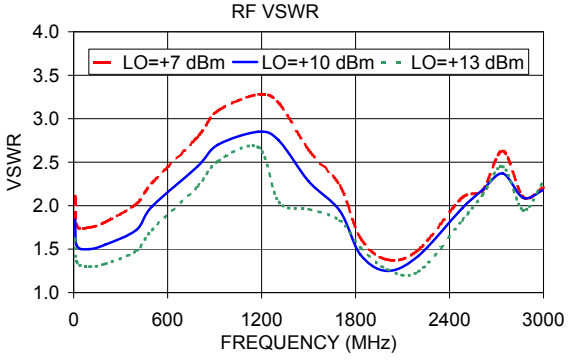

ZFM-15
LO VSWR

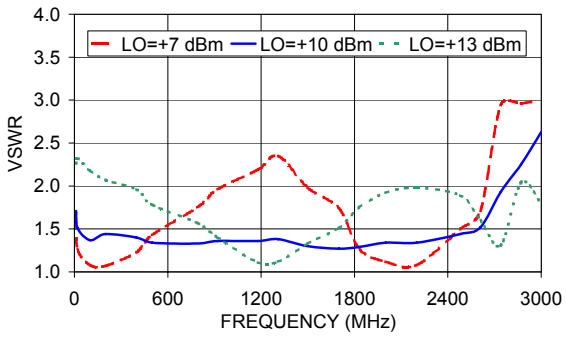

ZFM-15
IF VSWR

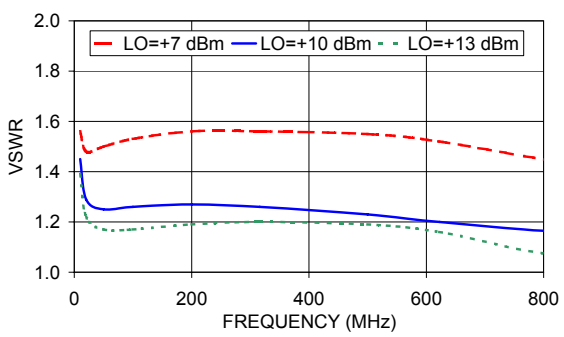

Notes: 1. Performance and quality attributes and conditions not expressly stated in this specification sheet are intended to be excluded and do not form a part of this specification sheet. **2.** Electrical specifications and performance data contained herein are based on Mini-Circuit's applicable established test performance criteria and measurement instructions. **3.** The parts covered by this specification sheet are subject to Mini-Circuits standard limited warranty and terms and conditions (collectively, "Standard Terms"); Purchasers of this part are entitled to the rights and benefits contained therein. For a full statement of the Standard Terms and the exclusive rights and remedies thereunder, please visit Mini-Circuits' website at www.minicircuits.com/MCLStore/terms.jsp.

Coaxial

Amplifier

ZFL-500+
ZFL-500

50Ω Low Power 0.05 to 500 MHz

SMA version shown

CASE STYLE: Y460

Connectors	Model	Price	Qty.
SMA	ZFL-500(+)	$69.95	(1-9)
BNC	ZFL-500-BNC	$74.95	(1-9)
BRACKET (OPTION "B")		$5.00	(1+)

Features

- wideband, 0.05 to 500 MHz
- rugged, shielded case
- low noise, 5.3 dB typ.
- protected by US Patent, 6,943,629

Applications

- instrumentation
- lab use
- VHF/UHF

+RoHS Compliant

The +Suffix identifies RoHS Compliance. See our web site for RoHS Compliance methodologies and qualifications

Amplifier Electrical Specifications

MODEL NO.	FREQUENCY (MHz)		GAIN (dB)		MAXIMUM POWER (dBm)		DYNAMIC RANGE		VSWR (:1) Typ.		DC POWER	
	f_L	f_U	Min.	Flatness Max.	Output (1 dB Compr.)	Input (no damage)	NF (dB) Typ.	IP3 (dBm) Typ.	In	Out	Volt (V) Nom.	Current (mA) Max.
ZFL-500(+)	0.05	500	20	±1.0	+9	+5	5.3	+18	1.9	1.9	15	80

Open load is not recommended, potentially can cause damage.
With no load derate max input power by 20 dB

Maximum Ratings

Operating Temperature	-20°C to 71°C
Storage Temperature	-55°C to 100°C
DC Voltage	+17V Max.

Permanent damage may occur if any of these limits are exceeded.

Outline Drawing

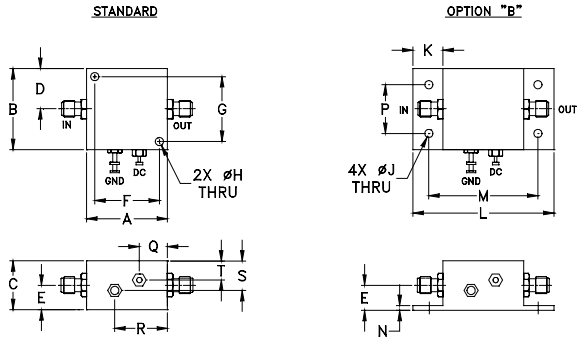

Outline Dimensions (inch / mm)

A	B	C	D	E	F	G	H	J	K	L	M	N	P	Q	R	S	T	wt.
1.25	1.25	.75	.63	.36	1.000	1.000	.125	.125	.46	2.18	1.688	.06	.750	.50	.80	.45	.29	grams
31.75	31.75	19.05	16.00	9.14	25.40	25.40	3.18	3.18	11.68	55.37	42.88	1.52	19.05	12.70	20.32	11.43	7.37	38

Notes

A. Performance and quality attributes and conditions not expressly stated in this specification document are intended to be excluded and do not form a part of this specification document.
B. Electrical specifications and performance data contained in this specification document are based on Mini-Circuit's applicable established test performance criteria and measurement instructions.
C. The parts covered by this specification document are subject to Mini-Circuits standard limited warranty and terms and conditions (collectively, "Standard Terms"); Purchasers of this part are entitled to the rights and benefits contained therein. For a full statement of the Standard Terms and the exclusive rights and remedies thereunder, please visit Mini-Circuits' website at www.minicircuits.com/MCLStore/terms.jsp

Typical Performance Data/Curves

FREQUENCY (MHz)	GAIN (dB)			DIRECTIVITY (dB)			VSWR (:1) 15V		NOISE FIGURE (dB)	POUT at 1 dB COMPR. (dBm)
	12V	15V	16V	12V	15V	16V	IN	OUT	15V	15V
0.05	20.18	21.24	21.41	18.10	17.50	17.40	1.59	1.69	—	10.52
0.33	21.00	22.06	22.23	16.40	15.70	15.60	1.17	1.11	—	10.82
3.90	21.03	22.08	22.27	16.30	15.60	15.50	1.09	1.11	—	10.84
47.90	21.08	22.13	22.30	16.10	15.40	15.30	1.07	1.11	5.72	10.87
192.30	20.96	21.93	22.07	15.40	15.90	17.10	1.01	1.01	5.74	10.31
243.60	20.79	21.74	21.90	16.80	17.20	16.80	1.01	1.01	5.76	10.28
307.70	20.74	21.70	21.84	16.20	16.60	16.60	1.01	1.02	5.77	10.26
371.80	20.58	21.55	21.70	16.40	17.20	17.60	1.01	1.02	5.77	10.23
435.90	20.69	21.65	21.80	15.70	16.80	16.10	1.01	1.03	5.78	10.14
500.00	20.40	21.36	21.52	17.10	17.70	16.70	1.01	1.02	5.79	10.05

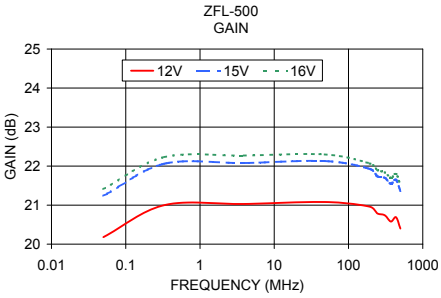

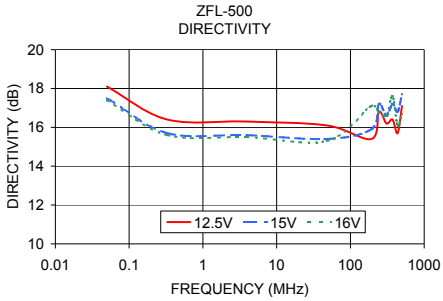

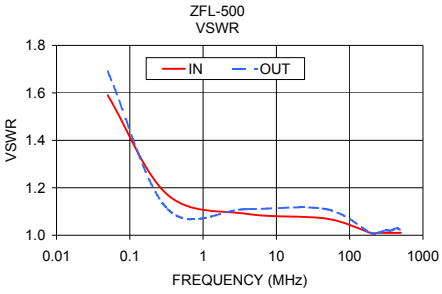

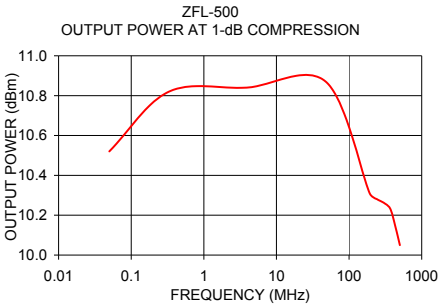

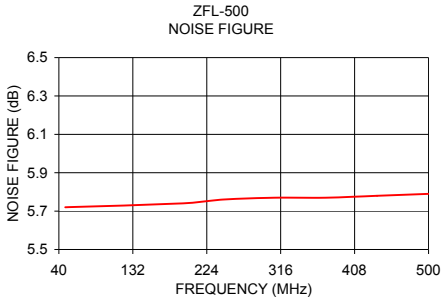

Notes
A. Performance and quality attributes and conditions not expressly stated in this specification document are intended to be excluded and do not form a part of this specification document.
B. Electrical specifications and performance data contained in this specification document are based on Mini-Circuit's applicable established test performance criteria and measurement instructions.
C. The parts covered by this specification document are subject to Mini-Circuits standard limited warranty and terms and conditions (collectively, "Standard Terms"); Purchasers of this part are entitled to the rights and benefits contained therein. For a full statement of the Standard Terms and the exclusive rights and remedies thereunder, please visit Mini-Circuits' website at www.minicircuits.com/MCLStore/terms.jsp

BIBLIOGRAPHY

[1] D. McLaughlin, D. Pepyne, V. Chandrasekar, B. Philips, J. Kurose, M. Zink, K. Droegemeier, S. Cruz-Pol, F. Junyent, J. Brotzge, D. Westbrook, N. Bharadwaj, Y. Wang, E. Lyons, K. Hondl, Y. Liu, E. Knapp, M. Xue, A. Hopf, K. Kloesel, A. DeFonzo, P. Kollias, K. Brewster, R. Contreras, B. Dolan, T. Djaferis, E. Insanic, S. Frasier, and F. Carr, "Short-wavelength technology and the potential for distributed networks of small radar systems," *Bulletin of the American Meterological Society*, pp. 1797–1817, Dec. 2009.

[2] M. Weadon, P. Heinselman, D. Forsyth, W. E. Benner, G. S. Torok, and J. Kimpel, "Multifunction phased array radar," *Bulletin of the American Meterological Society*, pp. 385–389, Mar. 2009.

[3] F. Junyent Lopez, "The design, development and initial field deployment of an X-band polarimetric doppler weather radar," Master's thesis, University of Massachusetts Amherst, Sep. 2003.

[4] K. Orzel, V. Venkatesh, T. Hartley, and S. Frasier, "Development and calibration of a X-band dual polarization phased array radar," in *IEEE Radar Conference*, Ottawa, Canada, May 2013.

[5] V. Chandrasekar, H. Chen, B. Philips, D.-j. Seo, F. Junyent, A. Bajaj, M. Zink, J. Mcenery, Z. Sukheswalla, A. Cannon, E. Lyons, and D. Westbrook, "The CASA Dallas Fort Worth Remote Sensing Network ICT for Urban Disaster Mitigation," in *EGU General Assembly Conference Abstracts*, Vienna, Austria, Apr. 2013, p. 6351.

[6] K. Orzel, V. Venkatesh, R. Palumbo, R. Medina, J. Salazar, A. Krishnamurthy, E. Knapp, D. McLaughlin, R. Tessier, and S. Frasier, "Mobile X-band dual polarization phased-array radar: System requirements and development," in *American Meterological Society 35th Conference on Radar Meteorology*, Pittsburg, PA, Sep. 2011.

[7] R. H. Medina, E. J. Knapp, J. L. Salazar, and D. J. McLaughlin, "T/R module for CASA phase-tilt radar antenna array," in *7th European Microwave Integrated Circuits Conferences*, Amsterdam, the Netherlands, Oct. 2012, pp. 913–916.

[8] J. L. Salazar Cerreño, "The feasability of low-cost, dual-polarized, phase-tilt antenna arrays for dense radar networks," Ph.D. dissertation, University of Massachusetts Amherst, Sep. 2012.

[9] Y. Golestani, V. Chandrasekar, and R. J. Keeler, "Dual Polarized Staggered PRT Scheme for Weather Radars: Analysis and Applications," *IEEE Transactions on Geoscience and Remote Sensing*, vol. 33, no. 2, pp. 239–246, Mar. 1995.

[10] R. J. Doviak and D. S. Zrnić, *Doppler Radar and Weather Observations*, 2nd ed. Dover Publications, 1993.

[11] V. N. Bringi and V. Chandrasekar, *Polarimetric Doppler Weather Radar: Principles and Applications*. Cambridge University Press, 2001.

[12] S. J. Frasier, F. Kabeche, J. Figueras i Ventura, H. Al-Sakka, P. Tabary, J. Beck, and O. Bousquet, "In-place estimation of wet radome attenuation at X band," *Journal of Atmospheric and Oceanic Technology*, vol. 30, pp. 917–928, May 2013.

[13] J. D. Hunter, "Matplotlib: A 2D graphics environment," *Computing In Science & Engineering*, vol. 9, no. 3, pp. 90–95, 2007.

[14] M. Heistermann, S. Jacobi, and T. Pfaff, "Technical note: An open source library for processing weather radar data (wradlib)," *Hydrology and Earth System Sciences*, vol. 17, pp. 863–871, Feb. 2013.

[15] K. Orzel, L. Masiunas, T. Hartley, and S. Frasier, "Deployment of the X-band dual polarization phased array radar in the Dallas-Fort Worth Urban Demonstration Network," in *Eigth European Conference on Radar in Meteorology and Hydrology*, Garmisch-Partenkirchen, Germany, Sep. 2014.